ASPECTS OF ENERGY REQUIREMENTS FOR ROCK DRILLING

by

DAVID WOOTTON, B.Sc.

A thesis presented to the University of Leeds in fulfilment of the requirements for the degree of Doctor of Philosophy.

Department of Mining and Mineral Sciences,
University of Leeds

August, 1974.

CONTENTS

ABSTRACT

Development of laboratory rock breakage techniques to relate energy and surface area produced by slow compression, drop hammer and stamp mill.

A detailed study of laboratory rotary-percussive drilling in a wide range of rocks under different conditions, with the collection of drill cuttings and measurement of the drill parameters. The correlation of drill parameters with rock indices by energy concepts and the developed empirical formula.

Field rotary-percussive drilling studies and collection of drill cuttings on the basis of laboratory analysis.

INTRODUCTION

Where the drilling of rock is necessary in mining, the cost incurred forms a very large part of the mining budget. The most important drilling factors relating to cost are the penetration rate, bit wear and the efficient use of energy. The penetration rate being dependent on time will directly determine the length of a drilling operation. This can increase or decrease the overall production rate and this in turn will effect capital and running costs. The bit life must be prolonged to reduce the need for resharpening and continual new purchases. Energy has become a much more important factor due to the world energy situation and should be used effectively. The efficient use of energy is also particularly relevant when working with portable power packs, whereby the need is to make maximum use of the energy available.

With these factors in mind the complete understanding of drilling from the design through to the application has become an essential goal to be obtained. Obviously, this is an extremely wide field and various research organisations have examined specific areas with varying degrees of success.

The most common method of analysis has been to try to predict performance by correlating the penetration rate with a rock property. A large number of rock properties have been correlated with penetration rate, some reasonably well, others show little or no correlation. However,

even the best correlations found by complicated regression analysis have not given the desired accuracy and this is clearly shown with field drilling.

Hence the fairly simple idea on drillability was to be extended to measure all the drilling parameters both in the laboratory and field. Furthermore, to develop a more detailed analysis of laboratory methods of rock breakage to give (a) an accurate index and (b) to examine the efficiency of a process with regard to energy input and the resulting rock breakage. This was then the basis of this investigation.

General Outline of the Research Programme

A model of a rotary-percussive drill was made to carry out laboratory drilling and designed so it was possible to measure the speed of rotation, torque, penetration rate, thrust, percussive action and for the collection of drill cuttings for analysis. The important variable of bit wear was for the purpose of this present research eliminated by drilling short holes, resharpening after each hole and having a supply of 40 drills. The omission was because the design and analysis of bits is an extremely large area of research itself and work is being carried out with the sole intention of solving this problem.

When the model was made, tests were carried out to show that the standard characteristics of drilling were exhibited. Drilling was then started on a large range of

rocks and the data collected for each rock. So that detailed information was obtained for the drilling characteristics showing the advantages of using one type of drilling as opposed to another. Then relationships of performance in different rocks were compared to the rock indices.

Field rotary-percussive drilling was done by Halifax Tool Company and the results were analysed in detail. Further field work was carried out in collecting data and drill cuttings for laboratory tests.

The other important part of the research was the development of the rock breakage indices. Previous researchers used compressive strength, the most common index, as the index for correlation, but a more simple method was developed by Protodyakonov M.M. This has been refined by the U.S. Bureau of Mines to give the index 'coefficient of rock strength' and Leeds University rock mechanics section to give the 'rock impact hardness' index. Both these methods are ones of drop hammer breakage which were found to correlate best with rotary-percussive drilling. The most efficient method of breakage is by slow compression, so a comparison of this method with drop hammer was made by measuring the energy inputs and the surface area produced by each method.

This analysis was extended to a stamp mill method of breakage, the idea being that short hammer drops could be more applicable to rotary-percussive drilling than the

longer fall of the drop hammer.

Therefore the indices used for correlation purposes were those developed, i.e. slow compression, drop hammer and stamp mill, also the standard compressive strength index, rock impact hardness number and values of dynamic Young's Modulus from an ultrasonic tester.

CHAPTER I

LITERATURE REVIEW

CHAPTER I

LITERATURE SURVEY

The main methods of rock drilling are rotary, percussive and the combination of the two, rotary-percussive. The post-war need for greater speed in drilling, especially drilling in hard rocks, led to the development of rotary-percussive drilling. The idea was conceived in Britain as early as 1922, but the first production model was shown at the Essen Mining Exhibition in 1950 by the Salzgitter Company. It was only in the middle-fifties where rotary-percussive drilling was developed to the point to carry out commercial drilling.

This method of drilling combines the advantages of both drilling by rotary and by percussion giving better penetration rates and longer bit life, the drill parameters being changed to suit the rock conditions.

1.1 Characteristics of Rotary-Percussion Drilling

Lacabanne and Pfleider (1) showed the characteristics (Fig.1.1) of rotary-percussive drilling and its advantages in their paper 'Rotary Percussive Blasthole Machine may Revolutionise Drilling'. Indeed, this has proved to be true with the vast majority of quarry blast hole drilling being carried out by rotary-percussive machines. However, they were over-optimistic in relating bit rotation and penetration rate to the Shore Hardness, a linear relationship was obtained with four rocks (Fig.1.2). Fish (2) at the N.C.B. Mining Research Establishment carried out

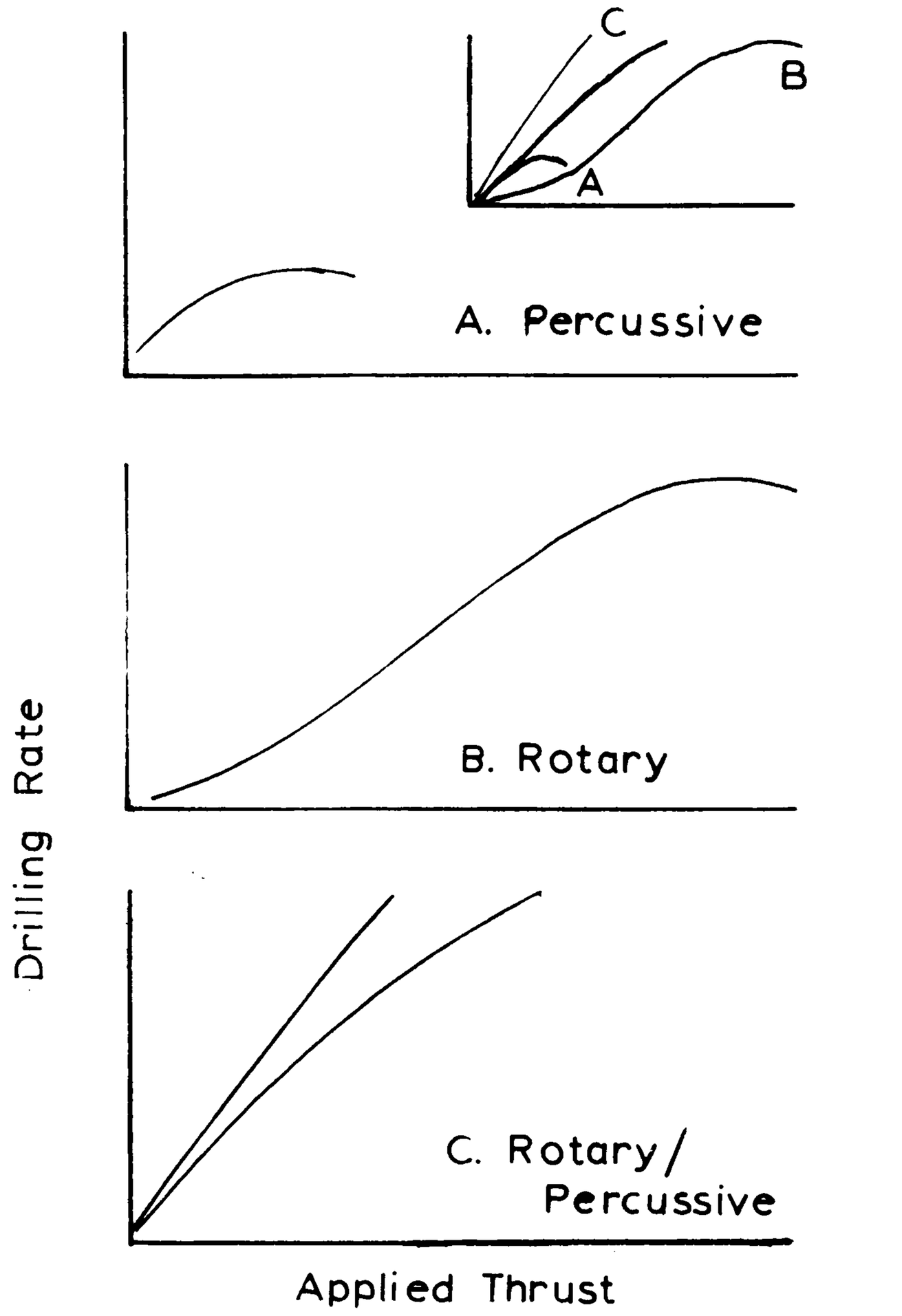

FIGURE 1.1: CHARACTERISTICS AFTER LACABANNE AND PFLEIDER (1).

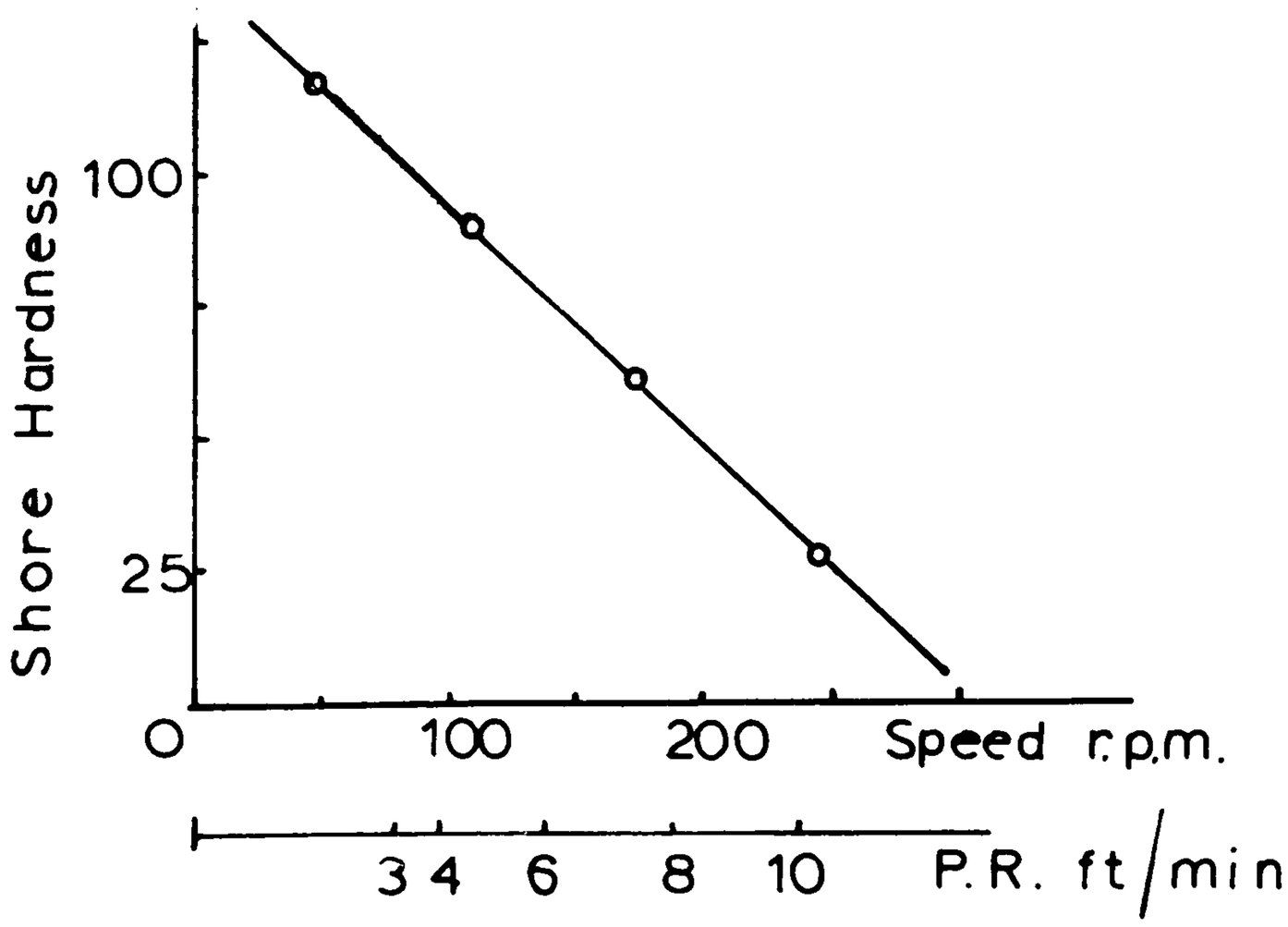

FIGURE 1.2: RELATIONSHIP AFTER LACABANNE AND PFLEIDER (1)

work on a rotary-percussive Hauscherr DK7ES drill. He drilled in a soft sandstone, i.e. Darley Dale sandstone, in a hard sandstone, i.e, Pennant sandstone, and Cornish granite. The results from his tests agreed with those of Lacabanne and Pfleider. Fish suggested that the efficiency of performance regarding the consumption was less when compared to percussive drilling. The hope was to rectify this by changing the drill design such as weight, number of blows, change of feed and rotation.

From this initial work quite a number of papers (3,4,5,6,7,8,9,10) were published in the late-fifties and early-sixties on the fundamentals of rotary-percussive drilling, so as to establish drilling rates, thrusts, speed, torque, strength of blows, number of blows etc.

1.2 Stress Wave Energetics in Impacting

The early-sixties saw the introduction of the digital computers and this was particularly relevant in the study of stress wave energetics in impacting. One dimensional stress wave theory already existed more than a hundred years ago (11,12) and the first to apply this theory was Donnel (13) and Dahl (14) in the early 1930's. A graphical analysis was developed by De Juhasz (15,16) and this was later refined and applied by Fischer (17). However, it is in the sixties when the important part of energy transfers in drilling was investigated in detail, through the elimination of the computational problems. Fairhurst (18), Fischer (19), Bailey (20) and Simon (21) all studied

the wave mechanics of percussive drilling. Hustrulid and Fairhurst (22) predicted penetration rate and thrust by considering stress wave interactions in developing the theoretical mechanics of percussive drilling. They found that the energy transfer to the rock only occurs during the first and possibly the second stress wave interaction; therefore it is advantageous to transfer the maximum amount in the first wave. Dutta (23) at Sheffield determined the stress wave forms produced by percussive drill pistons of various geometrical designs.

The most recent study of stress wave energetics is by B. Lundberg (24), his paper published in the International Journal of Rock Mechanics is divided into three parts. Part one compares the percussive methods of churn, down-the-hole and hammer drilling by considering the first impact wave and the efficiency is found in that order. Part two considers the second wave and concludes that design done on the first wave is all right because the efficiency reaches 90%. However, when not drilling under optimum conditions the energy transfer from subsequent waves is still important. Part three studies the transfer of energy through joints in two models, elastic and rigid. Also transfer through rigid models for a number of joints which Lundberg says that transfer becomes more favourable because each joint is acting as a low pass filter and there are less high frequency components after passing each joint. In the case of long-hole percussive drilling

we do know that drilling does become more inefficient at depth because of friction and dissipation of energy. There is not much left of the incident wave compared to when it first starts, even though what is left is favourable. Indeed, down-the-hole drilling attempts to eliminate this problem.

1.3 Drillability Studies

In the study of drilling a number of methods have been suggested for the evaluation of rock drillability which is defined as the rate of penetration of a drill into a rock. The idea being that on being presented with a rock sample one could carry out a laboratory test so as to predict the penetration rate of the drill. In general terms establishing a relationship between the machine performance and a rock property for a range of rocks one could predict the performance of the machine from laboratory testing of the rock by graphical interpretation or a regression equation for that range and particular machine. It is the attempt to establish such a relationship that has directed researchers into this field of study, firstly by fairly simple techniques and then by more detailed machine and rock examinations.

A. Hardness

Hardness has been most commonly used for predicting the drillability of rocks (25,26,27,28,29,30,31), Gyss and Davis (26) defined hardness of homogeneous rocks as its resistance to a penetrating medium such as a drill bit.

Hardness is also expressed by the familiar scratch hardness of mineralogists and rebound hardness determined by the rebound of a hammer dropped on the surface of the rock. Furby (32) used a rebound hammer consisting basically of a spring-loaded piston that was projected under controlled conditions against an anvil. Singh (30) used a rebound Sklerograph hardness tester and plotted these values for rocks against a drillability number obtained by drilling with a chisel bit (3/8" x 3/8" x 3/32") on a laboratory drilling machine made after suggestions by R.H. Goodrich of the Joy Manufacturing Company. This was done under a constant thrust of 40 lbs. with 150 revolutions and the drillability number calculated on the assumption that a hole of 1 inch depth has a drillability number of 254. The resulting graph (Fig. 1.3) showed a wide scatter and only indicated a general trend. Shore Schleroscope hardness tester, another rebound method of hardness, also gives wide scatter and general trend shown by Misra (34) in his rotary-percussive drill studies over a range of rocks and different rock properties. Misra also used the N.C.B. cone indentor for hardness determination whereby the rock specimen is indented with a tungsten carbide conical point. The force used to effect the indentation is measured indirectly by the deflection of a steel spring against which the specimen abuts. If the deflection and indentation are noted by D and I respectively then the ratio of D/I represents the cone indentation

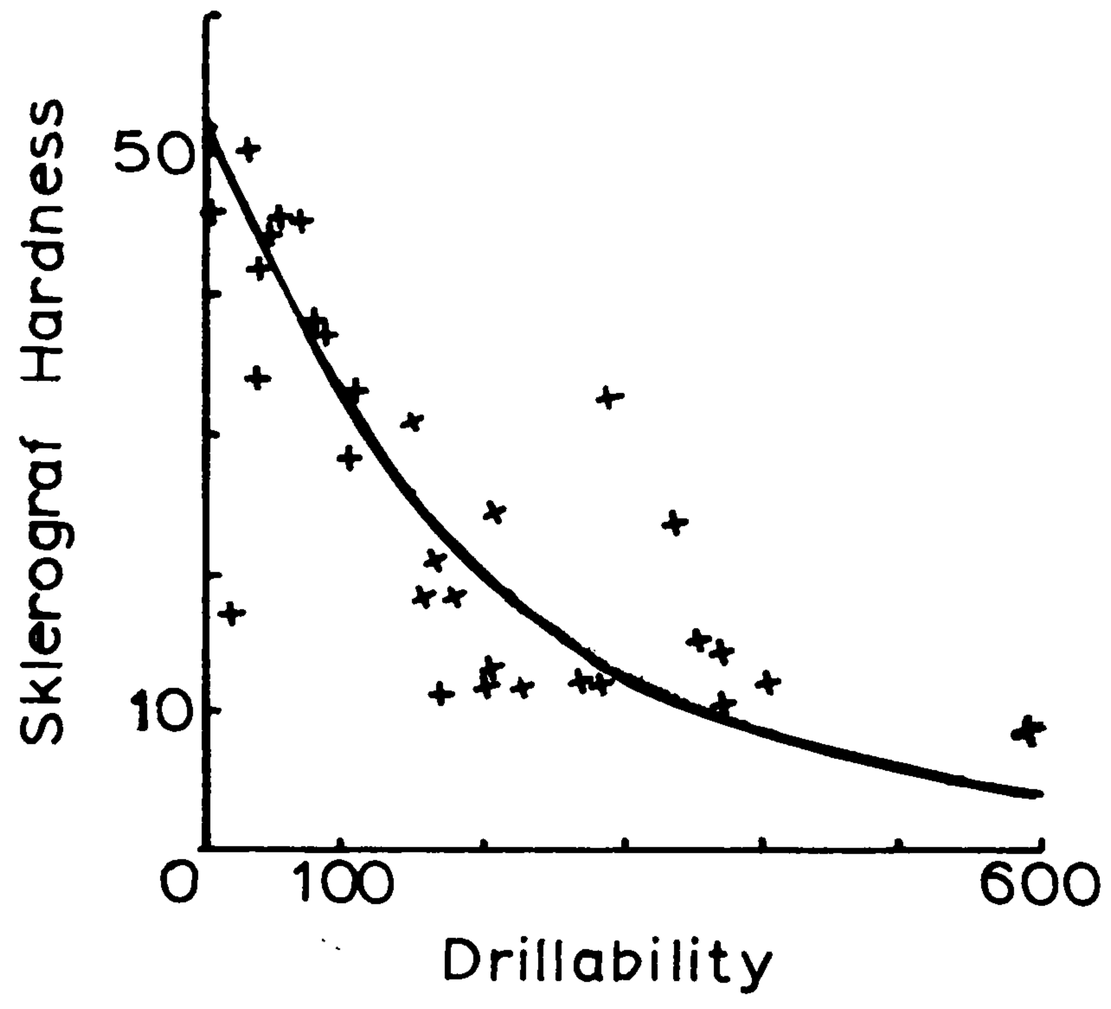

FIGURE 1.3: RELATIONSHIP AFTER SINGH (30).

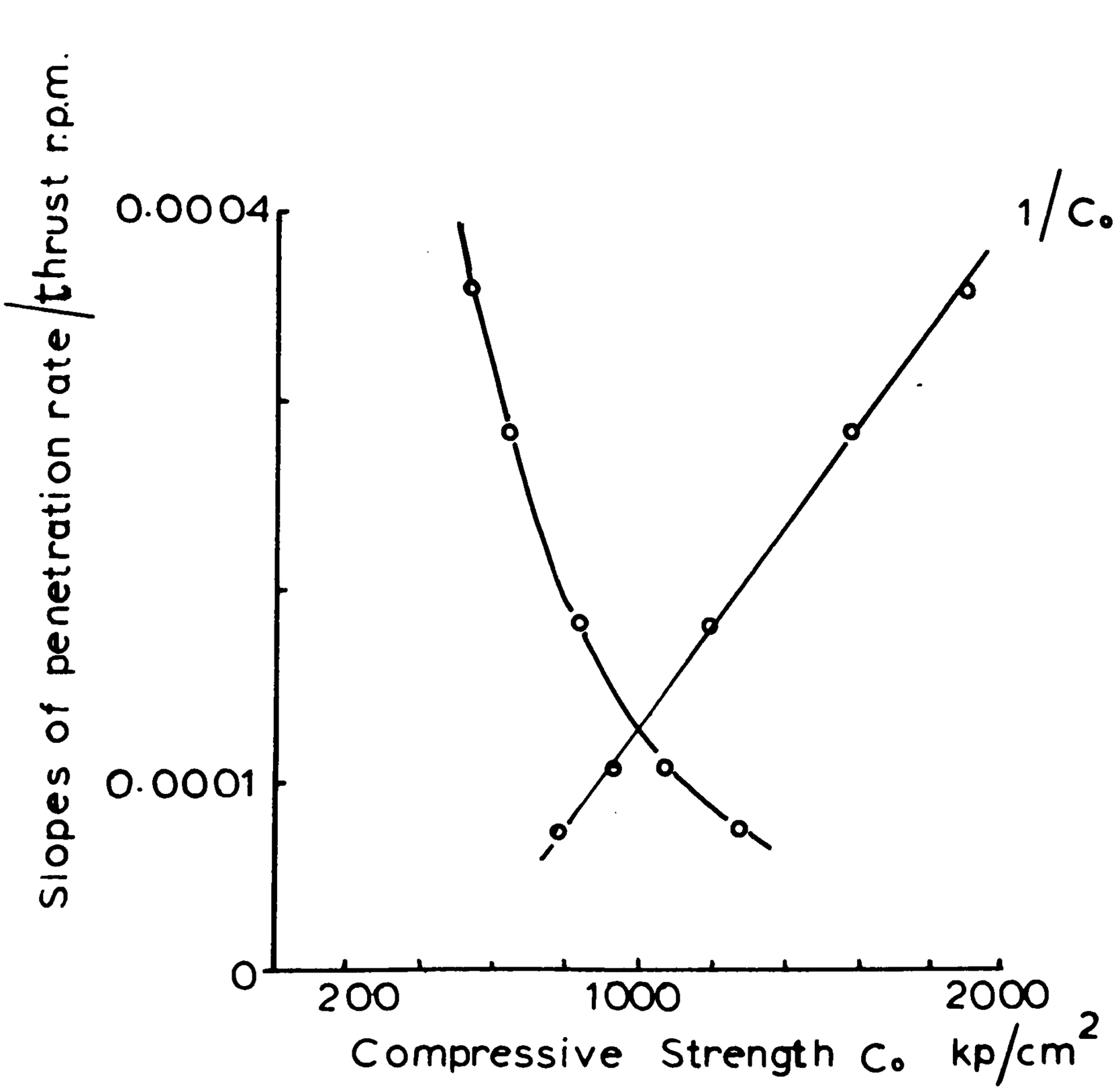

FIGURE 1.4: RELATIONSHIP AFTER TSOUTRELIS (39).

hardness (35). He concluded that results on limestones were reasonably constant, but the results on sandstones varied and that it could not be used on all rocks. It was therefore not capable of providing a comprehensive hardness index. Van del Vlis (36) has used a steel ball indentor expressed as the Brinell hardness number and obtained an empirical relationship with Young's Modulus, but as yet no published applications to machine performance.

In conclusion with regard to hardness indices only a general trend is obtained in correlation with drillability and cannot be taken as a reliable guide to drillability. The reason for this can be explained by the fact that generally the harder the rock the more difficult it is to drill, but many hard rocks have been drilled more easily compared with soft rocks. One may also have two hard rocks, but one is tough and the other brittle; the brittle rock provides easier drilling with the formation of bigger chips, as long as there is still a cutting edge on the bit. Similarly the abrasivity of a hard or soft rock will affect the drillability and a rock composed of hard minerals but loosely bound can be easily drilled

B. Strength

Indices developed from strength have given a more definite relationship. This was to be expected because during the process of drilling the rock either fails in compression, tension or shear depending on which type of stress exceeds the appropriate strength. A large amount

of interesting and useful work on drilling and its relation to rock properties has been carried out by the United States Bureau of Mines.

Paone and Bruce (37) studied surface set diamond coring bits and developed an equation for predicting the depth of penetration per revolution from the compressive strength:

$$d = \frac{2(T - VFr)}{SA - F}$$

where, d = penetration depth per revolution, inches

T = applied torque

V = coefficient of resistance

F = applied thrust lb/in^2

S = drilling resistance lb/in^2

A = cross-sectional area

r = bit radius.

Where the two unknowns are coefficient of resistance and the drilling resistance, these were taken as 0.4 and the compressive strength respectively. Plotting d against the compressive strength gave a good relationship for different rocks under one drilling condition. In a later paper Paone and Madson (38) gave their results on surface set and impregnated diamond bits for laboratory and field drilling. Their laboratory results of ordinary penetration rate versus compressive strength gave a good trend; field results indicated a general trend. However, they did not use an analysis by the above derived equation simply because it did not work for impregnated diamond bits

but their work showed a good relationship of diamond drilling to compressive strength.

Tsoutrelis (39) used a dimaond drill and obtained the penetration rate-thrust characteristics for five rocks. Plotting the rock drilling constant against the reciprocal of the compressive strength gave a linear relationship (Fig. 1.4). The rock drilling constant is the slope of the penetration rate-thrust graphs per rev/min. The equation of the straight line was proposed for the determination of the compressive strength of rock by drilling in situ or in test blocks. The advantages claimed by the method are that it avoids difficulties of preparation of the rock specimens and it is not affected by the presence of any invisible cracks or discontinuities in the rock. Also by increasing the distance drilled in the rock the compressive strength becomes more and more representative of the whole rock mass. To substantiate these claims further tests would be needed over a large number and range of rocks for the prediction of drillability.

An indirect method of measuring rock strength was developed by Protodyakonov M.M. (29) and he found that it correlated better with percussive drilling. Paone et al (40) derived the coefficient of rock strength from the Protodyakonov test and found a good correlation with two laboratory percussive drills (Fig. 1.5). Misra (34) also found the Rock Impact Hardness Number Test, a test also derived from Protodyakonov, to correlate with a

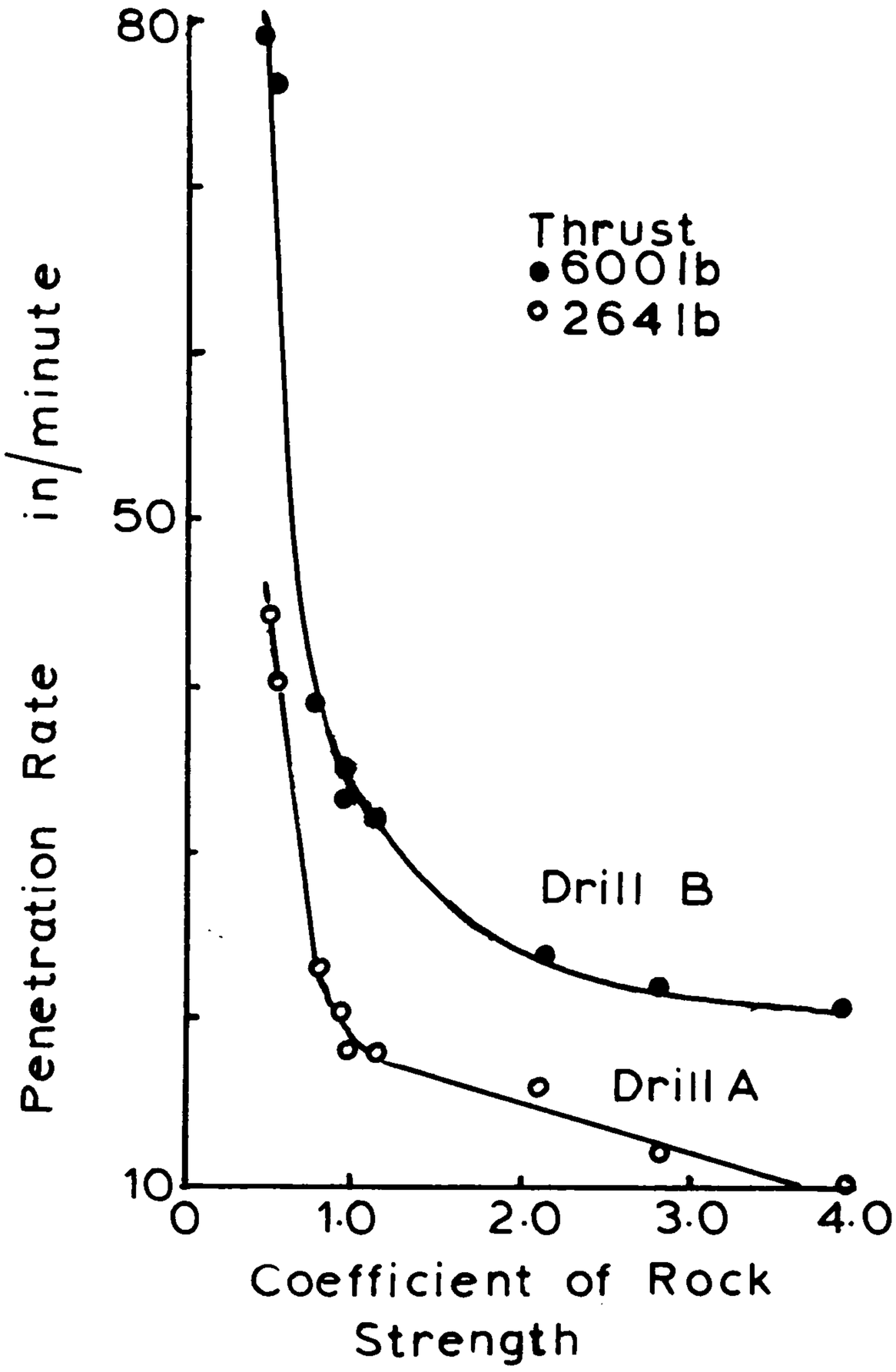

FIGURE 1.5: RELATIONSHIP AFTER PAONE ET AL(40).

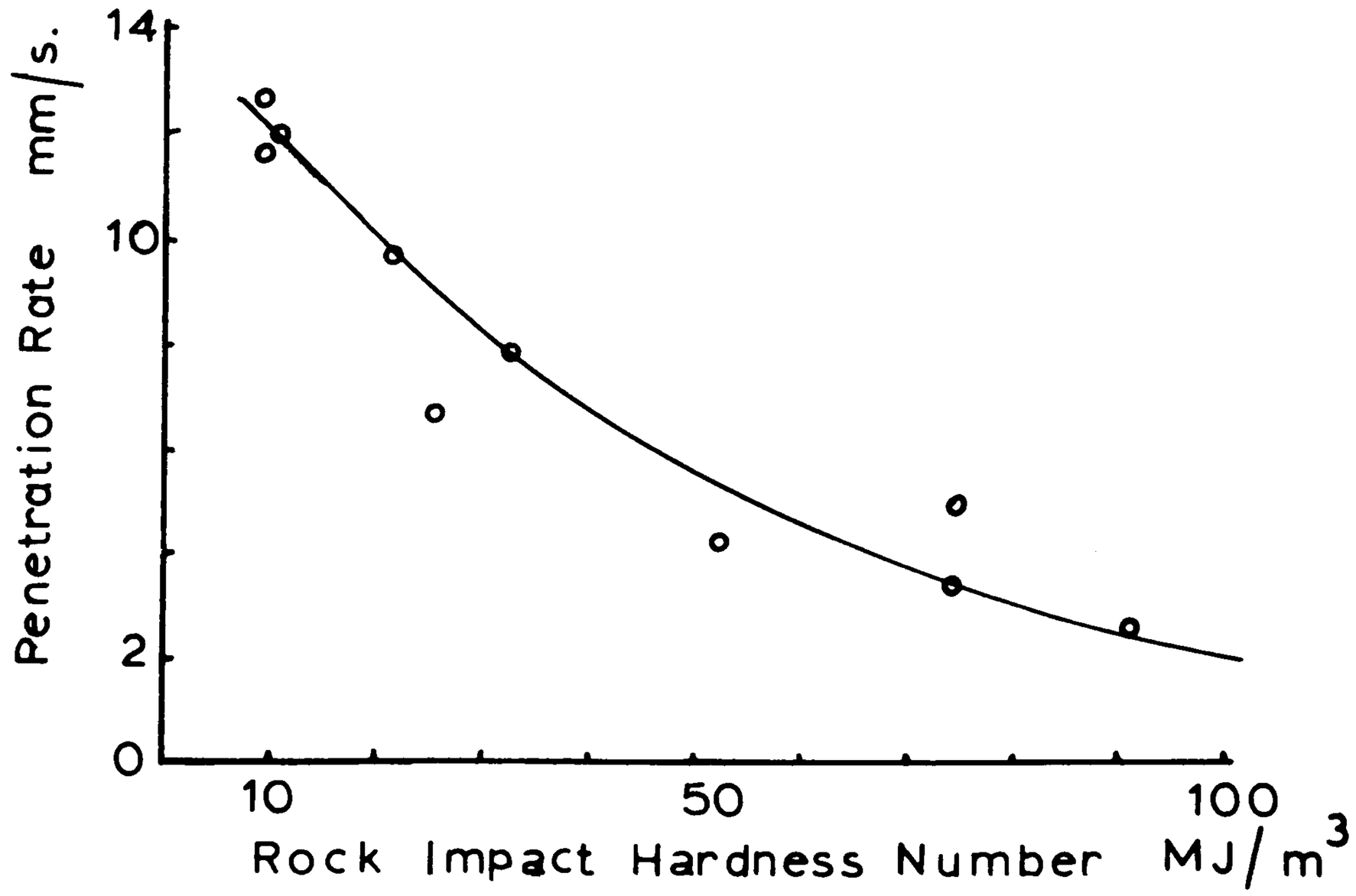

FIGURE 1.6: RELATIONSHIP AFTER MISRA(34).

rotary-percussive laboratory drill (Fig. 1.6) and a general trend with a field rotary-percussive drill. The methods involve breaking rock specimens in a mortar by drop hammer and measuring the fines produced below 500 microns. Through this research it was decided in the present research programme to examine this method by a more detailed analysis hence to compare the efficiency of laboratory breakage techniques and consequently with actual drilling. Therefore I will describe the three methods of determining the indices as the research builds on the basis of them.

(a) Protodyakonov Test

Professor Protodyakonov devised this method for the assessment of coal hardness in Russian mines. The same method was extended by Protodyakonov (Jnr) to include rocks. The Protodyakonov Test is also known as "Basic Method" or "Stamp Method" or "Pounding Method" in the Soviet Union. The standard procedure applied to rock is as follows:

(i) Each sample to be tested is broken up with a hammer and five specimens, consisting of chunks 20-40mm are picked and the volume of each specimen being 10-20 cm^3. Sharp edges in the specimens are avoided.

(ii) Each specimen is placed in a mortar (90mm diameter) of a tubular drop tester designed by Professor Syskov and is impacted with a 2.4 kg weight dropping freely from a height of 0.6m. The number of blows given to a particular rock varies from 5 to 15 according to the strength of the rock.

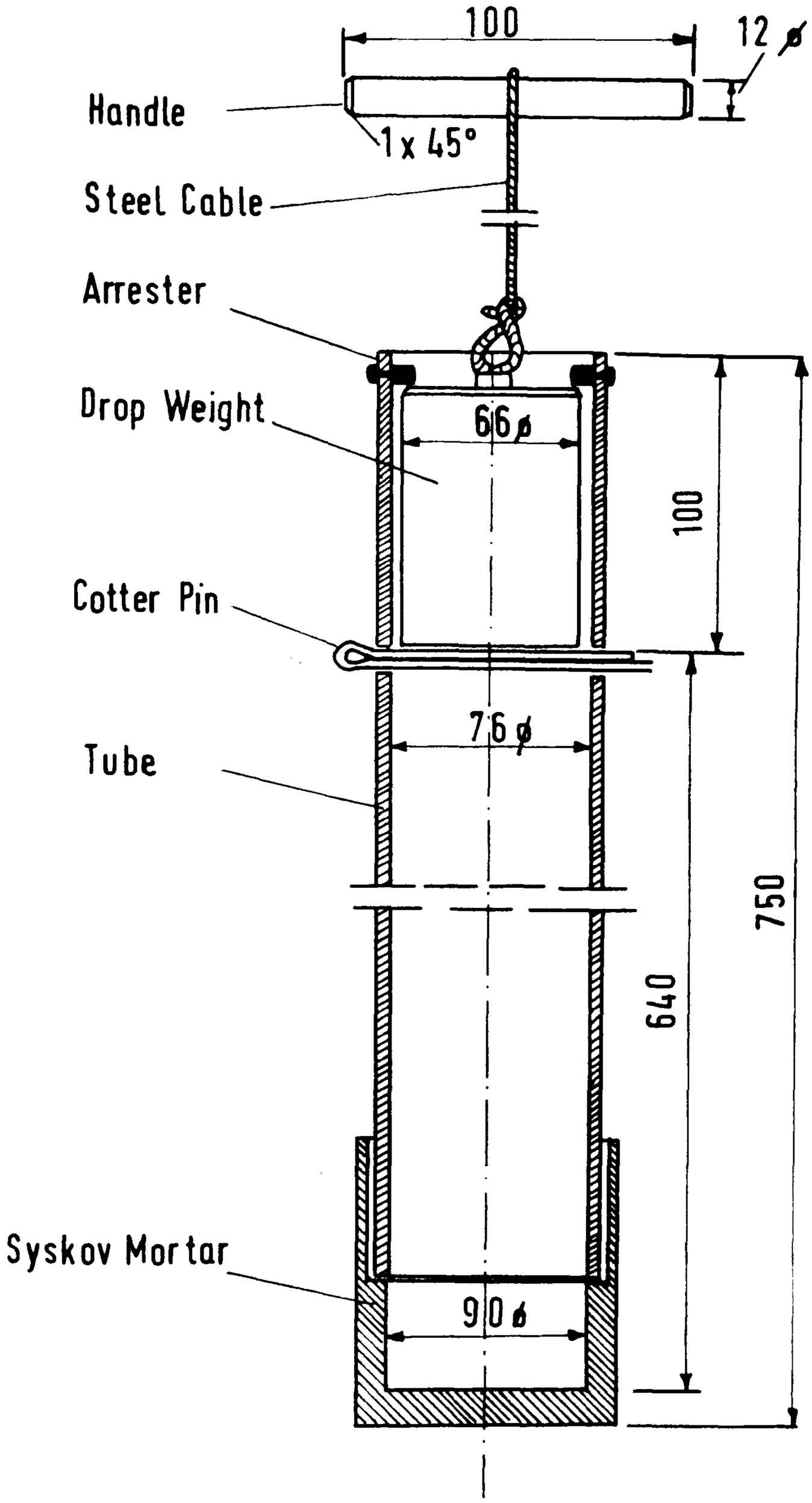

FIGURE 1.7: THE PROTODYAKONOV DROP HAMMER APPARATUS.

(iii) All five separately crushed specimens are placed on to a sieve of 500 microns and are sieved together.

(iv) The undersize product of the 500 microns sieve is poured into the tube of a volumemeter of 23mm diameter and with a piston length calibrated to 160mm. The tube is gently tapped to level the fines and allow a small amount of compaction. Then the piston is lowered into the tube until it just touches the top of the fines and the height of the column of dust (l) is recorded.

(v) The "strength coefficient" or the "Protodyakonov Number" according to Protodyakonov (Snr) will be:-

$$f = \frac{20n}{l} \quad \ldots\ldots\ldots\ldots\ldots\ldots \text{(I)}$$

where, n = number of blows

l = height of fines column in mm

produced by the corresponding n.

The above formula (I) is based upon the physical law

$$H = \frac{A}{S} \quad \ldots\ldots\ldots\ldots\ldots\ldots \text{(II)}$$

where, A = total work performed

H = the specific work consumed for crushing

S = total surface of particles after crushing

(b) Coefficient of Rock Strength

Paone et al (40) describes the method derived from Protodyakonov; the procedure is

(i) Five irregularly shaped rocks are prepared, each having a volume of about 15 cm^3. The total weight in grams of the five specimens should be 75 times the specific gravity of the material, $\pm$ 2 grams.

(ii) Each specimen is placed on the bottom of a hollow cylindrical drop tester and impacted with a 2.4 kg weight falling from a height of 0.6m. The cross-sectional area of the cylinder is 7.30 sq.in.

(iii) The number of drops for each specimen may vary from 3 to 40, with the stronger rocks requiring more drops. The broken material for each sample is combined and shaken on a 500 micron sieve.

(iv) The minus 500 micron material is weighed and divided by the specific gravity to determine the solid volume of the sample. The coefficient of rock strength is then determined by dividing the volume of the minus 500 micron material of the five specimens by the number of drops used.

(v) After the coefficient of rock strength is determined for one sample, a larger and smaller number of drops are tried to determine the minimum coefficient of rock strength. After a minimum number has been found, two additional determinations are made to verify the results.

Schmidt (42) in a later U.S. Bureau of Mines report describes the above test and shows a detailed diagram of the testing apparatus. Schmidt has made a slight modification of the above method in that 10 irregularly shaped specimens averaging 7.5 cm^3 are placed in the mortar two at a time instead of 5 specimens of volume 15 cm^3 individually broken. The U.S. Bureau of Mines mortar has 8 holes drilled in the mortar of 5/16" diameter. Sieving of the material was carried out on a 500 micron sieve for 40 seconds. Schmidt's

objective was to determine the minimum coefficient, as this represents the most efficient use of energy to produce the minus 500 microns of material. After one determination was made, another set of 10 specimens was tested with a larger or smaller number of impacts. His procedure was to plot the number of impacts versus coefficient of rock strength and let the trend of the curve indicate whether more or fewer impacts were in the direction of the minimum.

The equation for determining rock strength is:

$$f' = \frac{n}{V} = np/w$$

where, f' = coefficient of rock strength

n = number of drops

p = specific gravity

w = total weight of minus 500 microns from five groups, gms.

and V = solid volume of minus 500 microns from 5 groups, cu.cm.

Comparison of results on the coefficient of rock strength carried out by researchers at the U.S. Bureau of Mines show discrepancies for different rocks. This could be due to the slightly changing method or different sampling of rock. These discrepancies are particularly evident with Dresser basalt and Aurora taconite, as shown in Table 1.

TABLE 1

Comparing Values of Coefficient of Rock Strength

Rock Name	Paone et al (Ref.40)	Schmidt (Ref.42)	Unger et al (Ref.56)
Kasota Stone	0.50	-	0.72
Mankato Stone	0.54	0.45	0.51
Rockville Granite	0.82	0.84	0.86
Rainbow Granite	0.97	-	0.87
Jasper Quartzite	1.00	1.01	1.1
Charcoal Granite	1.11	1.21	1.4
Aurora Taconite	2.08	2.62	3.4
Babbitt Taconite	2.84	2.84	-
Dresser Basalt	3.94	2.86	3.7

Despite these discrepancies the important point that arises is that good correlation was still obtained providing that the same rock sample to be drilled is also that which is to be tested for strength.

(c) Rock Impact Hardness Number Test (R.I.H.N.)

This method was developed by researchers (43,44, 45,46,34) at the Mining and Mineral Sciences Department, Leeds University and has proved to be an extremely consistent index. The method of finding Protodyakonov Number by the pounding method was first examined, and the effect of the initial size of specimen thoroughly investigated. The inaccuracies involved in the original

method, which stem from the measurement of a volume of fines below 500 microns are avoided by using weight measurements expressed as a percentage of the original weight of the regular specimen. Misra (34) in his Ph.D. thesis details the development from Protodyakonov through to R.I.H.N. and also outlines other methods of drop hammer breakage.

The R.I.H.N. method is as follows:

(i) Four or five regular specimens (25mm diameter and 50mm long) are diamond cored.

(ii) Each are placed separately in the Syskov mortar with the cylindrical axis horizontal and comminuted by a 2.4 kg. weight from a drop height of 0.6m.

(iii) The material is then sieved by hand for 45 seconds on a 500 micron sieve.

(iv) The minus 500 micron fines material is then weighed and expressed as a percentage of the original specimen weight.

(v) This procedure is repeated at different numbers of blows until the percentage fines produced by a test was over 30%. A graph of percentage fines against number of blows is plotted.

(vi) The 'Rock Impact Hardness Number' is defined as the number of blows to produce 25% fines, found from the graph or alternatively by the best fit curve obtained from the least square method, using computer facilities.

A bit of confusion does appear in the literature with regard to drop height. Protodyakonov, in his paper, does state that the drop height is to be 0.6m, but in the drawing of the testing apparatus (Fig. 1.7) the distance from the start of the drop to the bottom of the mortar is 0.640m. Paone et al state that the drop is 0.6m, Schmidt states 0.640m and researchers at Leeds have quoted 0.6m. In fact when using irregular shaped specimens their approximate height is 0.040m, so that the drop is 0.6m At Leeds the total drop is the distance dropped when empty (0.640m) minus the specimen diameter (0.025m) for R.I.H.N. It is the exclusion or inclusion of the specimen size that caused the confusion, all the drops are the same when the mortars are empty. However, if one wanted to work out the energy input accurately, it would be necessary to measure the height of fall before each blow. Clearly this is very small when compared as a percentage of the total drop.

Selmer-Olsen and Blindheim (47) carried out controlled field drilling, then laboratory tests on rock samples from test sites to establish a drillability index for hard Norwegian rock. Correlation was between drilling rate and the Swedish brittleness value corrected by Sievers-J value (48), (Fig.1.8). This Swedish test is a drop weight test technique and the Sievers-J is the penetration of a Wolfram carbide drill into the rock

expressed in 1/10mm after 200 rotations carried out in the direction of drilling. To obtain the Swedish brittleness value the procedure is:

(i) Crush the rock 2 times in a laboratory crusher with an opening of 18mm, then sieve using sieve sizers 16mm and 11.2mm.

(ii) 500 gms of crushed rock between these sizes is placed in a mortar solidly mounted on a 5 ton concrete block.

(iii) A 14.5 kg weight is dropped through 25 cm on to the rock 20 times.

(iv) Measure the amount below 11.2mm as a percentage of 500 gms and this is the Swedish brittleness value.

The authors found this method as a good index to estimate drillability but mainly pertaining to hard Norwegian rocks.

Broch and Franklin (49) used the percussive drilling rates of Selmer-Olsen and Blindheim plotted against results from a diametral point-load strength (I_s) of cores drilled perpendicular to rock foiliation (Fig. 1.9). Points are scattered, but a general trend is obtained.

Hartman (50) concluded that the drop tester was a good rock drillability measuring device but found little benefit from indexing research.

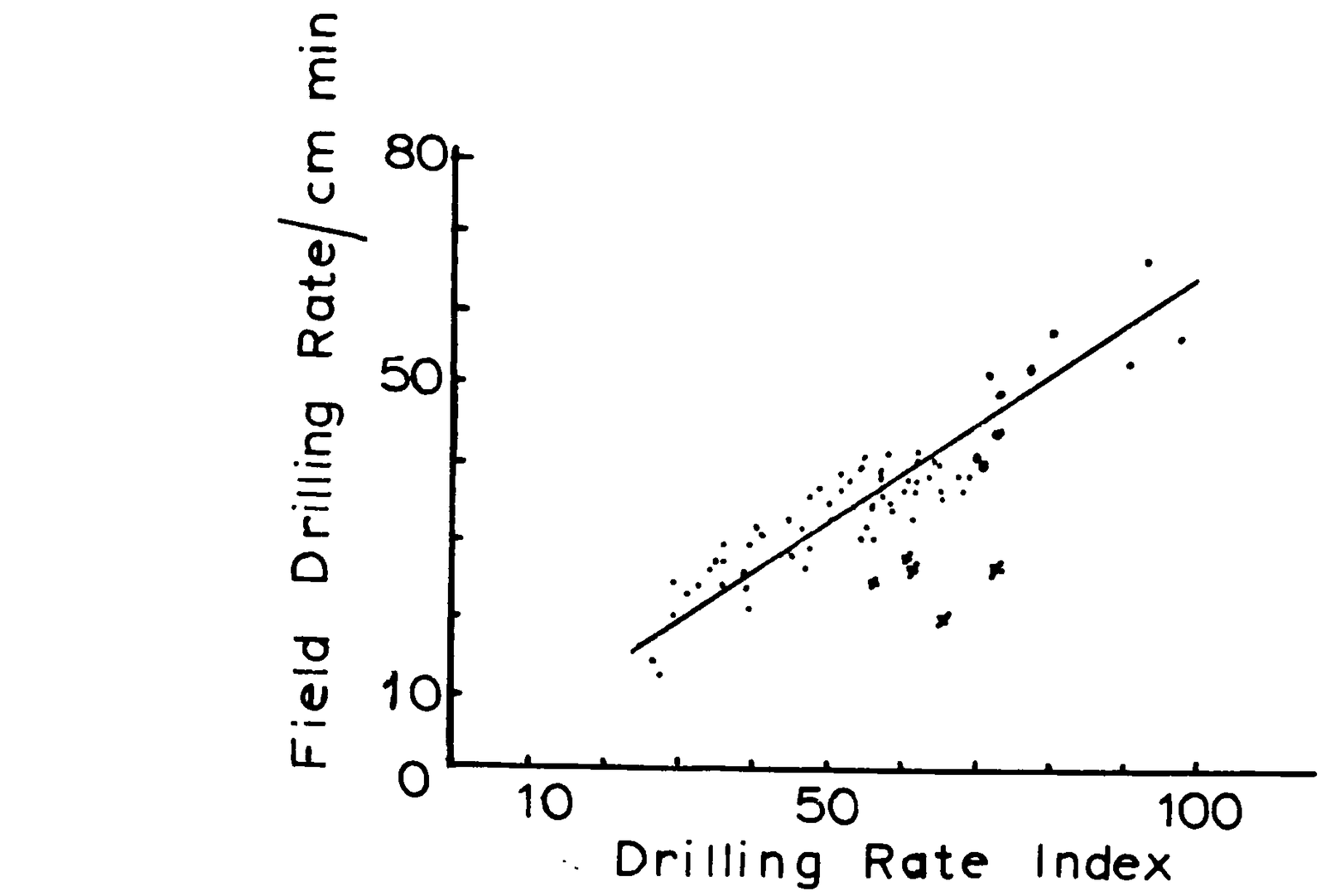

FIGURE 1.8: RELATIONSHIP AFTER SELMER-OLSEN BLINDHEIM (47).

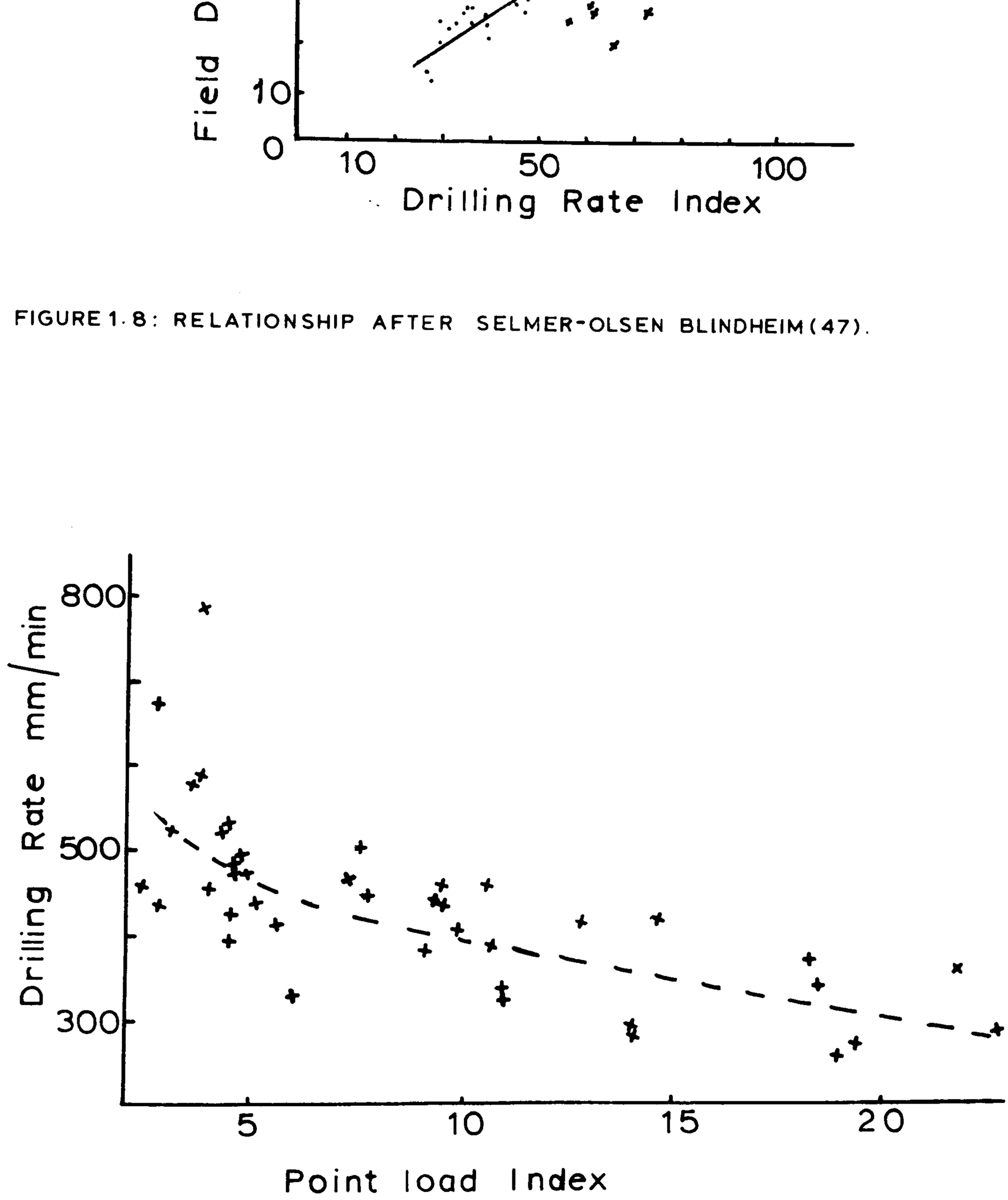

FIGURE 1.9: RELATIONSHIP AFTER BROCH AND FRANKLIN (49).

C. Energy Concepts in the Drillability of Rocks

Teale (51) proposed that the work done per unit volume excavated is the specific energy required for drilling. For rotary drilling he proposed the equation:

$$e = \frac{F}{A} + \frac{2\pi NT}{Au} \quad \text{..... in lb/in}^3$$

where, e = specific energy

F = thrust, lbs.

A = area of hole, in²

u = penetration rate, in/min.

N = speed, rev/min.

T = Torque, lb.in.

His idea was that minimum specific energy could be correlated with the compressive strength and could be extended to all methods of rock drilling.

Opoloski (52) calculated the drillability index for coal measures by taking into account the slope of the energy input/penetration rate curve. His drillability index T′ was defined as:

$$T' = \frac{60P}{FV} \quad \text{..... watt sec. per cm}^3$$

where, P = input power, watt.

V = penetration rate, cm/min.

F = area of hole, cm²

Cook and Hustrulid (52) in their efficiency analysis of three percussive rock drills at two different sites

said that the specific energy has a value of the same order as that of the co-axial compressive strength (C_o) of the rock. The power going into breaking the rock at the bottom of a drill is obtained from:-

$$W_R = A_H \times w \times E_v$$

where, W_R = power to break rock at bottom of drill

A_H = area of drill hole

w = rate of penetration

E_v = specific energy of drilling = C_o compressive stength.

Hustrulid (54) earlier presented the equation for percussive drilling:-

$$P.R. = \frac{12V \times f \times Tr}{A_H \times E_v} \quad \ldots\ldots\ldots\ldots \quad \text{Equation II}$$

where, P.R. = penetration rate, in/min.

V = blow energy, ft. lb.

f = blow frequency, blows/min

Tr = transfer ratio of energy transferred to the rock and energy available for each blow.

A_H = cross-sectional area of hole , sq. in.

E_v = energy required to remove unit volume of rock, in lb/cu.in.

Hustrulid's paper (55) on the percussive drilling of quartzite quotes Tr as being approximately equal to 0.8 and $E_v \simeq C_o$, the initial compressive strength of the rock.

Mellor (56) criticised the use of the compressive strength in the specific energy concept, but it would be extremely convenient if specific energy and compressive strength were correlated. However, he has found no information to support this over a wide range of rocks. Hughes (57) states that machine efficiency can be represented by the ratio of compressive strength to specific energy and by considering comparative efficiencies of tests in the laboratory and by a machine, an equation is derived:

$$\frac{C_o}{E_v} = 700 \frac{gD}{Gd} = \eta \times N_R$$

where, D/d is the ratio of the debris size for work in the laboratory (d) and that by a machine (D) equal to N_R, the rock number.

$\frac{g}{G}$ is the ratio of specific energy required for a given debris size in the laboratory with that required for the same debris size under operating conditions in the heading.

700 g/G is the efficiency for method of fracture equal to η .

Schmidt (42) at the U.S. Bureau of Mines made studies of percussive drilling in the field. The transfer ratio (Tr) was assumed to be 0.7 and the other unknown in Equation II, the specific energy (E_v), was calculated from

actual drill results to give apparent specific energy (E_{va}). So that,

$$E_{va} = \frac{12V \times f \times 0.7}{A_H \times P.R.} \quad \text{..... Equation III}$$

In making these calculations, the maximum penetration rate obtained at each level of operating air pressure was used. The apparent specific energy values (E_{va}) were plotted against the coefficient of rock strength (Fig.1.10) and a regression equation obtained. The procedure to predict the penetration rate is to determine the coefficient of rock strength and use the coefficient to determine the apparent specific energy of the rock. These values are then substituted for E_v in Equation II to predict the penetration rate. Predicted and actual penetration rates were correlated and the correlation coefficients ranged from 0.62 to 0.80 for both laboratory and field rocks. The higher correlation being with the field rocks from which the regression equation was obtained.

In Equations II and III, V x f is called the work rate W, ft.lb/min. and is usually obtained from the manufacturer or approximated by:-

$$W = (KE) \times (BPM)$$

where, KE = kinetic energy

BPM = blow per minute

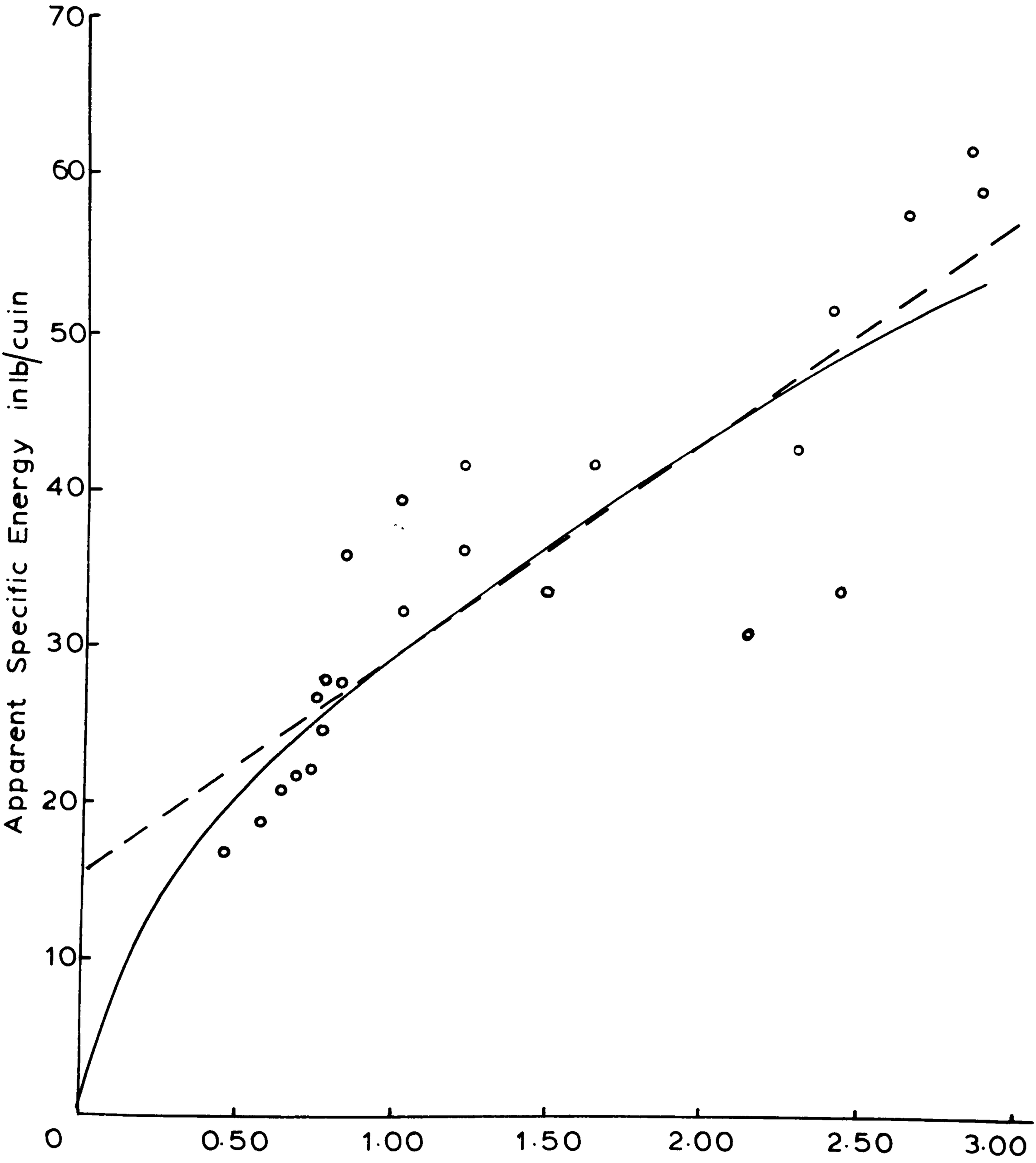

FIGURE 1.10: RELATIONSHIP AFTER SCHMIDT (42).

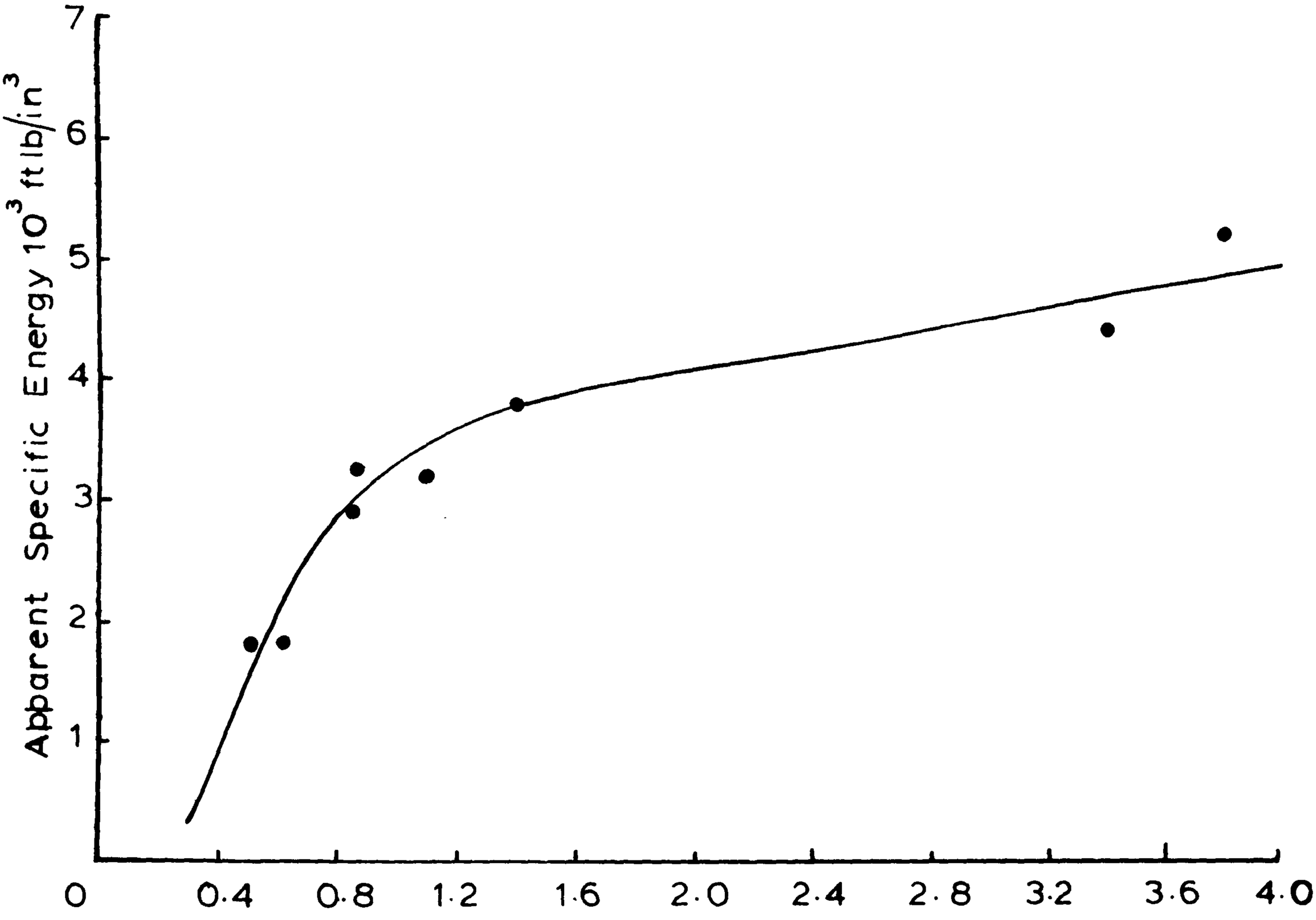

FIGURE 1.11: RELATIONSHIP AFTER UNGER AND FUMANTI(58).

Therefore for a constant hole size, work rate and transfer ratio, the regression equation is in fact the reciprocal of penetration rate, taken as the apparent specific energy, against coefficient of rock strength. This is then used to predict penetration rates.

Unger and Fumanti (58) investigated percussive drilling with independent rotation and assumed the transfer ratio (Tr) equal to 1 for eight rocks.

$$\text{Specific energy, } E_v = \frac{P \times Tr}{A_H \times P.R.} \quad \text{.....} \quad \overline{V}$$

P = power output of drilling system, ft.lbs/min = W

Data is presented as specific energy against coefficient of rock strength at 100 p.s.i. operating and rotational drilling pressures, making P constant. So that again:-

$$E_v = K \times \frac{1}{PR} \quad \text{.....} \quad \overline{VI}$$

where, K is a constant for one drilling condition. Calculating E_v for the 70 p.s.i. operating and 100 p.s.i. rotational drilling pressure gives a good general trend (fig. 1.11).

In conclusion, it is apparent that the difficulty in energy concepts is to measure the actual input power to the rock. Stress wave energetic studies have found the stress available at the bit in different forms of percussive drilling, but how and the amount that transfers to produce rock breakage is unknown. Assumptions of transfer ratios have to be made and the problem is further enhanced in rotary-percussive drilling, because of large losses in friction during rotation.

d. Regression Analysis

Selim and Bruce (59) describe the feasibility of

predicting percussive drilling rates by equations derived from statistical regression analysis. The least squares statistical method was used and the analysis performed both by direct and by stepwise linear regression analysis. The predicted penetration rate is a function of drill power and the physical properties of the nine rocks penetrated. The drill power was calculated by measuring the maximum piston velocity and the blow frequency from photographed oscilloscope traces, produced by a linear velocity transducer, consisting of a cylindrical permanent magnet moving with a coil. A number of equations were developed for prediction of the performance of two laboratory percussive drills (A and B). Their best prediction equation for drill A was:-

$$Y = 10.0+0.0001255x, - 353.0\left(\frac{1}{x_4}\right) - 64.76\left(\frac{1}{x_5}\right) + 72.0\left(\frac{10^6}{x_6}\right) + 11.90\left(\frac{10^6}{x_8}\right) + 11.23\left(\frac{1}{x_9}\right).$$

where, x, is the work rate for drill A in ft.lb/min, x_4 is Shore Hardness in scale units, x_5 is apparent density in gm/cm^3, x_8 is Shear Modulus in p.s.i., x_9 is coefficient of rock strength and Y is the predicted penetration rate.

Misra (34) decided to use the three most significant independent variables which showed the three best linear correlation coefficients with the laboratory rotary-percussive drill. The reason being that expressing penetration rates with a large number of variables (e.g. 10 rock properties some of which require a great deal of time and care to be found accurately) may not be of any practical use. The

regression equation with 28 rocks was:-

$$Y_p = 30.16 - 8.823x_6 - 0.01523x_1 - 0.00013x_2$$

(the multiple correlation coefficient = 0.8959)

where, x_6 is the apparent density in gm/cm^3, x_1 is the uniaxial compressive strength in MN/m^2, x_2 is the modulus of rupture (3-point circular) in MN/m^2 and Y_p is the penetration rate in mm/sec.

However, his best-fitted function for the prediction of penetration rate with the same data was:-

$$Y_p = 27.35 - 7.895\ (\ell n\ x_5) + 0.5857(\ell n\ x_5)^2$$

(correlation coefficient = -0.9555)

where, x_5 is the Rock Imput Hardness Number and Y_p is the penetration rate.

The predicted equations found by Misra and Selim and Bruce are only valid for the type and size of drills and bits, and the range of data used to form them.

1.4 Drill Cuttings

The examination of the debris produced from a rock breaking process gives a guide to the efficiency. In drilling the object is to remove the debris as quickly as possible so not to have reginding of particles. The maximum size of a particle able to be removed is determined by the design clearance for the exhausting system. The pressures involved in clearing the debris is another important factor. Breakage and ginding of debris more than necessary is wasting energy.

Patzold (60) carried out a screen analysis to compare

the cuttings from rotary-percussive drilling and percussive drilling. He noted that for rotary percussive drilling there was a wide distribution of large cuttings up to diameters of more than 5 mm, whereas with percussive drilling the largest diameter cuttings were 1 to 2 mm.

The percentage of fines of -0.75 mm was 38 to 61% for rotary-percussive and 81 to 90% for percussive, clearly better rock fragmentation takes place with rotary-percussive drilling using the same energy.

Analysis of debris has been carried out by screening methods because of the ease and simplicity. Barker (61) in his laboratory investigations of rock cutting using large picks examines rock debris by sieve analysis. Whereby, the cumulative percentages of material in the sieve size fractions is added and called the Coarseness Index. The higher the index the greater is the coarse debris.

Dubnie and Tervo (62) evaluated drill cuttings from a long-hole drilling project by sieve analysis. A large number of cuttings samples (114 samples) were collected and a simple comparison of the cumulative percentage retained on a 100 mesh screen was made. Depths of holes at different inclinations were plotted against the cumulative percentage cuttings on the 100 mesh. Reduction in size of cuttings with depth is apparent in all holes, regardless of inclination. In inclined vertical holes debris is coarser than those inclined down from the horizontal.

Unger and Fumanti (58) in their study of percussive drilling with independent rotation collected drill cuttings

with a vacuum system and sized them with a set of laboratory screens. Results from Mankato stone drilled at air motor operating pressures of 50 and 100 p.s.i. with other conditions kept constant, show that coarser cuttings are produced at the higher operating pressures. The same result was obtained for cuttings collected during the drilling of Rainbow granite, giving an indication of more efficient drilling.

Schmidt et al (63) compared mining coal seams by borer, ripper and conventional mining by drilling, under cutting and shooting with compressed air, with regard to size of product. Sizing was first carried out by sieve analysis after scalping, then sonic sifting and then by ultrasonic sizing to 10 microns. The conventional product had the least fines of the three production methods. The borer product had more fines than did the ripper product, but it also had a greater amount of large pieces. All three products, as samples, had essentially the same amount of minus 10 micron particles. Photomicrographs and surface-area measurements by gas absorption under 37 microns, were compared. Gas absorption essentially gave the same values and surface area calculations, assuming spherical particles and no porosity, gave a smaller area to the conventional product.

The examination and analysis of debris from drilling and indeed from other forms of rock breakage is extremely important.

1.5 Crater formations

The formation of craters in rocks by various methods

have been tried by a number of researchers to establish an index. Simon (8) studied the formation of craters produced by a drop tester to try to determine fundamental rock failure criteria in percussive drilling. He formulated the following equation:-

$$R = \frac{2.4\ (P - P_t)}{D^2\ S}$$

where, R is the penetration rate in in/min., P is mechanical power imput to the rock, in lb/min, P_t is the threshold power in lb/min, D is the hole diameter in inches, and S is drilling strength.

From the above equation S was determined and the reciprocal of this was proposed as the drillability index.

Hartman (6) extending Simon's work, conducted dynamic wedge indentation tests at varying energies and index distances, noting the difference in crater volumes. He proposed the following equation for predicting penetration rate:-

$$S = \frac{VBW}{A}$$

where, S is the penetration ratio, ft/min, V is single blow crater volume, ft^3, B is the blow frequency in cycles/min, W is number of bit wings, A is cross-section of the hole, ft^2.

Hartman (64) made further studies in relationships between crater volume and rock resistance using a laboratory drop tester. Pariseau and Fairhurst (65) studied force-penetration characteristics for wedge penetrations into rocks.

Morris (66) investigated the basic penetration mechanism of roller cone drilling and concluded that by indentation of a 1/8" radiused, hemispherical ended cone of tungsten carbide into rock, a drillability index P'/E would be established, (where P' = crater depths in inches, E = ram load in lbs). The values obtained from the laboratory were related to field drilling by the empirical formula:-

$$R = CN \frac{(P')}{E} \times \frac{W}{C}$$

where R is the penetration rate, C is a constant, N is revolution speed R.P.M., P' is crater depth in inches, E is threshold strength in lbs, W is effective drilling weight in lbs, C is total number of bit elements. Lightfoot (67) correlated Morris's index P'/E with penetration rate for a raise drill (fig.1.12) and states that the predicted penetration rates were less than 25 per cent of the actual field rates. However, fig. 1.12 shows that there is a large deviation for some rocks when considering the plot is log penetration rate.

With indentation and crater methods there is no allowance for variation in jointing, faulting or intrusions, therefore to be able to make predictions it is necessary to sample widely and make a large number of tests.

General Conclusion and directions for research

The literature review shows that the essential goal of understanding and quantifying drill performance is an

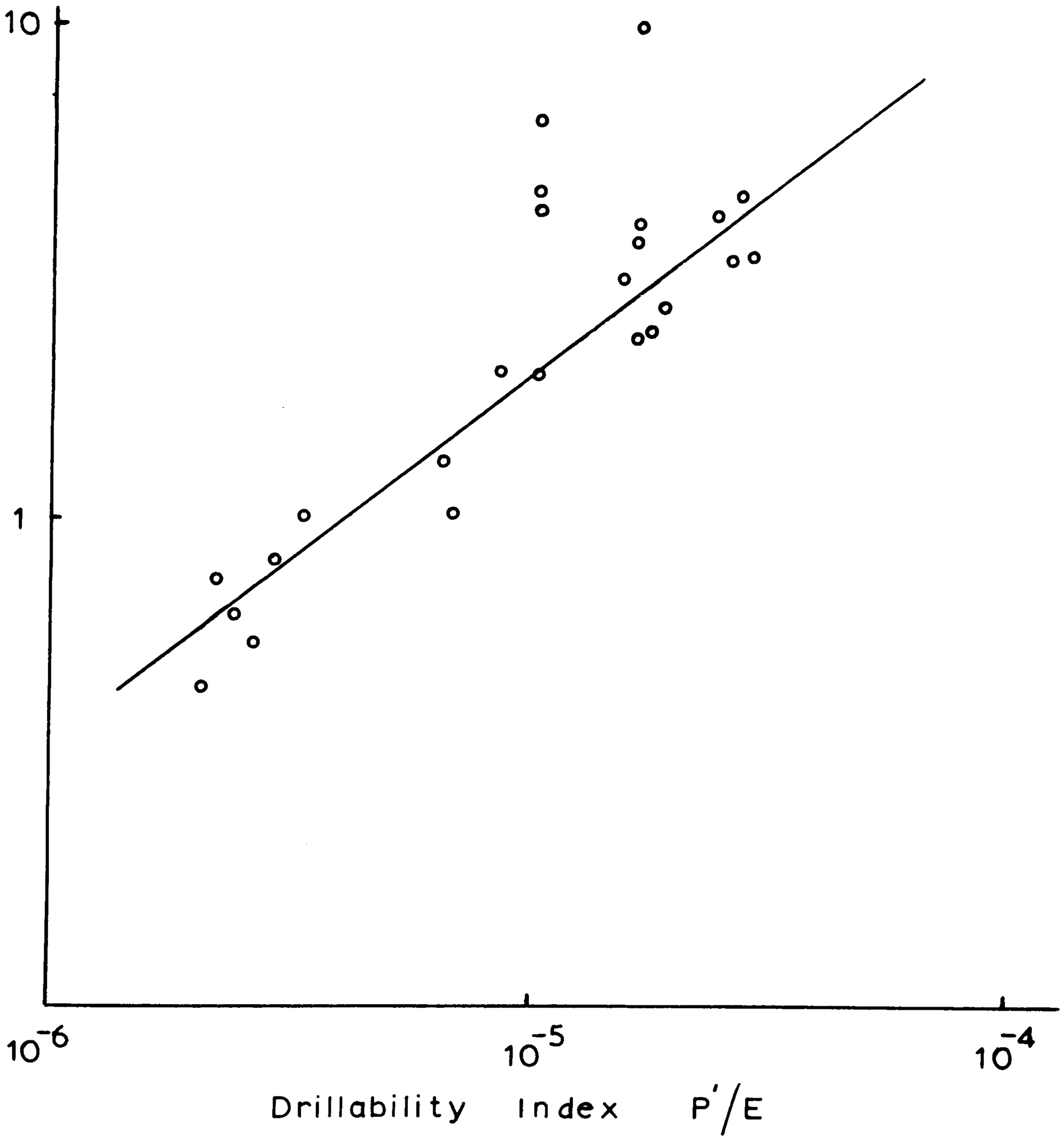

FIGURE 1.12: RELATIONSHIP AFTER LIGHTFOOT (67).

extremely difficult attainment. A great deal of interesting and varied work has been carried out by researchers from different angles in order to achieve this goal. The achievement of which is necessary because drilling plays an important part in the world's mining, oil and construction industries.

The directions for this research are considerations of laboratory rock breakage techniques developed from Protodyakonov, which show good correlations with percussive and rotary-percussive drilling. So that an accurate rock index could be established and at the same time compare the energy requirements to produce breakage. The compressive strength as an index is included as it is a standard rock test and is also related to drillability. Measurement of all the drilling parameters of a laboratory drill on the idea that the best method to understand drill performance in different rocks is to actually drill it. Analysis of data and drill cuttings from laboratory and field drilling to be an important part of the research project.

CHAPTER II

DEVELOPMENT OF EXPERIMENTAL AND ANALYTICAL TECHNIQUES IN ROCK BREAKAGE

CHAPTER II

DEVELOPMENT OF EXPERIMENTAL AND ANALYTICAL TECHNIQUES IN ROCK BREAKAGE

2.1 Introduction

This area of work overlaps with the theories and research in comminution. The study of comminution theory is over 100 years old. Numerous experiments have been performed, mathematical studies made and many papers written. On reading papers concerned with comminution, it becomes apparent that there are many conflicting views and theories. The reason for this is that there is no easy answer to the actual mechanism of rock breakage only theories. This doesn't mean that valid information cannot be gained by applying a particular theory to the type of breakage. Indeed systems have been analysed with success using one theory to solve a particular problem. Generally, people have used the theory that has best suited their needs and kept to it.

A brief description of the theories is given with a view that this project is concerned with using comminution theories for application from a rock mechanics point of view and not to be drawn too extensively into comminution research no matter how fascinating the subject.

2.2 The 'Laws' of Comminution

Early attempts at using models to predict energy consumption are well-known, namely the laws of crushing of Kick (68) and Rittinger (69). Both of these take the assumed relationships:-

Kick: energy proportional to volume crushed (i.e. strain energy requirement).

Rittinger: energy produced proportional to surface produced (i.e. cleavage energy requirements).

Bond's (70) Third Theory of Comminution attempts a compromise involving both strain energy and surface produced based on a linear regression analysis of experimental results and is essentially empirical. Hukki (71) has presented experimental evidence that no definite 'law' applies, but there is a gradual transition from one 'law' to another as comminution conditions change. Jowett (72) in his "introduction to the assessment of energy requirements and product size in comminution", states that all the differential equations can be criticized for implying a continuous process for what is in fact a series of catastrophic events; but the equations are intended to express trends in statistically based processes.

Walker et al (73) proposed the equation:-

$$\frac{dE}{dL} = - C.L^{p}$$

where, dE is the energy required to effect an infinitesimal change in particle size (dL) is a simple power function of size.

The constant, C, represents basic fracture properties of material subjected to comminution.

Substitution of appropriate values of p in this equation leads to mathematical forms of the 'laws' of crushing:-

(1) Kick's Law (p = -1)

$E = C. \ \ell n \ (L_1/L_2)$ and L_1/L_2 is the reduction ratio.

(2) Kittinger's Law (p = -2)

$E = C(\frac{1}{L_2} - \frac{1}{L_1})$, and 1/L is a measure of surface area.

(3) Bond's Law (p = -3/2)

$$E = 2C \ (\frac{1}{\sqrt{L_2}} - \frac{1}{\sqrt{L_1}})$$

$$= 2C \ \frac{1}{\sqrt{L_1}} \ (1 - \frac{1}{\sqrt{L_1/L_2}})$$ which combines reduction ratio and surface area functions.

A similar equation was devised by Holmes (74):-

$\frac{dN}{dE} = KNL^r$ where, N = number of particles

K, r are parameters.

Substituting in this equation, r = 0, r = 0.5 and 1 gives the same laws. Surface area S may also be substituted for N to give another form.

Another equation used by many is that developed by Charles (75):-

$$E = AK^{-m}$$

where, E is the energy required, A is the parameter representing mineral strength, K is size modulus, and m the distribution modulus of the Schuhmann (76) plot, figure 2.1 shows a Schuhmann plot. The Schuhmann equation is $Y = (\frac{x}{K})^m$

where, Y is the cumulative fraction passing size x.

The change in energy on size reduction (i.e. feed to product) is:-

$$\Delta E = A(\frac{1}{K_1^m} - \frac{1}{K_o^m})$$

and if m is unity, the equation has the same form as the

Rittinger equation, and if m is a half it has the form of the Bond equation.

Figure 2.1. Size distribution approximating to Schuhmann distributions.

(constant slope with energy input increasing)

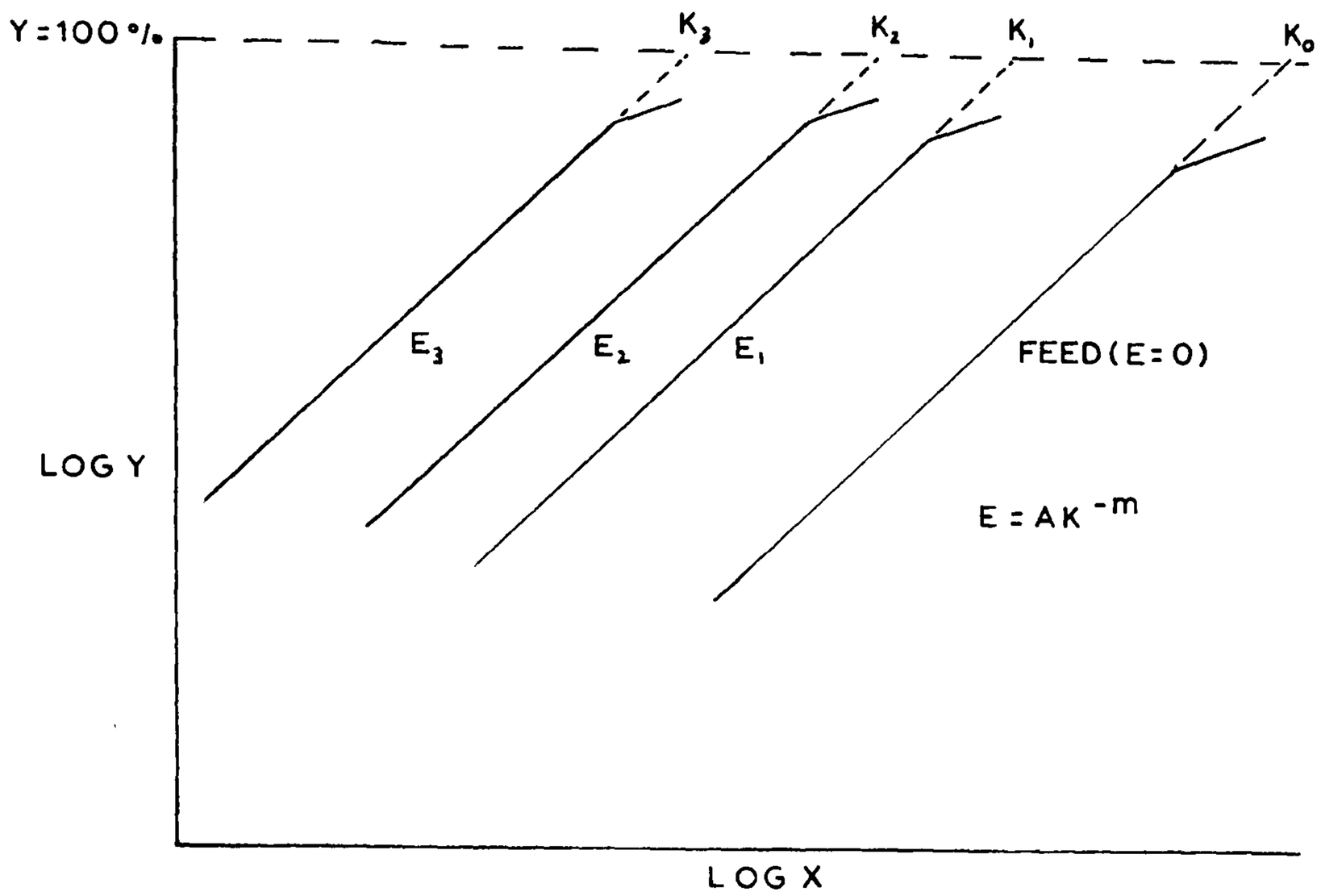

2.3 Use of the Schuhmann Method in Slow Compression

The application of the Schuhmann method was carried out on Galena and Fluorspar particles. The particles were evenly spread in a small hardened steel mortar and crushed by slow compression after Carey and Stairmand (77) in an Instron testing machine. The energy required to crush the particles, which had been graded to a size approximately 3/16", was measured. (Details of energy measurements, the small steel mortar, are given in Chapter III, Section C on slow compression, along with photographs). The reduction was by one half. The crushed particles were carefully removed

placed in a nest of sieves and sieved by hand for 3 minutes. The weights on each sieve were obtained. The larger particles were replaced in the mortar for re-crushing and the method repeated for a number of crushes. The results of crushing Galena and Fluorspar are given in tables 2 and 3 respectively. Hence for both Galena and Fluorspar, the Schuhmann plot can be made after calculating the cumulative percentage from tables 2 and 3. Figures 2.2 and 2.3 show the Schuhmann plots for Galena and Fluorspar respectively. Good results were obtained and straight lines were drawn for the different energy levels. K values (K is the size modulus) at Y = 100% can then be plotted against the energy levels as shown in figures 2.2 and 2.3. This gives the characteristic of energy consumed for that mineral. On the basis of this analysis the method was applied to a rock as opposed to a pure mineral. The rock examined was Elland Edge sandstone, the results are shown in table 4 and the Schuhmann plot in figure 2.4. From figure 2.4 it can be seen that a linear relationship does not hold, where does one take the K modulus to give a consistent interpretation? The possibilities are to take the K values at Y = 100% as normal or take the values of K at lower values of Y or to take tangents to the curves. The possibilities however, would over emphasize the coarse product as opposed to the fines and vice-versa depending on where the K values or tangents were taken on the curves. With respect to this difficulty encountered in finding K values, it was necessary to develop a more consistent way of analysing the result.

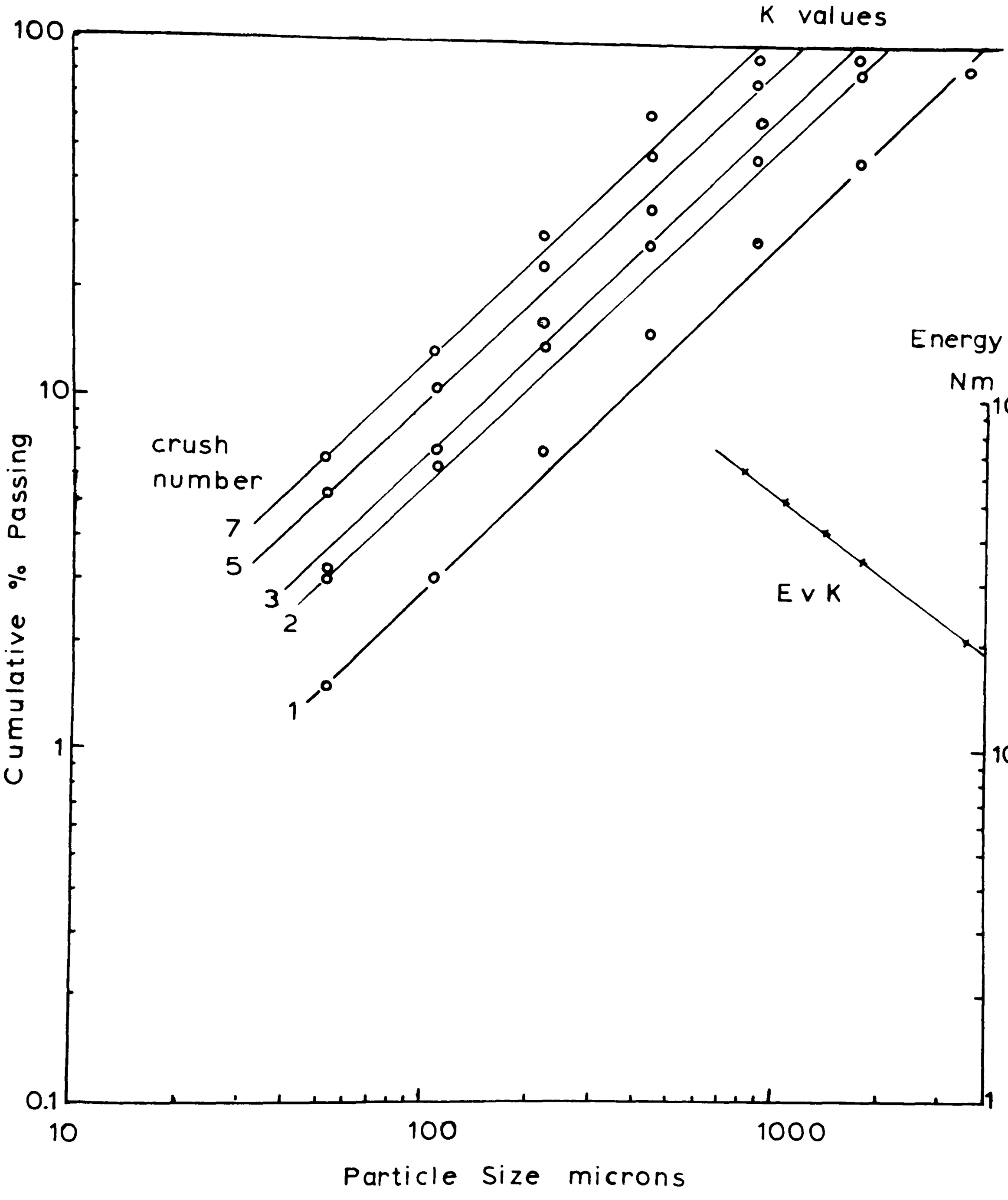

FIGURE 2.2: SCHUHMANN PLOT, SLOW COMPRESSION OF GALENA.

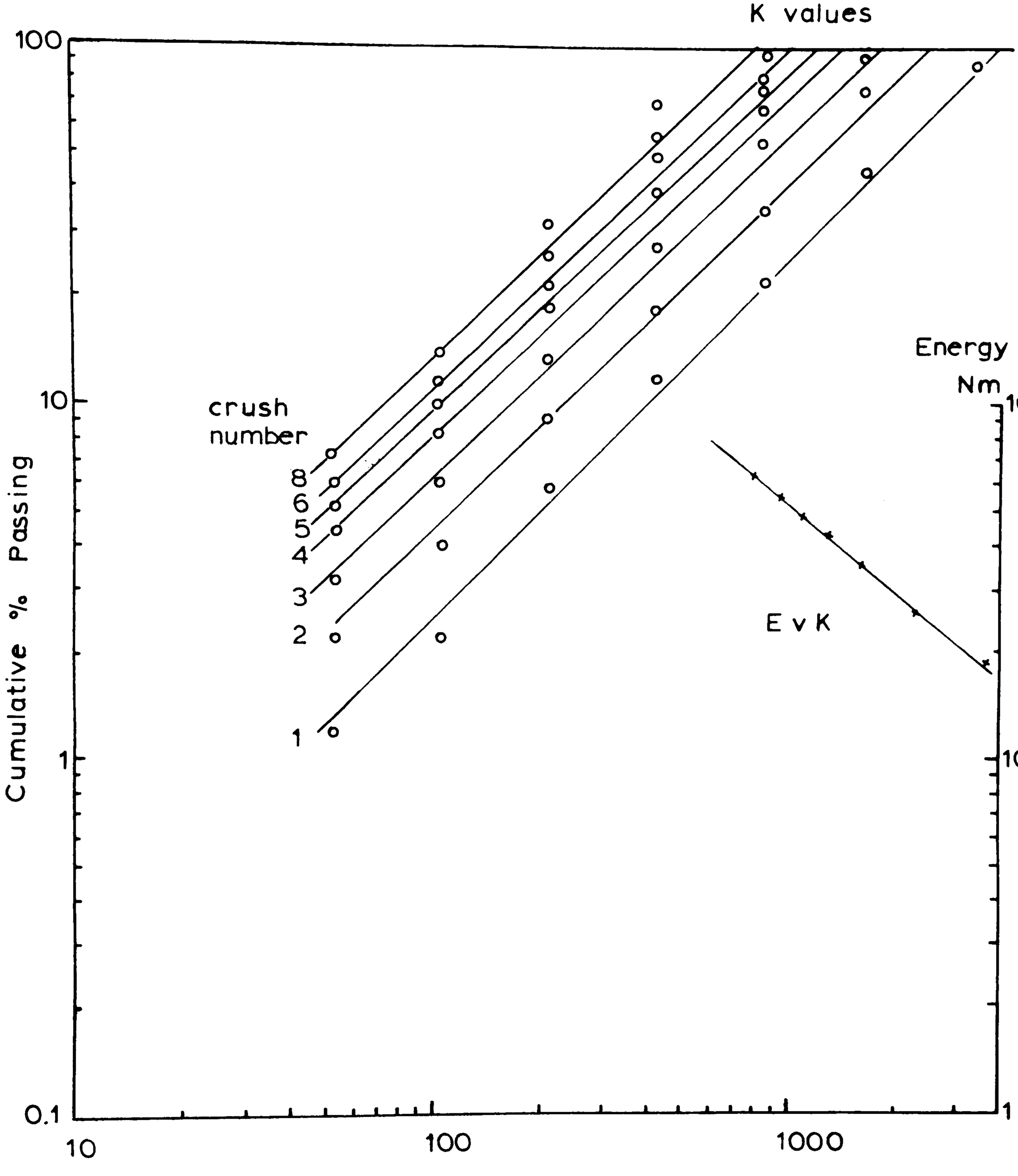

FIGURE 2.3: SCHUHMANN PLOT, SLOW COMPRESSION OF FLUORSPAR.

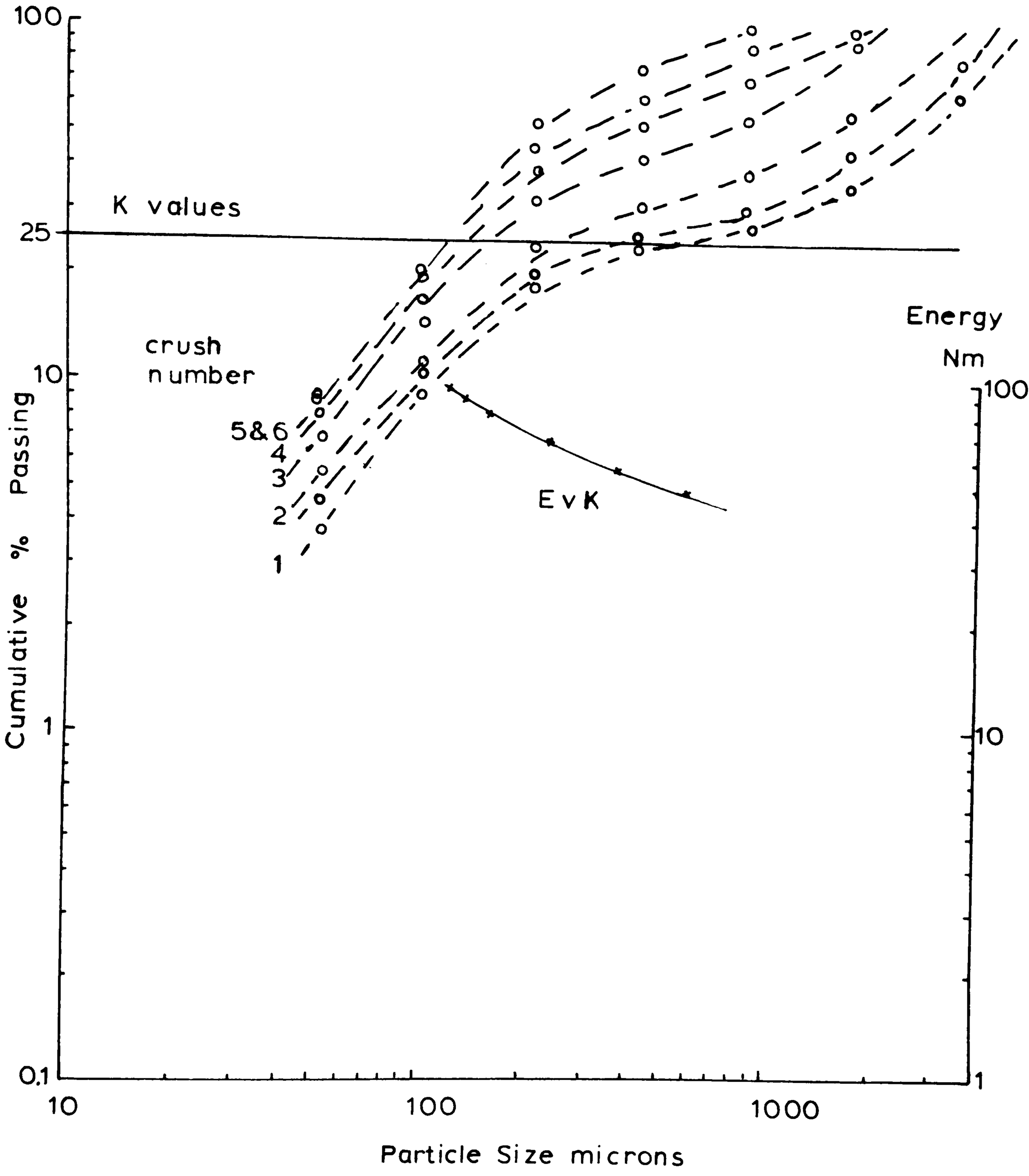

FIGURE 2.4: SCHUHMANN PLOT, SLOW COMPRESSION OF ELLAND EDGE SST.

TABLE 2

Galena crushed by slow compression

Number of Crushes	Energy Input Joules	SIEVE MESH NUMBERS 5	10	18	36	72	150	300	BASE	TOTAL WT. in gms.
		FRACTIONS IN GRAMS								
1	21.528	13.260	39.138	19.592	12.670	8.116	3.958	1.564	1.533	99.831
2	34.488	0.130	15.334	35.783	20.783	13.620	7.564	3.265	3.076	99.328
3	40.824	0	5.834	31.149	27.269	17.597	9.498	3.889	3.168	98.407
4	45.324	0	0.968	26.348	31.634	20.490	10.626	4.624	4.677	99.369
5	53.352	0	0.327	21.110	30.157	24.861	12.254	5.950	5.386	99.390
6	58.032	0	0.045	13.847	28.730	30.483	13.979	6.172	5.970	99.225
7	63.000	0	0	8.690	26.729	34.893	15.500	6.795	6.567	99.174
8	67.536	0	0	4.346	24.193	39.052	16.975	7.443	7.101	99.109

TABLE 3

Fluorspar crushed by slow compression

Number of Crushes	Energy Input Joules	SIEVE MESH NUMBERS 5	10	18	36	72	150	300	BASE	TOTAL WT. in gms.
		FRACTIONS IN GRAMS								
1	18.648	6.071	21.777	11.242	5.046	2.965	1.779	0.472	0.649	50.001
2	25.420	0.687	11.733	20.163	8.387	4.540	2.757	0.953	1.065	50.103
3	35.928	0	3.965	19.053	13.265	6.837	3.703	1.421	1.636	49.880
4	43.742	0	1.729	14.838	13.571	10.361	5.235	1.880	2.214	49.828
5	48.312	0	0.631	11.774	12.495	13.438	6.402	2.361	2.607	49.708
6	54.720	0	0.167	8.970	12.162	15.434	7.258	2.697	2.951	49.639
7	59.184	0	0.022	5.692	12.505	17.152	7.965	2.970	3.244	49.550
8	62.604	0	0	3.148	11.691	18.911	8.724	3.332	3.631	49.437

TABLE 4

Elland Edge crushed by slow compression

Number of Crushes	Energy Input Joules	SIEVE MESH NUMBERS FRACTIONS IN GRAMS 5	10	18	36	72	150	300	BASE	TOTAL WT. in gms.
1	48.004	14.830	12.035	3.391	1.619	1.652	3.399	1.193	1.467	39.931
2	68.180	0.856	16.125	7.561	2.848	2.659	5.279	2.026	2.165	39.518
3	79.952	0	4.476	13.496	4.840	3.886	7.237	2.825	2.713	39.473
4	87.440	0	1.095	10.153	7.304	5.175	9.066	3.490	3.085	39.369
5	93.587	0	0.013	4.827	10.045	6.492	10.538	3.935	3.466	39.302

2.4 Further Analysis

Carey and Stairmand (78) discussed the successive crushing of a single, brittle homogeneous particle and state that this could be plotted in the Schuhmann way. The linear slope of the plot would be about 45^{o} and such gradings would be known as "naturals". Curves were presented showing "naturals" for freely crushed limestone and these constant curves instead of straight lines were ascribed to sieving difficulties. However, the curves were almost linear and were treated as "naturals". A jaw-crusher product was obtained and sized. The amounts from each free crushing

were then expressed as a percentage of the jaw-crusher product. Hence, this is a method that could be used for grading as "naturals" with minerals that do give a slope of approximately 45^{o}, but clearly Elland Edge Sandstone is not a "natural". Further work has shown that rocks generally are far from "naturals" when analysed in this manner.

Another method tried was to consider that to produce a particular size fraction, so much energy of the total energy supplied to produce a distribution is constantly attributed to that fraction. This idea can then be expressed as an 8 x 8 simultaneous equation for 8 crushes of the mineral or rock:-

$$E_1 = e_1x_{11} + e_2x_{21} + e_3x_{31} + \ldots\ldots\ldots + e_8x_{81}$$

$$E_2 = e_1x_{12} + e_2x_{22} + e_3x_{32} + \ldots\ldots\ldots + e_8x_{82}$$

$$\vdots$$

$$E_8 = e_1x_{18} + e_2x_{28} + e_3x_{38} + \ldots\ldots\ldots + e_8x_{88}$$

where, E_n is the total energy input for that crush, e_{1-8} is the energy fraction for that size and x_{nn} is the weight of material on the sieve.

This information was fed into a Wang desk top computer using the Wang library program. This printed out the values of e_1, e_2 ..... e_8, galena is a typical result:-

$e_1 = -0.1491$, $e_2 = 1.124$, $e_3 = 4.627$, $e_4 = -4.318$,

$e_5 = 0.799$, $e_6 = -3.931$, $e_7 = 7.594$, $e_8 = -2.854$.

Obviously, this analysis is wrong because negative energies were obtained for a particular fraction and from the initial statement this cannot be true.

At this stage the energy proportional to the area of new surfaces created (according to Rittinger) was considered. This approach seemed a logical step from the 'K-size modulus' analysis, whereby a linear relationship could be obtained between energy and 'K', but the problem of obtaining a consistent value of K in all cases is difficult as described. Protodyakonov also states that by measuring fines below 500 microns in a volumemeter after breakage gives a fixed measure of surface area created.

2.5 Analysis of surface-area

The surface area can be derived in simple terms by:-

the area of new surfaces created is "so many" m^2 per gram.

So that the number of particles in a fraction of W grams

$$= \frac{W}{s, d^3} \times \frac{1}{\text{density}} \quad \ldots\ldots\ldots \text{ a number}$$

$$\therefore \quad \text{the surface area} = \frac{W}{s, d^3} \times \frac{1}{\text{density}} \times s_2 \, d^2 \ldots\ldots m^2$$

where, d is the dimension,

s, and s_2 are shape factors.

- so that the surface area created is proportional to:-

$$\frac{W}{d} \times \frac{1}{\text{density}} \quad \text{- for one fraction}$$

$$\text{total area for a nest of sieves} \propto \sum \frac{W}{d} \times \frac{1}{\text{density}} \ldots\ldots m^2$$

$$\text{and total area/gram} = \frac{C,}{\text{density}} \times \frac{\sum W/d}{\sum W} \ldots\ldots m^2/gm.$$

hence, specific energy $E/\sum W$

$$= \quad C \times \frac{\sum W/d}{\sum W}$$

For the three sets of results (i.e. Galena, Fluorspar and Elland Edge) the surface areas can be calculated for the different energy inputs. At this stage, the values of C, and C are omitted for simplicity, so that surface areas were just calculated as $\frac{\sum W/d}{\sum W}$. The weight on each sieve fraction is W gms and d is taken as the arithmetic mean size for that fraction. The ends of the range are completed by using an imaginary sieve size of 6706 microns at the coarse end and 26.5 microns at the finer end.

Mesh no.....	-	5	10	18	36	72	150	300	BASE
Size in microns	6706	3353	1676	863	422	211	104	53	26.5
'd' values in microns ..	-	5030	2515	1295	638	317	158	78.5	39.75

Table 5 shows the values of energy/gram and areas/gram for Galena, fluorspar and Elland Edge. On plotting energy/gm againg area/gm (fig.2.5) extremely good linear relationships were obtained. This indicates that breaking rocks starting from the same size, would give an index and it would be possible to compare the energy required to break a particular rock. Examination of energy requirements and correlation with surface area measurements by sieve analysis was now tried for the drop hammer test.

TABLE 5

Calculated Energy/gram and Area/gram for crushing of Galena, Fluorspar and Elland Edge by slow compression

Galena

Number of Crushes	1	2	3	4	5	6	7	8
Energy/gram $\frac{Nm}{gram}$	0.216	0.347	0.415	0.456	0.537	0.585	0.635	0.681
Area/gram $\frac{\sum W/d}{\sum W}$	1.631	2.788	3.199	3.820	4.260	4.735	5.134	5.509

Fluorspar

Number of Crushes	1	2	3	4	5	6	7	8
Energy/gram $\frac{Nm}{gram}$	0.373	0.507	0.720	0.878	0.972	1.102	1.194	1.266
Area/gram $\frac{\sum W/d}{\sum W}$	1.393	2.065	2.842	3.598	4.182	4.626	5.012	5.457

Elland Edge

Number of Crushes	1	2	3	4	5
Energy/gram $\frac{Nm}{gram}$	1.202	1.730	2.025	2.222	2.381
Area/gram $\frac{\sum W/d}{\sum W}$	2.302	3.526	4.628	5.490	5.700

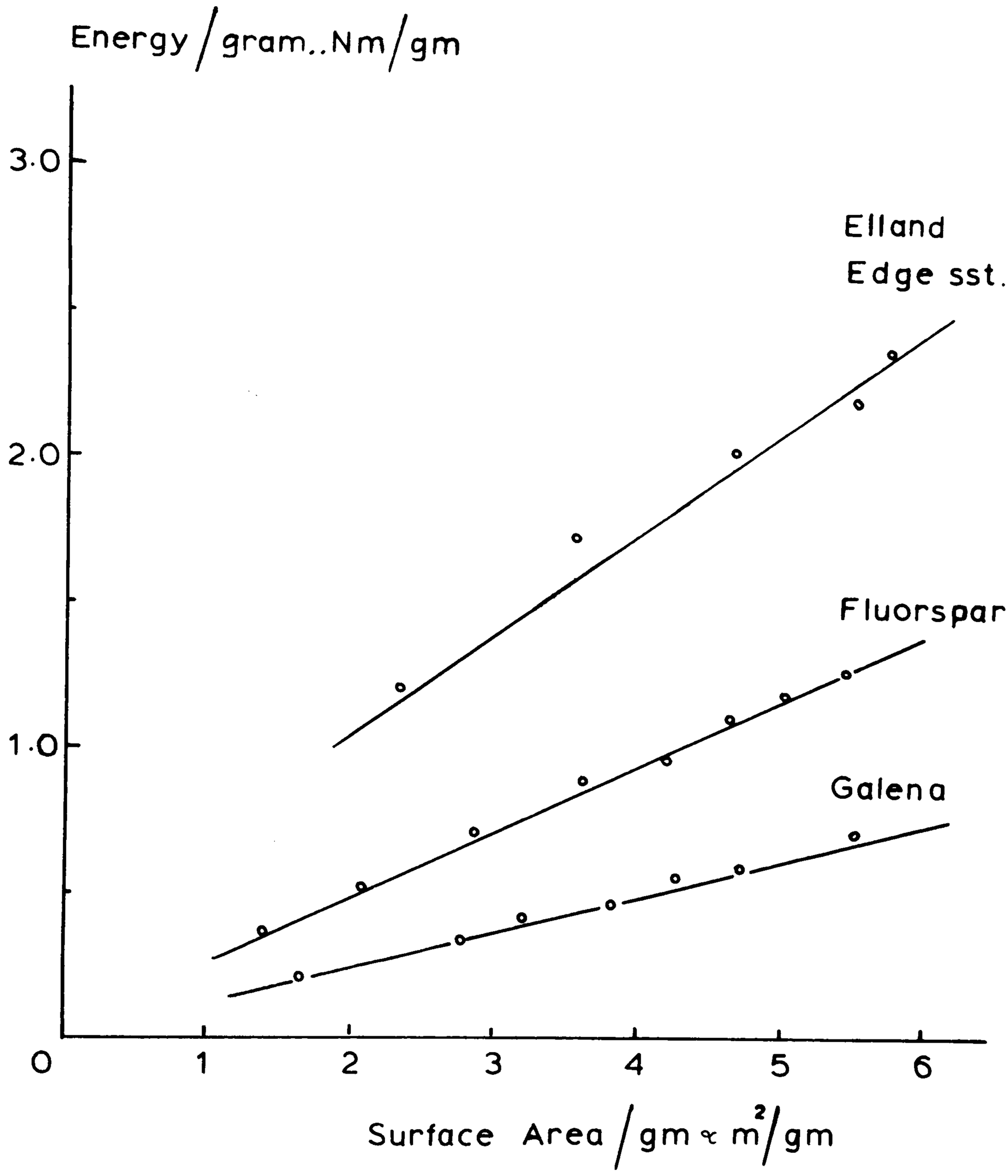

FIGURE 2.5: ENERGY/GRAM AGAINST SURFACE AREA/GRAM FOR SLOW COMPRESSION OF GALENA, FLUORSPAR & ELLAND EDGE SST.

2.6 Drop Hammer Test

Again Elland Edge Sandstone was used, but this time 50mm long and 25mm diameter specimens were used. One specimen was placed horizontally in the Syskov mortar as done in the rock impact hardness number test. The 2.4 kg. weight was dropped from a fixed height on to the rock for a number of blows, then the product was removed and sieved by hand for 3 minutes in the nest of sieves. Further specimens were individually broken in the mortar at different numbers of blows. The specific energy $(\frac{E}{\sum W})$, proportional to the number of blows, and surface area created/gram $(\frac{\sum W/d}{\sum W})$ are calculated and the results shown in table 6 were plotted in figure 2.6. An excellent linear relationship was obtained between the specific energy and the surface area. The Schuhmann plot was drawn (fig. 2.7) which still shows the difficulty of extracting K values.

In the testing of Elland Edge further results were obtained by using 1.2 kg and 3.6 kg weights dropped from the same height for 8 blows and then for 25 blows each. These fitted perfectly on to the graph (fig.2.6) and this indicated that varying the energy input as well as the blows for a particular method, a fixed relationship is still obtained between the energy/gram and surface area for the rock. Further work was carried out with regard to this point and the findings are detailed in Chapter III, Section A on drop hammer tests.

Correlation coefficients for the linear regressions:-

Slow compression:	Galena	0.99816
	Fluorspar.....	0.99866
	Elland Edge ...	0.99228
Drop Hammer:	Elland Edge ...	0.99517

In view of the high correlation coefficients obtained, the expression for surface area was redefined starting from basic principles, in order to give a more realistic value to include C, and density for the equation of area/gram derived on page 43.

TABLE 6

Elland Edge broken by drop hammer

Number of blows	Energy/gram Nm/gram	Area/gram α $\Sigma W/d/\Sigma W$
2.4kg.wt.		
5	1.089	0.942
8	1.922	1.341
10	2.258	1.364
15	3.388	2.106
20	4.774	2.882
25	6.123	4.110
35	8.477	5.512
1.2kg.wt.		
8	0.999	0.481
25	3.007	2.120
3.6 kg.wt		
8	2.981	1.918
25	9.273	5.709

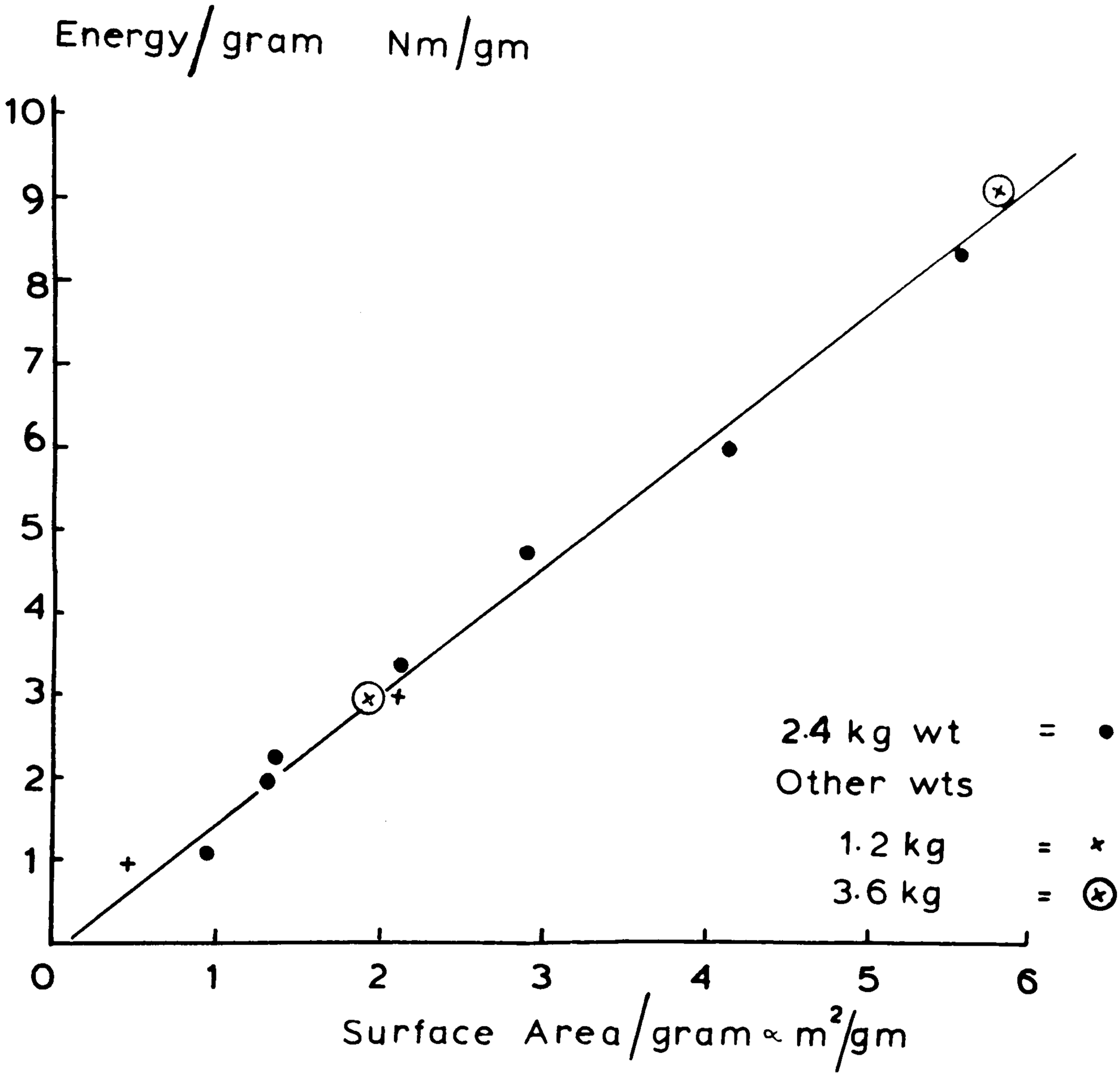

FIGURE 2.6: ENERGY GRAM AGAINST SURFACE AREA GRAM FOR DROP HAMMER BREAKAGE OF ELLAND EDGE SANDSTONE.

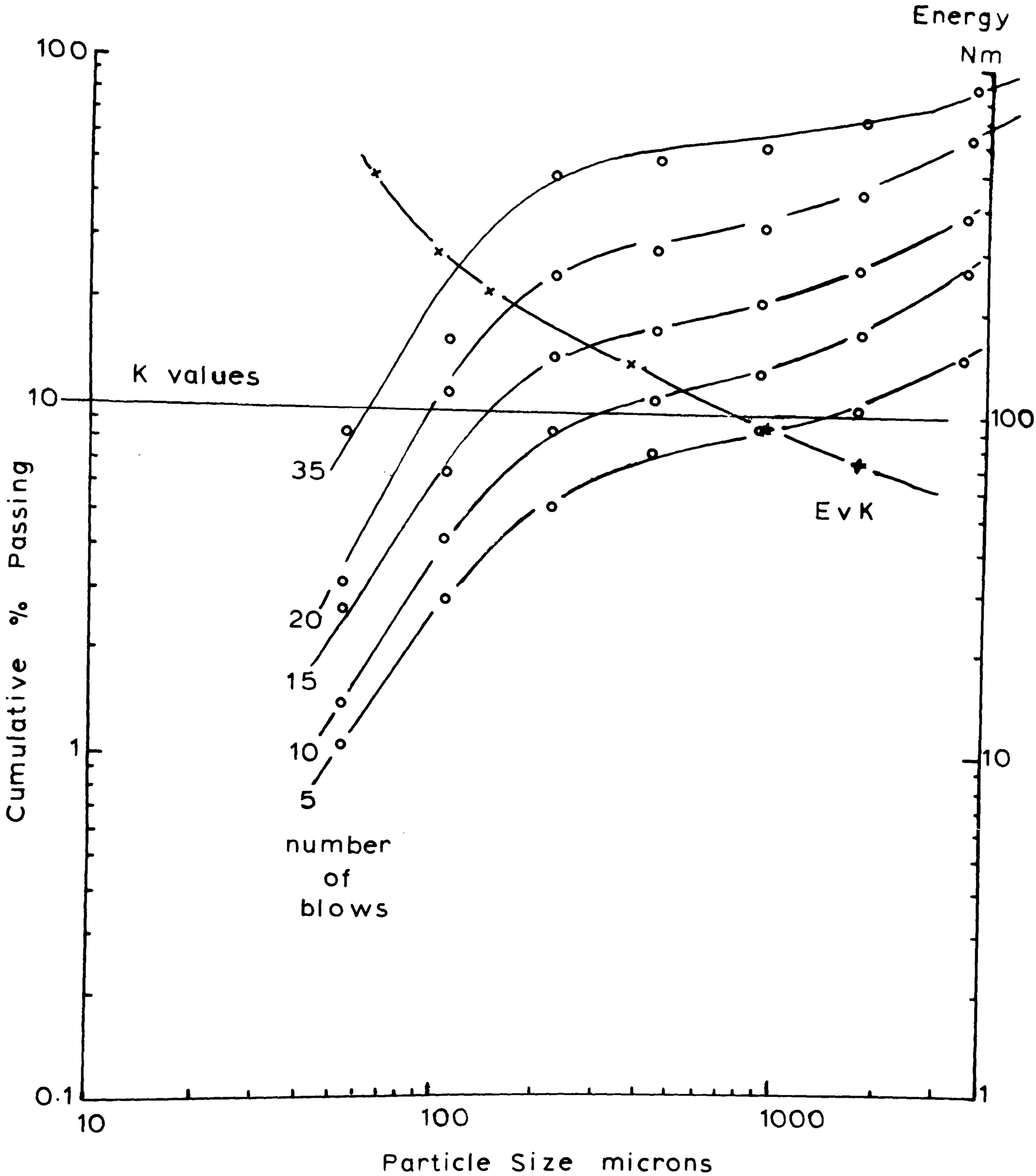

FIGURE 2.7: SCHUHMANN PLOT, DROP HAMMER BREAKAGE OF ELLAND EDGE SST.

2.7 Complete Derivation of Surface Area from Basic Principles.

Considering a graph of cumulative weight against size, and a small element of this graph of weight interval dw, size interval da. Over a small range, the graph can be considered as a straight line:-

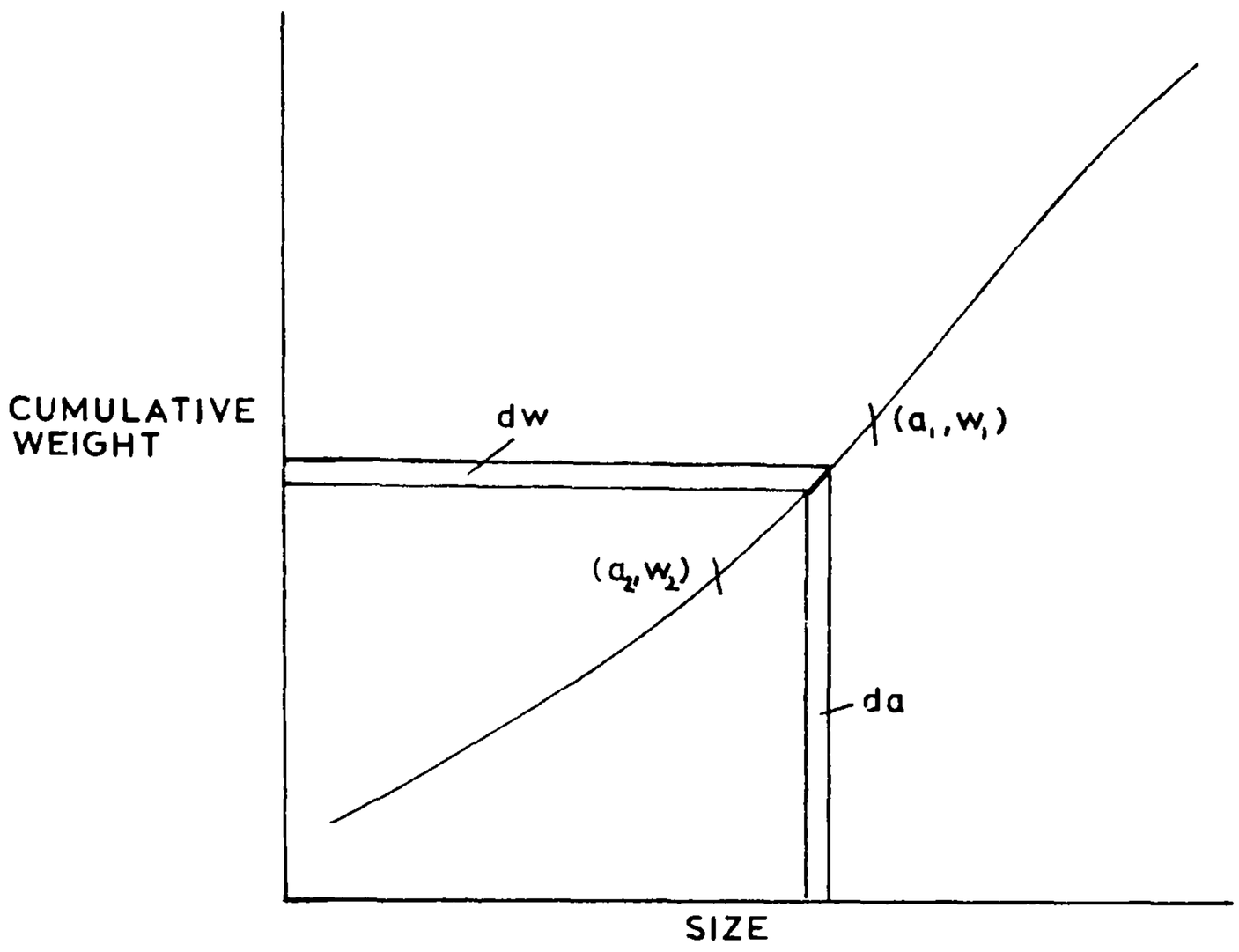

The size range considered as a straight line is from $a_1 w_1$ to $a_2 w_2$. In general a_1, a_2 are two consecutive sieve size apertures and $w_1 - w_2$ is the weight of material retained on the a_2 size sieve. If no particles of size a_1, a_2 were in the initial size distribution, all the area of the particles in the a_1 to a_2 range is newly created surface area.

If the specific gravity of the fraction dw is s, then the volume is dw/s, at a size a.

If there are n such particles in fraction dw, then the volume will be nVp, where Vp is a single particle volume.

Then, $\frac{dw}{s} = nVp$ $\qquad$ $n = \frac{dw}{s}.\frac{1}{Vp}$

The area of n particles is nAp, where Ap is a single particle area.

So that the area of fraction dw, dA is given by:-

$$dA = nAp = \frac{dw}{s}.\left(\frac{Ap}{Vp}\right)$$

or as previously stated on page 43.

$$dA = \frac{W}{\text{density}} \times \frac{1}{d}$$

For <u>spheres</u> of diameter a and radius r,

$$\frac{Ap}{Vp} = \frac{4\pi r^2}{\frac{4}{3}\pi r^3} = \frac{3}{r} = \frac{6}{a}$$

For <u>cubes</u> of side a,

$$\frac{Ap}{Vp} = \frac{6a^2}{a^3} = \frac{6}{a}$$

So that $\frac{Ap}{Vp}$ can be taken as $\frac{6}{a}$ for all shapes which are regular.

Then, $dA = \frac{dw}{s} \times \frac{6}{a}$

for a straight line interval

$$\frac{dw}{da} = \frac{w_1 - w_2}{a_1 - a_2}$$

and $dA = \frac{6}{s}.\frac{da}{a}.\left(\frac{w_1-w_2}{a_1-a_2}\right)$

For the interval being considered $\frac{w_1-w_2}{a_1-a_2}$ is a constant, but will be different for different intervals.

Then,

$$\int dA = \frac{6}{s}.\left(\frac{w_1-w_2}{a_1-a_2}\right) \int \frac{da}{a}$$

$$A = \frac{6}{s} \times \frac{(w_1-w_2)}{(a_1-a_2)} \times \ell na$$

putting in limits,

$$A_1 - A_2 = \frac{6}{s} \cdot \left(\frac{w_1 - w_2}{a_1 - a_2}\right) \ell n \left(\frac{a_1}{a_2}\right)$$

For a size range a_1 and a_2 can be substituted, except at the ends of the scale, but a fictitious size of 2 x maximum size and ½ x smallest size in a 2 to 1 scale for example, can be used to complete the range.

The total area is then found by the sum of all the terms:-

$$\frac{6}{s} \ell n \frac{a_1}{a_2} \cdot \left(\frac{\text{wt.of fraction}}{a_1 - a_2}\right)$$

The series is "non-converging", and that if very small sieves were available, the area values would be larger.

2.8 Choice of Sieves

On closely examining the Schuhmann plots for Galena and Fluorspar, figures 2.2 and 2.3 respectively, the sieve sizes of 422 microns and 211 microns are slightly off the lines for all the different crushes. However, this had little effect on the energy/gram versus area/gram graph, figure 2.5, through the high correlation coefficients being obtained. Even so this does suggest that the sieves may be slightly in error and as a lot of research was to be carried out in the three years, new sieves were purchased. Whereas the first sieves were chosen on availability just to give a range, the choice of size of the new sieves was made after the following considerations:-

Protodyakonov chose a 500 micron sieve for his work and similarly this is used in coefficient of rock strength and rock impact hardness number tests. This sieve size is approximately in the middle of a general sieve size range, so the choice of sieves would include 500 microns and sieves on either side to give a reasonable range.

A 2 to 1 scale of sieves would make $\ell n \frac{a_1}{a_2}$ equal to $\ell n 2$ and the ends of the scale would be simple to complete, so making the areas easier to calculate, The 2 to 1 range chosen starting around 500 microns was:-

4mm, 2mm, 1mm,/500 microns/, 250 microns, 125 microns, 63 microns, BASE.

This choice fits the standard U.S. mm sizes, Tyler mesh designation - 5, 9, 16, 32, 60, 115, 250, the standard

Canadian sizes and the British Standard sieve series nominal mesh numbers - 4, 8, 16, 30, 60, 120, 240,

so that the surface area equation becomes:-

$$\text{Surface Area} = \frac{6}{s} \ell n\ 2\ \frac{w_1 - w_2}{a_1 - a_2} \quad \text{where, } a_1 = 2a_2$$

Considering one fraction of material, $w_1 - w_2$, s are constants and $K = \frac{\text{wt of fraction}}{\text{density}}$,

$$\text{Surface Area} = K.6\ \ell n 2 x \frac{1}{a_2}$$

$$= \left(\frac{K}{a_2}\right) \times \frac{4.16}{}$$

Comparing this with the Geometric mean size and arithmetic mean size methods of obtaining surface area:-

$$\text{Gm, Geometric mean} = \frac{6}{s}\ \frac{w}{\sqrt{a_1 a_2}} = \frac{6}{s}\ \frac{w}{\sqrt{2a_2^2}}$$

$$= \frac{6}{s}\ \frac{w}{a_2}\ .\ \frac{1}{\sqrt{2}}$$

$$= \left(\frac{K}{a_2}\right) \times \frac{4.28}{}$$

$$\text{Am, Arithmetic mean} = \frac{6}{s}\ \frac{w}{\frac{a_1 + a_2}{2}} = \frac{6}{s}.\ \frac{w}{3a_2}\ .\frac{2}{}$$

$$= \left(\frac{K}{a_2}\right) \times \frac{4.0}{}$$

It is interesting to note that the method derived from basic principles when compared to the geometric mean and arithmetic mean values for this system, gives surface area values which fall almost exactly in the middle of values which would be obtained from using the Gm or Am. Also knowing one value, the other two values can be computed by using the above constants if so desired. This would be

applicable to all the fractions obtained.

In sieve analysis there is no specific reason for using either Gm or Am when applied to surface area. In this light it appeared a better idea to derive an expression from basic principles when there is no yardstick to go by, and then make the above comparison. The derived expression does not give a larger or smaller value and can be directly compared with Gm and Am as shown.

From this point all areas/gram were calculated by using the derived expression and a Wang computer programme was written. The input to the Wang was the fractional weights and density and the output was area/gram and total weight.

2.9 Sieving Techniques

A number of tests were carried out on material produced by drop hammer in order to find a consistent method of sieving and to note the effect on energy-area relationships.

The work that was carried out on Galena, Fluorspar and Elland Edge by hand sieving gave excellent results. However, to gain consistent, reproducable results, a machine method of sieving should be used.

Comparison of an Endecott sieving machine and a Rotap sieving machine was made using the drop hammer product of Groby Granite broken at different energy levels. The Endecott machine sieves by the action of vibrating the particles and the Rotap by a rotating action with tapping

to assist the sieving.

The results of energy/gram were plotted against area/gram, shown in fig.2.8, for the same sieving time of ten minutes. The graph shows that the Rotap is more efficient than the Endecott machine and the efficiency of the Endecott decreases as the product becomes finer in size.

Linear regression on the two methods:-

	ENDECOTT	ROTAP
Slope,energy/area	2600.76	2205.14
Intercept	-1.784	-2.055
Correlation Coefficient..	0.9914	0.9988
Standard error of Deviation	1.287	0.4414

The linear regression results give the Rotap a higher correlation and a smaller standard deviation. Though correlation coefficients are both very high, the Rotap technique was chosen to be used because of the reducing of efficiency by sieving with the Endecott machine as the product becomes finer. Also the energy/area slopes for the Rotap are substantially smaller, which shows that the area/gram is larger for the energy input. Therefore, a more "true" measure of the surface area is obtained by using the Rotap.

Further tests were carried out on three different rocks broken by drop hammer and sieved on the Rotap. This time the minus 63 microns product was further sieved on precision micro-plate sieves of 30 and 15 microns. Normally, dry sieving methods are not carried out below 37 microns. However, the idea was to see the effect of extending the

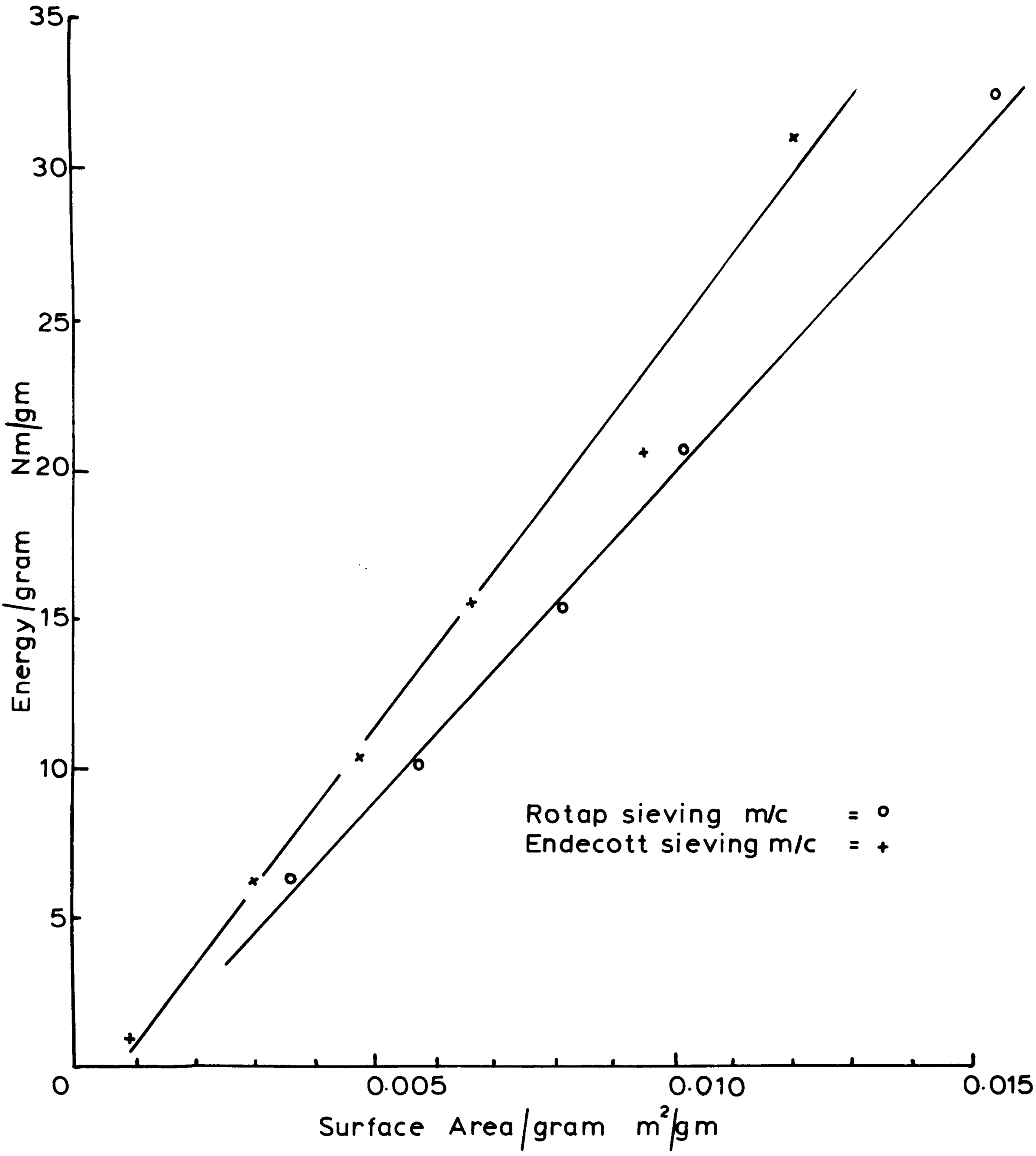

FIGURE 2.8: COMPARISON OF ROTAP AND ENDECOTT SIEVING USING GROBY GRANITE.

size range even though sieving is not recommended. If a large difference was obtained in the areas/gram between seven sieves and nine sieves, the extended range would then be included to give a more accurate measure of area. The three rocks used were: St. Bee's sandstone, Cornish granite and Giggleswick limestone. The energies per gram and areas per gram were calculated and computed. Figure 2.9 shows a typical plot of energy/gram versus area/gram for Giggleswick limestone. Linear regression analysis was carried out on the six lines, i.e. three rocks with two graphs, one for seven sieves and base and one for nine sieves and base.

Summary of linear regression for the three rocks:-

	St. Bee's		Cornish		Giggleswick	
	7sieves	9 sieves	7 sieves	9 sieves	7 sieves	9 sieves
Slope, energy/... area	423.22	378.96	1094.10	967.97	1042.78	1035.96
Correlation coefficient	0.9964	0.9958	0.9980	0.9969	0.9985	0.9977

All the correlation coefficients are still high, but the differences in slopes are not as high as those obtained for the Groby Granite on the Endecott and Rotap test. A more "true" figure is obtained with the 9 sieves, but the effort involved, and the time and care necessary to do the extra sizing does not give the large difference which would warrant the effort.

In conclusion, seven sieves with a base sieved on

the Rotap sieving machine is definitely adequate for comparing laboratory rock breakage techniques and the establishment of an accurate index.

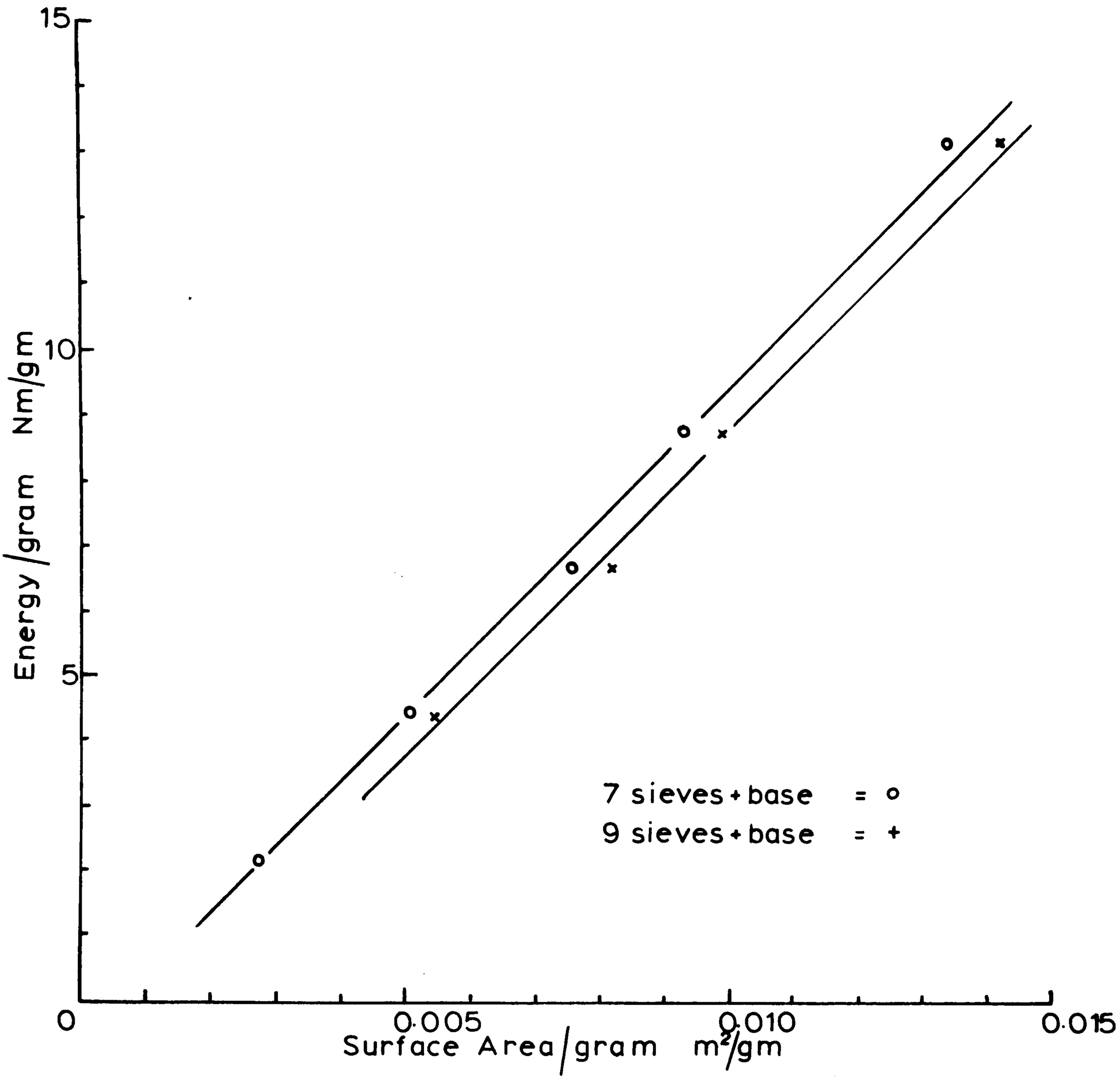

FIGURE 2.9 : COMPARISON OF 7 AND 9 SIEVES USING GIGGLESWICK LST.

2.10 Laboratory Drill Cuttings

The quantifying of the drill cuttings produced using a laboratory drilling rig, described in Chapter IV and shown in photograph 4, was to be an important part of this research programme. A simple and accurate method of measuring the area of the drill cuttings was needed. This section describes the work that was done to find a suitable means of measuring the drill cuttings.

Fourteen rocks covering a wide range of strength, hardness and different rock types, were drilled in the laboratory. The rocks were drilled with the same thrust, speed, percussion and depth of penetration. The cuttings produced by drilling five holes per rock were carefully collected.

A size analysis was carried out on the 7 sieves for each rock, hence the surface - areas could be computed. From the size analysis it could be seen that with all the rocks drilled the bulk of cuttings were less than 500 microns. Examples of this fact are shown below in table 7, where the fractional percentages are calculated for three rocks, a sandstone, a limestone and a granite:

TABLE 7

Laboratory Drill cuttings for three rocks expressed as fractional percentages

Rock:-	Darley Dale Sandstone	Giggleswick limestone	Mount Sorrel granite
sieve size	Fractional %	Fractional %	Fractional %
+4mm	0	0	0
+2mm	0.55	0	0
+1mm	1.83	0	0.20
+500 microns	2.84	1.53	0.39
+250 microns	10.23	4.03	1.31
+125 microns	20.68	15.65	7.35
+63 microns	20.43	21.56	20.45
BASE minus 63	43.44	57.23	70.30
TOTAL	100%	100%	100%

These results indicated that sieving with seven sieves would be insufficient and the base fractions needed to be further analysed to give a more "true" measure. Tests were conducted on the base fractions of Elland Edge sandstone and Darley Dale sandstone using a microscope, Quantimet 720 and a Fisher sub-sieve sizer. Microscope work was extremely tedious and the disadvantage with this method is that one always measures the largest diameter of the particle on the

plate as one looks vertically on to the plate. The Quantimet has been simply described as an "expensive microscope". The samples are mounted on slides, the microscope is focussed on to the slide and automatically traverses the sample counting the particles. The view through the microscope is shown on a colour television screen. A print out of sizes is obtained via the computer giving the number of particles counted for each size chosen by the operator. The slide can be rotated to give another area of view through the microscope and counting can commence again.

Quite a number of difficulties were encountered in carrying out this work. The preparation of slides was no easy task, just viewing dry powder on a slide was useless because of agglomeration and lack of dispersion. Mixing water with the powder was found to be more consistent as the powder dispersed and settled on the slide when the water evaporated. However, water cannot be used if there is any possibility of the powder dissolving. Glycol was good for dispersing, but this gives particles on different planes of suspension. Araldite can also be used for slide preparation. Background effects can be eliminated by doing an empty run, but this wasn't a constant value.

The biggest problem as with all microscope work is deciding which particles on which to focus. If the larger particles are brought into focus and measured then the smaller ones are not measured and vice-versa.

For a few minutes work on the Quantimet a large amount of data was obtained and this provided a difficulty of interpretation. Every count appeared different and each would need a detailed statistical analysis. However, with experience I feel that some of the difficulties could be eliminated.

The Fisher sub-sieve sizer gives the average particle diameter by air-permeability measurements and is a standard undergraduate laboratory apparatus. The average particle diameters for Elland Edge and Darley Dale sandstone were 5.00 microns and 4.25 microns respectively.

There are quite a number of different methods for sub-sieve sizing and the three methods I used gave different results. Muta and Watanabe (79) submitted results at the 1970 conference on particle size analysis held at Bradford University, where analysis of two powders was carried out by various methods in the size range of 100 microns to 1 microns. The methods used were the Coulter counter, optical microscopy, sedimentation balance, Andreasen pipette, light transmission and hydrometer method. From figures 2.10 and 2.11 it can be seen that all the methods do give different results for the same powder. As yet, no one method gives the "true" particle size distribution, Hindle (80) in his review of 'real' time size analysis also concluded that a method of complete analysis has yet to be developed. This applies to surface-area measurements, because surface-area is related to size and

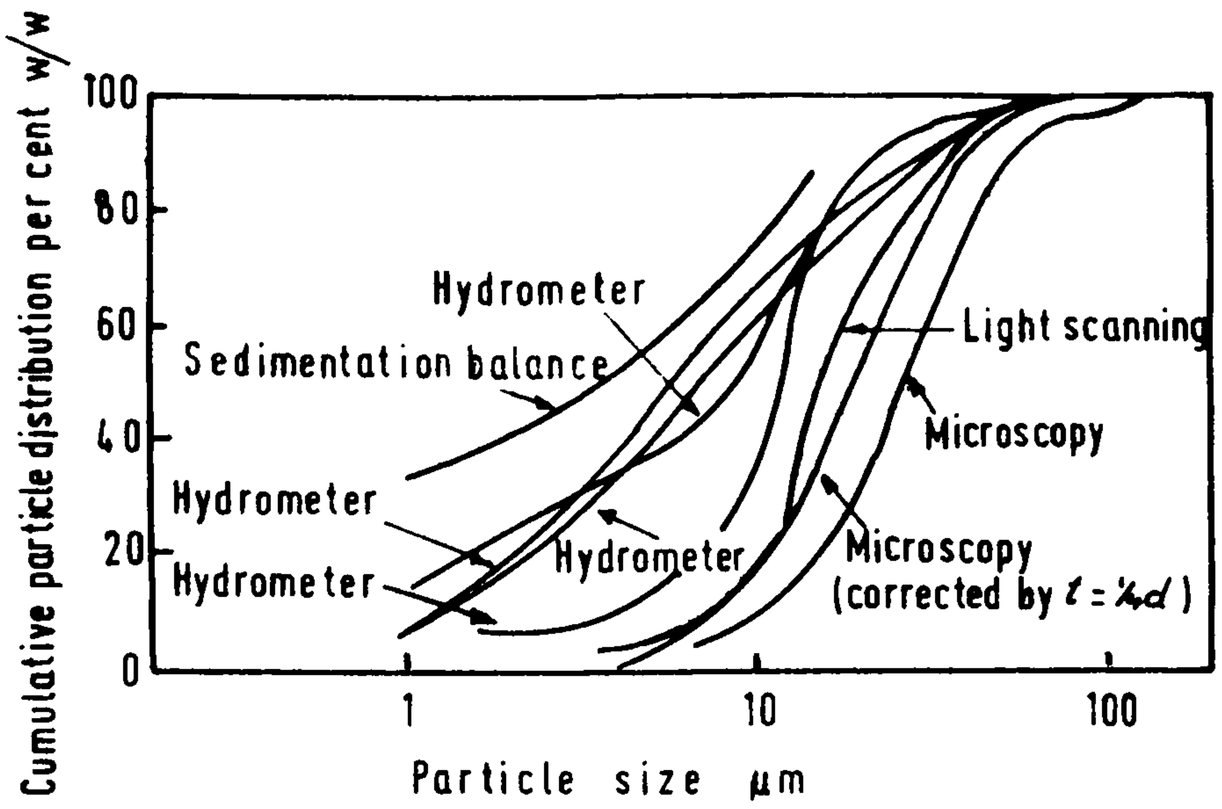

FIGURE 2.10: CUMULATIVE DISTRIBUTION, w/w, FOR CLAY BY VARIOUS ANALYTICAL METHODS AFTER MUTA AND WATANABE(79).

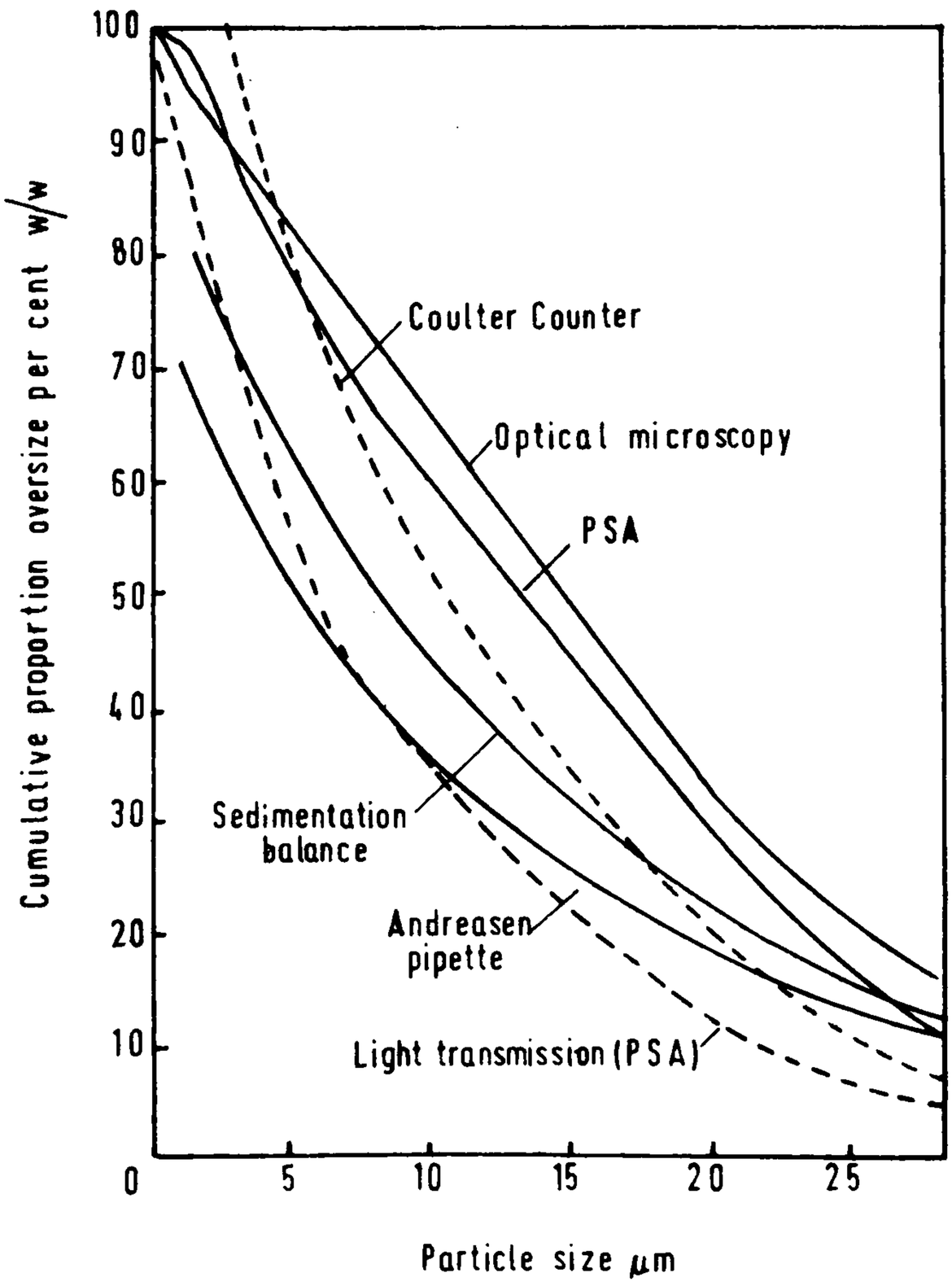

FIGURE 2.11: PARTICLE SIZE DISTRIBUTION OF KANTO LOAM POWDER AS MEASURED BY VARIOUS METHODS AFTER MUTA AND WATANABE(79).

furthermore this relationship depends on the assumptions of regularly-shaped particles. The general attitude for small particle size is to use one of the standard methods and stick to it for all subsequent tests.

It was felt that for all the analysis of the minus 63 micron drill cuttings fractions it would be advantageous to use micro-sieving techniques in order to have continuity and convenience. This is because dry sieving has so far been used needing no long statistical analysis and all the drilling and rock breaking is under dry conditions. Also changing the method of particle analysis 'midstream' produces a distinct change in the size analysis curve as shown diagrammatically below in figure 2.12.

Figure 2.12. Diagram showing the effect on the size analysis curve when changing method of analysis in a run.

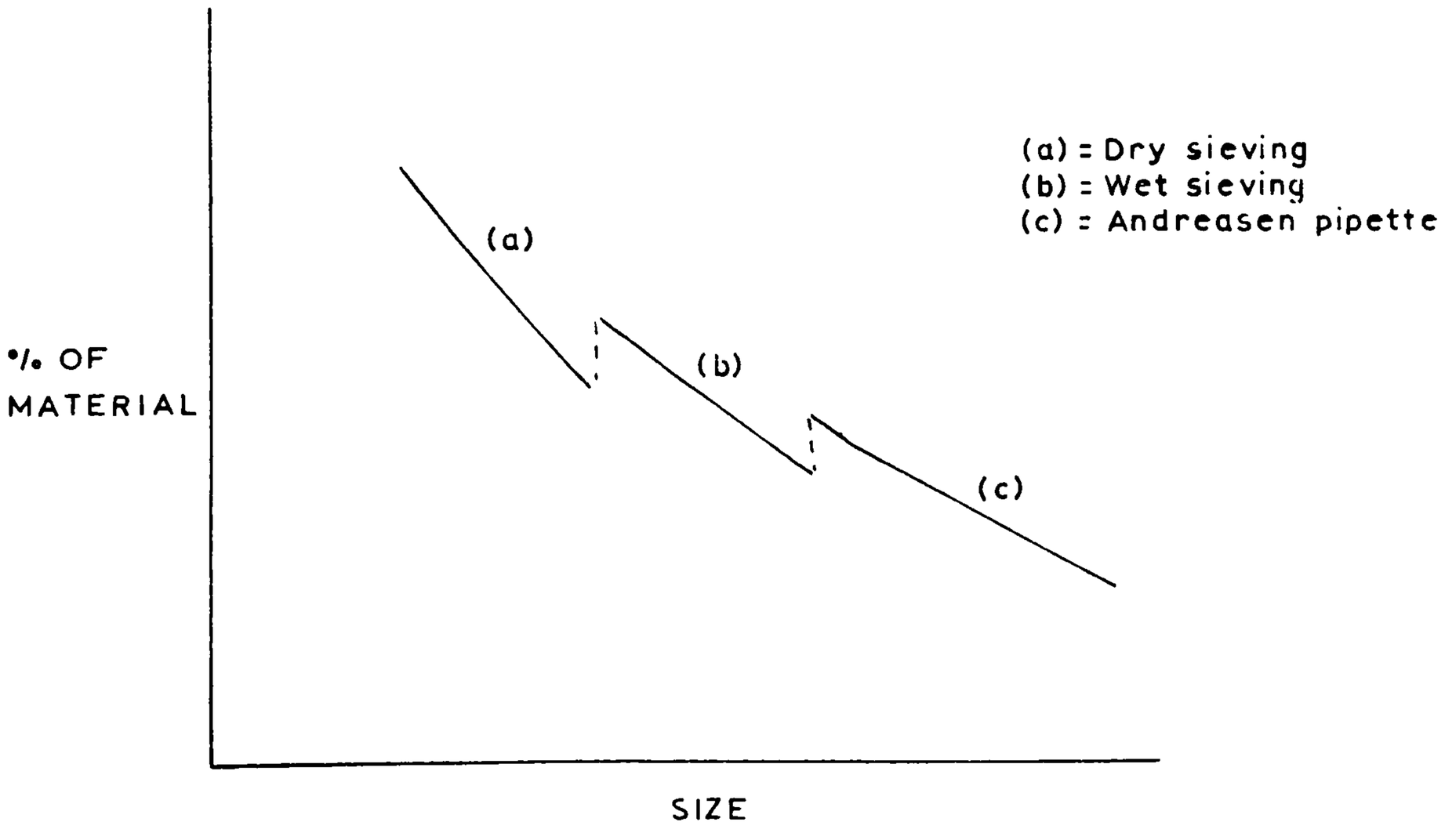

There are a few micro-sieving apparatus on the market, one is the Alpine air jet sieve. This apparatus was used to sieve the base fractions on 30 and 15 micron sieves.

2.11 Alpine Sieving Techniques

Figure 2.13 shows the apparatus mounted on a table. The apparatus consists of a sieve housing (detailed in figure 2.14) with a contact switch clock, a vacuum motor with a suction-pipe, a negative pressure measuring device in inches W.G., a fines collecting filter and a plexiglas cover.

From figure 2.14 showing the sieve housing, it is possible to understand the working action of the apparatus. The slit nozzle in figure 2.14, is rotated underneath the seive and the vacuum motor draws air through the system. The slit-nozzle is placed near to the sieve, the air is in fact jetted up through the sieve and in doing so raises and agitates the particles. As soon as the jet rotates to another area the particles are sucked downwards. The undersizes go through the sieve down the discharging socket and can be collected on the fines filter. As there was no further use for the fines they weren't collected.

The sieves were cleaned using an Ultrasonic cleaner containing water and alcohol. This gave fast drying and excellent cleaning, proved by examination under a microscope where all the sieve-perforations were completely cleared. With ultrasonic cleaning one has normally to be extremely careful in choosing the correct frequency for cleaning the sieves. Sieves can easily be damaged using the wrong

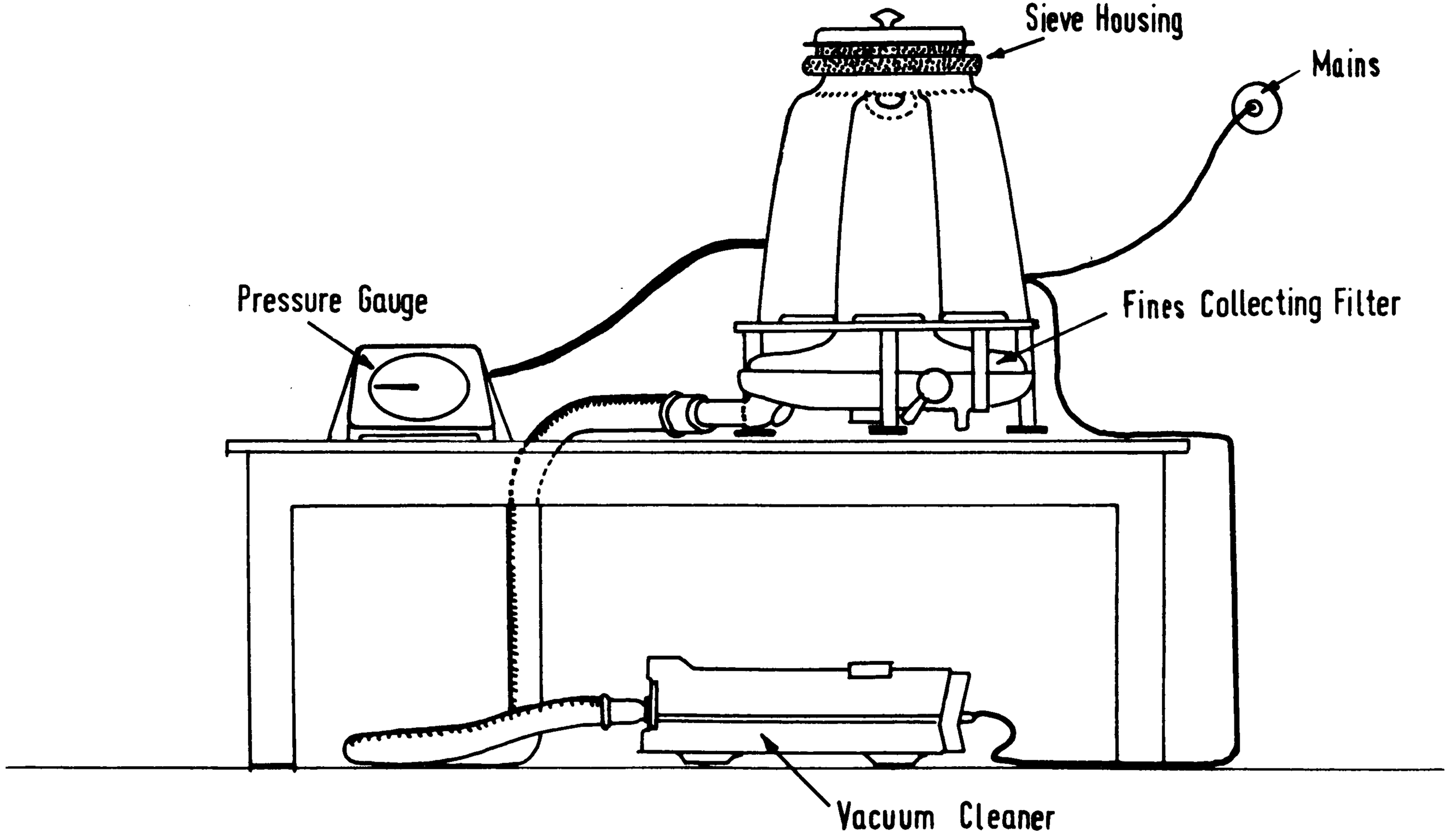

FIGURE 2.13: THE ALPINE SIEVING APPARATUS.

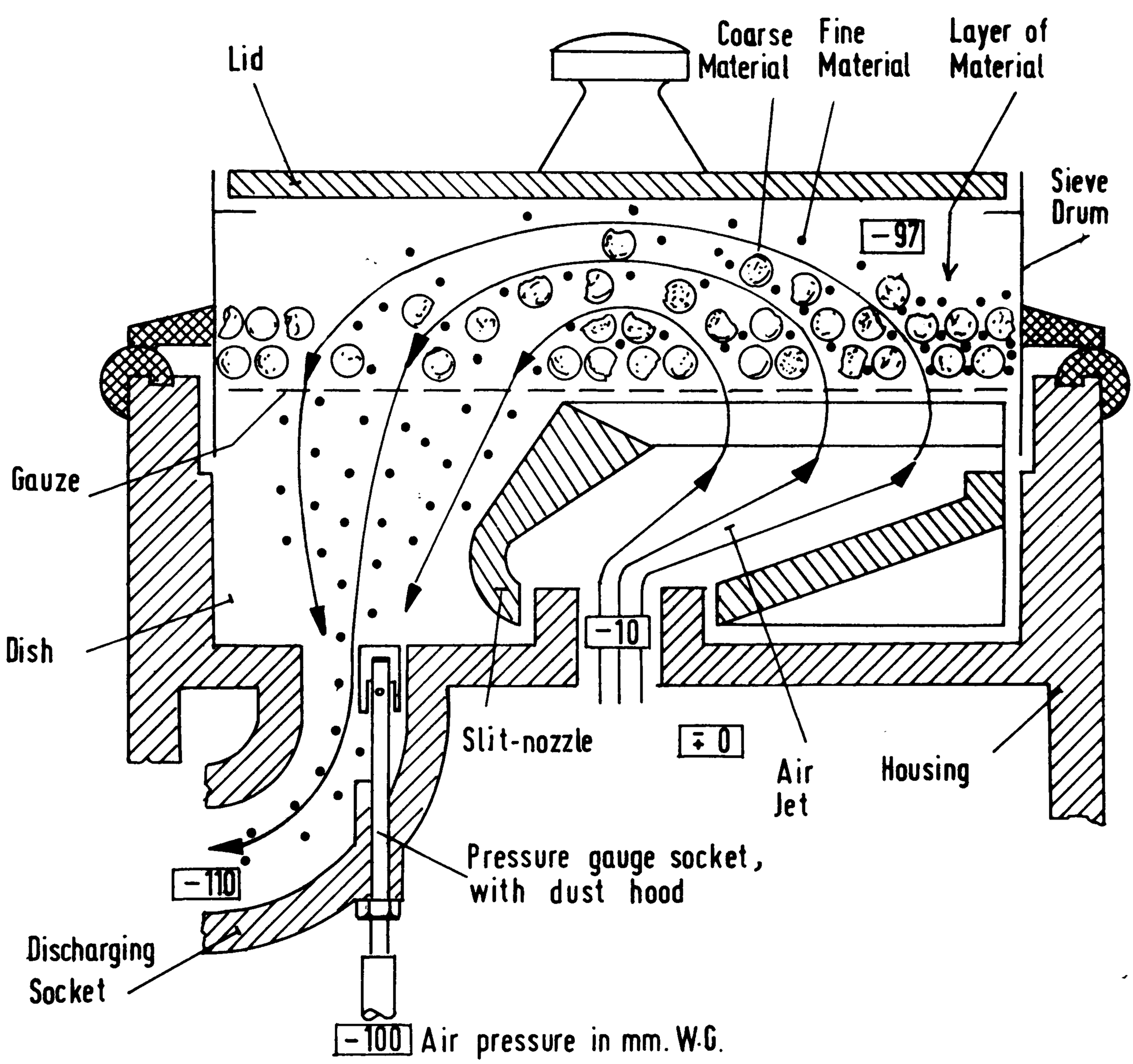

FIG 2·14 THE ALPINE SIEVE HOUSING

frequency and the correct frequency should be obtained from the manufacturer. Micro-sieves should always be used with extreme care. The 30 and 15 micron sieves used were Endecott 4" diameter stamped stainless steel plate.

The 15 micron sieve was first placed in the sieve housing and a known weight (W_1) of material was sifted on to the sieve. Air jet sieving was then done for 3 minutes. The weight (W_2) remaining subtracted from the original weight gives the minus 15 microns ($W_1 - W_2$). The remaining weight (W_2) is then similarly sieved on the 30 micron sieve for 3 minutes, the weight left on the 30 micron sieve is (W_3) which is the undersize of 63 microns. The minus 30 microns is ($W_2 - W_3$). A source of error here is the transferring and weighing of the weights W_2 and W_3 remaining on the 15 and 30 micron sieves, respectively. The material has to be carefully brushed from the sieve, so it is possible to leave an amount of material on the extremely fine sieves. However, with careful work this was found to be a small percentage, shown by:-

Weight of dry sieve after ultrasonic cleaning	=	118.0578 grms.
Weight of sieve after brushing out material	=	118.0620 grms.
Amount left on sieve	=	0.0042 grms.

Therefore, out of five grams this is only 0.084%. A five gram sample would be split into five approximately

equal fractions for the 15 micron sieve.

The original minus 63 microns in the base has then been further sieved into 3 fractions i.e. +30 microns, +15 microns, -15 microns and the surface area for this longer range calculated with a Wang computer programme.

During the sieving process, the sieve sides and lid were gently tapped to clear collected material. The operating pressure for the 30 micron sieve was 17" W.G. and for the 15 micron 22" W.G., but for the smaller sieve a greater pressure should have been used. Despite efforts to seal any leaks, higher pressures were unobtainable.

From the results it is clear that this sieving technique at 15 microns is greatly inefficient even by using small samples. However, with regard to this work the final analysis shows that this is irrelevant. Table 8 shows the three fractional percentages calculated for the same three rocks in table 7, as examples to show the inefficiency of 15 microns:

TABLE 8

Minus 63 micron laboratory drill cuttings for three rocks examined by Alpine air jet sieving expressed as fractional percentages.

Rock:-	Darley Dale Sandstone	Giggleswick Limestone	Mount Sorrel Granite
Total weight: (Minus 63 microns)	4.2571 gms.	4.8891 gms.	3.3775 gms.
Sieve size:	Fractional %	Fractional %	Fractional %
+30 microns	57.55	34.95	50.30
+15 microns	40.73	60.85	48.01
-15 microns	1.72	4.82	2.55

TABLE 9

The areas/gram of cuttings for 14 rocks drilled in the laboratory using the Rotap and Alpine sieving machines.

Rock	Area/gram .. m^2/gram Rotap 7 sieves + base	Area/gram .. m^2/gram Rotap and Alpine 9 sieves + base
Yellow Oolitic limestone	0.0257963	0.0371517
Darley Dale sandstone	0.0310271	0.0524096
St. Bee's sandstone	0.0363621	0.0637632
Elland Edge sandstone	0.0390165	0.0638189
Horsforth sandstone	0.0313493	0.0489311
Denbigh limestone	0.0338160	0.0523492
Whinstone	0.0328684	0.0475201
Cornish granite	0.0413904	0.0705092
Groby granite	0.0326729	0.0502091
Mount Sorrel Granite	0.0426497	0.0705179
Giggleswick limestone	0.0359191	0.625445
Bardon Hill granite	0.0347467	0.0556717
Craigenlow Pink granite	0.0436130	0.0710010
Bath limestone	0.0239419	0.0339495

Table 9 shows the values of area/gram for the fourteen laboratory drilled rocks, calculated from using the Rotap 7 sieves + base, then calculated from using the Rotap and Alpine air jet sieve 9 sieves and base. A graph of 7 sieves and base was plotted against 9 sieves and base area/gram values shown in figure 2.15. Allowing for experimental error, an extremely good straight line relationship is obtained, therefore 7 sieves and base are adequate for the examination of drill cuttings. So further analysis of particle size to obtain a more "true" measure would only give a line with greater area values anyway, similarly if a correct value for 15 microns was obtainable there is no reason why another linear relationship should not be found.

The final analysis is in fact a comparison of areas/gram for any rocks drilled and 7 sieve and basic sieving method provides a simple and relatively accurate method of enumerating the cuttings produced.

2.12 Field Drill Cuttings

Drill cuttings from a field rotary-percussive drill were collected for examination in the laboratory. This was done to quantify the cuttings in the hope of further understanding drill performance. The cuttings obtained were coned and quartered. The sample was further reduced in volume by using a small standard laboratory sample splitter, the final two halves were sieved on the Rotap with 7 sieves and base. The areas/gram computed and the mean value of the two halves taken, all agree closely.

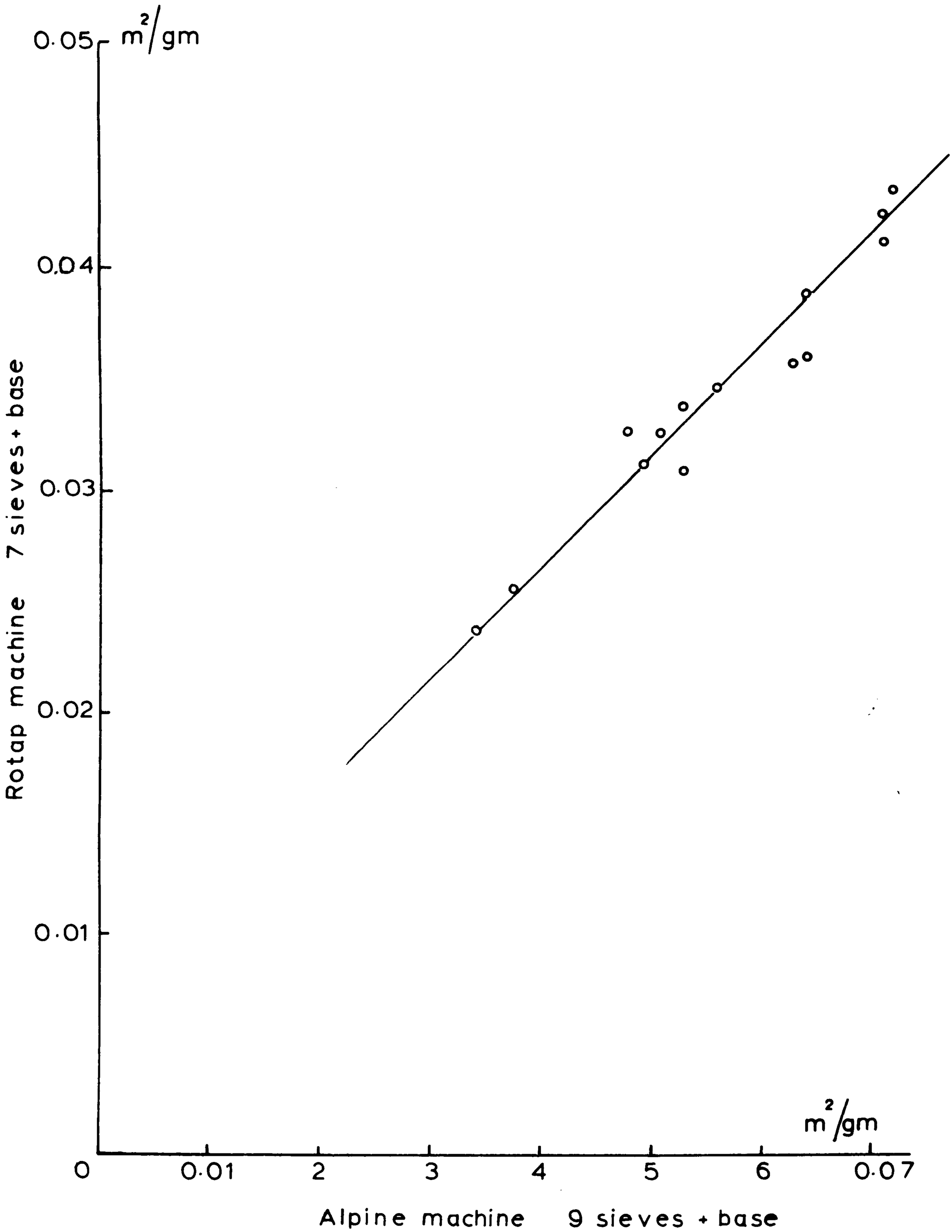

FIGURE 2.15: ROTAP 7 SIEVES AGAINST ALPINE 9 SIEVES.

The areas/gram for the field drilling ranged from 0.0038 to 0.0162 m^2/gram, which is the same order as breakage by laboratory techniques (i.e. slow compression, drop hammer etc.) and about half that of laboratory drilling.

2.13 Summary

a) The derivation of energy/gram and surface area/gram relationships have been presented. From graphs of energy/gram versus area/gram, an index can be obtained and it is possible to compare the efficiencies of different rock breaking processes.

b) After several tests, surface area has been finally calculated from carrying out a sieve analysis with a nest of seven sieves and base on a Rotap sieving machine for 10 minutes.

c) Laboratory drill cuttings containing lots of fines have been examined in detail. Seven sieves and base on the Rotap for 10 minutes still give a good measure of surface-area for the whole range of rocks drilled.

d) Reducing the large bulk of field drill cuttings enables the cuttings to be easily examined by the same nest sieves on the Rotap for 10 minutes.

CHAPTER III

ROCK BREAKAGE IN THE LABORATORY

CHAPTER III

ROCK BREAKAGE IN THE LABORATORY

INTRODUCTION

This chapter is divided into six sections and a summary of the findings is given at the end.

Section A deals with the drop hammer tests carried out in order to determine an accurate rock index in terms of energy/surface area relationships. Regular cylindrical specimens are used in the drop hammer tests. This section also gives the results of varying the drop weight and drop height to see the effect on the energy/area relationship.

Section B develops another index in terms of energy/surface area by the Stamp Mill method of breakage. In this method the drop height is approximately 35 times less than in the drop hammer tests and has smaller initial size specimens for crushing.

Section C describes the slow compression tests that have been introduced to compare the efficiency of the drop hammer method of breakage. Slow compression is used for this purpose as it has been proposed (72,86) that slow compression provides the most efficient known method of breakage. The efficiency is obviously high because the design of slow compression crushing is such that little energy is lost due to friction, noise, vibration and

compaction. The same size cylindrical specimens are used as with the drop hammer tests.

The method and results of slow compression breakage are presented and an index is also obtained. By considering energy/surface area relationships a graphical comparison of drop hammer and slow compression is made in Section D. This section includes tests on Bath limestone to compare the stamp mill with the drop hammer by using the smaller initial sizes as used in the stamp mill tests for crushing in the drop hammer apparatus.

Section D also includes the interrelationship of the three developed indices by means of a linear regression analysis. The equations for the linear regression and the correlation coefficients are listed.

Section E presents a literature review of recent publications, so that the results of this work can be compared where possible, to other people's work in this field.

Section F includes three more rock indices, these are the Compressive Strength, Rock Impact Hardness Number and Dynamic Young's Modulus. The modulus is measured by Ultrasonic testing and the techniques involved have been described. The compressive strength has been determined by a standard laboratory method and Rock Impact Hardness Number after Brook and Misra (46).

To conclude this chapter a summary of the findings is given.

SECTION A: DROP HAMMER TESTS

Photograph 1 shows the apparatus used in these tests, which was made from Protodyakonov's (29) specifications, figure 1.7 shows the dimensions of the apparatus. The base of the apparatus is firmly secured with clamps. Regular specimens are used, these are prepared by diamond coring giving 25mm diameters, the cores are then cut to 50mm lengths. The same rock samples are used for the taking of all subsequent cores and specimens for rock testing and drilling in this research programme.

A 2.4 kg. weight is allowed to fall freely from a fixed height on to the cylindrical specimen to cause breakage. The energy input to the specimen is then the weight of the hammer x the height of fall x the number of blows x acceleration due to gravity.

3.A1. Energy Input

To calculate the energy input to the rock certain considerations had to be made with regard to the height of fall. Previous research workers at Leeds (34, 43, 44, 45) have used 0.600m as the height of fall, but this is not the actual fall. When using cylindrical specimens of 50mm length and 25mm diameter which are placed horizontally in the Syskov mortar, the first drop height is the fall in the empty mortar minus the specimen diameter i.e. 0.640m - 0.025m. After the first blow a new height is obtained and similarly after every blow. Therefore, to gain an exact measurement of energy input, the height of fall would have

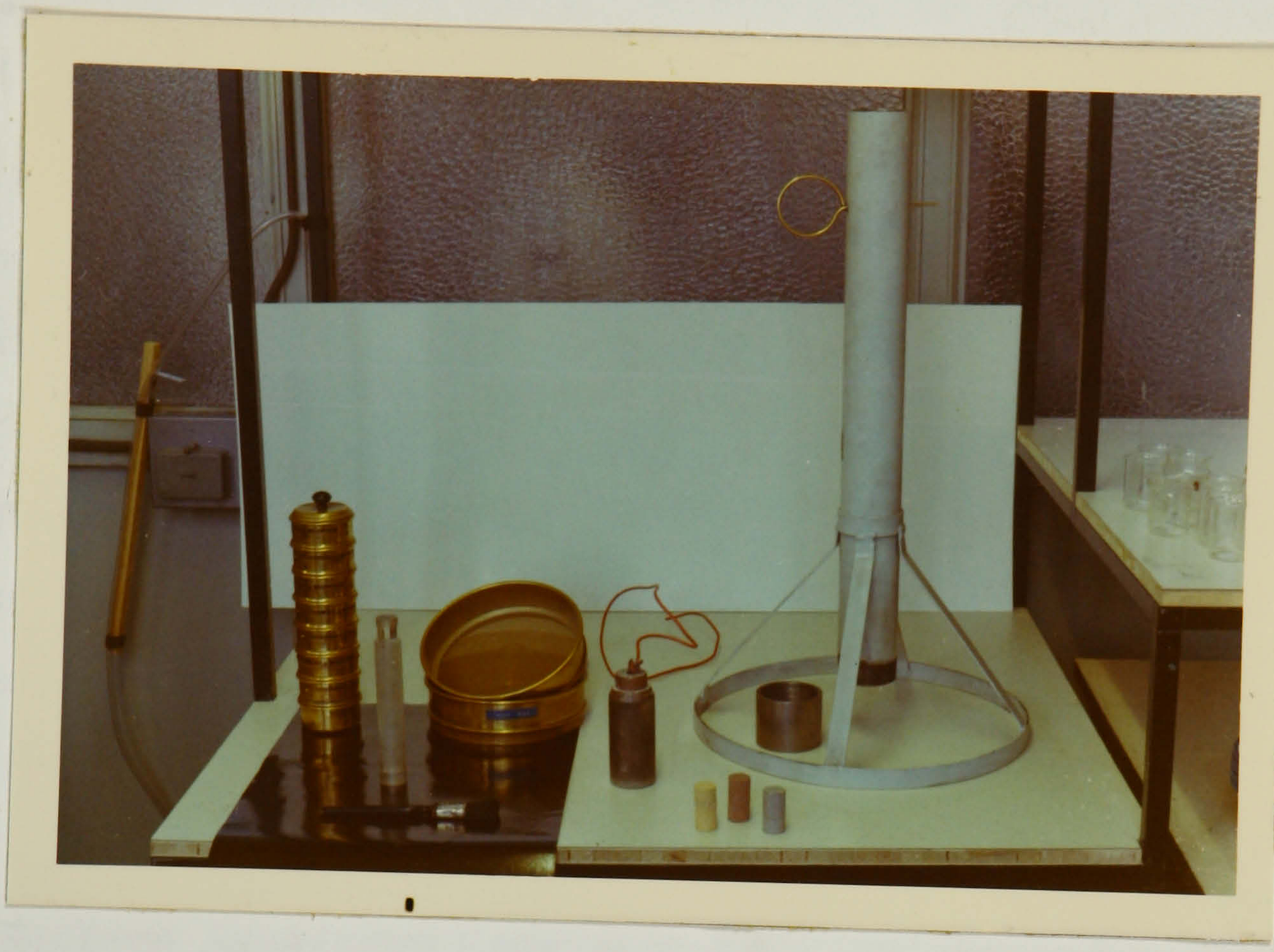

PHOTOGRAPH 1 : The Drop Hammer Apparatus

to be measured after each blow. If we assume a constant fall of 0.600m and that a maximum possible error by not measuring the true drop height after every blow is 0.020m, then the error in calculating the energy will be $\frac{0.020}{0.600} = \frac{1}{30}$ = 3.33% at the most. This value is quite small and is negligible, as a graphical method of obtaining the rock index is used. Also the energy input to the rock is calculated in the same manner for each rock.

For the purposes of this research a constant drop height was assumed, and to have a value of 0.600m. This value was also chosen as the drop height then all the results if required, can be compared to the previous results on Rock Impact Hardness.

3.A2 Surface Area/gram Measurement

The comminuted product is sieved on the Rotap for 10 minutes and the weights of the fractions on each sieve obtained. The surface area/gram is computed from $\sum \frac{6}{s} \ell n\ 2\ (\frac{\text{wt. of fraction}}{a_1 - a_2})$/gm on the Wang desk top computer.

At the start of the breakage, a small surface area i.e. the cylindrical specimen exists. This area equals $2\pi rl + 2\pi r^2$, where l = 50mm and r = 25mm. This gives an area of 0.004908m² and when divided by the weight of the specimen it has to be subtracted from the computed area/gram (i.e. from $\sum \frac{6}{s} \ell n\ 2(\frac{\text{weight of fraction}}{a_1 - a_2})$/gm to give the new surface area/gram created.

By varying the number of blows to give new energy levels on different cylindrical specimens the new surface areas can be obtained and a graph of energy/gram versus new area/gram can be established. Figures 3.1 and 3.2 show the energies/gram plotted against the new areas/gram for fourteen different rocks covering a wide range of properties and these results are tabulated in table 11. All the rocks give extremely good straight lines, the linear regression analysis giving very high correlation coefficients. The slopes of the lines, energy/area is taken as the rock index because of the high coefficients. Table 11 gives the correlation coefficients and the slope values.

An example of a size analysis and energy calculation, Denbigh limestone is given overleaf in table 10:

Table 10: Denbigh limestone Size Analysis showing weight retained on each sieve for 5 different energy levels.

Density ; 2.674 gm/cc

Sieve sizes	10 blows	25 blows	40 blows	60 blows	75 blows
4mm	53.363	38.093	29.126	12.820	6.302
2mm	5.612	9.061	11.221	14.604	15.556
1mm	3.608	6.329	7.716	11.039	11.544
0.5mm	2.179	4.649	6.297	8.870	9.656
0.25mm	1.230	2.932	4.162	5.721	7.656
0.125mm	0.743	1.870	2.979	4.462	5.074
0.063mm	0.471	1.135	1.953	2.765	3.538
BASE	0.988	2.860	4.590	7.714	11.534
Total wt. in gms.	68.193	66.929	68.045	67.996	70.860
1. Surface ..m^2/gm area/gram	0.0016903	0.0038588	0.0057559	0.0088966	0.0117893
2. New Area/ gram m^2/gm	0.0016180	0.0037862	0.0056838	0.0088251	0.0117182
3. Energy/ gram Nm/gm	2.072	5.277	8.304	12.465	15.601

3,A3. Determination of S.G. or density, s.

All the densities for the computation of surface area are calculated from the Pyknometer (specific gravity bottle) method. The sample of rock used is about 3 grams in weight and less than 500 microns in size, filling approximately 1/4 of the bottle.

Weight of empty bottle = w_1 gms.

Weight of sample = w_2 gms.

Weight of bottle full of distilled water and containing sample = w_3 gms.

Weight of bottle full of distilled water = w_4 gms.

$$\text{S.G. of sample} = \frac{\text{wt. of sample}}{\text{wt. of an equal volume of water}}$$

$$= \frac{(w_2 - w_1)}{(w_4 - w_1) - (w_3 - w_2)}$$

When filling the bottle with a liquid, sufficient must be added to ensure that on inserting the stopper, the hole in it will also be completely filled. The excess of liquid which oozes out of the stopper hole when inserted, must be completely removed and the outside of the bottle must be completely dry before weighing. Greater accuracy was obtained by using the wetting agent benzene.

So that, S.G. of sample = $\frac{\text{(S.G. of benzene)} \times (w_2 - w_1)}{(w_4 - w_1) - (w_3 - w_2)}$

A list of all the specific gravities of the rocks used in this work is given in the Appendix.

TABLE 11

RESULTS OF DROP HAMMER TESTS

Yellow Oolitic lst.		Darley Dale sst.		Horsforth sst.	
s = 2.642		s = 2.588		s = 2.860	
Energy/gm.	New Area/gm.	Energy/gm.	New Area/gm.	Energy/gm.	New Area/gm.
0.6417	0.004811	0.5276	0.003421	0.5565	0.003046
1.2513	0.006689	1.0988	0.005429	1.0954	0.005079
1.6010	0.007899	1.8875	0.007756	1.6429	0.006490
1.9224	0.008935	2.6118	0.009833	2.2967	0.008036
		3.3725	0.011218	2.7387	0.008844
Slope E/A = 309.470		Slope E/A = 357.467		Slope E/A = 376.223	
c.c. = 0.99972		c.c. = 0.99453		c.c. = 0.99221	

St. Bee's sst.		Elland Edge sst.		Bath Lst.	
s = 2.569		s = 2.644		s = 2.659	
Energy/gm.	New Area/gm.	Energy/gm.	New Area/gm.	Energy/gm.	New Area/gm.
0.5244	0.003176	0.4923	0.001648	1.2930	0.002677
1.3159	0.005040	2.4641	0.005068	2.5998	0.003999
1.9415	0.007240	3.5009	0.007129	3.8374	0.005592
2.6190	0.008765	4.9383	0.009613	5.1736	0.007682
4.8188	0.013185	(9.3501	0.014321)	6.3769	0.008880
(11.0102	0.016201)				
Slope E/A = 424.107		Slope E/A = 554.836		Slope E/A = 787.184	
c.c. = 0.99456		c.c. = 0.99971		c.c. = 0.99721	

....cont.

(Table 11 cont.)

Craigenlow Pink Gr.		Giggleswick Lst.		Cornish Gr.	
s = 2.646		s = 2.687		s = 2.651	
Energy/gm.	New Area/gm.	Energy/gm.	New Area/gm	Energy/gm.	New Area/gm.
2.1569	0.002494	2.1841	0.002630	2.1526	0.002268
4.3872	0.004532	4.4032	0.004979	4.3467	0.005098
6.5881	0.006433	6.6518	0.007452	8.6332	0.008899
8.7983	0.008395	8.7228	0.009175	13.0392	0.012678
10.8062	0.011230	13.1612	0.013175	16.2997	0.015404
Slope E/A = 1009.280		Slope E/A = 1042.791		Slope E/A = 1094.045	
c.c. = 0.99499		c.c. = 0.99853		c.c. = 0.99797	

Denbigh Lst.		Whinstone		Mount Sorrel Granite	
s = 2.674		s = 2.932		s = 2.576	
Energy/gm.	New Area/gm.	Energy/gm.	New Area/gm.	Energy/gm.	New Area/gm.
2.0715	0.001618	1.8962	0.001345	2.1090	0.001876
5.2766	0.003786	4.7418	0.0030721	5.2726	0.004141
8.3042	0.005684	9.4934	0.005915	10.5604	0.008040
12.4652	0.008825	14.2608	0.008809	15.8582	0.011405
15.6012	0.011718	19.0358	0.013258	21.1695	0.014006
Slope E/A = 1348.564		Slope E/A = 1460.816		Slope E/A= 1541.405	
c.c. = 0.99752		c.c. = 0.99491		c.c. = 0.99694	

Groby Granite		Bardon Hill Granite	
s = 2.681		s = 2.849	
Energy/gm.	New Area/gm.	Energy/gm.	New Area/gm.
6.3602	0.003482	1.9470	0.000625
10.1558	0.005668	3.8953	0.001630
15.4633	0.008133	11.7230	0.003925
20.6566	0.010086	17.6007	0.007333
32.4001	0.015490	23.4955	0.007333
Slope E/A = 2205.595		Slope E/A = 3269.839	
c.c. = 0.99881		c.c. = 0.99832	

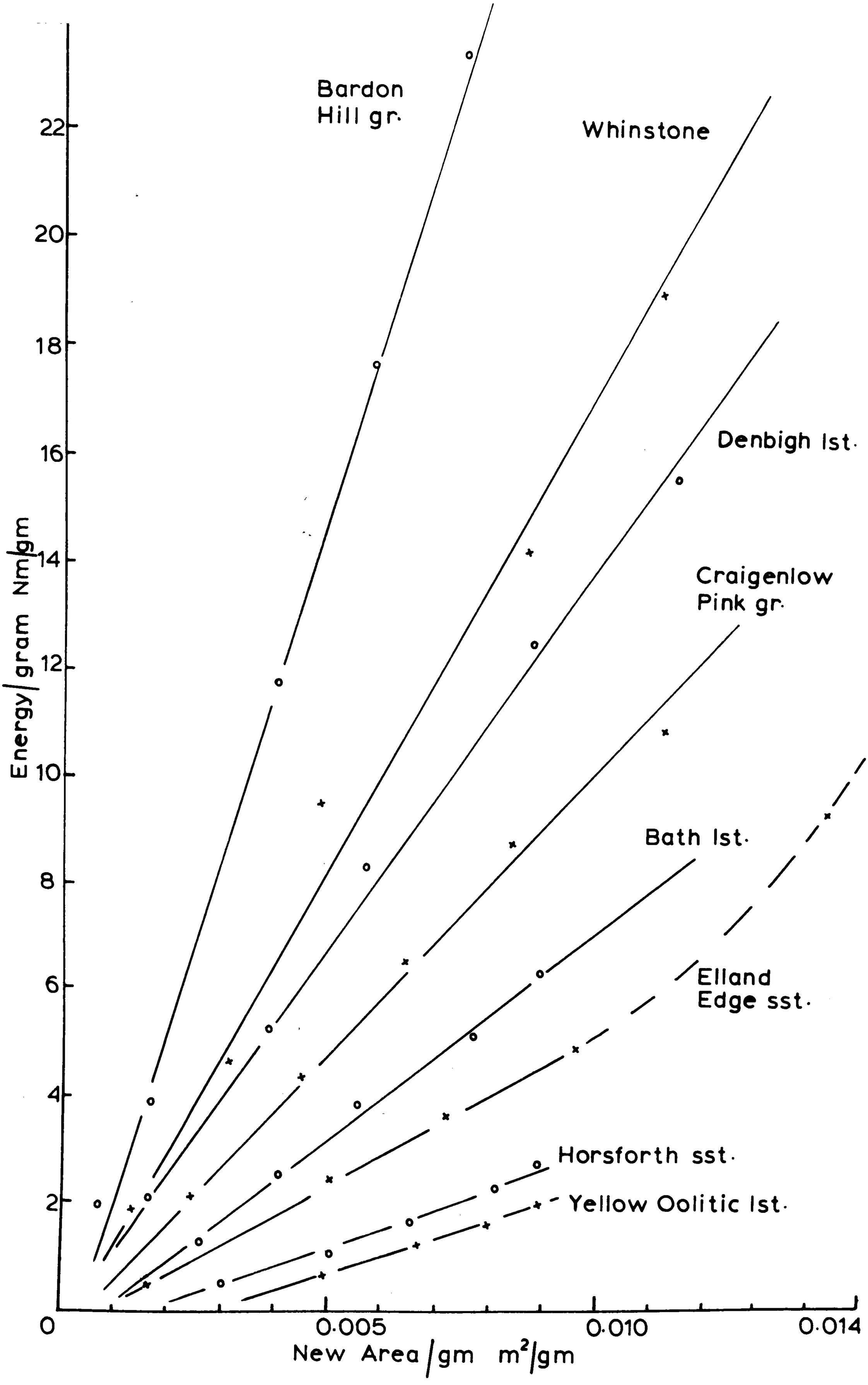

FIGURE 3.1: DROP HAMMER TESTS.

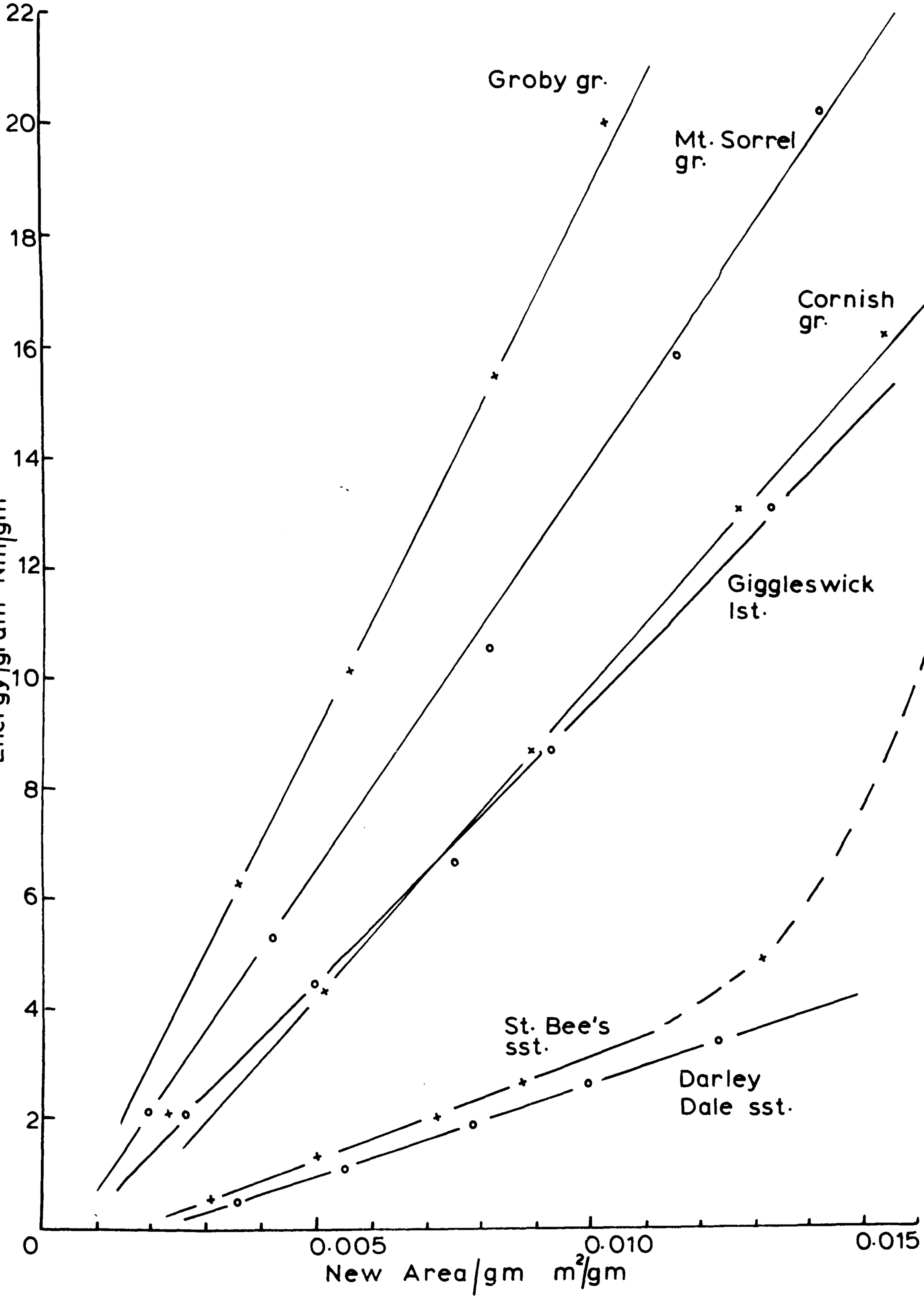

FIGURE 3·2: DROP HAMMER TESTS.

3.A4. Variation of drop height and weight in drop hammer tests.

In chapter II work on Elland Edge sandstone showed that by varying the drop weight to 1.2 and 3.6 kg, a fixed energy/area relationship was still obtained. Further tests were carried out varying both the drop weight and height on three different rocks Yellow Oolitic limestone, Crystalline limestone and Larvikite granite.

A graph of Energy/gram against area/gram for each rock was established in the normal way using 2.4 kg. weight and 0.6m drop height, then for each rock five more cores were tested in the following manner:-

a) 1 core with the 3.6 kg. mass at normal height of fall (0.6m).

b) 1 core with the 3.6 kg. mass at 1/2 normal height of fall (1/2 x 0.6m).

c) 1 core with the 2.4 kg. mass at 1/2 normal height of fall (1/2 x 0.6m).

d) 1 core with the 1.2 kg. mass at normal height of fall.

e) 1 core with the 1.2 kg. mass at 1/2 normal height of fall.

Larvikite granite was tested with core (a) having 20 blows (b) 44 blows (c) 46 blows (d) 50 blows (e) 60 blows in the Syskov mortar.

Crys. limestone with core (a) having 20 blows (b) 36 blows (c) 44 blows (d) 70 blows (e) 68 blows in the Syskov mortar.

Yellow Oolitic limestone with core (a) having 5 blows (b) 12 blows (c) 14 blows (d) 10 blows (e) 12 blows in the

Syskov mortar.

(All cores of standard 50 mm length and 25 mm diameter).

Energy inputs are calculated from number of blows x height of fall x drop weight x g and the areas by using the Wang Computer Programme for calculating surface areas $\left(\sum \frac{6}{s} \ell n\ 2 \frac{\text{wt. of fraction}/_{gm}}{a_1 - a_2}\right)$ from the normal sieve analysis. Table 12 gives the calculated results for the three rocks with the five different energy inputs as well as the 2.4 kg. weight dropped from 0.6m results. The surface areas given are the new surface areas/gram created obtained by taking away the small original rock cylinder area/gram. The results from table 12 are plotted in figures 3.3 and 3.4, which show good linear relationships for the rocks. Correlation coefficients are high, as shown in table 12 but the lowest value for Yellow Oolitic limestone is to be expected as there is a large difference between the two highest points on the graph. This is because with the 2.4 kg. weight, dropped from 0.6m producing 0.013196 m^2/gram of area, the efficiency has not begun to reduce.

The interesting point from these tests is that by using the same apparatus, but varying the method of energy input, with regard to height and weight, linear relationships are still obtained. This applies for the variations of height and weight in these tests, though the variations are large, any larger variations would not necessarily fall on to the energy/area line for a rock. However, the fact that these variations in height and weight do fall on the graphs is

significant for design purposes. In rotary-percussive drilling for instance, changes in piston weight and number of blows/minute would be a parallel to these tests and in ball milling, changing the weight of balls would be another parallel.

TABLE 12

Energy/gram and New Area/gram values for three different rocks after the variation of drop height and weight in drop hammer tests.

Yellow Oolitic limestone

2.4 kg.wt 0.6m drop height		Other combinations		
Energy/gram	New Area/gram		Energy/gram	New Area/gram
0.5973	0.004477	a)	2.0870	0.010204
1.1394	0.005711	b)	2.7339	0.014541
1.2513	0.006689	c)	2.0557	0.010009
1.6993	0.008529	d)	1.4454	0.008402
1.9224	0.008935	e)	0.8528	0.005664
2.9743	0.013196			

correlation coefficients ... 2.4 kg.wt. at 0.6m = 0.99530

... all eleven points = 0.97460

Crystalline limestone

2.4 kg.wt 0.6m drop height		Other combinations		
Energy/gram	New Area/gram		Energy/gram	New Area/gram
1.0550	0.001423	a)	6.2787	0.007636
2.0900	0.002622	b)	5.7776	0.007232
3.1416	0.003717	c)	4.5942	0.005970
4.2158	0.004821	d)	7.3682	0.007862
5.2360	0.006272	e)	3.4780	0.004581

correlation coefficients ... 2.4 kg.wt. at 0.6m = 0.99827

... all ten points = 0.98565

(Table 12 cont)

Larvikite granite

2.4 kg.wt. at 0.6m drop height		Other combinations		
Energy/gram	New Area/gram		Energy/gram	New Area/gram
2.0620	0.002463	a)	6.2015	0.006157
4.1592	0.004358	b)	6.8349	0.007112
6.2967	0.006372	c)	5.0719	0.005314
8.2747	0.007935	d)	5.1448	0.004809
10.3829	0.009919	e)	3.0652	0.003219

correlation coefficient ... 2.4 kg.wt. at 0.6m = 0.99969

... all ten points = 0.99537

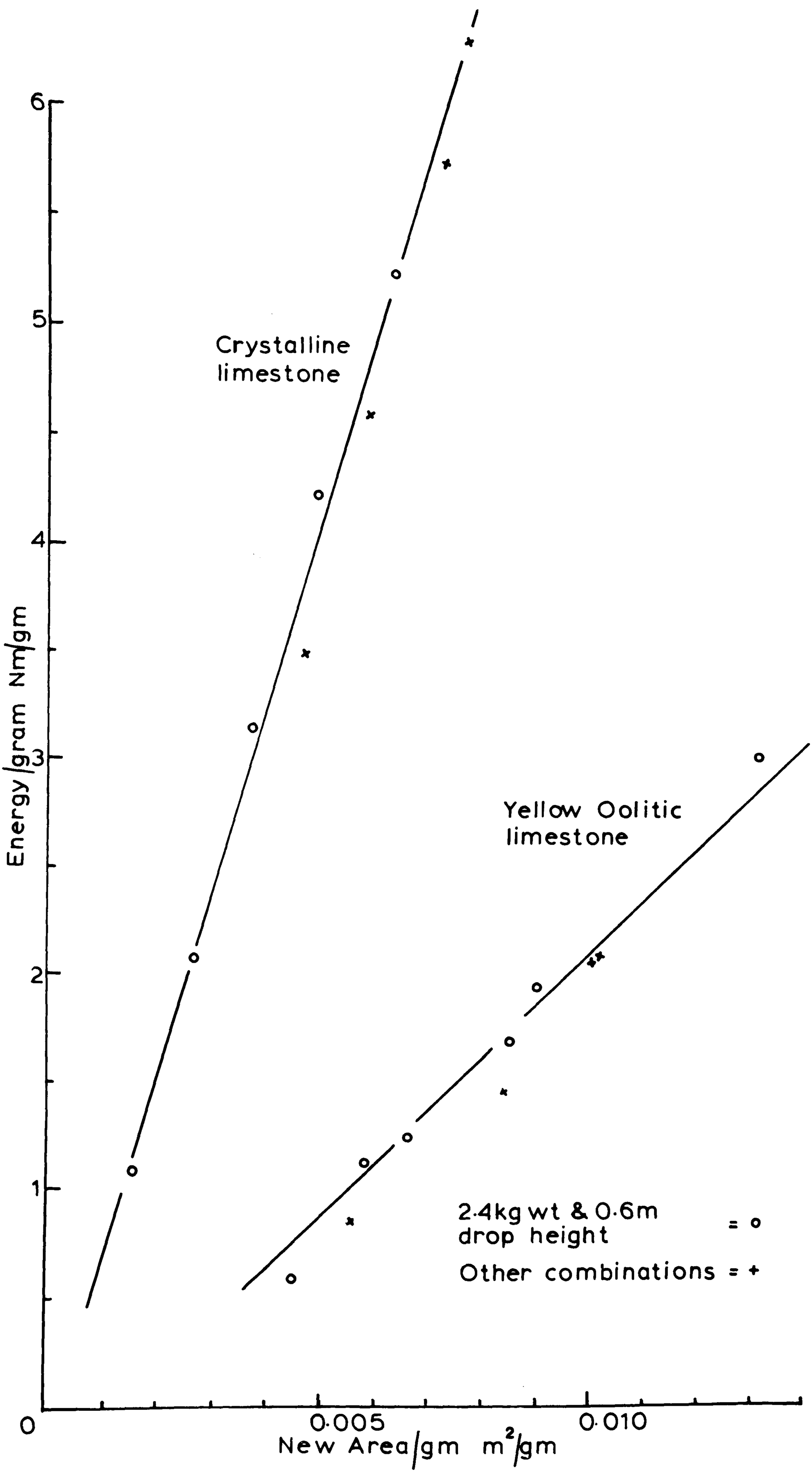

FIGURE 3·3: DROP HAMMER TESTS WITH DIFFERENT DROP HEIGHTS & WEIGHTS.

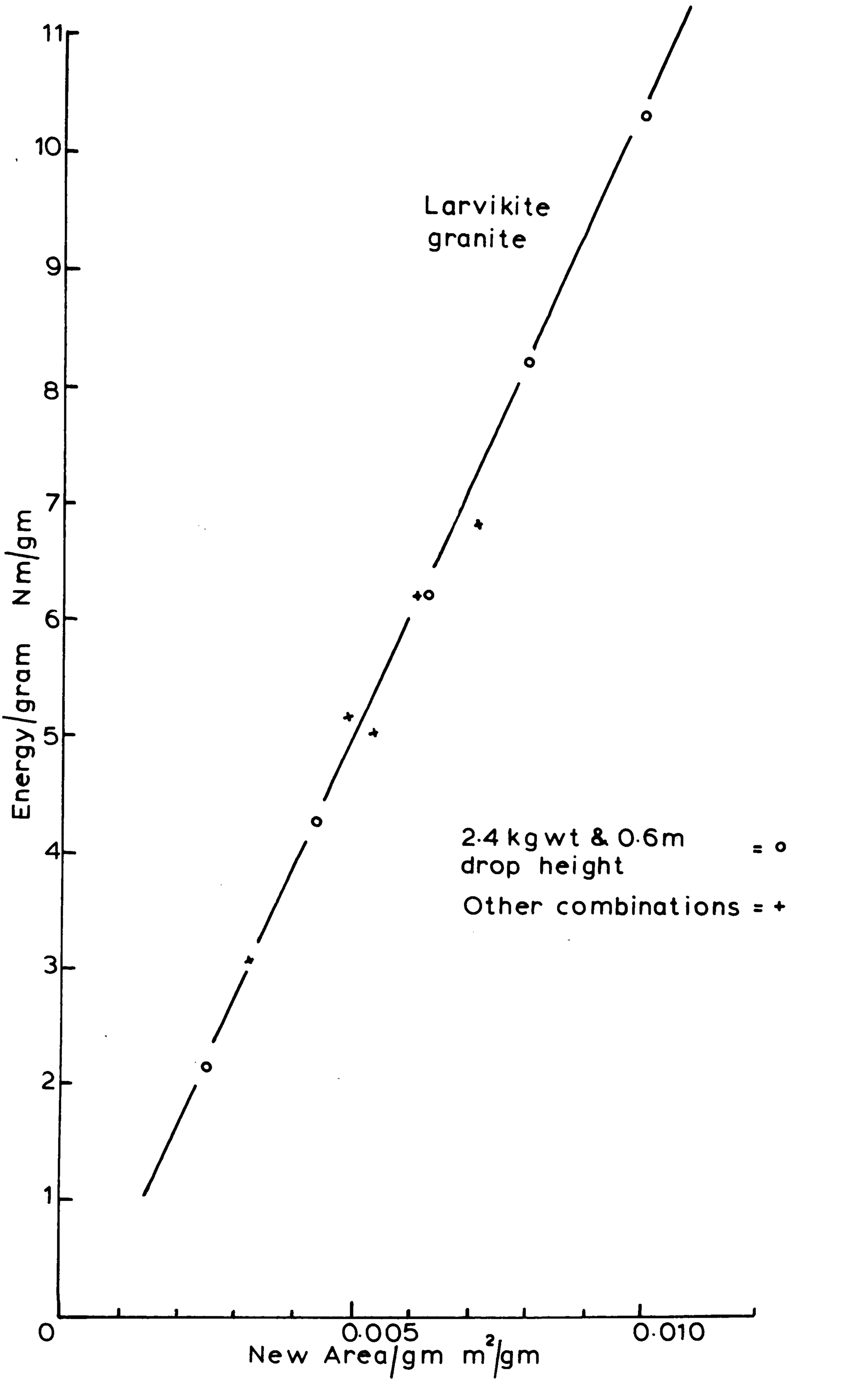

FIGURE 3.4: DROP HAMMER TESTS WITH DIFFERENT DROP HEIGHTS & WEIGHTS.

SECTION B STAMP MILL TESTS

Stamp mill tests were done in order to establish an index that might give a good correlation with rotary-percussive drilling. In the stamp mill method of breakage, the weight falls through a small drop height (about 1.6cm) and to achieve comparable energy inputs with the drop hammer and slow compression tests more blows must be applied. The height of fall is measured accurately before and after breakage using a micrometer mounted on the aparatus.

The diagram of the stamp mill is shown in figure 3.5. This apparatus was designed by Frangiskos (81) and consists of an A.C. motor (1/6 H.P.) which via a belt and pulley system rotates a cam shaft. The cam shaft has four cams, hence for one rotation of the cam shaft the weight (2.0264kg) is raised and allowed to fall freely four times. The number of rotations of the cam shaft is recorded on the counter, the number of blows is obtained by multiplying the rotations by four.

Particles between -4mm and +2mm in size are placed in the hardened steel mortar, these are spread evenly so that the interference of particles is diminished. The weight of the charge therefore, does vary from rock to rock and the criterion is an even spread of particles not a charge of constant weight as recommended by Frangiskos (81). In drop hammer and slow compression tests the regular size of the specimens (50mm long by 25mm diameter) is the criterion also giving varying weights of charge.

The blow rate of 200 blows/min at 50 R.P.M. cam shaft

STAMP MILL

KEY

A	CRUSHING HEAD
B	STEM
C	MORTAR BOX
D	ROTATING CAM
E	CAM SHAFT
F	TAPPET
G	WASHERS
H	POINTER
I	STEM BEARINGS
J	FRAME
K	MORTAR SECURING WEDGE
L	SMALL FLY WHEEL
M	MOTOR
N	REVOLUTION COUNTER
O	CAM SHAFT BEARINGS
P	WINDLASS FOR MORTAR
Q	WINDLASS PULLEYS
R	V BELTS
S	DRIVING SYSTEM
T	CONCRETE FOUNDATION

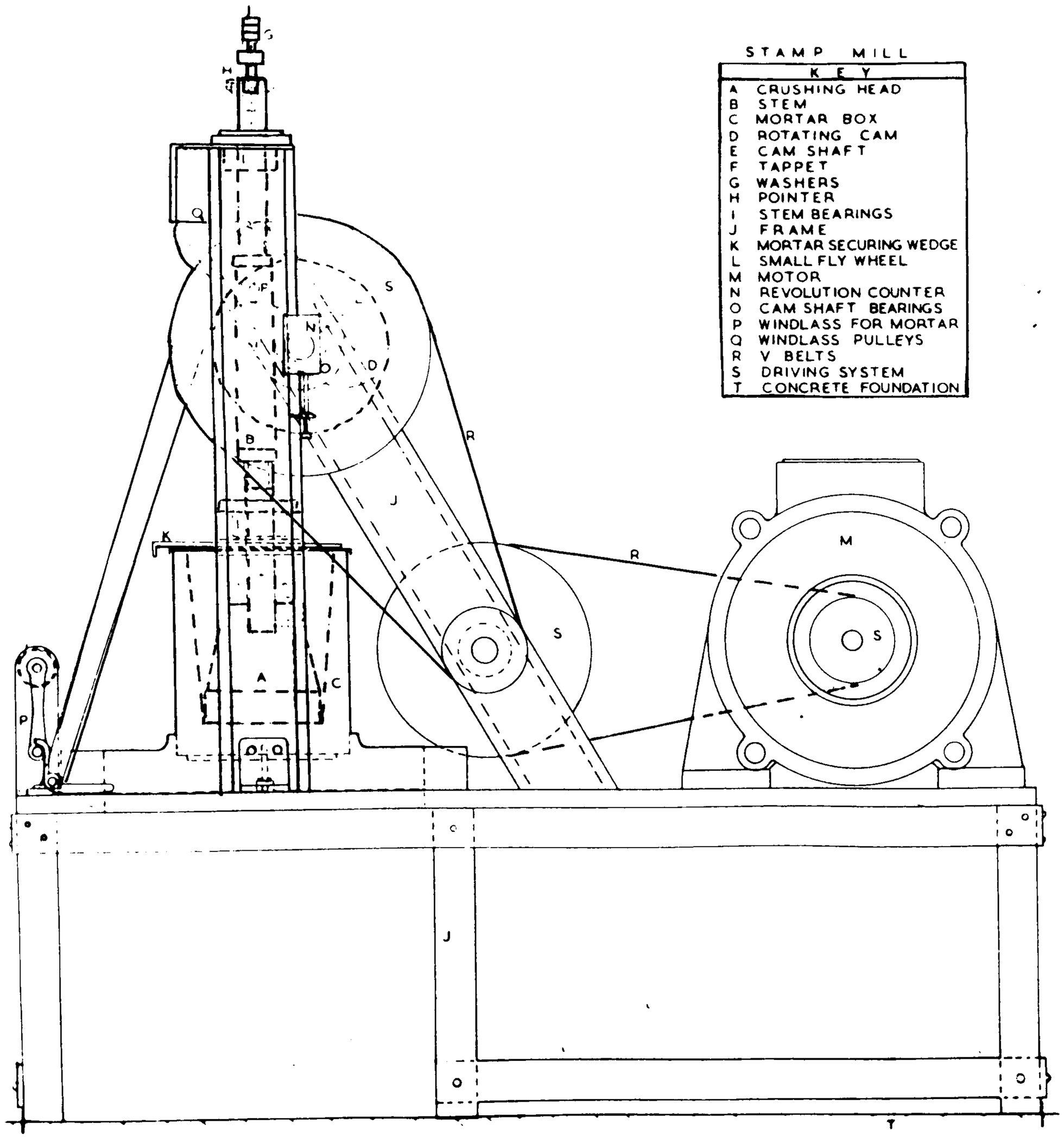

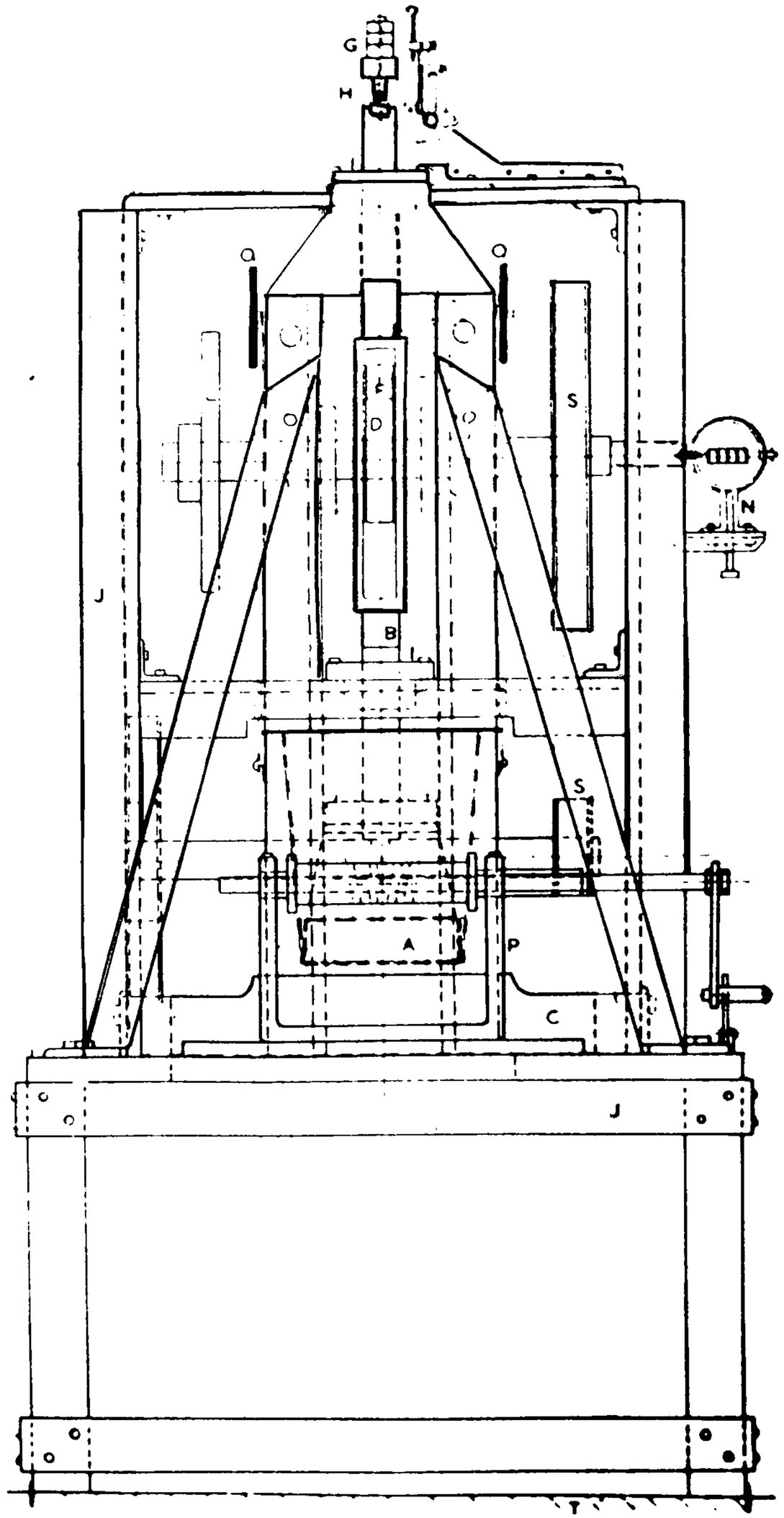

FIGURE 3.5: THE STAMP MILL .

speed recommended by Chakravarti (82) was used. An example of a size analysis and energy input calculation is shown below in table 13. After the first breakage the large particles are replaced in the mortar for further breakage at a higher energy level, then this product is sieved with the previous fines product for the calculation of surface area. This process is continued to give a reasonably spaced energy/gram against area/gram graph. Each energy level is added to the previous because it is the total energy input up to that size distribution to give that distribution. Table 13 gives an example of the size analysis for St. Bee's sandstone.

TABLE 13

St. Bee's sandstone. Size analysis showing weight retained on each sieve for 5 different energy levels.

Density, s = 2.569 gm/cc.

Blows	19	20	20	26	28
Total no. of blows..	19 blows	39 blows	59 blows	85 blows	113 blows
4mm	0	0	0	0	0
2mm	7.910	0.555	0	0	0
1mm	2.669	5.453	3.265	0.171	0.006
0.5mm	0.759	2.065	3.226	3.626	0.771
0.25mm	0.653	1.413	1.897	2.514	3.335
0.125mm	1.532	3.265	4.092	5.476	6.994
0.063mm	0.562	1.135	1.347	1.861	2.384
BASE	0.212	0.357	0.396	0.563	0.709
Total wt. in gms.	14.296	14.243	14.223	14.211	14.199
Surface area/gm. .....m^2 /gm.	0.004242	0.008096	0.009590	0.012430	0.015013

In the stamp mill tests by starting with particles betweeen 4 and 2mm there is a significant area/gram to start with, to obtain the new surface areas created the value for this initial area must be subtracted. This initial area is computed in the usual way from $\sum \frac{6}{s} \ell n\ 2 \frac{\text{wt of fraction}}{a_1 - a_2}$ and will be different for each rock. For St. Bee's sandstone the new surface areas created will be the surface areas/gms shown in table 12 minus $\frac{6}{2.569} \times \ell n\ 2 \times \frac{14.296}{4-2mm}$/14.296 the original surface area/gram which equals 0.000809 m^2/gram. The new surface areas/gram for St. Bee's sandstone are shown in table 15 along with the values for other rocks tested.

3.B1. Calculation of Energy/gram

The reading on the micrometer when the weight is at the position of the maximum lift of a cam is 2.480 cm. When particles are placed in the mortar, the weight is allowed to rest on them and the reading xcm on the micrometer is noted. After breakage the weight is again rested on the particles and the new reading ycm is noted.

So that,

$2.480 - x_n$ = the minimum height of fall in cm.

$2.480 - y_n$ = the maximum height of fall in cm.

where, n is the energy level for that rock.

Graphs were drawn using both values of x_n and y_n for each energy level, Groby Granite being the strongest rock tested and St. Bee's sandstone being one of the weakest were

plotted in this manner as examples shown in figure 3.6. Calculations of energy/gram values from weight of hammer x height of fall x number of blows x g/gram for the minimum and maximum heights of fall are shown in table 14.

TABLE 14

Energy/gram calculations for St. Bee's Sandstone and Groby Granite

St. Bee's Sandstone

Total number of blows	Minimum height of fall	Minimum Energy/gm	Maximum height of fall	Maximum Energy/gm	New surface area/gm
19	1.404	0.3709	1.431	0.3780	0.003345
39	1.429	0.7778	1.561	0.8496	0.007287
59	1.545	1.2741	1.610	1.3280	0.008781
85	1.602	1.9048	1.657	1.9701	0.011621
113	1.642	2.5788	1.730	2.7104	0.014204

Groby Granite

Total number of blows	Minimum height of fall	Minimum Energy/gm	Maximum height of fall	Maximum Energy/gm	New surface area/gm
80	1.387	1.7152	1.531	1.8933	0.0006780
281	1.318	5.7401	1.610	7.0110	0.002614
482	1.528	11.4651	1.581	11.8628	0.005143
682	1.586	16.8986	1.707	18.1878	0.007778
882	1.597	22.1031	1.672	23.1411	0.01043

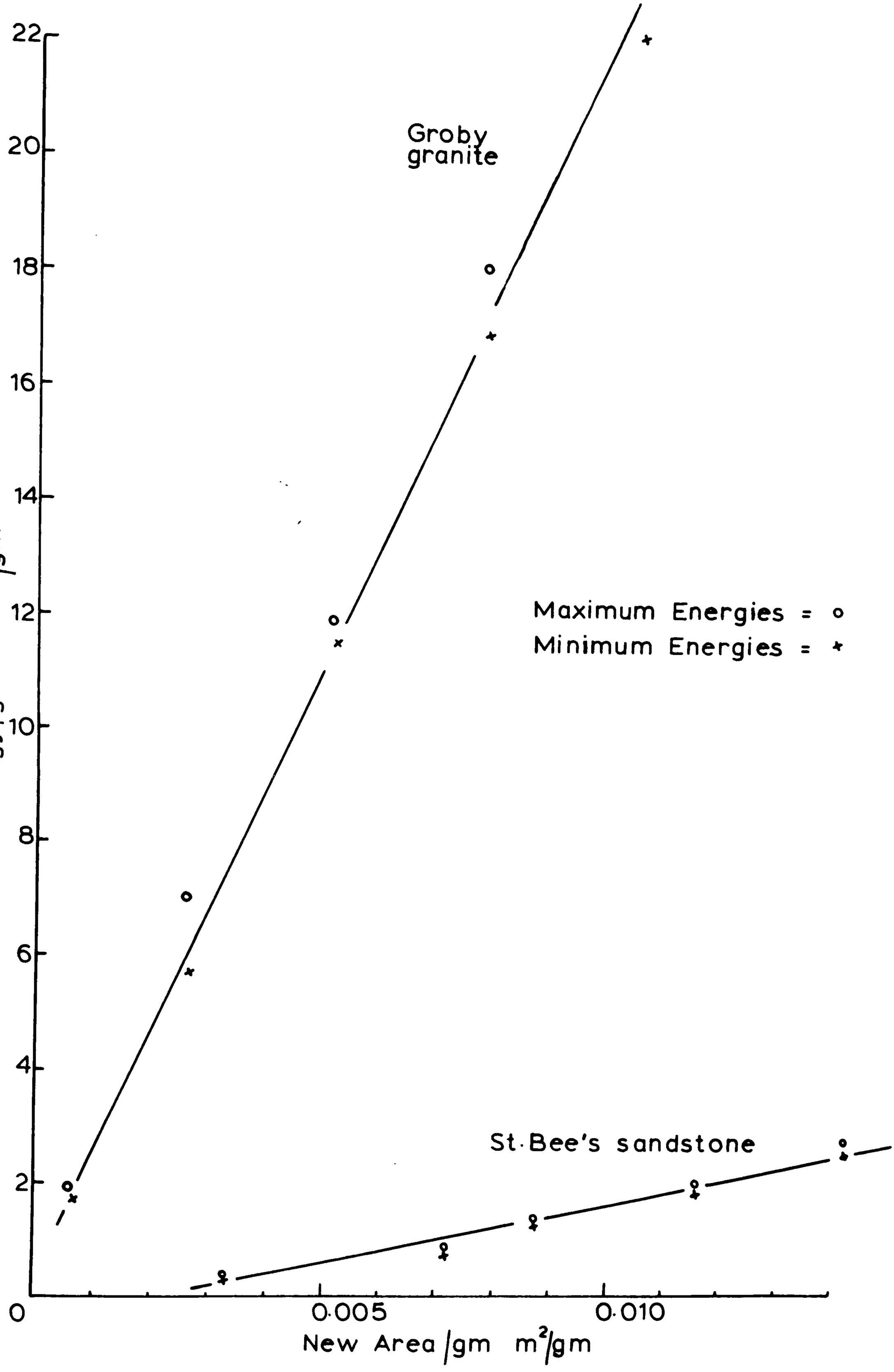

FIGURE 3.6: STAMP MILL TESTS SHOWING MAXIMUM AND MINIMUM ENERGY PER GRAM VALUES AGAINST THE NEW SURFACE AREA PER GRAM.

From figure 3.6 it can be seen that a good linear relationship is obtained whether minimum or maximum height of fall was used to calculate the energies/gram with little difference between the graphs. Therefore it was decided all energies/gram for all the rocks tested would be calculated by taking the mean height of fall of the weight.

Table 15 gives the energies/gram (mean energy values) and new surface areas/gram for all the rocks tested and these are plotted in figures 3.7 and 3.8. Table 15 also gives the values of the slopes of the lines and the correlation coefficients from the linear regression analysis for all the rocks tested. The rock index being taken as the slopes of the lines.

High correlation coefficients were obtained except for Yellow Oolitic limestone, Horsforth sandstone and St. Bee's sandstone where, the coefficients were slightly lower due to the upward curving through the method becoming inefficient when breaking the smaller particles.

TABLE 15

RESULTS OF STAMP MILL TESTS

Yellow Oolitic Lst.		Darley Dale Sst.		Horsforth Sst.	
Energy/gm	New Area/gm	Energy/gm	New Area/gm	Energy/gm	New Area/gm
0.2133	0.002150	0.1676	0.004115	0.3059	0.003601
0.4586	0.003191	0.3702	0.005057	0.6611	0.004911
1.1988	0.007062	0.7393	0.008039	1.0152	0.005700
2.0776	0.009420	1.1128	0.009614	1.3758	0.0062501
(2.9516	0.010102)	(2.0011	0.011143)	1.7940	0.006680
Slope E/A = 245.064		Slope E/A = 161.509		Slope E/A = 464.030	
c.c. = 0.988304		c.c. = 0.99121		c.c. = 0.96818	

St. Bee's Sst.		Elland Edge Sst.		Bath Lst.	
Energy/gm	New Area/gm	Energy/gm	New Area/gm	Energy/gm	New Area/gm
0.3745	0.003343	0.1998	0.001110	0.1130	0.000796
0.8137	0.007287	0.7072	0.002612	0.4711	0.001425
1.3011	0.008781	1.5121	0.005224	1.2070	0.003107
1.9375	0.011621	2.3012	0.008314	2.5492	0.005395
2.6446	0.14204	3.1553	0.011520	3.9593	0.007485
Slope E/A = 213.004		Slope E/A = 281.289		Slope E/A = 567.573	
c.c. = 0.98401		c.c. = 0.99875		c.c. = 0.99717	

....cont.

(Table 15 cont)

Craigenlow Pink Gr.		Cornish Granite		Denbigh Lst.	
Energy/gm	New Area/gm	Energy/gm	New Area/gm	Energy/gm	New Area/gm
1.1081	0.001290	0.4030	0.000371	0.2725	0.000423
3.8725	0,004409	1.6251	0.001170	0.9154	0.000911
5.4688	0.006271	2.8792	0.002159	2.2231	0.001894
7.1866	0.008297	4.4775	0.003341	3.9536	0.003215
9.3125	0.010610	6.2398	0.004682	5.5328	0.004471
Slope E/A = 869.043		Slope E/A = 1344.019		Slope E/A = 1301.750	
c.c. = 0.99990		c.c. = 0.99973		c.c. = 0.99994	

Whinstone		Mount Sorrel		Groby Granite	
Energy/gm	New Area/gm	Energy/gm	New Area/gm	Energy/gm	New Area/gm
1.8858	0.001261	1.1068	0.000663	1.8043	0.000678
6.2554	0.003718	3.5546	0.002171	6.3756	0.002614
8.8165	0.005772	7.6529	0.004710	11.6640	0.005143
11.8399	0.007980	11.8814	0.009651	17.5389	0.007778
		16.0427	0.007132	22.6221	0.01043
Slope E/A = 1541.957		Slope E/A = 1666.588		Slope E/A = 2137.001	
c.c. = 0.99821		c.c. = 0.99991		c.c. = 0.99951	

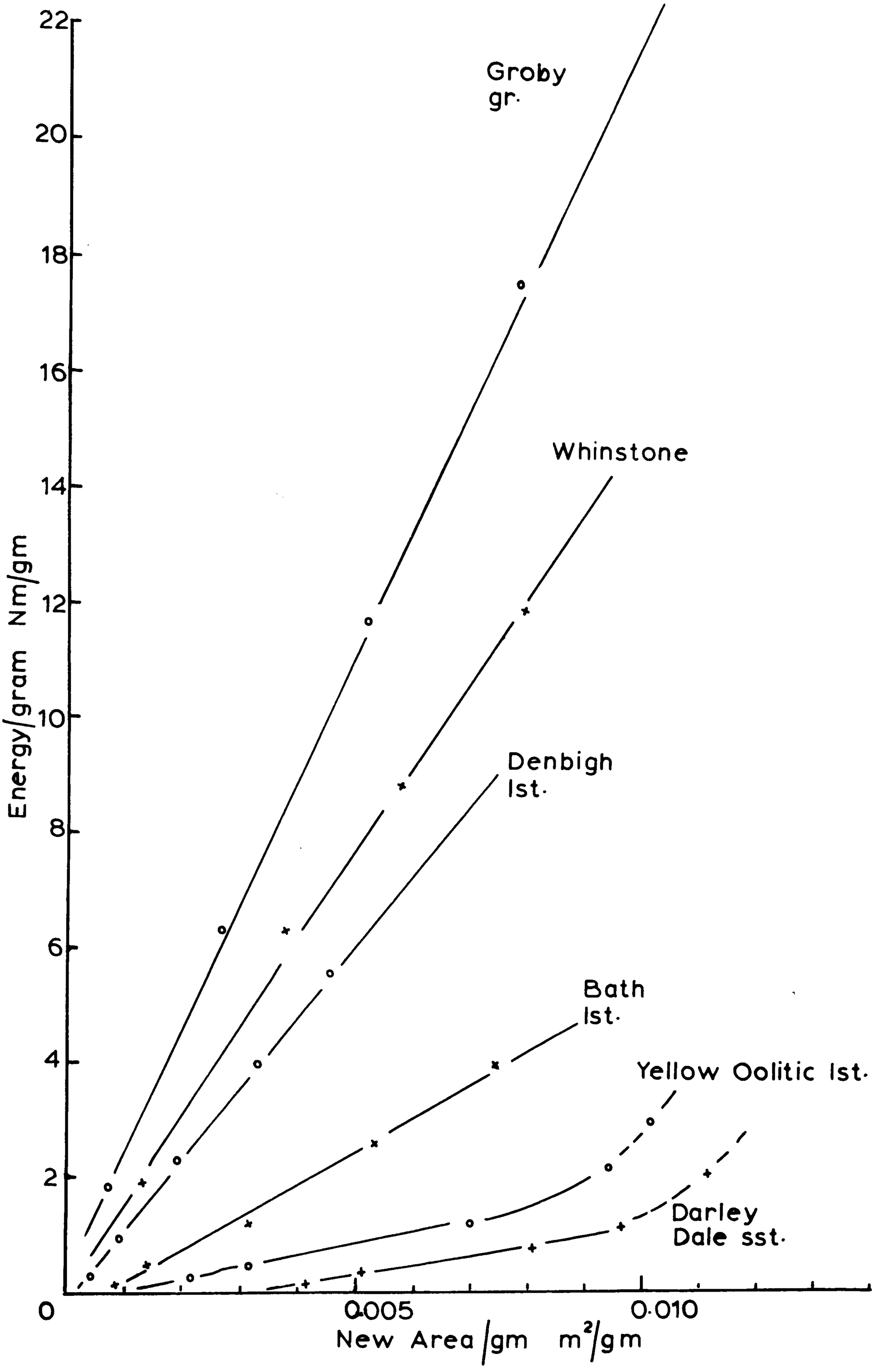

FIGURE 3.7: STAMP MILL TESTS.

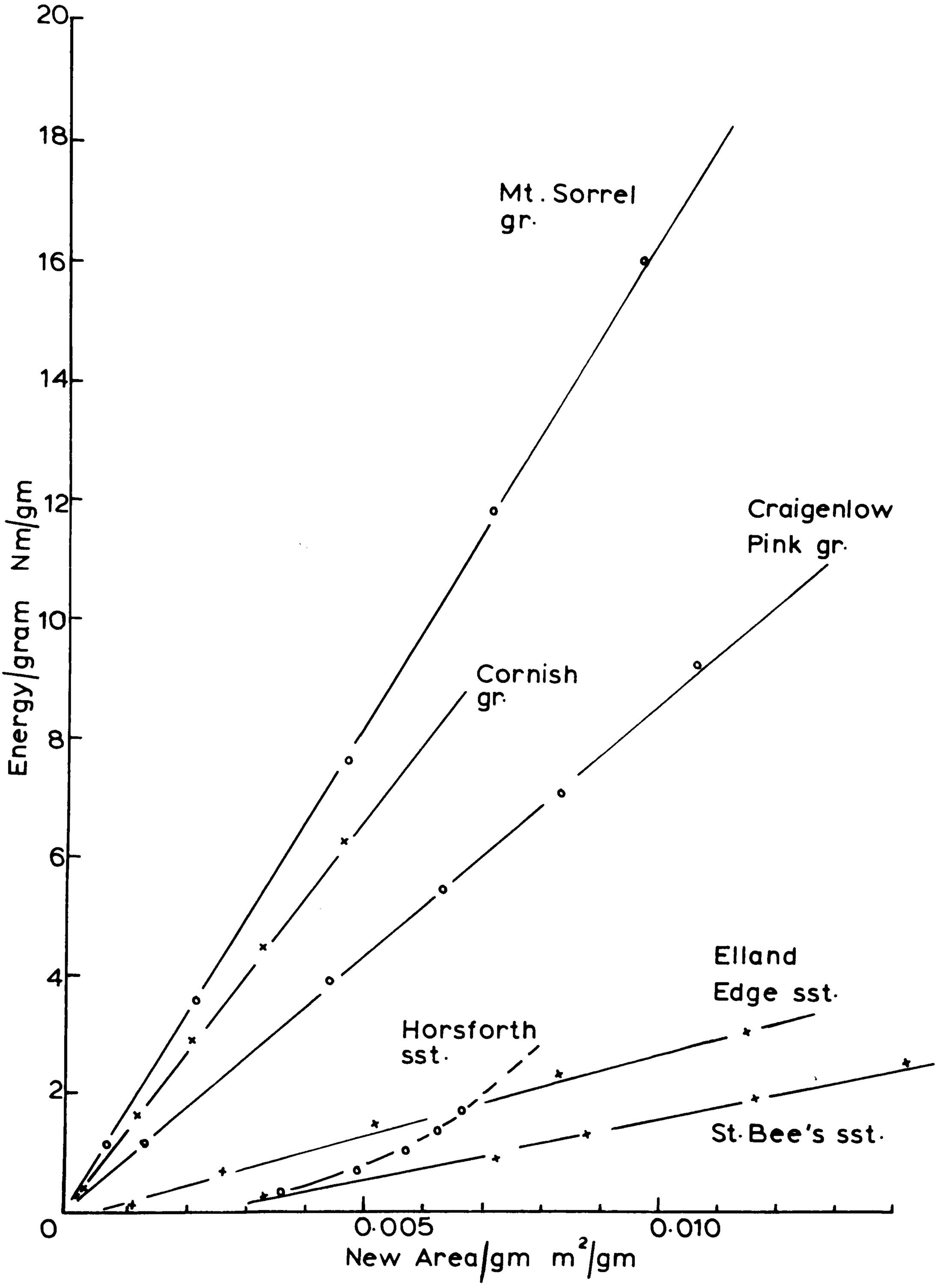

FIGURE 3.8: STAMP MILL TESTS.

SECTION C SLOW COMPRESSION TESTS

Two mortars are used for the purposes of crushing. The cores are first crushed in the large mortar, which has an internal diameter of 255mm and an internal depth of 50mm. A large mortar was used so that the drop hammer test in which 50mm long and 25mm diameter specimens were used could be compared directly with slow compression values. Also the large mortar is extremely useful for testing the larger particles in order to see the effect of breakage by slow compression. In the development tests described in chapter II only the small mortar was used as the large mortar hadn't then been made. After two or three crushes, depending on the rock being crushed, when there are no particles greater than 6mm in height crushing is done in a smaller mortar for convenience. The smaller mortar has an internal diameter of 119mm and a depth of 11mm. Photograph 2 shows the two mortars used in this work along with the nest of sieves.

Loading is carried out on the Instron testing machine, with the load range set at the maximum of 0 to 5000kg. Photograph 3 shows the large mortar being loaded in the Instron.

3.C1. Rocks under test

Ten rocks were tested Yellow Oolitic limestone, St. Bee's sandstone, Darley Dale sandstone, Bath limestone,

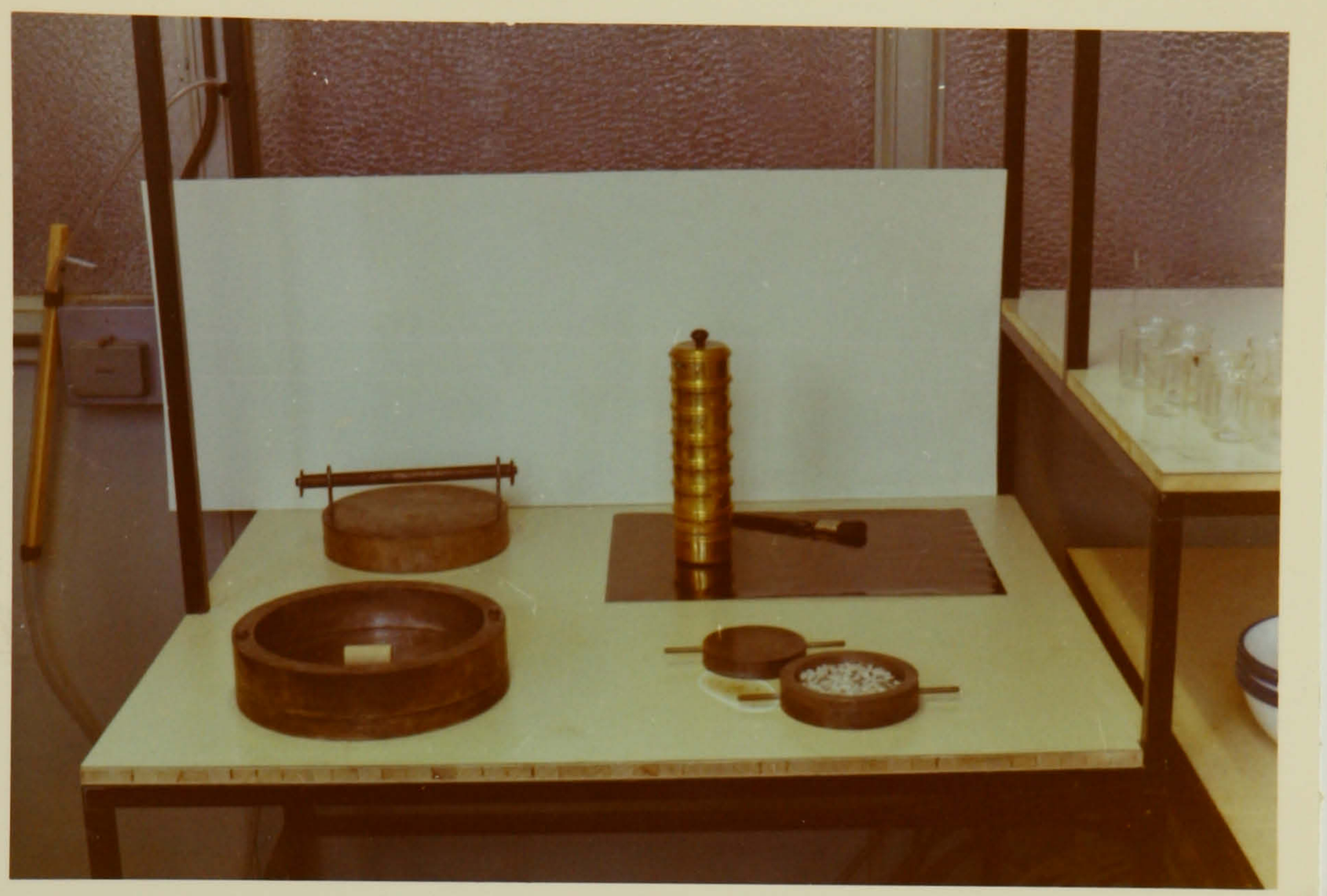

PHOTOGRAPH 2 : The Large and Small Mortars used for Slow Compression Testing.

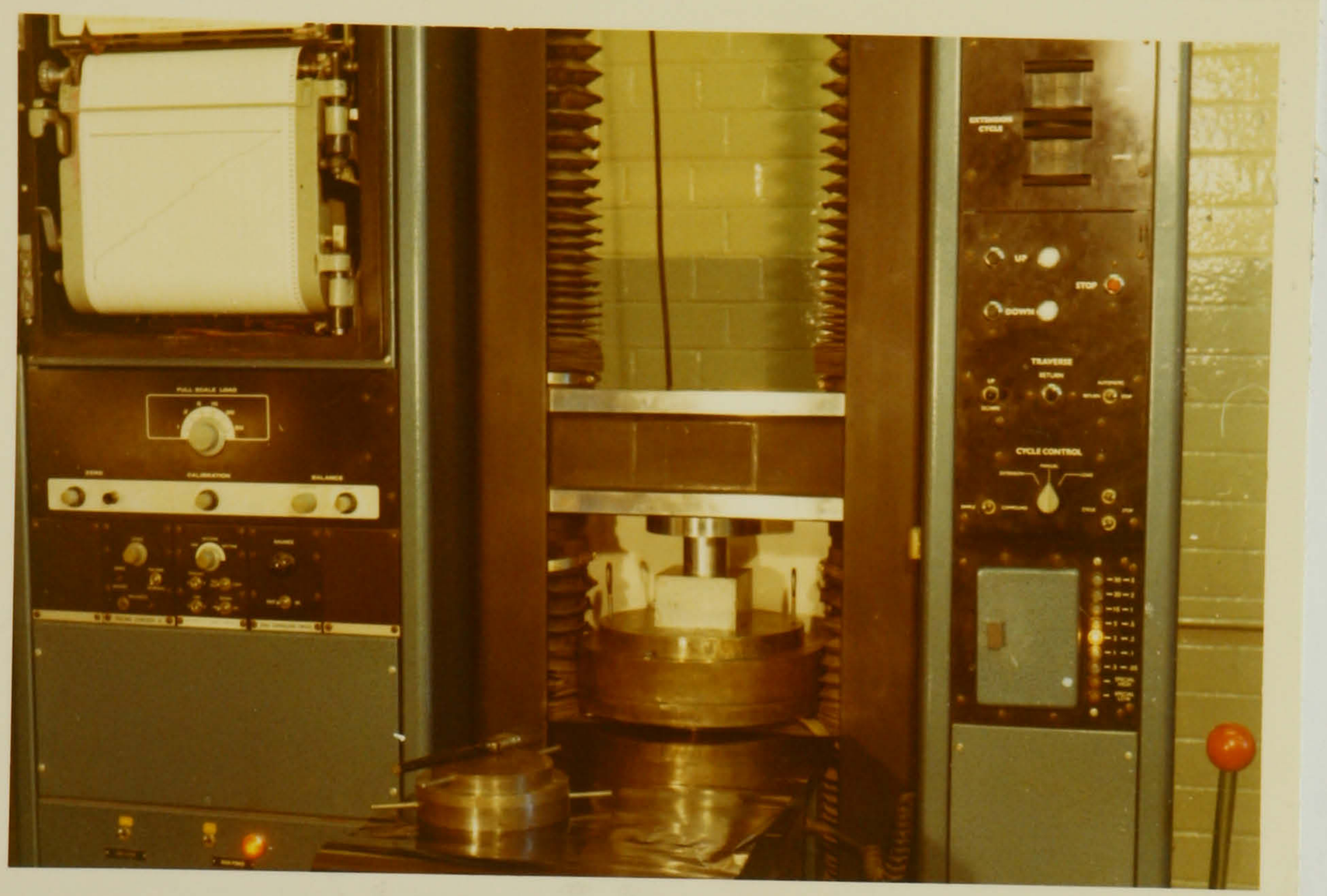

PHOTOGRAPH 3 : The Large Mortar Loaded in the

Instron Testing Machine

Elland Edge sandstone, Craigenlow Pink granite, Denbigh limestone, Cornish granite, Mount Sorrel granite and Groby granite.

3.C2. Method

The specimen is placed horizontally in the large mortar which is carefully centralised in the Instron. The cross-head was set to load at a rate of 0.2 cm/min and the chart to record at 5cm/min, a graph is plotted by the Instron recording the energy input to the specimen, the mortar and the machine. An empty run is made so that the energy input to the mortar and machine can be obtained. Figure 3.9 shows a typical output with the straight line for energy input to the mortar and machine drawn in. The shaded area represents the energy that has been used to crush the material.

Figure 3.9 Typical chart output shown digrammatically

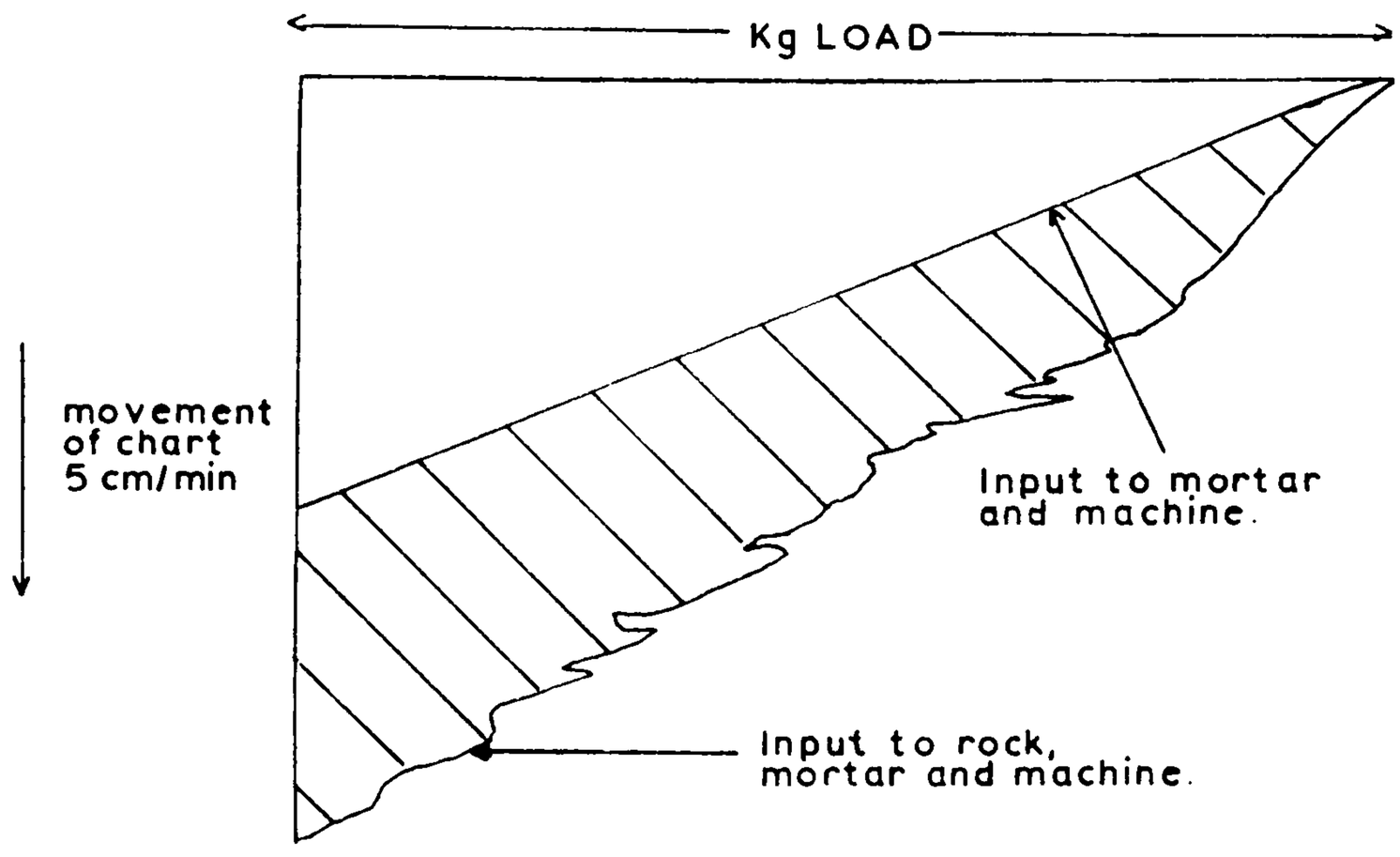

Load is applied via a loading block on to the mortar until the specimen breaks. The mortar is removed from the machine, then the particles are carefully brushed from the mortar. The crushed product is sieved on the Rotap for 10 minutes, and all the fractions are weighed. From the weights and sieve size, the surface area/gram is computed. For continuing runs to produce the energy/area graph, the large particles are replaced in the mortar, taking care to spread evenly, then loaded. The above process is repeated for as many times as required, firstly using the large mortar then later transferring to the smaller one for convenience. A reduction ratio of around 2 to 1 was used to give a well spaced graph of energy/gram versus area/gram.

3.C3. Surface Area/gram measurement

The areas/gram are computed on a Wang desk top computer from the derived expression $\sum \frac{6}{s} \ell n\ 2\ \frac{\text{wt. of fraction}}{a_1 - a_2}$ as detailed in chapter II.

An example of a sieve size analysis for the calculation of the surface area created per gram is shown in table 16 overleaf. Darley Dale sandstone has been chosen to show the analysis for 5 crushes in the Instron testing machine.

TABLE 16

Size analysis showing weight retained on each sieve for 5 crushes.

Darley Dale sandstone.

Density, s = 2.588 gm/c.c.

	1	2	3	4	5
4mm	46.446	22.246	0	0	0
2mm	1.463	7.967	1.919	0	0
1mm	1.026	3.562	11.083	0.195	0.030
0.5mm	1.045	3.560	9.186	10.441	7.545
0.25mm	2.170	7.852	15.945	23.176	24.218
0.125mm	1.739	5.713	9.867	12.737	14.212
0.063mm	0.786	2.248	3.583	4.270	4.602
BASE	0.867	2.403	3.722	4.248	4.406
Total wt. in gms.	55.543	55.412	55.305	55.066	55.013
Surface Area/gram ....m^2/gm	0.0022674	0.0058542	0.0101573	0.0122546	0.0128617
New Area/gm	0.0021781	0.0057630	0.0100692	0.0121661	0.0127729

(The New surface areas created are 0.000089m^2/gram less than the surface areas/gram quoted above. This is because the cylindrical specimen has this small area to start with.)

3.C4 Energy/gram Calculations

The energy inputs are obtained by measuring the shaded area shown in figure 3.9 either by weighing or planimetering. A conversion factor was calculated for 1 gm of chart paper, this was done by weighing a rectangle of graph paper 2 units by 4 cm. 2 units represents a load of 1000 kg. and 4 cms is proportional to the distance moved by the cross-head.

Four different rectangles were averaged, 0.1022, 0.1021, 0.1023, 0.1024, mean weight = 0.10225 gms. At 5cm/min chart speed and 0.2cm/min cross head speed, 0.10225 grams represents:-

$$1000\text{kg} \times \frac{4\text{cm}}{5\text{cm/min}} \times \frac{9.81}{100\text{cm}} \times 1\text{m} \times 0.2\text{cm/min of energy}$$

$$= 15.6960 \text{ Joules}$$

$$1\text{gm} = \frac{153.5061 \text{ Joules}}{} = \text{The Conversion Factor, C.F.}$$

Each energy value is added to the previous to give total energy values for each crush.

TABLE 17

Energy/gram calculations for Darley Dale sandstone.

Crush number	Wt. of graph paper gms. W	Energy values Joules WxC.F.	Total energy values Nm	Energy per gram Nm/gm of rock
1	0.1758	26.979	26.979	0.4857
2	0.2871	44.072	71.051	1.2790
3	0.0924	14.189	85.250	1.5415
4	0.0315	4.835	90.085	1.6361
5	0.0208	3.185	93.270	1.6952

Hence a graph of Energy/gram against New Area/gram can be drawn from the above calculations. The results of tests for the nine other rocks by slow compression have been treated in the same way and table 18 gives Energy/gram and New Area/gram values. The plots of Energy/gram against New Area/gram are shown in figures 3.10 and 3.11 for the nine rocks and Darley Dale sandstone.

TABLE 18

Slow Compression on nine rocks, Energy/gram and New Area/gram values.

Yellow Oolitic Lst.		St. Bee's Sst.		Elland Edge Sst.	
Energy/gm	New area/gm	Energy/gm	New area/gm	Energy/gm	New area/gm
0.2161	0.004848	0.4056	0.002027	0.2502	0.000769
0.2735	0.006217	0.8236	0.005498	0.8711	0.002930
0.4531	0.008970	1.1110	0.008828	1.6399	0.005747
0.6375	0.010809	1.3410	0.013552	2.2955	0.009721
0.8724	0.011812	1.4005	0.0153890	2.5163	0.012274

Bath Limestone		Craigenlow Pink Granite		Cornish Granite	
Energy/gm	New area/gm	Energy/gm	New area/gm	Energy/gm	New area/gm
0.4683	0.001638	0.1984	0.000618	0.1778	0.000623
0.1060	0.003680	1.5329	0.003501	1.3300	0.001990
1.4247	0.004938	2.6970	0.006820	2.9226	0.004407
1.8419	0.007031	2.9551	0.007700	3.3387	0.005603
2.0476	0.008574	3.2971	0.009366	3.7027	0.006940

Denbigh Limestone		Mount Sorrel Granite		Groby Granite	
Energy/gm	New Area/gm	Energy/gm	New Area/gm	Energy/gm	New Area/gm
1.0593	0.001031	0.3092	0.000852	0.7561	0.001048
2.1768	0.002523	2.0892	0.003456	2.6174	0.002585
2.9313	0.003723	3.3624	0.005456	3.4910	0.003349
3.1917	0.004682	4.2214	0.007999	4.0442	0.004123
3.3473	0.005443	5.0218	0.009850	4.5848	0.004883
				5.4570	0.006568

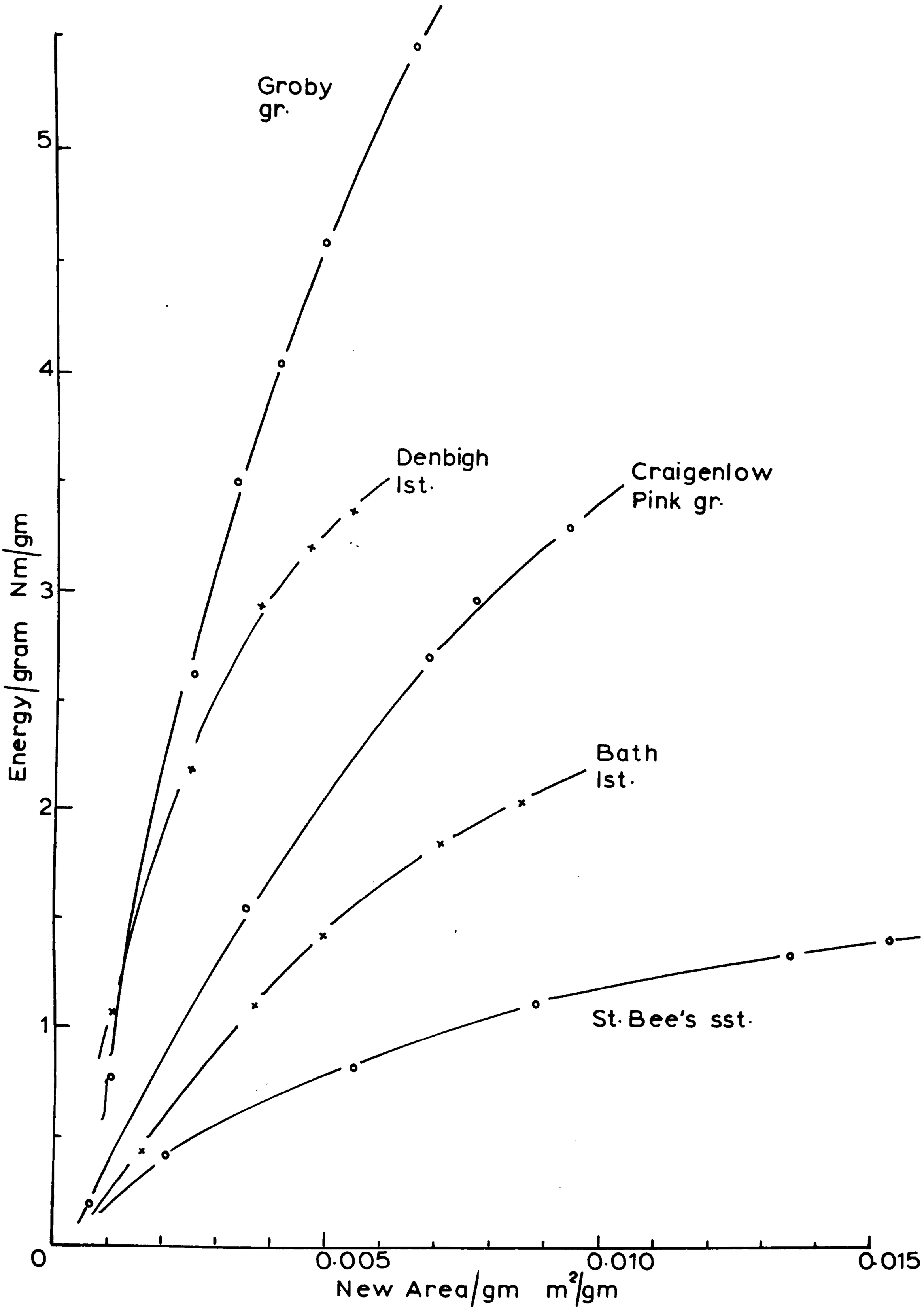

FIGURE 3.10: SLOW COMPRESSION TESTS.

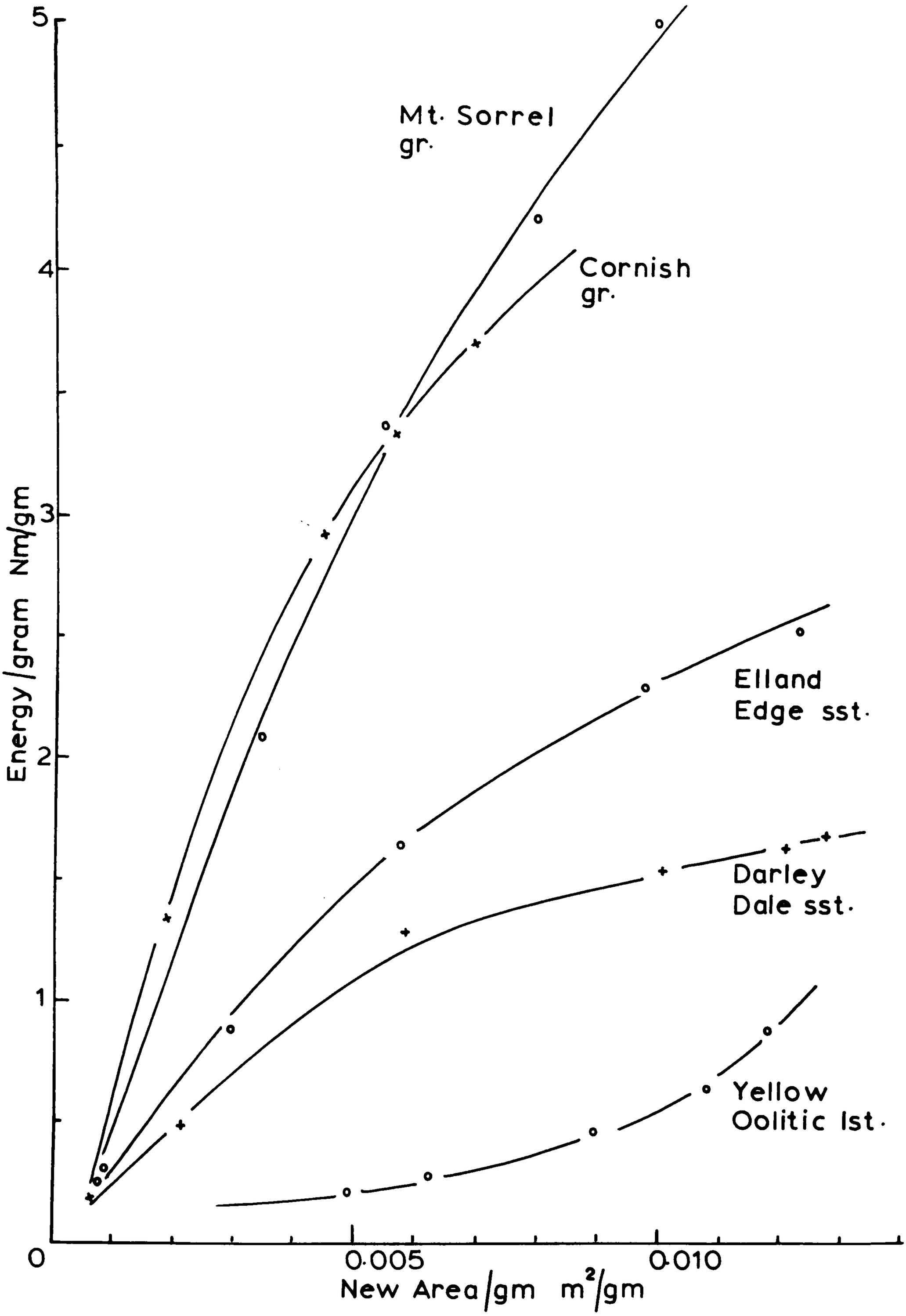

FIGURE 3.11: SLOW COMPRESSION TESTS.

SECTION D Comparison and Discussion of Drop Hammer Stamp Mill and Slow Compression Tests.

3.D1 Higher Energy Levels in Slow Compression and Drop Hammer Breakage

The expected Energy/area relationship can be divided into three regions, a) linear b) curvilinear and c) asymptotic region. These regions are shown diagrammatically in figure 3.12 below.

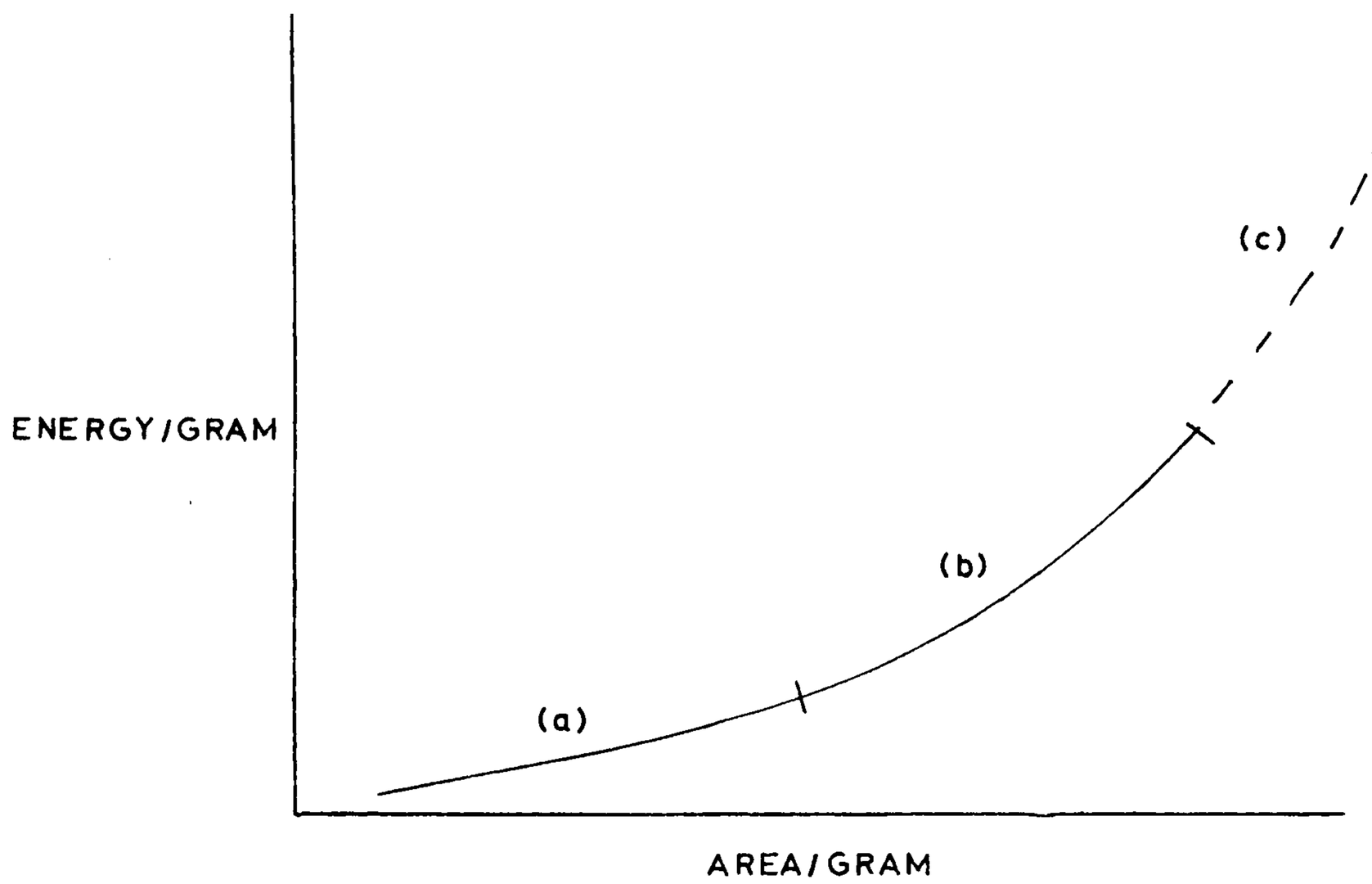

Figure 3.12
The graphical Energy/area relationship

The results for the drop hammer and stamp mill tests do conform to this relationship but the slow compression results give an opposite curvature shown in figures 3.10 and 3.11. In the view of these results it was felt that higher energy levels should be applied to see the effect on the slow compression tests. Three rocks, Yellow Oolitic limestone, Elland Edge sandstone and Craigenlow Pink granite, were further tested at higher energy levels. These rocks were also tested

at higher energy levels by drop hammer just to compare this effect. Figure 3.13 shows the Energy/gram against New Area/gram for the three rocks tested by slow compression and figure 3.14 for the same rocks tested by drop hammer. The figures 3.13 and 3.14 have the same Area/gram scale, but the Energy/gram scale for the drop hammer results is twice as small as Energy/gram scale for slow compression.

From figure 3.13 for slow compression, it can be seen that the results do eventually conform to the expected Energy/area relationship. Unfortunately, there is no obvious explanation for the phenomena of the initial curvature in slow compression testing. Figure 3.14 for drop hammer shows the Energy/area relationship without any complications, though tests haven't been fully extended to region (c).

3.D2. Indices for Drop Hammer, Slow Compression and Stamp Mill.

As the slow compression graphs of Energy/area are curvilinear, obtaining an index can be done by taking a fixed value of Area/gram for all the rocks and the corresponding Energy/gram will be the rock index. $0.0050 m^2$/gram was chosen as the fixed value of Area/gram. For the drop hammer and Stamp Mill tests the slope of the Energy/area line obtained from linear regression is taken as the index. Table 23 gives a list of the indices developed and other indices used in this work.

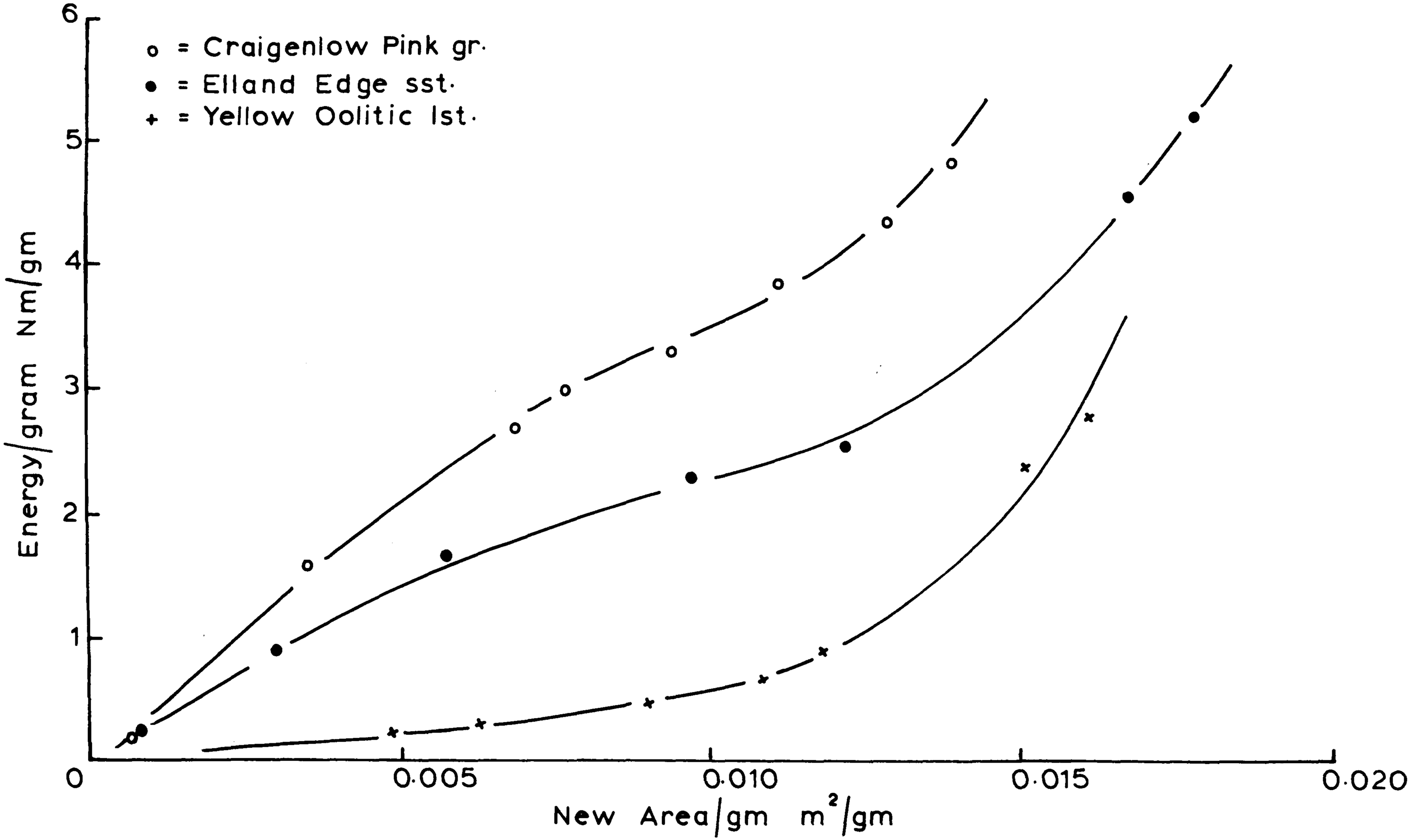

FIGURE 3.13: SLOW COMPRESSION TESTS WITH HIGHER ENERGY INPUTS.

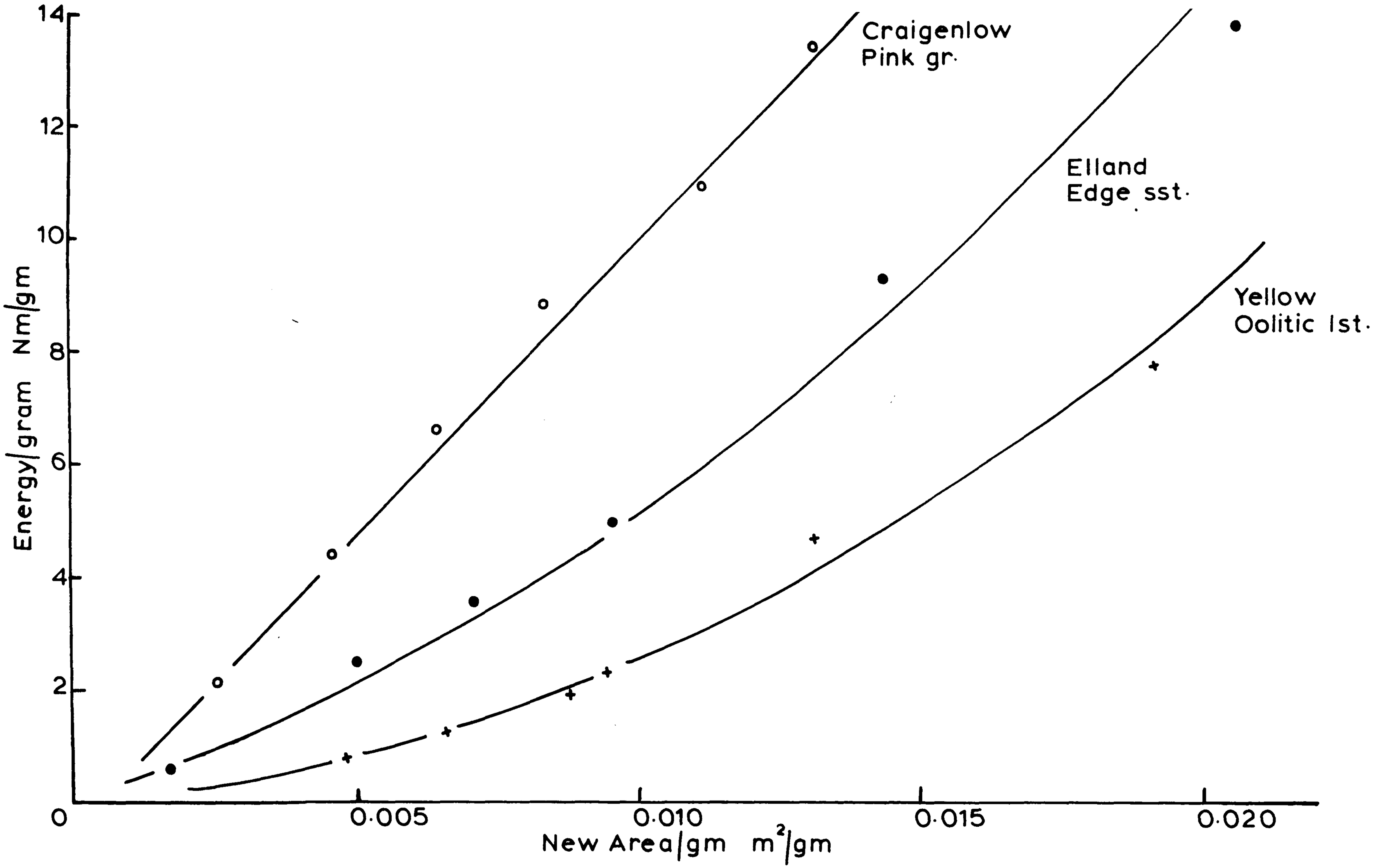

FIGURE 3.14: DROP HAMMER TESTS WITH HIGHER ENERGY INPUTS.

Hence the indices can be used as rock properties to try to predict machine performance and also to compare energy usage in other rock breaking processes. In chapter IV, where laboratory rock drilling is reported, the indices have been used to try to predict machine performance and to compare the efficiency of the drilling process.

3.D3. Comparison of the Drop Hammer and Slow Compression Tests.

The efficiency of the drop hammer tests can be compared directly with the slow compression tests as the same size cylindrical specimens have been used and the results analysed in the same manner. However, to show that the differences between the drop hammer and slow compression tests are not due to the fact that in slow compression, after the initial breakage of the cylindrical specimen, only the larger particles are replaced in the mortar. [With the drop hammer tests, coarse and fine particles are both in the Syskov mortar after the first drop on the cylindrical specimen. Coarse and fine particles are crushed by the hammer until the desired energy level is reached. To reach another energy level, a new cylindrical specimen is used and is crushed in the Syskov mortar until the new energy level is reached.] Therefore, Bath limestone was crushed in the drop hammer apparatus, following the slow compression technique of only replacing the larger particles at each new energy level, as opposed to using

a new cylindrical specimen for each energy level.

The results on the drop hammer test on Bath limestone are shown in table 19 and the Energy/gram against New Area/gram values are plotted in figure 3.15. Figure 3.15 also shows the normal method of determining Energy/area relationships, with the cylindrical specimens, so as to compare these with the values obtained by replacing the larger particles into the Syskov mortar after the slow compression method.

TABLE 19

Bath limestone crushed by drop hammer with the replacement of the larger particles in the Syskov mortar.

Number of blows	Total number of blows	Energy/gm Nm/gm	New Area/gm m^2/gm
5	5	1.3130	0.002768
5	10	2.5138	0.003548
5	15	3.7722	0.006197
5	20	5.0317	0.007385
5	25	6.2926	0.009003

correlation coefficient = 0.98955

slope E/A = 748.782

Graphically (from figure 3.15) there is no significant difference between the two methods i.e. the normal way of using rock cylinders and that of using one cylinder and replacing the larger particles. However, the linear

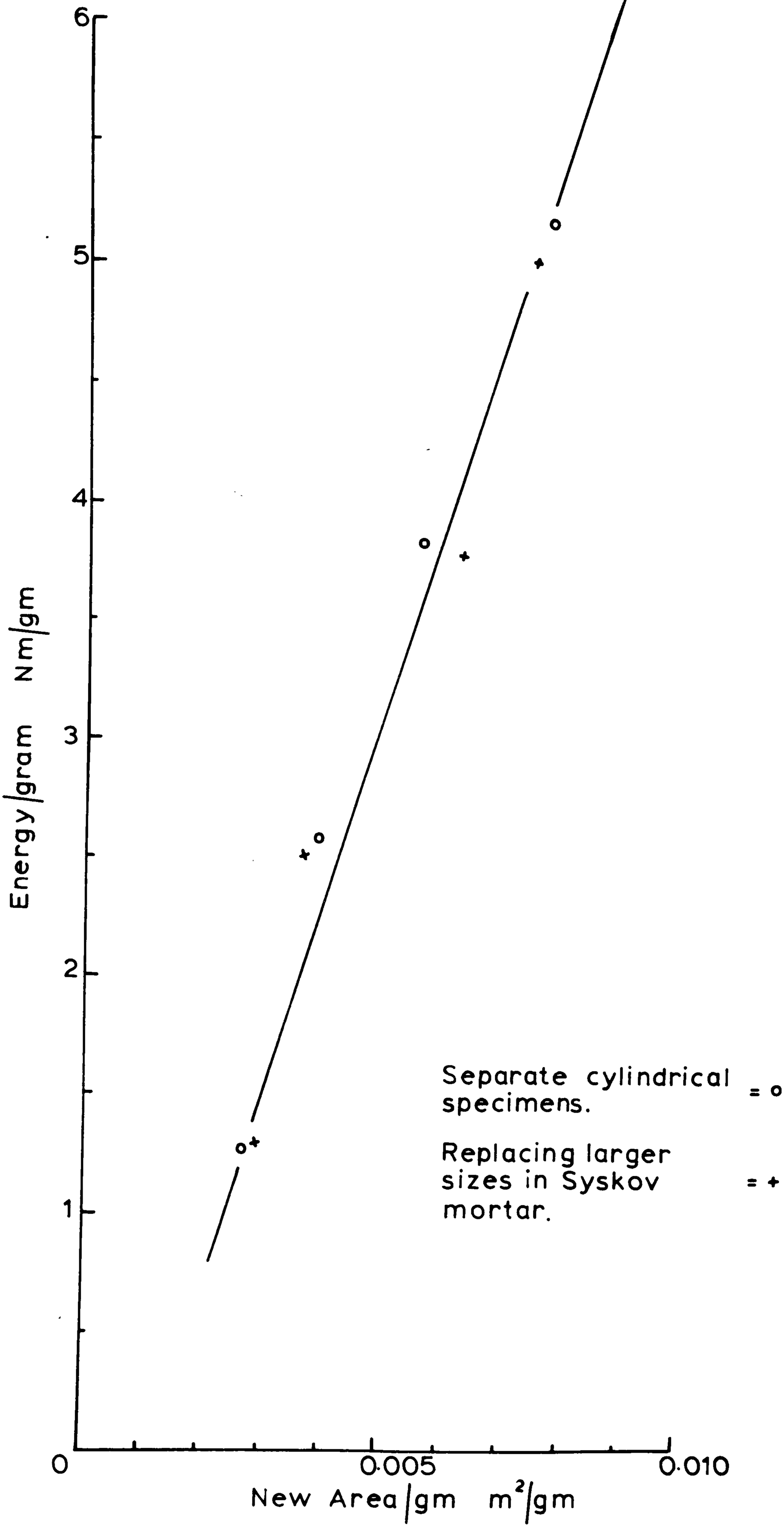

HAMMER TESTS ON BATH LIMESTONE.

regression analysis gives a lower correlation coefficient 0.98955 as opposed to 0.99721 and a slope of 748.782 as opposed to 787.184. The correlation coefficients indicate that by using the one specimen the method is slightly less accurate, but becomes a little more efficient as seen from the slopes. As this difference is very small and with a graphical representation there is very little change, it can be concluded that a graphical comparison of slow compression and drop hammer would be sufficient, because any difference will be due to the method of breakage or the efficiency of the process.

3.D4. Graphical comparison of Slow Compression and Drop Hammer Tests.

Figures 3.16 and 3.17 show the graphical comparison of slow compression to drop hammer for ten different rocks. Clearly the two methods have very different efficiencies and at the smaller values of New Area/gram, efficiency varies from rock to rock. With Yellow Oolitic limestone, Darley Dale, St. Bee's and Elland Edge sandstones, the drop hammer tests at the smaller values of area/gram are more efficient when compared to slow compression. This is understandable as it is easier for a drop hammer to break the bonding or cementing in the softer rocks and cause more initial destruction than slow compression. This fact of drop hammer being more efficient than slow compression in the smaller regions of area/gram ties in with the primary

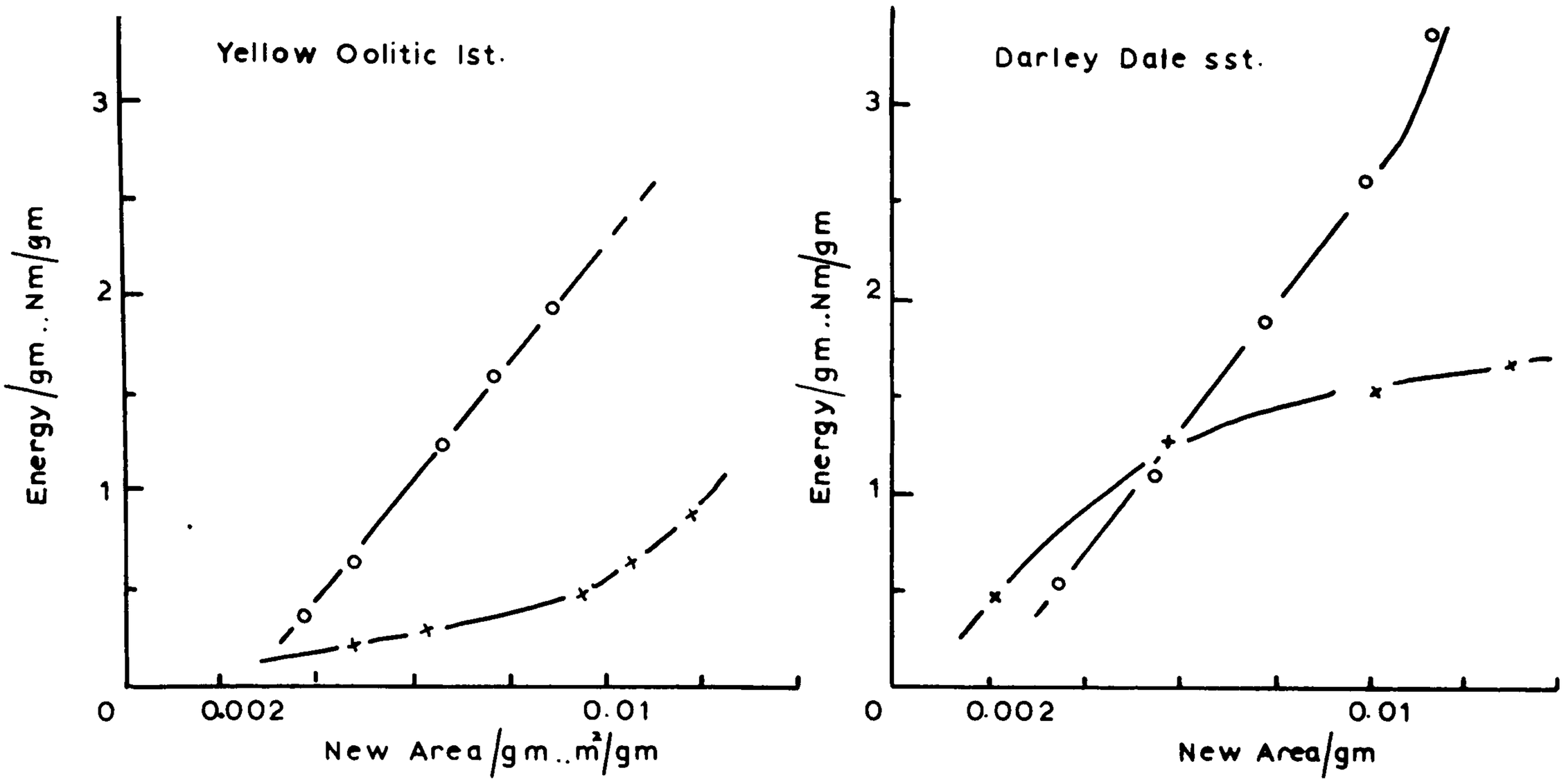

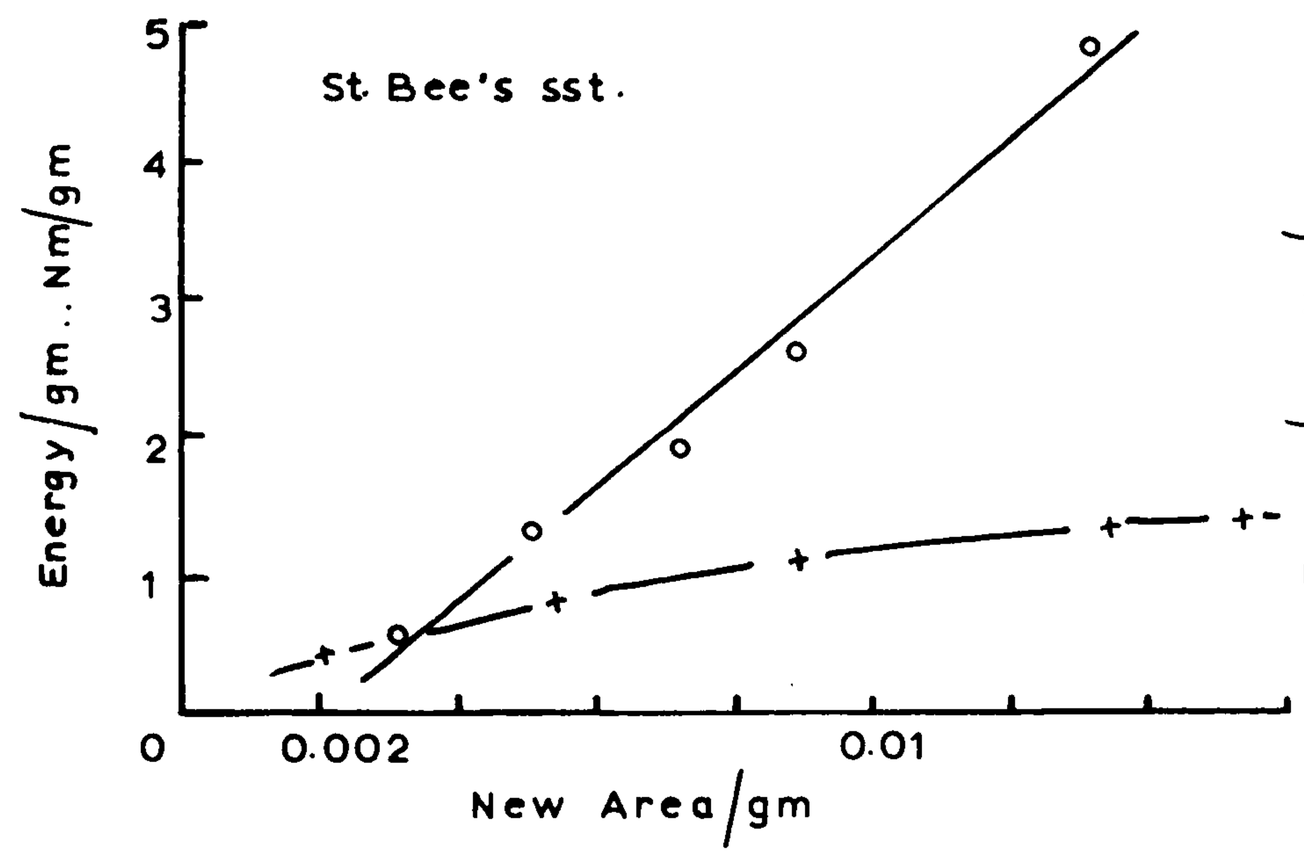

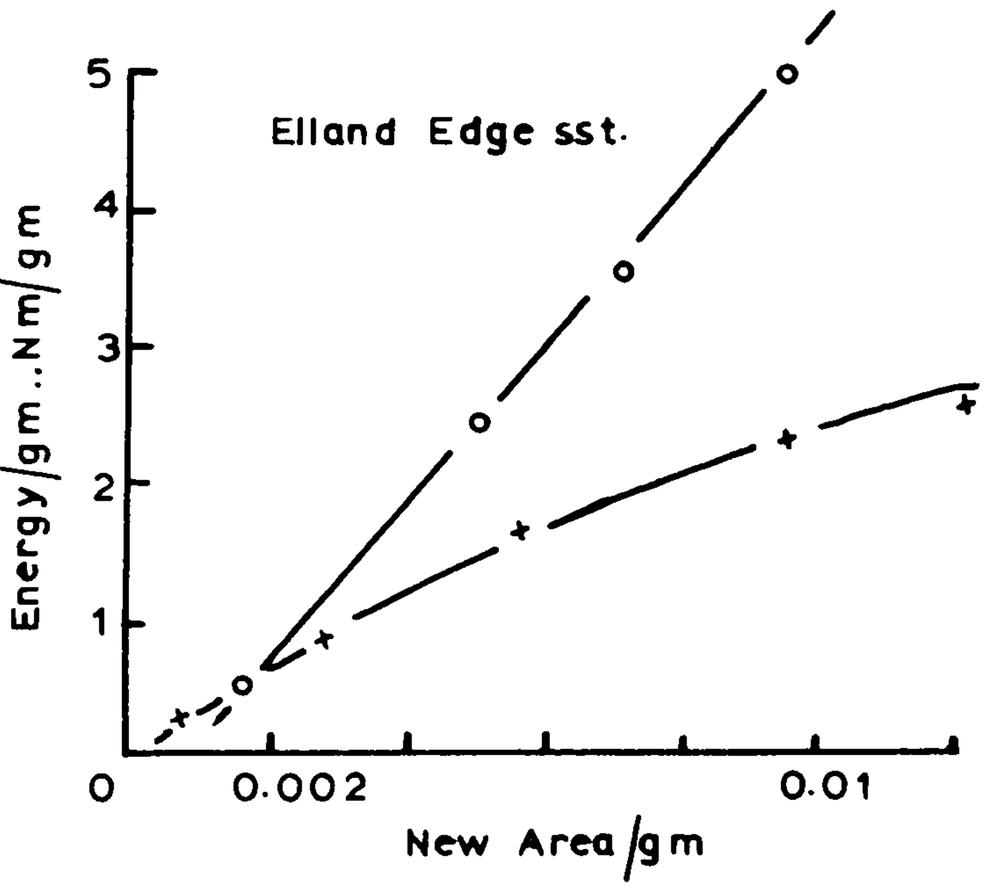

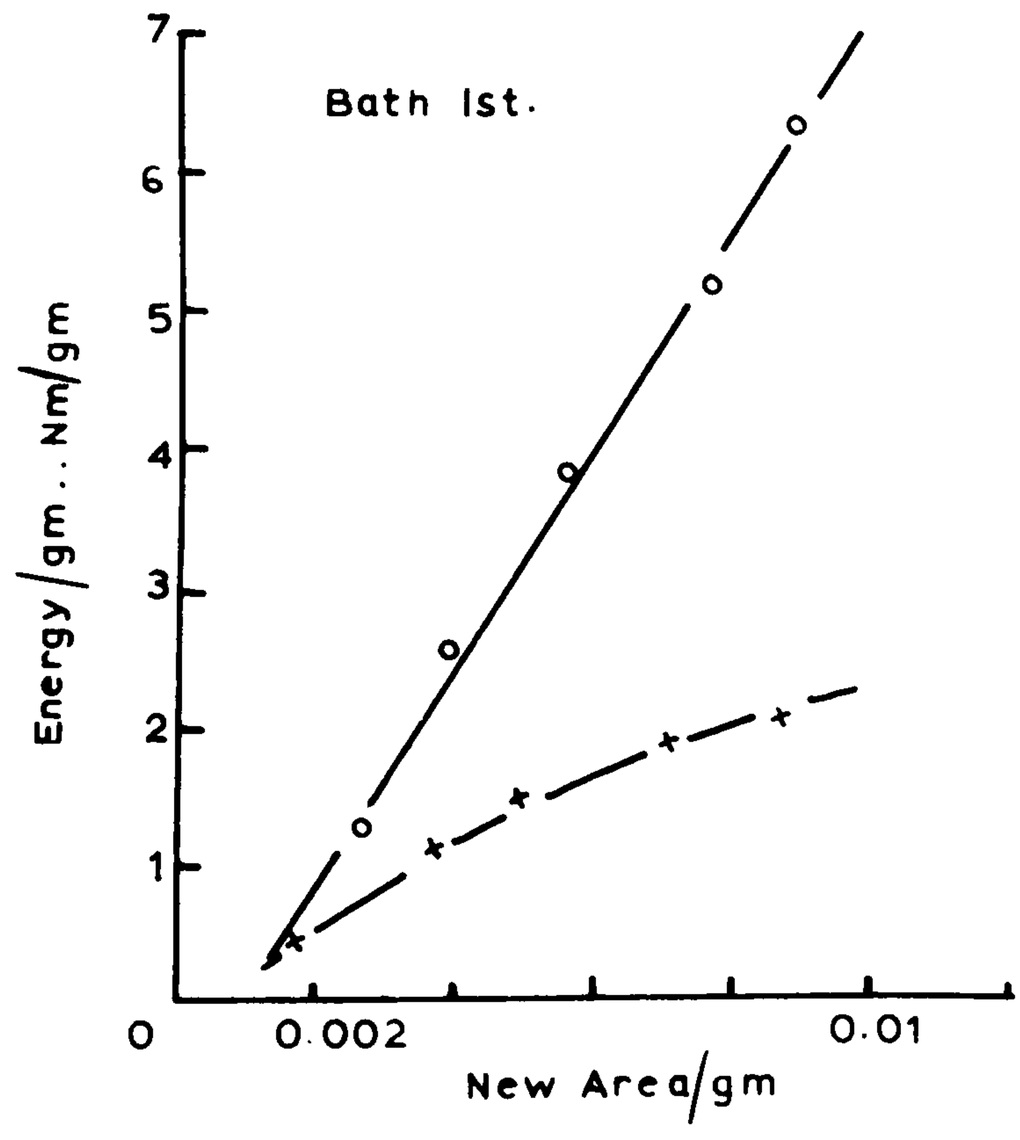

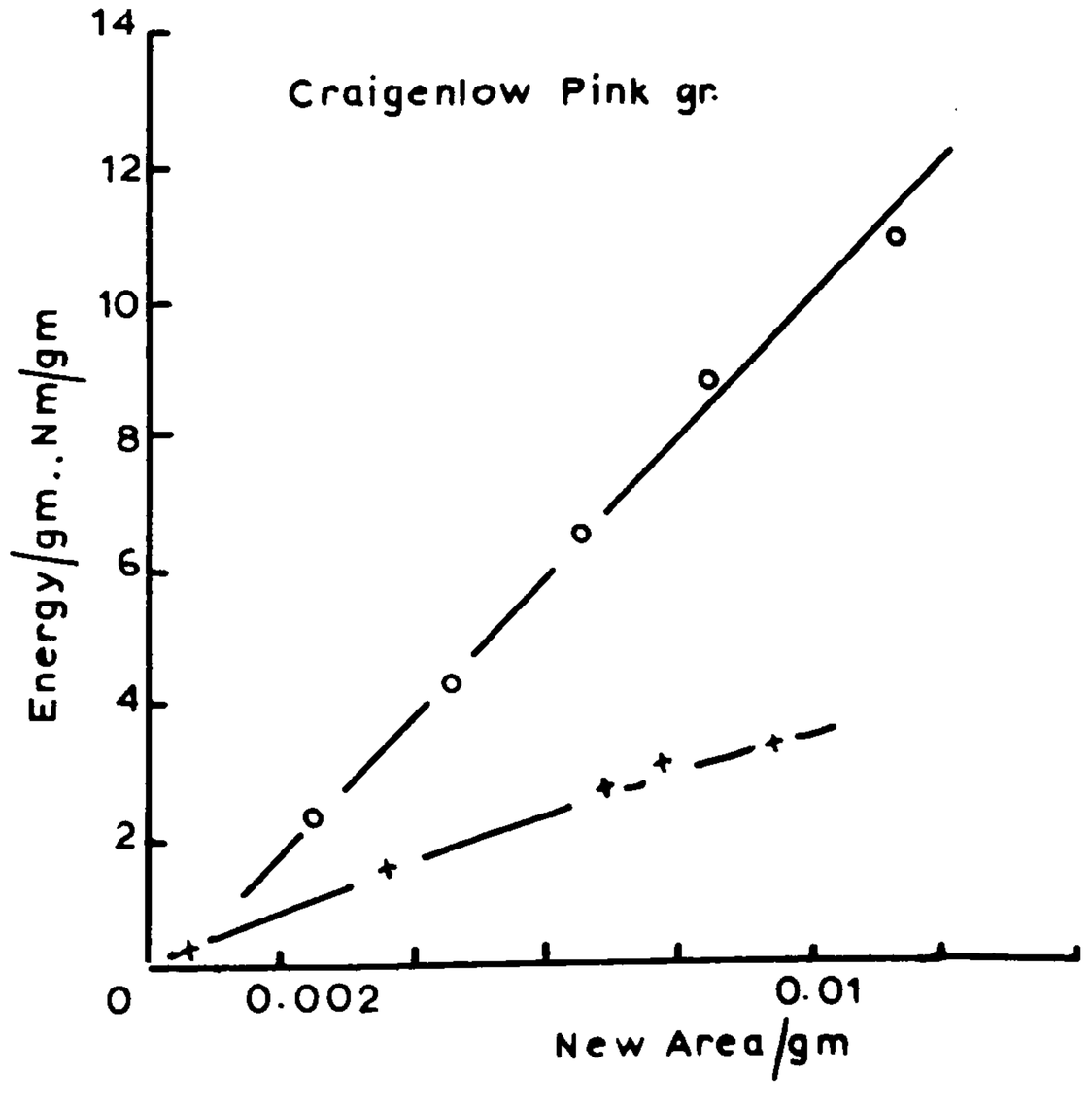

FIGURE 3.16: COMPARISON OF SLOW COMPRESSION & DROP HAMMER TESTS.

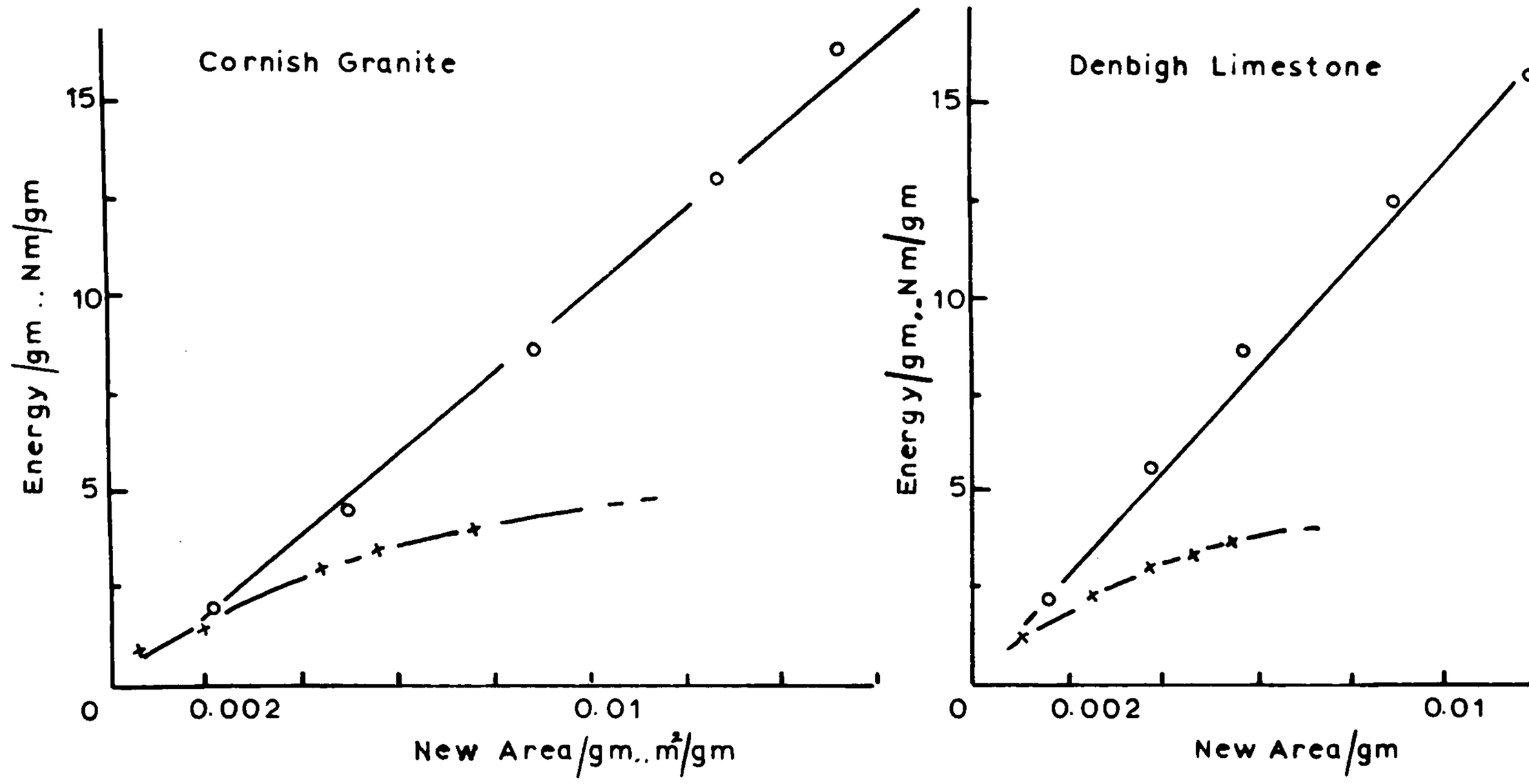

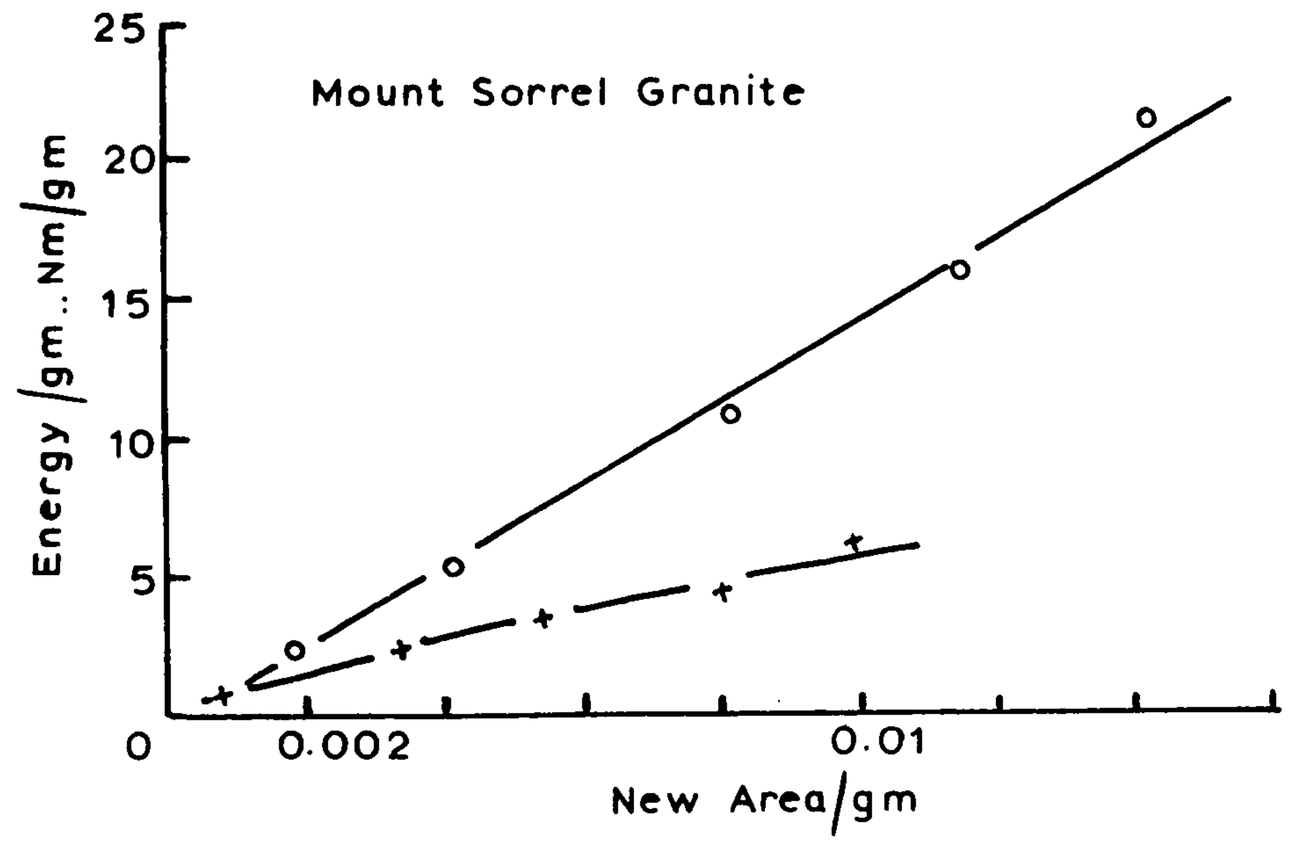

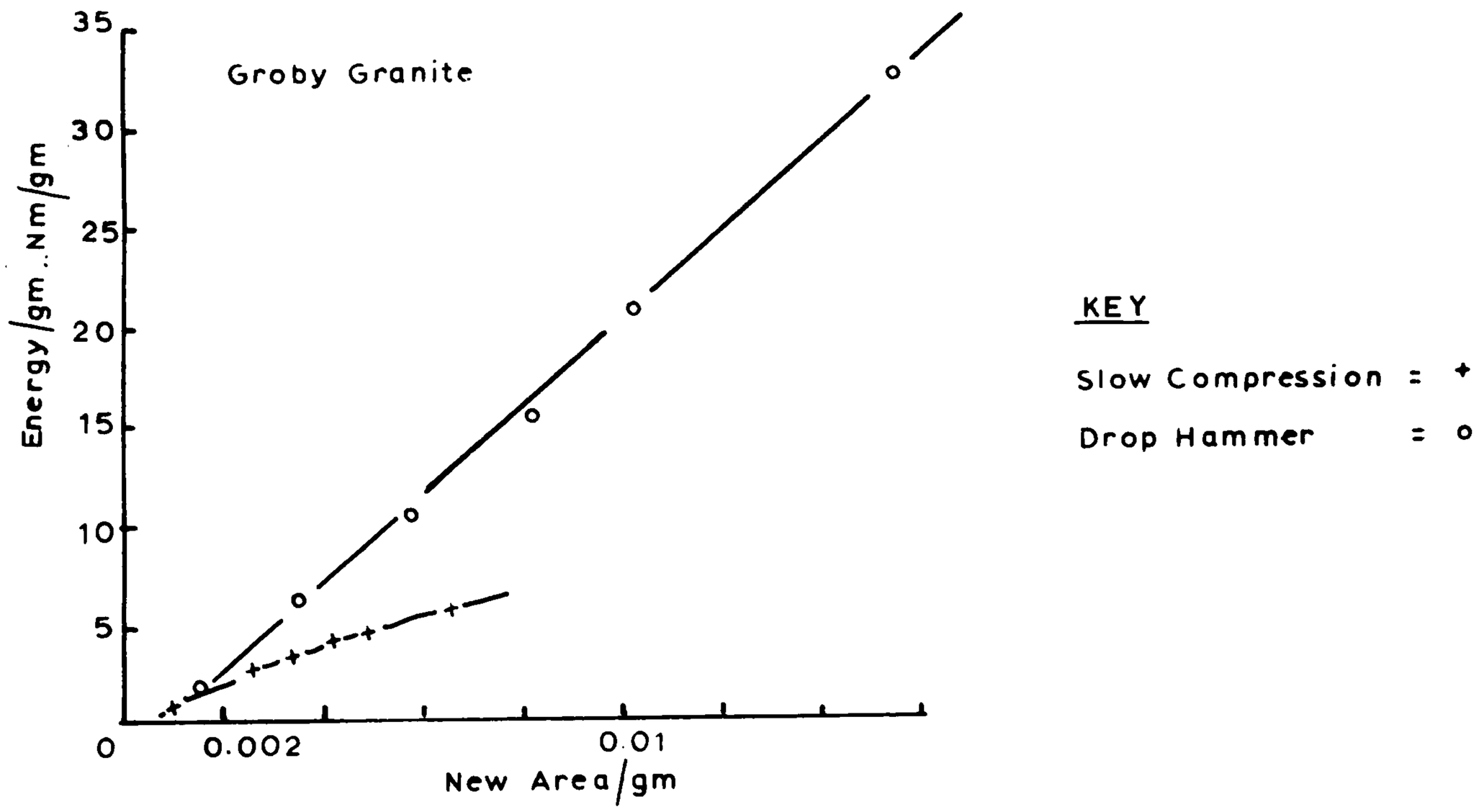

FIGURE 3.17: COMPARISON OF SLOW COMPRESSION & DROP HAMMER TESTS.

crushing of rock, for instance, primary jaw crushing or demolition drop balls. Though these comminution methods are used because of convenience and experinece, the laboratory work shows that the choice is justified in terms of efficiency.

These smaller values of Area/gram where drop hammer is more efficient than slow compression is dependent on the physical make up of the rock. For instance, with Darley Dale sandstone, drop hammer is more efficient than slow compression up to the change over point of 0.0057m^2/gram, after this point slow compression becomes much more efficient. This is the highest value of Area/gram for the change point for any of the rocks and is also understandable as Darley Dale sandstone is weakly bonded and has large lattice structures that can easily be reduced.

As the rocks tested became stronger and tougher in their physical make up, these initial Areas/gram are more difficult to pick out. In all cases, after the initial Area/gram. Where present in the test range, slow compression is substantially more efficient than drop hammer.

In using the Instron machine for slow compression loading, the range for reducing stronger rocks is diminished because the capacity of the machine was reached. To obtain the last points on the Energy/area graphs for the stronger rocks, the larger particles had to be replaced in the mortar five or six times to give a reasonable reduction. This is not the fault of the process and could be

overcome by using a larger capacity loading machine. In impacting one can obtain a larger range by applying more blows, i.e. greater physical effort. Using a larger capacity machine for slow compression more than one cylindrical specimen could be broken, so giving that extra accuracy.

3.D5 Drop Hammer and Stamp Mill Comparison

Stamp mill tests cannot be directly compared to drop hammer and slow compression tests as the starting point is with much smaller particles. However, a comparison was made between drop hammer and stamp mill using Bath limestone with particles between -4mm and +2mm (i.e. same size as the charge in the Stamp Mill) in the drop hammer apparatus. The particles were evenly spread in the Syskov mortar and broken by the drop weight of 2.4kg from the normal drop height, the larger particles were replaced in the mortar to obtain a new energy level as done with the Stamp Mill. Energy/gram and Area/gram values were computed and table 20 gives those values, these were plotted in figure 3.18 (line A) along with those obtained by Stamp Mill crushing (line B).

TABLE 20

Energy/gram	1.1200	2.6101	3.5135	8.2039	11.7112
New Area/ gram	0.003010	0.004002	0.004210	0.006412	0.008213

Energy/gram and Area/gram results for Bath limestone particles between -4mm and +3mm crushed by drop hammer.

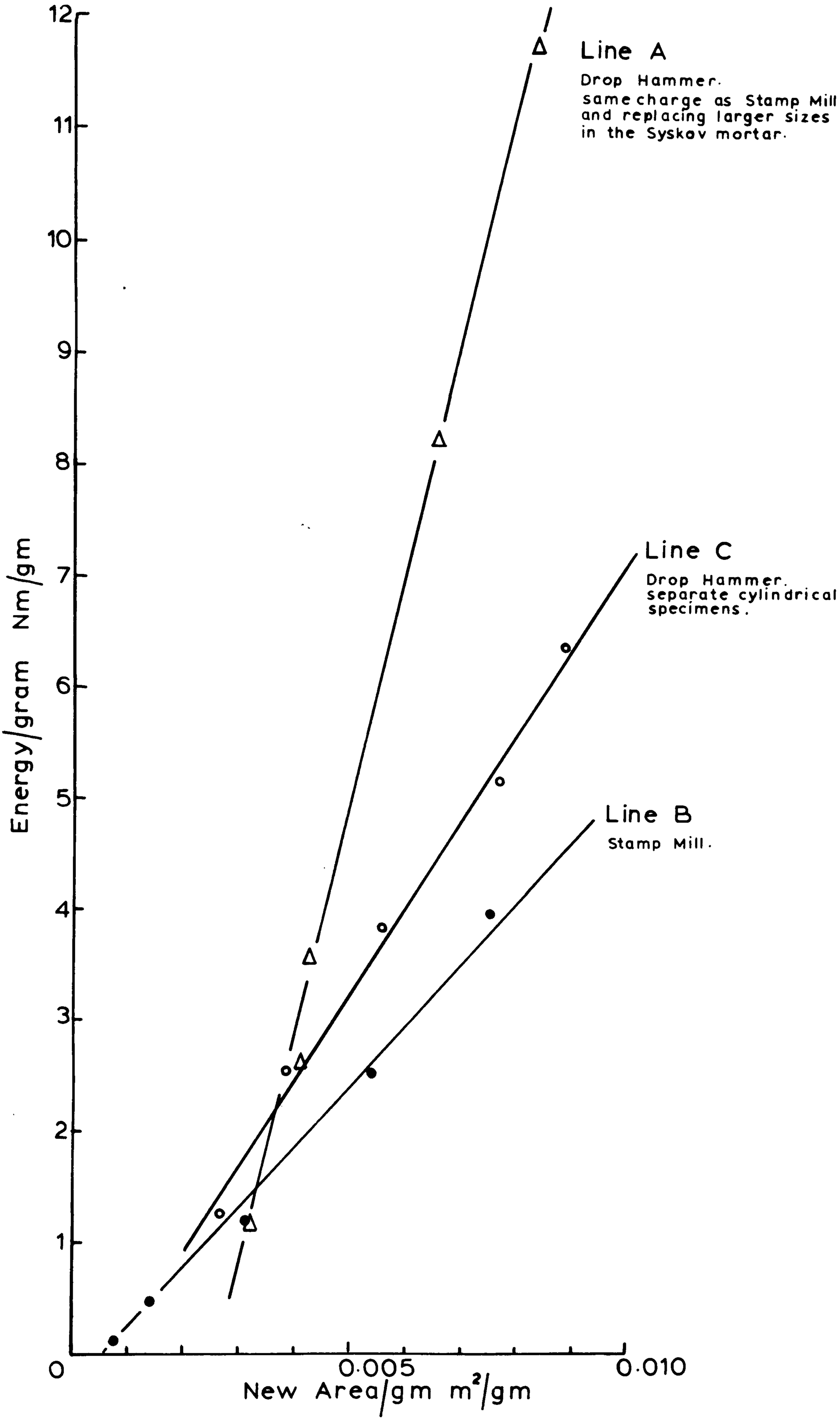

FIGURE 3.18: COMPARISON OF DROP HAMMER & STAMP MILL USING BATH LIMESTONE.

From figure 3.18 it appears that the drop hammer breakage is more efficient again at the smaller areas, but the Stamp Mill becomes increasingly efficient compared to the drop hammer at the larger areas.

The drop hammer tests on the cylindrical specimens (line C in figure 3.18) compared to the above results for drop hammer on small particles, have very little difference in efficiency at the smaller areas/gram but the efficiency soon changes as the area increases. The drop hammer being inefficient in comparison when breaking the smaller particles.

3.D6 Interrelationship by linear regression analysis of the three developed indices

The three indices, drop hammer, StampMill and slow compression, were correlated against each other to show their interrelationship. All three correlated with each other fairly well by a linear regression analysis and the three regression equations are listed below, giving the correlation coefficients (c.c.) and standard error of deviation. The best correlation is that between drop hammer testing and Stamp Mill testing, this equation also has the lowest percentage standard error of deviation.

1. Stamp Mill (y) against drop hammer (x)

$$y = 1.1031x - 154.8864$$

$$\frac{S.E.}{\bar{y}} = \frac{144.1693}{899.402} = 16.03\%, \text{ c.c.} = 0.97484$$

2. Slow compression (y) against Drop Hammer (x)

$$y = 0.00213x + 0.04345$$

$$\frac{S.E.}{\bar{y}} = \frac{0.34960}{2.0955} = 16.68\%, \text{ c.c.} = 0.961847$$

3. Slow compression (y) against Stamp Mill (x)

$$y = 0.001848x + 0.47137$$

$$\frac{S.E.}{\bar{y}} = \frac{0.35411}{2.0955} = 16.89\%, \text{ c.c.} = 0.96083$$

SECTION E RECENT PUBLICATIONS

In this section a review of recent publications on research relating to work described in this chapter, is presented.

St. Clair and Brown (83) studied particle size and size distribution of uniformly sized quartz crushed by impact in a simple drop weight machine. Energy was applied up to about 10Nm/gram and a screen analysis of the crushed products was carried out. They examined the quantitative relationship between energy expended and size reduction for three initial starting sizes of mineral. The energy input is in the same order as the drop-hammer tests carried out in this research programme. Their energy versus size reduction graphs are curves and have been produced backwards to cut the energy axis on the assumption that a minimum amount of energy must be applied before any reduction takes place. The smaller the initial particle size, the minimum energy needed is greater.

Schoenert (84) made theoretical studies concerning the energy balance of a crack, starting on the basis of Griffith's crack theory (85). His work included the crushing of single particles by impacting and slow compression. He concludes that impact has less utilization of energy than slow compression which agrees with the findings presented in this chapter. However, working with larger specimens in the drop hammer and slow compression, our results have shown in some cases drop hammer is more efficient than slow compression. (Schoenert refers to

crushing by drop weight as impacting.) Bradley et al (86) looked at the slow crushing of quartz and Witwatersrand reef in a stiff testing machine. The results were compared to the comminution of the materials in a ball-mill under optimum conditions. The efficiency of the ball-mill in comparison to the slow compression energy utilization is about 80%. Bradley et al concluded that as ball-milling is a relatively efficient process when compared with all other known comminution processes, there would seem to be evidence to support the validity of the proposal by Jowett (72). The proposal being that the standard 100 per cent efficiency should be based on some standard slow crushing test. Also the efficiency of any other comminution process should be assessed on this basis and not in terms of a theoretical efficiency, which because of present lack of knowledge of the fundamentals of brittle fracture is a misleading and misunderstood concept.

Jomoto and Majima (87) did experimental work to attempt to find a useful criterion of comminution which can be determined simply in the laboratory. Young's modulus (E), tensile strength (T) and critical height for a drop weight impact were measured for five different rocks. The best relationship was found between the critical height and the square of the tensile strength. The square of the tensile strength also gives the best relationship with an energy index (150 mesh 80% passing) for tumbling mill grinding of the sample rocks. Jomoto states that the

the square of the tensile strength determined using irregularly shaped rock specimens, is a useful criterion of comminution of rocks, not only for impact crushing but also for tumbling mill grinding. These results and relationships are extremely interesting, but a greater number of rocks should be further tested for verification. Analysing Misra's (34) results of tensile strength (T) and impact test (R) for 28 rocks showed that correlation coefficients for $R_v T$ was 0.897, $R_v \ell n T$ was 0.806, and $R_v T^2$ gave 0.865, these are nowhere near as good as Jomoto's results for five rocks.

Drop weight tests as a basis for the calculation of the performance of ball mills using cement clinker have been presented by Rose (88) and the conclusions are applicable to the comminution of most heterogeneous materials. Tests have been carried out on single particles and comminution in a bed. Curves presented of energy against area (cm^2) (figure 3.19) are of the same numerical order as those presented in this thesis. However, smaller initial particle diameters are used and this is the reason for the curves becoming asymptotic to area value, i.e. large increases of energy producing little increase in surface area. This becomes apparent in the work presented in this thesis for softer rocks such as Yellow Oolitic limestone, which agrees with the above results by Rose.

The observation of fracture phenomena in comminution experiments has been described by Rumpf (89). He has

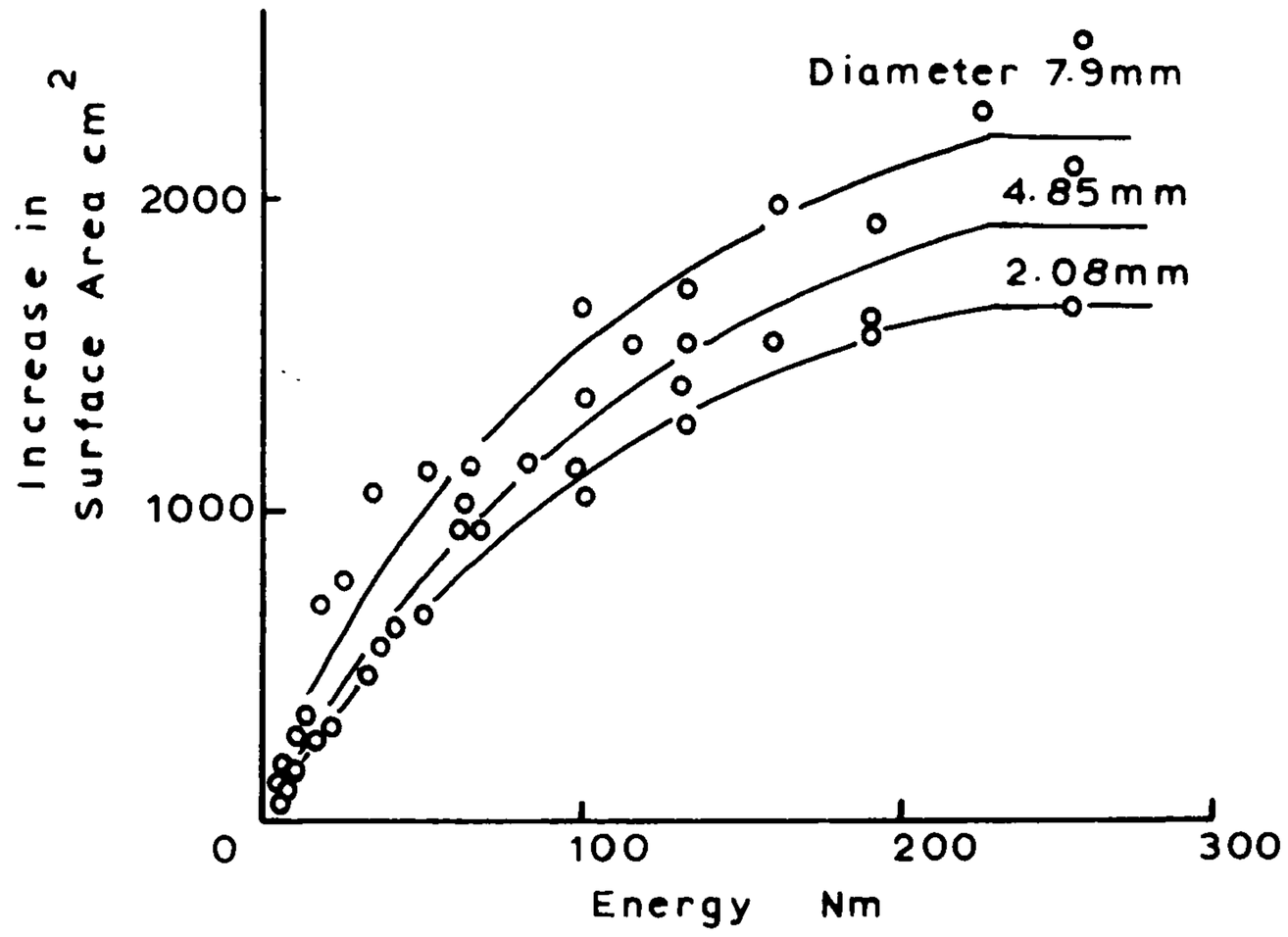

FIGURE 3.19: THE INCREASE IN SURFACE AREA FOR VARIOUS ENERGIES OF BLOW AND SIZES OF PARTICLE AFTER ROSE (88).

derived a similarity law of comminution which is based on physical assumptions and leads to Rittinger's Law. Rumpf examined single particle comminution by slow compression, falling weight and by impact, he concluded that energy utilization decreases in that order.

Agar and Somasundaran (90) review equations proposed in the past to relate particle size to energy consumption or similar quantities in crushing and grinding. An analysis of their own results and other people's results such as Bond (91,92) Meyers and co-workers (93) Smith and Lee (94), is presented in the forms of Schuhmann and Charles equations (i.e. $y = \frac{(x)^m}{(K)}$ and $E = AK^{-m}$ respectively). The various results presented for ball mill and rod mill grinding for different ores and rocks gave linear relationships between log cummulative fraction of material and log size. The work on galena and fluorspar detailed in chapter II also fits this analysis. The authors do mention the difficulty of determining K, the size modulus, and some results that do not give straight lines have been rejected. It could be seen from the report that the Schuhmann and Charles equations were adequate for the analysis of mineral crushing and grind-ability tests, but for the needs of this research programme energy versus surface area created was developed as detailed in chapter II.

The results in this thesis agree with those found recently by other workers, who have also studied energy/

surface area/particle size relationships in order to attempt to solve comminution problems. The original intention of the development of an accurate index and to compare rock breaking efficiencies has been fulfilled, but in addition to this a large amount of useful data has been collected which will contribute to the study of comminution.

SECTION F Indices of Compressive Strength, Rock Impact Hardness Number and Dynamic Young's Modulus

3.F1. Compressive strength

Compressive strength was included in this work as it has been proved to bear a relationship with drilling and is also a standard method of laboratory rock testing. Therefore, its exclusion would render this study incomplete.

The index of compressive strength was obtained by taking the mean load of six specimens individually stressed in a Denison testing machine until failure. A standard loading rate of 20KN/minute was used. The specimens used are the normal cylindrical type (50mm in length and 25mm diameter), but the ends are ground to 1/10,000 of an inch. The specimens are placed in a jig, six at a time, for grinding, so all the specimens are of the same length. Grinding the specimen ends equally, minimises the adverse 'ends' effect.

The method of obtaining the mean load of the six specimens was that recommended by Misra (34) which is to ignore the lowest and highest values and to average the remaining four. If large differences were obtained for all six specimens, then further specimens were tested.

The accepted values of compressive strength are listed in table 23.

3.F2. Rock Impact Hardness Number

This test has already been detailed in chapter I, giving its development and method. This index was chosen to be included in this research because it is an extension of the work by Protodyakonov, also Misra (34) has shown that it has a good correlation with rotary-percussive drilling.

The index is listed in table 23.

With both compressive strength and rock impact hardness number, values could be obtained from B. Misra (34) when the same rock samples were used in this study. However, if there was insufficient rock sample to provide enough specimens for the whole of this study, a different rock sample was used, and the values of compressive strength and rock impact hardness number determined for that rock sample. This rock sample was then used for all subsequent testing. Similarly if a new rock was introduced into the study, that rock sample was used for all the testing. The rock samples were in the order of 2 feet square by 4" deep. In the main sampling did not vary too much, nevertheless it was a precaution that was justified to give consistent results.

3.F3. Dynamic Young's Modulus

The Dynamic Young's modulus was determined by using an Ultrasonic Tester, which measures the time for low ultrasonic frequency waves to pass through the rock specimen.

The Modulus is a function of the speed of the wave pulse through the specimen and the bulk density of the rock. Ultrasonic testers were originally intended for the detection of flaws in concrete, but have been adapted for use as a method of rock indexing. It is not known whether such an index gives a high correlation with drilling, but as the method is simple and quick, the index was obtained in an afternoon's work for correlating with the laboratory rotary-percussive drilling.

The tester used was an Ultrasonic Materials Tester type UCT2/1822A, manufactured by Dawe Instruments of London. The instrument indicates the time taken for the earliest part of the pulse to reach the receiving transducer from the time it leaves the transmitting transducer. A quartz crystal is used to calibrate the time measuring system and a cathode-ray tube is used for the presentation of the transmitted and received signals. Barium titanate transducers enclosed in metal housings act as the transmitter and receiver of the ultrasonic pulse.

Cylindrical specimens of 50mm length and 25mm diameter, with the ends ground to 1/10,000 of an inch, are used for testing. The instrument is calibrated as detailed in the manufacturer's handbook, along with the simple operating techniques. It should be stressed that the instrument should be allowed 20 minutes to warm up before any readings are taken.

To improve contact between the transducer faces and the core end faces a light coating of vaseline grease was applied

to the core ends. (This was also recommended by the manufacturer and does not have any adverse effects on the readings). Using a wooden retort stand and clamps, the two transducers were supported and the rock specimen gripped between them. A resulting wave pattern of the transit wave was displayed on the cathode ray tube. Using the rotary scale, the transit time was read off. By accurately measuring the specimen length, the transit velocity can be calculated.

$$\text{transit velocity} = \frac{\text{length of specimen}}{\text{transit time}} = \text{m/s}$$

The transit velocity (V) and the bulk density (D) of the rock specimen are functions of Dynamic Young's Modulus (E), so that Dynamic Young's Modulus can be found from:-

$$E = V^2 D$$

where E, the Young's Modulus is in GN/m^2

V, the transit speed is in m/sec

and D, the bulk density is ton/m^3.

Table 21 gives the values of E, V and D for the rocks tested.

In Ultrasonic work it is more appropriate to use the bulk density of the rock, because it is the bulk of the rock that gives the pulse time its characteristic. It was thought at this time that perhaps the length of specimen could be subject to error, as there was no reason for choosing a 50mm length of specimen. It was decided that this would make a good final year project, to see the

effect of varying the lengths of specimens.

The results obtained were extremely encouraging in that a direct linear relationship between transit time and length was obtained for four rocks tested at different lengths of specimen. High correlation coefficients were obtained even though some of the rock samples were joined together and classed as one long continuous sample. The lengths of specimens varied between 9mm and 290mm with diameters of 25mm. Buckton sandstone was also tested at different lengths with specimen diameters of 48mm. This also gave a near perfect relationship.

Table 22 lists the linear regression analysis for each rock showing the slope of the line, the intercept value on the vertical axis, i.e. the transit length axis. All the lines intersect the y-axis below the origin, which demonstrates that there is an "end effect" present between the transducers of a very low magnitude. In fact the highest negative intercept value represents only 1.01% of the maximum sample length value. The measurement of the transit time is only accurate to ±.1%, therefore it can be concluded that any end effects which are present, although apparent can be regarded as negligible.

So that the using of 50mm lengths of specimens for all the rocks is as good as any length to choose to obtain the ultrasonic characteristic properties of the rocks.

The tests that were done on the Buckton sandstone with the two diameters (25mm and 48mm) at different lengths

of specimen, show very little difference in the gradients of the lines. The intercept is slightly greater for the larger specimen showing a larger "end effect", but nevertheless still quite small.

Work by Thill and Peng (95) at the U.S. Bureau of Mines has recently been published also confirming the high correlation between the transit time and length. They used 20mm diameter specimens and the transit time for varying lengths was measured. The resulting correlations coefficients being extremely high, verified the 50mm choice of length for determining the rock index.

TABLE 21

Results from Ultrasonic Testing

Rock	Bulk Density ton/m^3	Transit Speed km/sec	Dynamic Young's Modulus GN/m^2
Yellow Oolitic Lst.	1.880	2.663	13.332
Darley Dale sst.	2.206	2.3472	12.153
Horsforth sst.	2.166	2.8637	17.758
St. Bee's sst.	2.089	2.695	15.169
Elland Edge sst.	2.398	3.3418	26.779
Bath lst.	2.203	3.9768	34.841
Craigenlow Pink Granite	2.601	-	-
Giggleswick lst.	2.666	6.0073	96.209
Cornish Granite	2.615	5.2690	72.595
Denbigh lst.	2.643	4.7783	60.345
Whinstone	2.892	4.8756	68.746
Mount Sorrel Granite	2.660	5.6537	85.025
Groby Granite	2.536	5.6843	81.942
Bardon Hill Granite	2.862	6.0137	103.503
Horton Mudstone	2.641	6.2195	102.159

TABLE 22

Linear regression analysis for four rocks varying the specimen lengths and diameter in Ultrasonic testing.

Rock	Sample diameter	No. of different specimen lengths	Correlation coefficient	Intercept valve on vert. axis	Gradient of line
Buckton sst.	48mm	36	0.99969	-2.8126	3.7574
Buckton sst.	25mm	35	0.99974	-1.0627	3.7803
Darley Dale sst.	25mm	19	0.99981	-0.4161	2.4093
Kirbymoorside lst.	25mm	30	0.99887	-1.3759	6.2649
Metamorphosed lst.	25mm	29	0.99968	-1.2496	5.3773

TABLE 23

LIST OF ROCK INDICES

Rock	Drop Hammer E/A .. N/m	Stamp Mill E/A .. N/m	Slow Compression E/gm .. Nm/gm	Rock Impact Hardness Number ... MJ/m^3	Compressive Strength ... MN/m^2	Dynamic Young's Modulus ... GN/m^2
Yellow Oolitic Lst.	309.470	245.064	0.225	8.02	10.28	13.332
Darley Dale Sst.	357.467	161.509	1.07	9.75	41.47	12.153
Horsforth Sst.	376.223	464.030	-	9.16	44.33	17.758
St. Bee's Sst.	424.107	213.004	0.780	10.87	57.22	15.169
Elland Edge Sst.	554.836	281.289	1.475	25.6	95.50	26.779
Bath Lst.	787.184	567.573	1.40	20.97	46.91	34.841
Craigenlow Pink Gr.	1009.280	869.043	2.09	-	225.1	-
Giggleswick Lst.	1042.791	-	-	68.93	131.84	96.209
Cornish Gr.	1094.045	1344.019	3.075	76.09	168.29	72.595
Denbigh Lst.	1348.564	1301.750	3.25	96.62	178.57	60.746
Whinstone	1460.816	1541.957	-	113.22	175.27	68.746
Mount Sorrel Gr.	1541.405	1666.588	3.05	91.05	251.51	85.025
Groby Gr.	2205.595	2137.001	4.54	133.53	143.30	81.942
Bardon Hill Gr.	3269.839	-	-	210.52	330.47	103.503
Horton Mudstone	-	-	-	66.07	132.33	102.159

SUMMARY

a) An accurate index for drop hammer testing has been developed with very high correlation coefficients for a large range of different rock types by considering Energy/surface area relationships.

Indices for stamp mill and slow compression methods of breakage have also been developed. High correlation coefficients for Energy/surface area were obtained for the stamp mill, but slow compression had a non-linear relationship of Energy/surface area.

The indices for stamp mill and slow compression are not as accurate as the drop hammer index, because the drop hammer uses a new rock specimen for each energy level. However, the difference in accuracy is only relatively small as shown by the tests on Bath limestone.

b) A graphical comparison of drop hammer and slow compression has been made showing that in the main slow compression is an efficient process compared to the drop hammer. But, the drop hammer can be more efficient for the breaking of larger particles.

The comparison of drop hammer and stamp mill made graphically with Bath limestone, indicates that the drop hammer again can be more efficient for the breaking of larger particles, but does become inefficient for the breaking of smaller particles.

c) The literature review on recent publications pertaining to energy requirements in rock breakage has shown some

parallel results to this work.

d) Compressive Strength and Rock Impact Hardness Number indices have been given. Dynamic Young's modulus was easily determined from Ultrasonic testing and the transit time/transit length relationships have very high correlation coefficients.

CHAPTER IV

LABORATORY ROCK DRILLING

CHAPTER IV

LABORATORY ROCK DRILLING

Introduction

This chapter describes in detail the laboratory rock drilling that has been performed in order to try to achieve the objective of greater understanding and insight into drilling.

Determination of penetration rate-thrust characteristics has been carried out on a number of rocks covering a wide range of physical rock properties and the characteristics have been used for correlation with rock properties.

A new laboratory drilling rig was designed so that it was possible to measure all the drill parameters. A complete description of the drilling rig is given along with the methods used for measuring the drill variables. The calibrations of the measuring devices and the operation of the drilling rig are also described.

As stated earlier, the study of bit-wear is recognised as an important part of drill research, but for this programme it is omitted. This is purely because of the time that would be required would certainly greatly reduce the time available for the objectives of this research programme to be attained. The effect of bit-wear was removed by using a newly-sharpened bit for each hole drilled and also by drilling short holes of approximately 14mm depth.

Preliminary tests were conducted to see that the

laboratory drilling rig was in fact drilling in a rotary percussive manner and exhibiting the standard characteristics. The preliminary tests were thrust, speed and percussion tests, discussion and conclusions of the tests are included.

The results of drilling a range of rocks at a set drilling condition measuring all the drill parameters are tabulated and analysed after Teale (51) and Hustrulid (55). At this point an empirical formula is introduced, this formula combines all the drill parameters and was found to have an extremely good relationship with the compressive strength. The results from drilling more than one range of rocks under different drilling conditions are also presented and analysed.

Finally, an analysis combining more than one drilling condition has been made by considering the empirical formula at different speeds of rotation correlated with the compressive strength.

The work of laboratory drilling is summarised at the end of the chapter.

4.1. Penetration Rate/Thrust Characteristics

The first laboratory drilling tests carried out in this research were to establish the penetration rate-thrust characteristics for a range of rocks. An ordinary Black and Decker GD4 type 1, rotary-percussive drill was used for these tests. This drill was previously used by Misra and he has given a full description with diagrams in his thesis (34).

The drill is mounted on a vertical stand and is allowed to drill cylindrical rock specimens that are firmly clamped to the bench. A newly-sharpened bit is used for each hole drilled. The time to drill approximately 14mm depth is noted from the digital time clock and the depth of penetration measured to 1/10th of a millimeter. Each rock is drilled five times at different thrust levels and the average penetration rate (mm/sec) for the five is taken. The thrust levels applied were the machine weight only, that is 7lbs, then by adding weights secured on top of the drill to give 17lbs, 27lbs, 37lbs and 57lbs thrusts. Throughout the thrust tests, speed and percussion were kept constant at maximum values.

Hence for the rocks tested the penetration rate/thrust graphs can be drawn and figure 4.1 shows those for some of the rocks drilled, as examples. Table 24 gives the values of penetration rate for the varying thrusts for all the rocks tested.

The first part of the graphs, a near linear relationship

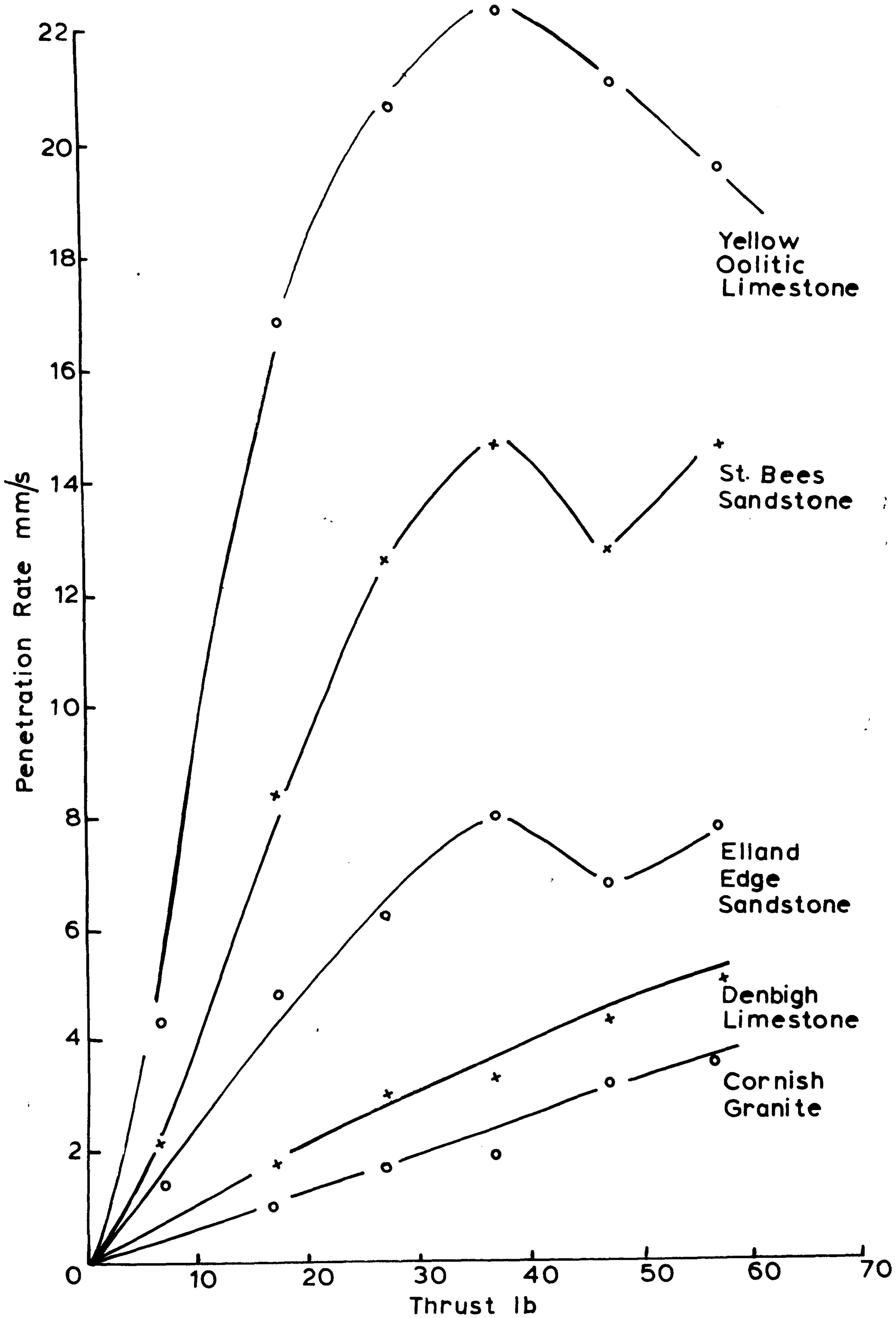

FIGURE 4.1: PENETRATION RATE - THRUST CHARACTERISTICS.

exists between penetration rate and thrust. So, it is possible to find a linear regression relationship between them and to use the slope of the lines as a machine property.

At 47lbs thrust the penetration rate decreases for the 'softer' rocks and for Horsforth, St. Bee's, Elland Edge sandstones and Bath limestone increases at 57lbs thrust. For the 'stronger' rocks after Bath limestone in table 24, the penetration rate/thrust relationships do not yet show this anomaly. (This anomaly can be fully seen in 4.5(a)(ii) of this chapter, where a slower speed has been used in some other thrust tests).

The slopes of the penetration rate/thrust graphs are therefore obtained from linear regression by using values between zero and the maximum penetration rate with the corresponding thrusts before the anomaly occurs. With the 'stronger' rocks all the values of penetration rate and thrust could be used for linear regression. The slope values for the rocks drilled are listed in table 24.

These slopes from the linear regression were then used for correlation with the rock indices listed in table 23, chapter III. Graphs of the slopes against the indices were drawn and the resulting graphs with the least scatter of points are presented. Figure 4.2 shows the slopes against the drop hammer index (E/A), figure 4.3 slopes against rock impact hardness number and figure 4.4 slopes against the compressive strength.

As stated in the literature review of chapter I, Tsoutrelis (39) plotted the slopes of penetration rate/ thrust characteristics at constant 260 R.P.M. for a diamond drill drilling five rocks, against the reciprocal of the compressive strength. That analysis was then tried for this laboratory rotary-percussive drill by linear regression, the correlation coefficients obtained are given in table 25.

Table 25 also gives the correlation coefficients for the penetration rate at 37lbs constant thrust (i.e. before the anomaly occurs) against the reciprocal of the rock indices. This is done so that a simple comparison of coefficients can be made using just penetration rate or using penetration rate/thrust slopes in the correlation with rock indices. Furthermore, to show that by trying different mathematical functions it is possible to find an improved correlation coefficient. As an example of an improvement, the reciprocal of the log squared was taken for the rock indices and correlated with both penetration rate/thrust slopes and penetration rate. The correlation coefficients are tabulated in table 25.

TABLE 24

Results of Penetration Rate/Thrust Tests in Laboratory Drilling

The rows give the penetration rate (mm/sec) for that rock and thrust.

Thrust	71bs	171bs	271bs	371bs	471bs	571bs	P.R/Thrust Slope mm/sec.lb.
			(mm/sec)				
Yellow Oolitic limestone	4.281	16.917	20.726	22.408	21.065	19.686	0.64698
Darley Dale sandstone	1.588	7.832	8.946	12.515	14.543	14.031	0.344176
Horsforth sandstone	2.016	8.559	12.580	14.768	12.621	14.701	0.42633
St. Bee's sandstone	2.201	5.369	8.527	11.701	10.620	10.810	0.31580
Elland Edge sandstone	0.613	4.850	6.185	8.147	6.680	7.906	0.23308
Bath limestone	1.880	4.590	7.012	10.190	8.811	9.723	0.27801
Horton Mudstone	-	1.812	3.109	3.197	4.334	5.219	0.08847
Denbigh limestone	-	1.589	2.845	3.863	4.551	5.057	0.09194
Whinstone	-	1.641	2.617	3.586	4.552	5.524	0.09692
Giggleswick limestone	-	1.566	3.120	3.624	3.571	4.738	0.07961
Craigenlow Pink granite	-	0.655	1.031	1.416	1.809	2.195	0.03851
Cornish granite	-	1.131	1.717	1.769	3.314	3.519	0.06275
Mount Sorrel granite	-	0.305	0.511	0.649	1.460	2.115	0.03534
Groby granite	-	1.653	2.512	3.586	4.414	5.535	0.09692
Bardon Hill granite	-	0.217	0.857	1.030	1.912	2.530	0.04539

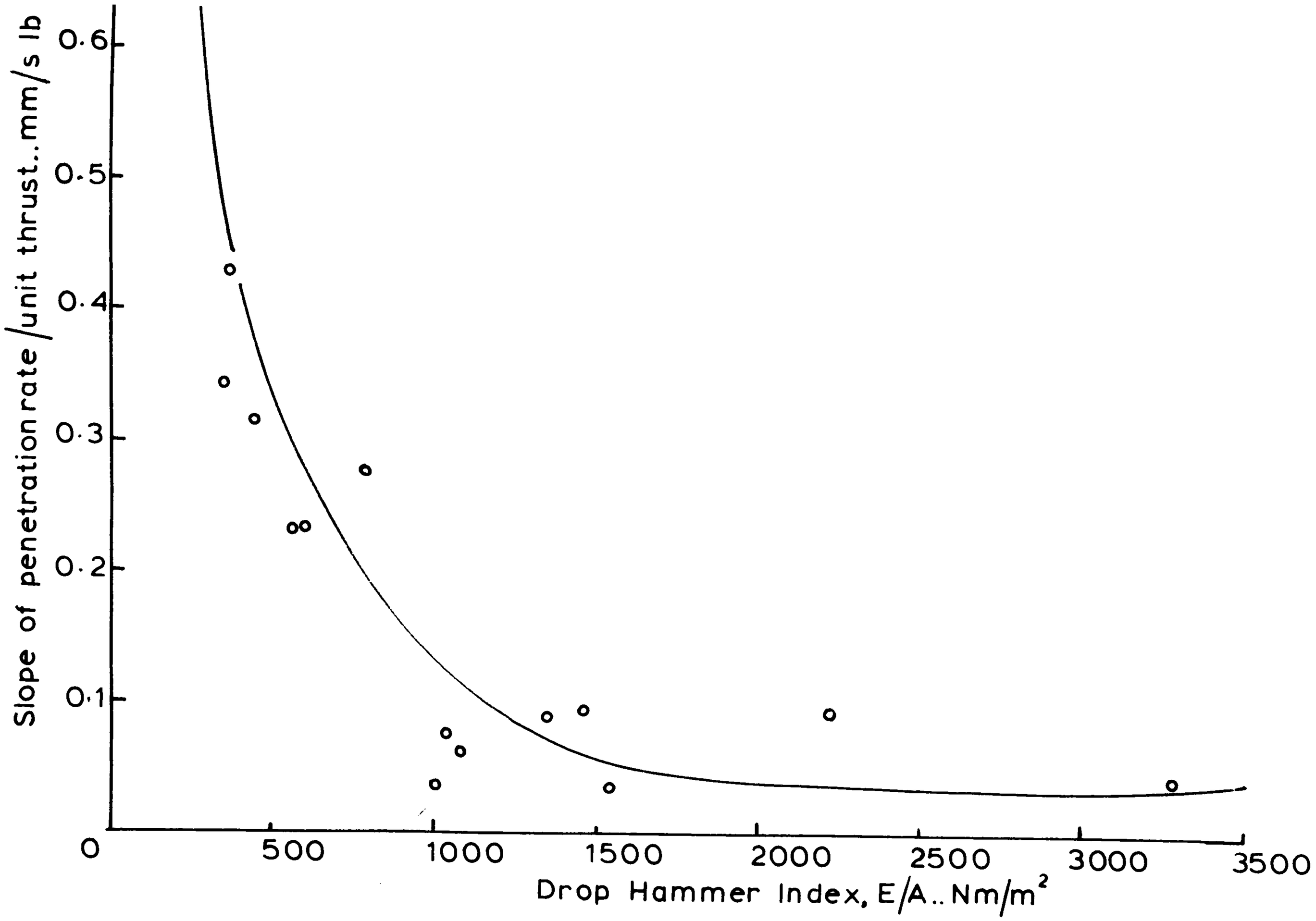

FIGURE 4.2: SLOPES OF PENETRATION RATE - THRUST GRAPHS VERSUS DROP HAMMER INDEX.

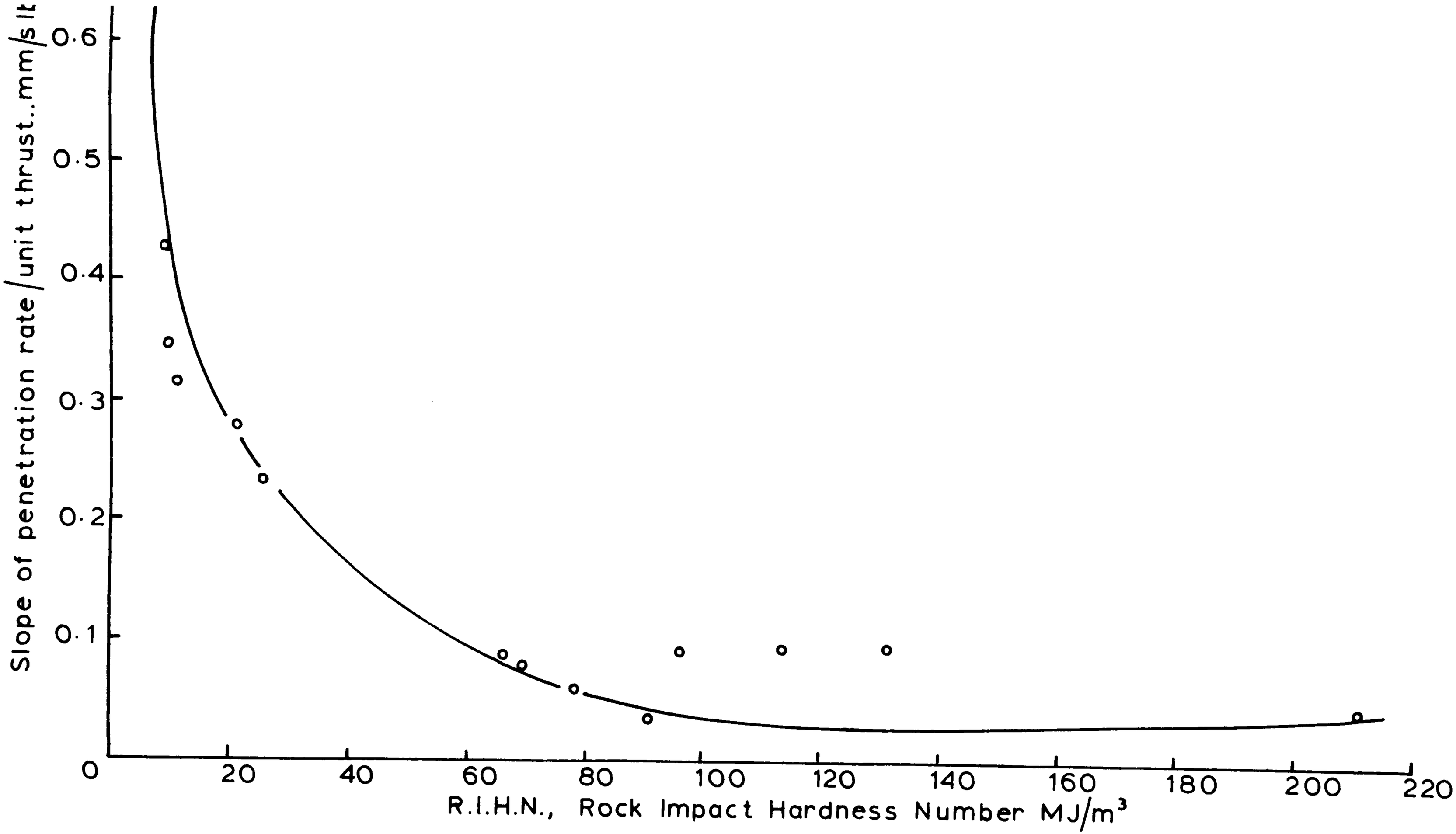

FIGURE 4.3: SLOPES OF PENETRATION RATE - THRUST GRAPHS VERSUS ROCK IMPACT HARDNESS NUMBER.

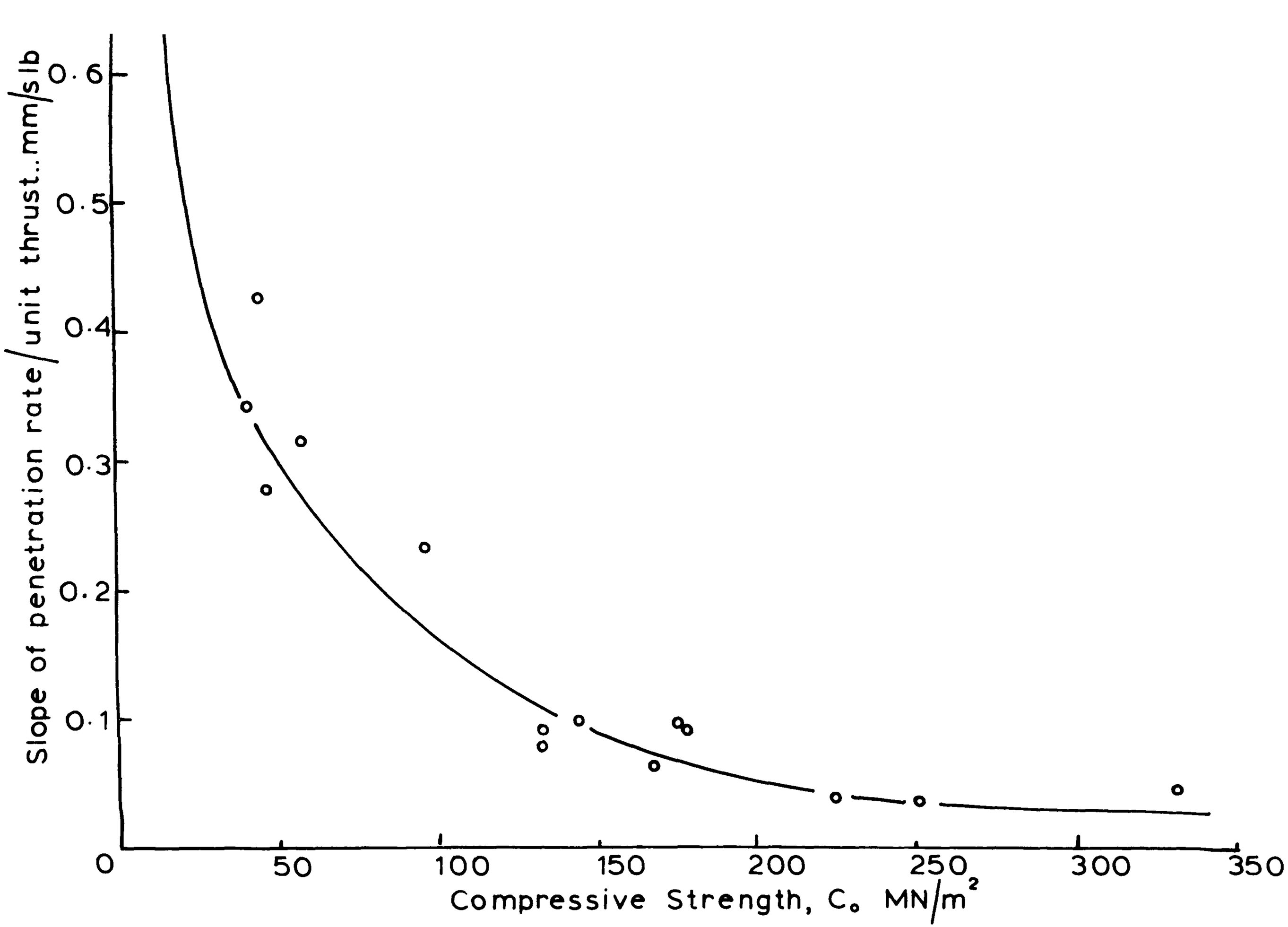

FIGURE 4.4: SLOPES OF PENETRATION RATE - THRUST GRAPHS VERSUS COMPRESSIVE STRENGTH.

TABLE 25

Correlation coefficients for two functions in the correlating of two machine parameters with three rock indices

The functions:- (a) $y = 1/x$, (b) $y = 1/(\ell nx)^2$

y, The Machine Properties:- (a) Penetration Rate P.R., mm/sec, at 37lbs from table 24.

(b) Penetration Rate/Thrust slopes P.R./Th, mm/sec.lb, from table 24.

x, The Rock Indices (a) Compressive strength, C_o, MN/m^2

(b) Drop Hammer Index, E/A, N/m^2

(c) Rock Impact Hardness Number, R.I.H.N., MJ/m^3

$\frac{P.R.}{Th}$ v $\frac{1}{C_o}$,	c.c.=0.87867	P.R. v $\frac{1}{C_o}$,	c.c.=0.86520
$\frac{P.R.}{Th}$ v $\frac{1}{(\ell n\ C_o)^2}$,	c.c.=0.904993	P.R. v $\frac{1}{(\ell n\ C_o)^2}$,	c.c.=0.89507
$\frac{P.R.}{Th}$ v $\frac{1}{E/A}$,	c.c.=0.92961	P.R. v $\frac{1}{E/A}$,	c.c.=0.932361
$\frac{P.R.}{Th}$ v $\frac{1}{(\ell n\ E/A)^2}$,	c.c.=0.89785	P.R. v $\frac{1}{(\ell n\ E/A)^2}$,	c.c.=0.905339
$\frac{P.R.}{Th}$ v $\frac{1}{R.I.H.N.}$,	c.c.=0.949514	P.R. v $\frac{1}{R.I.H.N.}$,	c.c.=0.950265
$\frac{P.R.}{Th}$ v $\frac{1}{(\ell n\ R.I.H.N.)^2}$,	c.c.=0.95229	P.R. v $\frac{1}{(\ell n\ R.I.H.N.)^2}$,	c.c.=0.953208

Discussion

Analysing the results of penetration rate/thrust tests has shown that correlation of the slopes against rock impact hardness number gave the best correlation coefficients for the range of rocks tested, the indices and the two mathematical functions considered. The log squared reciprocal function improved all the correlation coefficients except for the drop hammer index.

The coefficients for penetration rate against rock impact hardness number and the drop hammer index are slightly better than those for penetration rate/thrust slopes against the same indices, but for the compressive strength the penetration rate coefficients are slightly worse than the slope coefficients.

Hence, for prediction purposes there is not a great deal to be gained from using penetration rate/thrust slopes, except that it would be possible to have as good as a prediction as the penetration rate even if the drill was working at different thrusts. Penetration rate/rock property relationships are such that the drill must be operating at the same thrust for all the rocks or working at the optimum thrust. Whereas, penetration rate/thrust slopes against a rock property can be used for the prediction of penetration rate at any thrust. This is provided that the thrust applied is known and the drill is being operated in the near-linear region of the penetration rate/thrust graphs.

The finding of improved correlation coefficient by

regression analysis was done by Misra (34) and Selim and Bruce (59), who tried a large number of different functions for the relating of penetration rate with rock properties. The highest coefficients obtained were between 0.95 - 0.978, but even with these values large errors can still occur. Therefore, for accurate predictions the best fitted function should have a correlation coefficient greater than 0.98. To give such a coefficient or higher, the points on the graph should all be on or very near the curve. With the graphs of penetration rate/thrust slopes against the rock indices, an extensive curve fitting exercise is not necessary as the points are fairly scattered and this exercise would not be covering any new ground. The resulting coefficients would not be an improvement on penetration rate/rock property functions, because a good initial graphical relationship is not there to start with. However, as an example to show that a curve fitting exercise can give an improved correlation, an analysis was carried out on the index which gave the best graphical relationship. This was found on inspection to be the compressive strength and some of the functions fitted are given below with their correlation coefficients:-

y = Penetration rate/thrust slope, x = Compressive strength.

function	correlation coefficient
$y = ax^b$	- 0.934803
$y = ae^{bx}$	- 0.920868
$y = ab^x$	- 0.920874
$\ell ny = a\ell nx+b$	- 0.934812
$y = a\ell nx+b$	- 0.969874

function	correlation coefficient
$y = ax^2 + b$	- 0.638170
$y = a/x^2 + b$	0.756208
$y = a/(x)^{\frac{1}{2}} + b$	0.952900
$y = a/(\ell nx)^{\frac{1}{2}} + b$	0.961305
$y = a + b \log x + c(\log x)^2$	0.973941

This analysis further supports the fact that it is possible to obtain improved correlation coefficients, but the higher correlation coefficients for accurate predictions are unobtainable because of the scatter of points on the graph. Nevertheless, it can be said that more than just a general trend exists for penetration rate/thrust/strength index relationships.

The useful amount of work that could be done on the Black and Decker drill set up had now been completed. Therefore, it was necessary to design a laboratory drilling rig, whereby all the drilling parameters could be measured in order to attempt to fulfill the objectives of this research.

4.2 Design of the New Laboratory Drilling Rig

The drilling parameters that were to be measured are the thrust, speed of rotation, torque, percussion, drill cuttings and the penetration rate. Therefore, the energy or power inputs and outputs produced by varying combinations for a range of rocks can be examined.

Penetration rate and thrust measurements are done as with the Black and Decker G.D.4 drill. The time to drill approximately 14mm, measured to 1/10th of a millimeter, gives the penetration rate and the weight of the drill rig plus the weights secured on top to give thrust. Varying thrusts can be obtained by adding or subtracting different weights.

The drill cuttings produced are collected and quantified by sieve analysis, so the new surface/area gram can be computed from $\sum_{s}^{6} \ell n 2 \left(\frac{\text{weight of fraction}}{a_1 - a_2}\right)$/gram, as detailed in chapter II.

Hence the Drilling Rig had to be designed such that the speed of rotation, percussion and torque could be easily measured and the rotation and percussion varied independently.

The Laboratory Drilling Rig

Photograph 4 shows the completed laboratory drilling rig and fig. 4.5 shows a diagram of it. The electrical circuit is detailed in figure 4.6 and the key for figure 4.6 appears on the page after this figure.

Two drills are used to provide the rotary-percussive action, drill 1 provides purely rotation and drill 2 purely

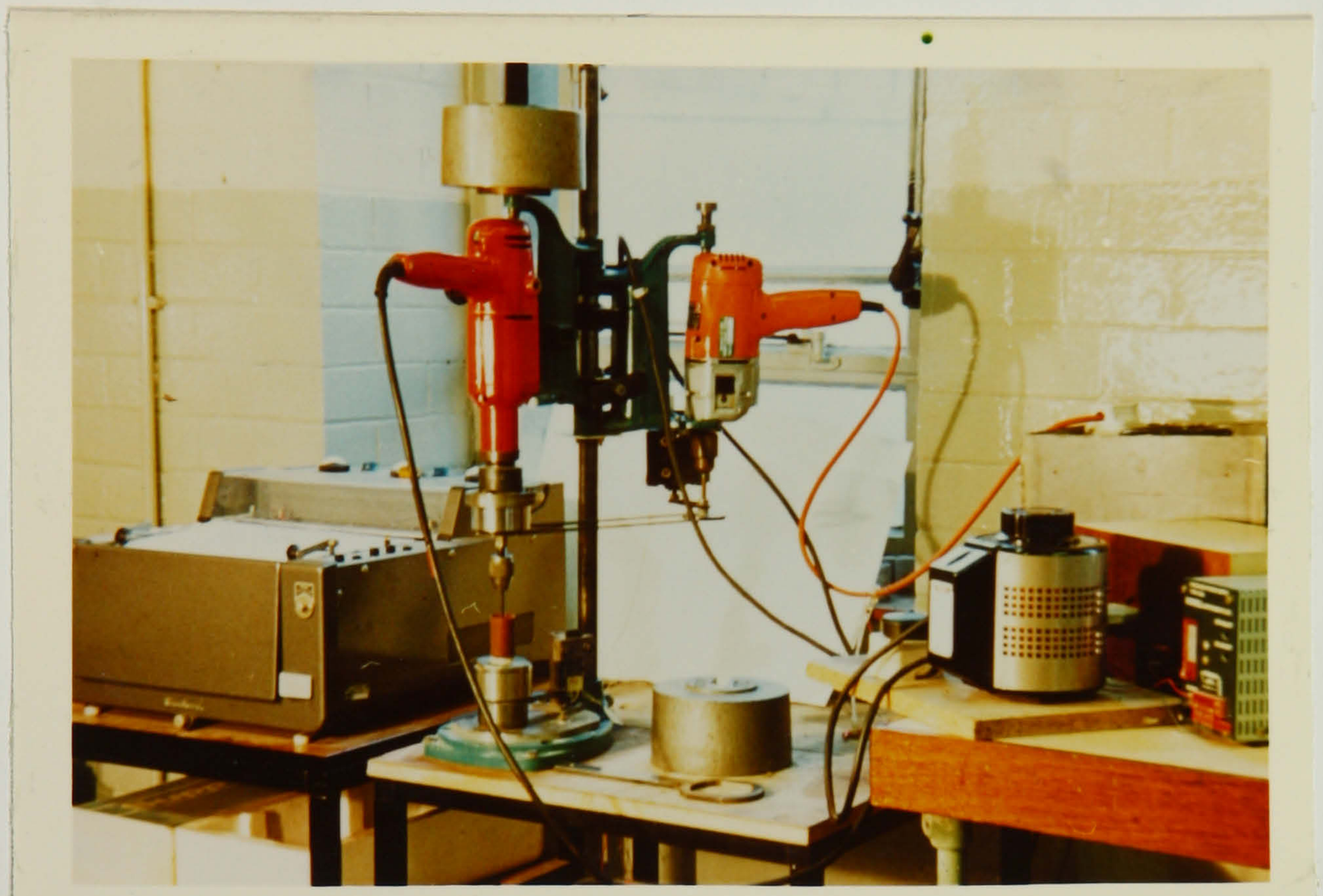

PHOTOGRAPH 4 : The Laboratory Drilling Rig

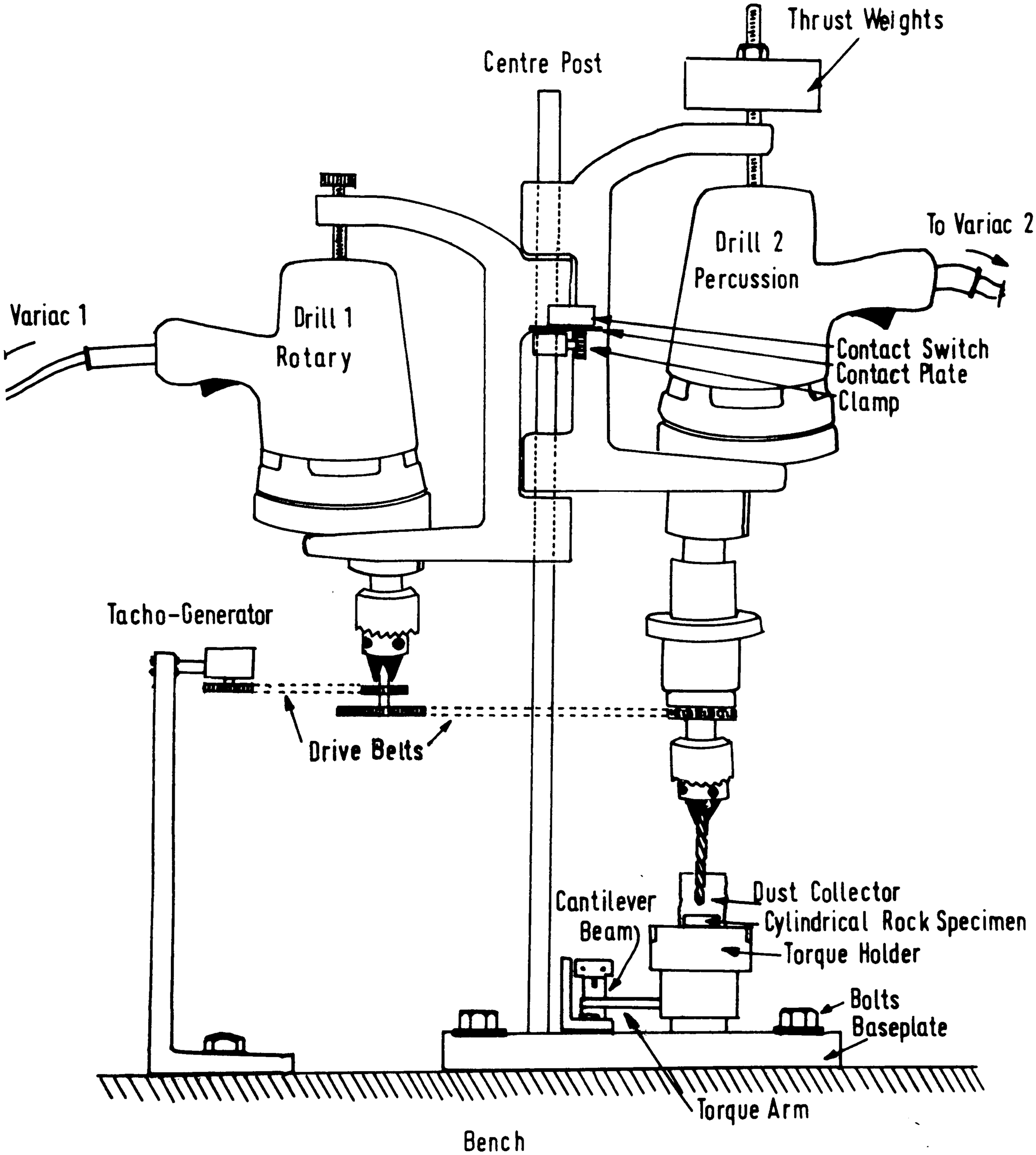

FIGURE 4.5: SCHEMATIC DRAWING OF THE LABORATORY ROTARY-PERCUSSIVE DRILLING RIG.

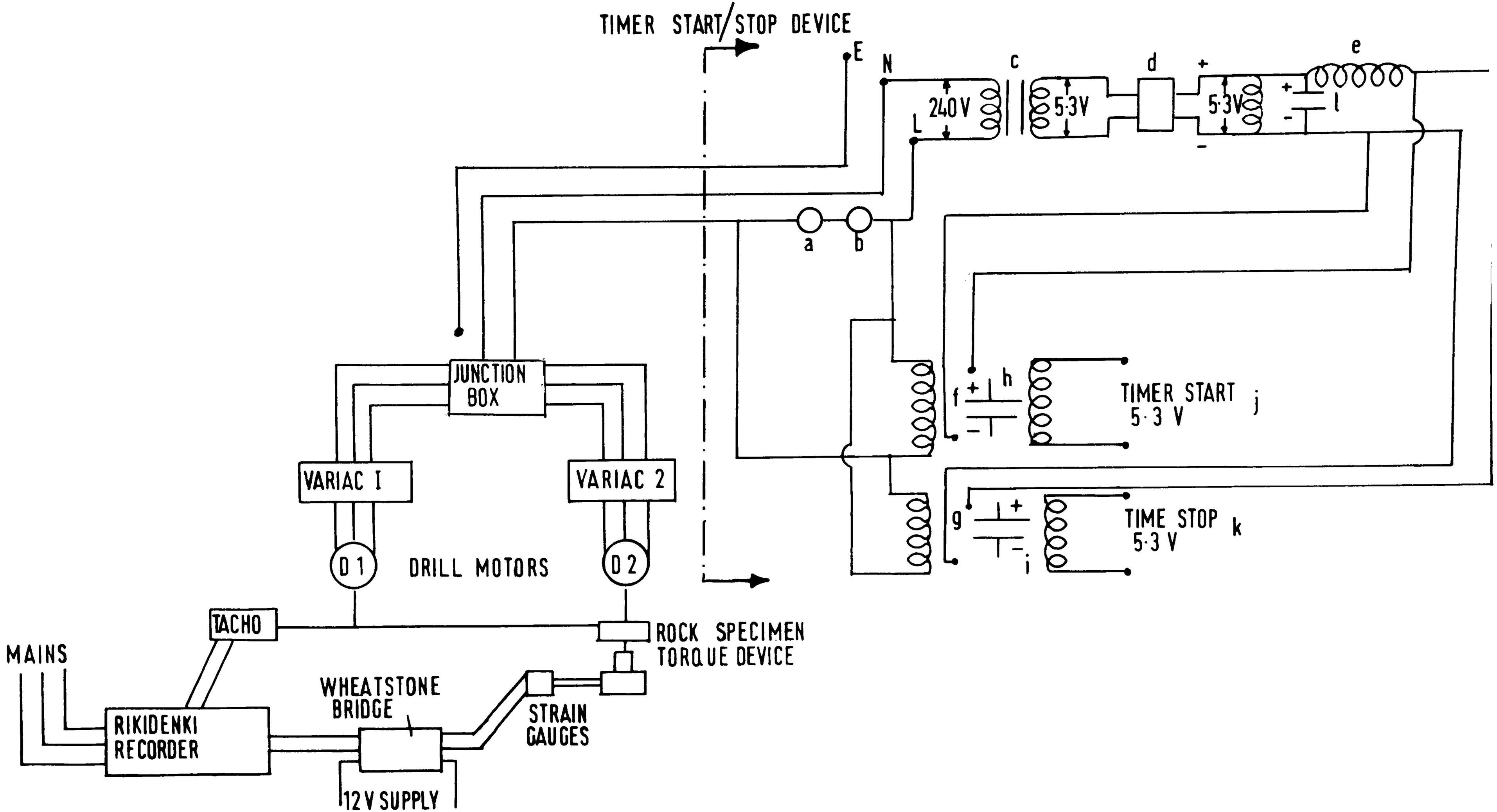

FIGURE 4.6: LABORATORY DRILLING RIG ELECTRICAL CIRCUIT.

Key to Figure 4.6. The Electrical Circuit

a - a toggle switch to start the drills and timer simultaneously.

b - a micro switch to stop the drills and timer simultaneously.

c - a step-down a.c. transformer with a voltage ratio 240:5.3V.

d - a full wave bridge rectifier suitable for a maximum current of 1 amp.

e - a 100 Ohms resistor (all other resistors shown in the circuit are also of this value).

f and g - mains coil double pole relays.

h and i - 100 micro F, 25V d.c. capacitors across the relays.

j - 5.3V d.c. terminals for the start socket of the timer.

k - 5.3V d.c. terminals for the stop socket of the timer.

l - a 250 micro F, 25V d.c. post rectification smoothing capacitor.

percussion. Each drill is connected to separate variacs to give independent variations.

In order to combine the two actions, a thrust bearing is incorporated into the system. This bearing has two functions (a) to allow the bit on drill 2 to be rotated by drill 1 and (b) to transfer the applied thrust to the bit so that neither rotation nor thrust interferes with the percussive action. The bearing can be seen in figure 4.5 as part of the whole drilling rig and the design is separately detailed in figure 4.7.

a) Measurement of Speed of Rotation

To measure the speed of rotation an Evershed FFIA tachogenerator was introduced at the point of rotation. The rotating shaft on drill 1 that provides rotation to the bit by means of two 2" pulleys and a drive belt, was also used to rotate the tachogenerator shaft. This was done by means of two ½" pulleys and a drive belt. The output from the generator was recorded on a Rikadenki three-pen chart recorder, so that the speed or rotation when drilling could be directly recorded and different speeds recorded by changing the setting of the variac for drill 1.

b) Measurement of Percussion

The percussive action of drill 2 is obtained by the armature shaft of the drill rotating a cam shaft and a double cam compresses a spring. When the spring is released

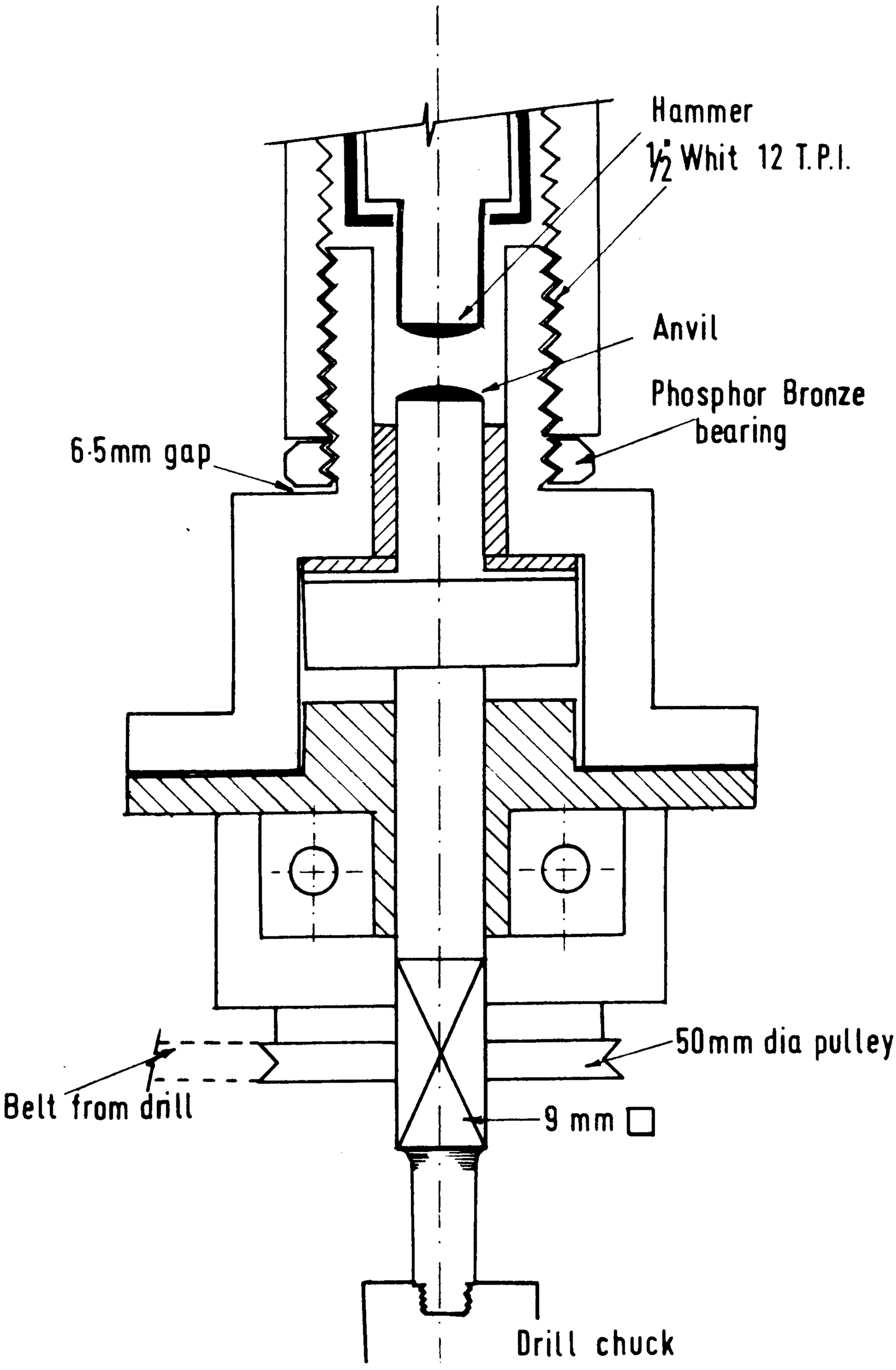

FIGURE 4.7: THE THRUST BEARING.

it pushes the percussive hammer downwards so striking the anvil at the top of the bit shaft to give the percussion.

A diagram of the percussive action is given in figure 4.8.

The percussion rate in blows/min is obtained by calibrating the armature shaft rotations for the variac settings. The number of blows will be the speed of the armature shaft divided by the gear ratio of the armature shaft to the cam shaft times two because of the double cam giving two blows for each revolution.

The energy per blow is a fixed value and is calculated from the energy imparted by the spring. Therefore, the power input by the percussive drill is the percussion rate times the energy/blow.

The details of calibration and power input are given in section 4.3 (b) on percussion calibration.

c) Measurement of Torque

In order to measure torque to enable the rotary power input to be determined from $2\pi NT$, where N is speed of rotation, and T is the torque, a torque measuring device was designed. This was to be a simple and accurate device to give the torques when drilling.

It was decided that a torque holder to grip the cylindrical rock specimens (50mm long and 25mm diameter) and to freely rotate on its base through a bearing would be used. To measure the torque a torque arm from the torque holder comes to rest on a cantilever beam and the torque developed when drilling produces a force which deflects the

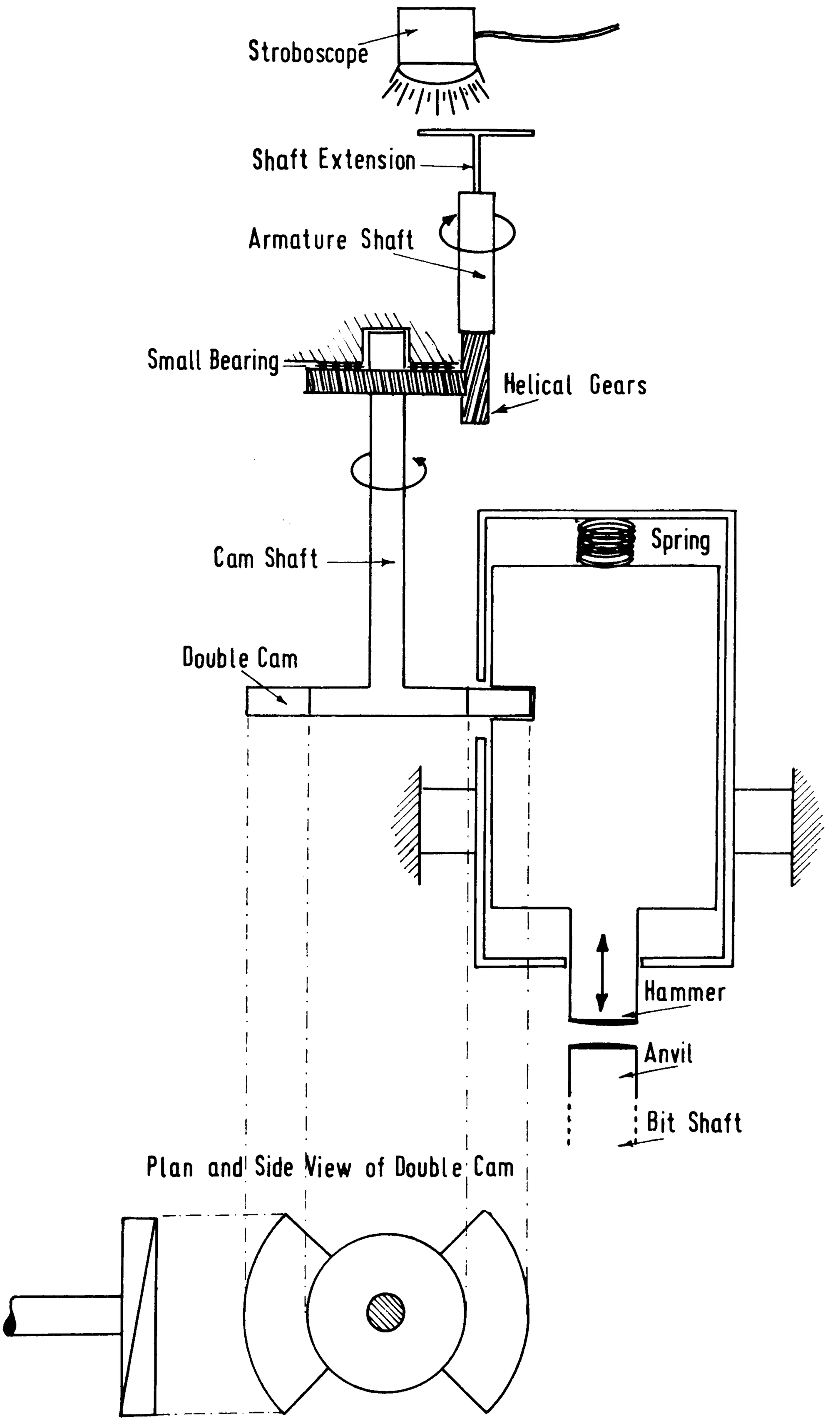

FIGURE 4.8: SCHEMATIC DRAWING OF THE PERCUSSIVE ACTION.

beam. Strain gauges are used to register the deflection which is recorded on the Rikadenki as a voltage. Hence by calibrating the beam for known torques, the torques when drilling can be obtained in terms of recorded voltage. The drilling torque $\propto$ force x arm length from centre of drill rock specimen to centre of beam $\propto$ deflection of beam $\propto$ recorded voltage.

In designing the torque measuring apparatus a convenient length of 4" from the centre of the drill specimen to the centre of the beam was chosen. Also to obtain a reasonable signal from the strain gauges (usually about 500 microstrains) it was necessary to determine the length and material of beam needed. Considering the bending moments in terms of strain equations:-

$$\frac{P}{y} = \frac{E}{R} = \frac{M}{I}$$

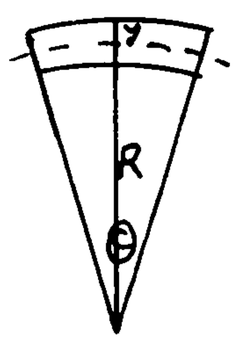

$$\text{Strain} = \frac{(R+y)\theta - R\theta}{R\theta} = \frac{y}{R} = y\,\frac{M}{EI}$$

where, y is the distance from the neutral axis

M is the bending moment

E is the Young's Modulus and

I is the second moment of area

The rectangular beam was to be deflected as a cantilever so that the strain equation becomes:-

$$\text{Strain} = \frac{d}{2} \times \frac{W\ell}{E} \times \frac{bd^3}{12} \qquad \text{Equation 1}$$

where, d = depth of the beam

b = breadth

W = applied load

ℓ = length of beam

E = Young's Modulus

and y maximum = $\frac{d}{2}$, M = $W\ell$ bending moment for a cantilever beam,

$$I = \frac{bd^3}{12}$$

Choosing a tempered steel beam of dimension breadth, b = 23.8mm and the depth, d = 1.346mm having a Young's Modulus between 30 x 10^6 to 40 x 10^6 p.s.i. as quoted in the Engineers handbook. Therefore, the unknown for designing the length of the cantilever beam is W, the applied load. This was obtained by measuring the maximum torque to cause stalling at maximum speed of rotation of the drilling rig. Using a spring balance, pulleys and weights this value of torque could be crudely determined and its value doubled to allow for any errors.

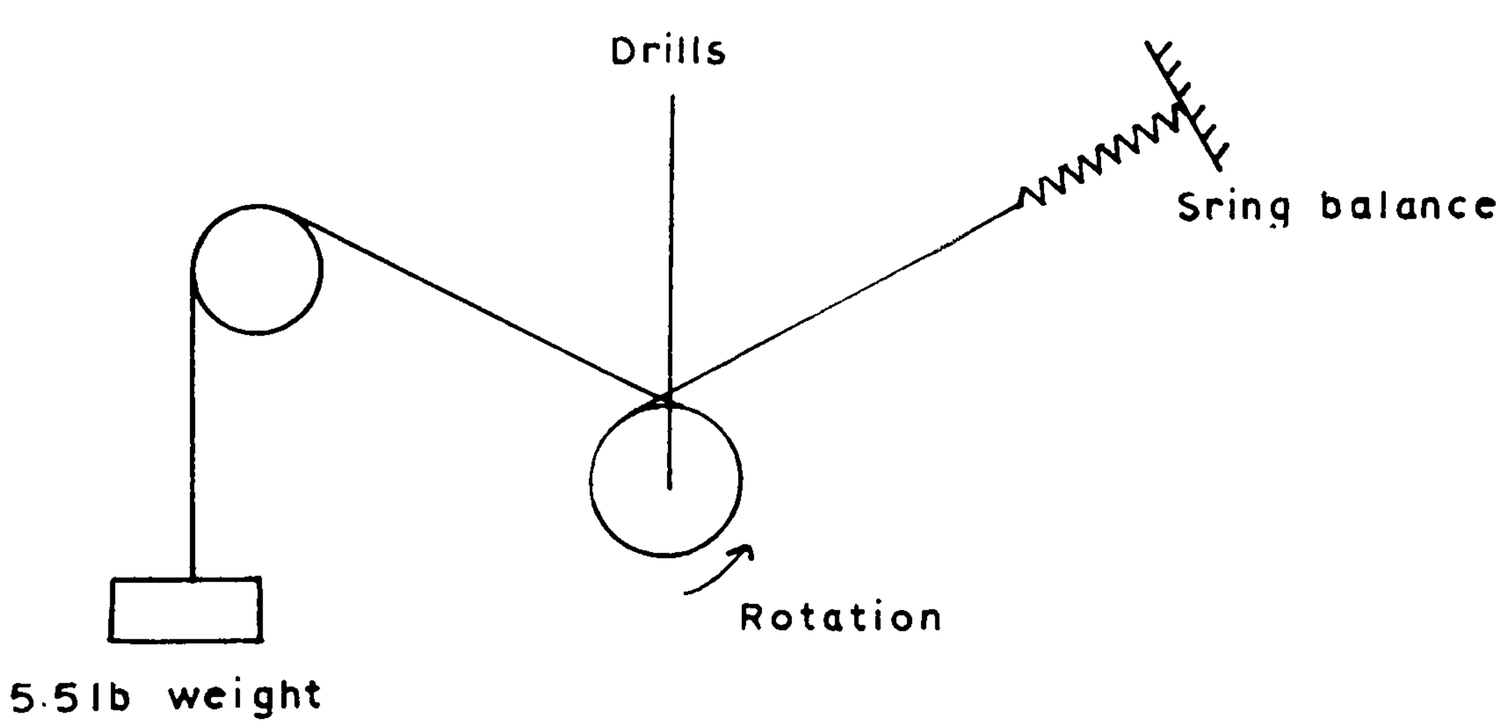

Therefore, Torque = (spring balance reading - hanging weight to cause stalling) x diameter of pulley.

= (20 - 5.5)lbs x $\frac{5}{8}$"

= 10lbs ins.

Maximum Torque allowing for errors = 20lbs ins.

As the torque radius of the torque holder from the centre of the cylindrical rock specimen to the centre of the beam was chosen to be 4" then W the maximum applied load equals 20lbs ins/4" = 5lbs.

Hence it is possible to determine the length of the cantilever beam from equation 1, however it was felt that Young's Modulus for the beam, should be accurately determined.

Young's Modulus

Young's Modulus was determined by 3 point loading a 150mm length of beam on the Instron using two dial gauges. The standard procedure was used with one dial placed at the centre of the beam to determine maximum deflection and the other dial at the end support to measure the downward movement of the measuring cell relative to the beam. The difference between the two dials gives the true deflection of the beam. Values of increasing loads producing increasing deflection were noted and a graph of load against true deflection was plotted which is shown in figure 4.9. The slope of the graph was then used to determine Young's Modulus from the equation:-

$$\text{Young's Modulus, } E = \frac{W}{d} \times \frac{L^3}{48I}$$

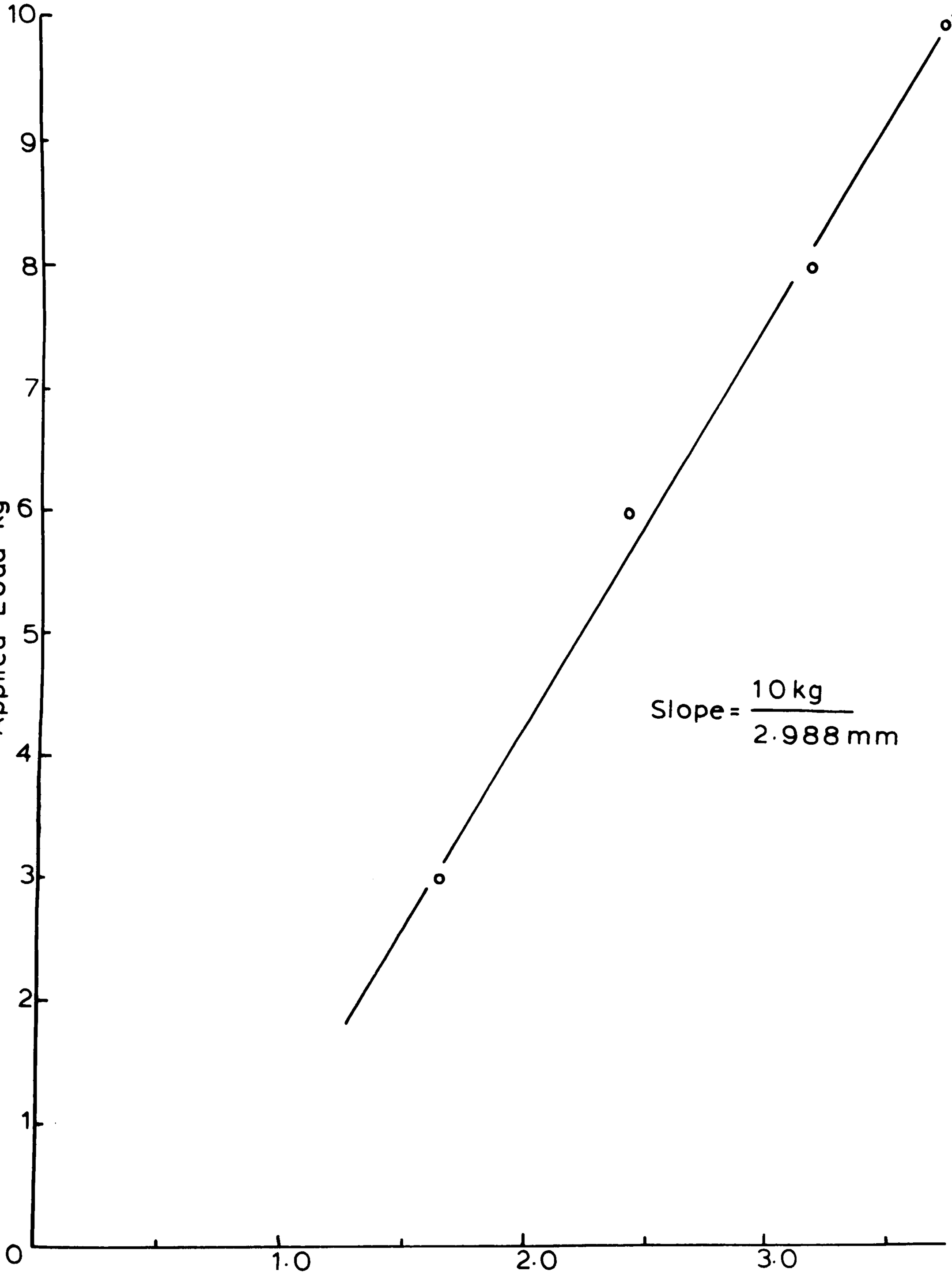

FIGURE 4.9: 3-POINT LOADING OF THE BEAM

where, W is the load applied to the 3 point loaded beam, d is the true deflection, L is the length of the span, I is the second moment of area $\frac{bd^3}{12}$.

$$E = \frac{10kg}{2.988mm} \times \frac{(119)^3 \times 12}{48 \times 23.8mm \times (1.346)^3}$$

$$= \underline{24,185.42kg/mm^2}$$

or 34.406×10^6 p.s.i.

This now completes the information required for determining the length of the cantilever beam for the torque measuring, equation 1 becomes:-

$$\text{Strain} = 500\times10^{-6} = \frac{6xW\ell}{Exbd^2} = \frac{6 \times 2.268kg \times \ell}{24,185.42kg/mm^2 \times 23.8mm \times (1.346)^2 mm^2}$$

length of cantilever, ℓ = 39.075mm

This cantilever will have a maximum deflection of

$$d = \frac{WL^3}{3EI} = \frac{2.2268 \times (39.075)^3 \times 12}{3\times24,185.42\times23.8\times(1.346)^3}$$

$$= 1.9024mm$$

Figure 4.10 shows the final torque measuring apparatus.

Strain Measurement

As stated earlier to measure the torque the deflection of the beam is registered by two strain gauges and the change in voltage is recorded on the Rikadenki recorder. To do this the gauges are placed at the end of the cantilever, one on each side, where the greatest bending occurs. The gauges are connected in a Wheatstone Bridge set up with resistances shown in the diagram on the next page:-

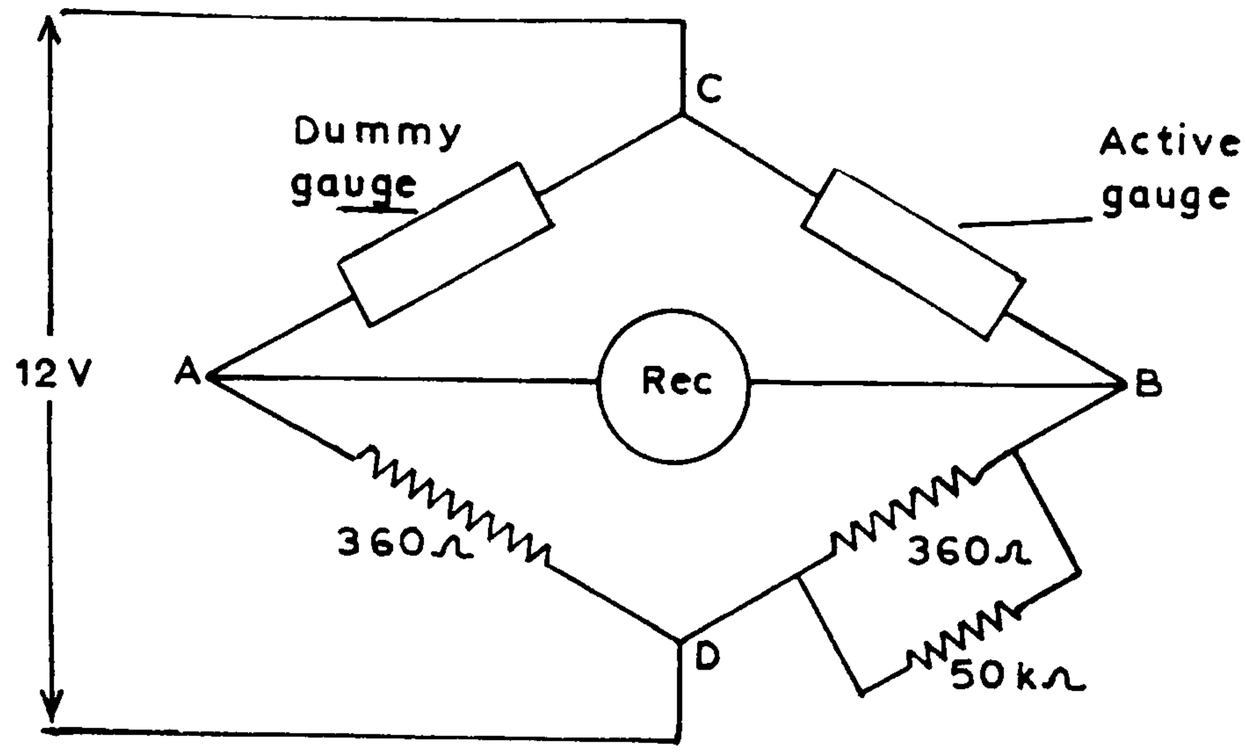

WHEATSTONE BRIDGE

Recorder to AB, active gauge to BC, Dummy Gauge to AC, and a 12 volt power supply to CD. With no bending the recorder is set to zero, with bending the unbalance is recorded as a voltage on the Rikadenki.

Before all of the drilling measurements could be made it was now necessary to calibrate the speed of rotation, the torque and the percussive action. Section 4.3 deals with the calibration of these parameters.

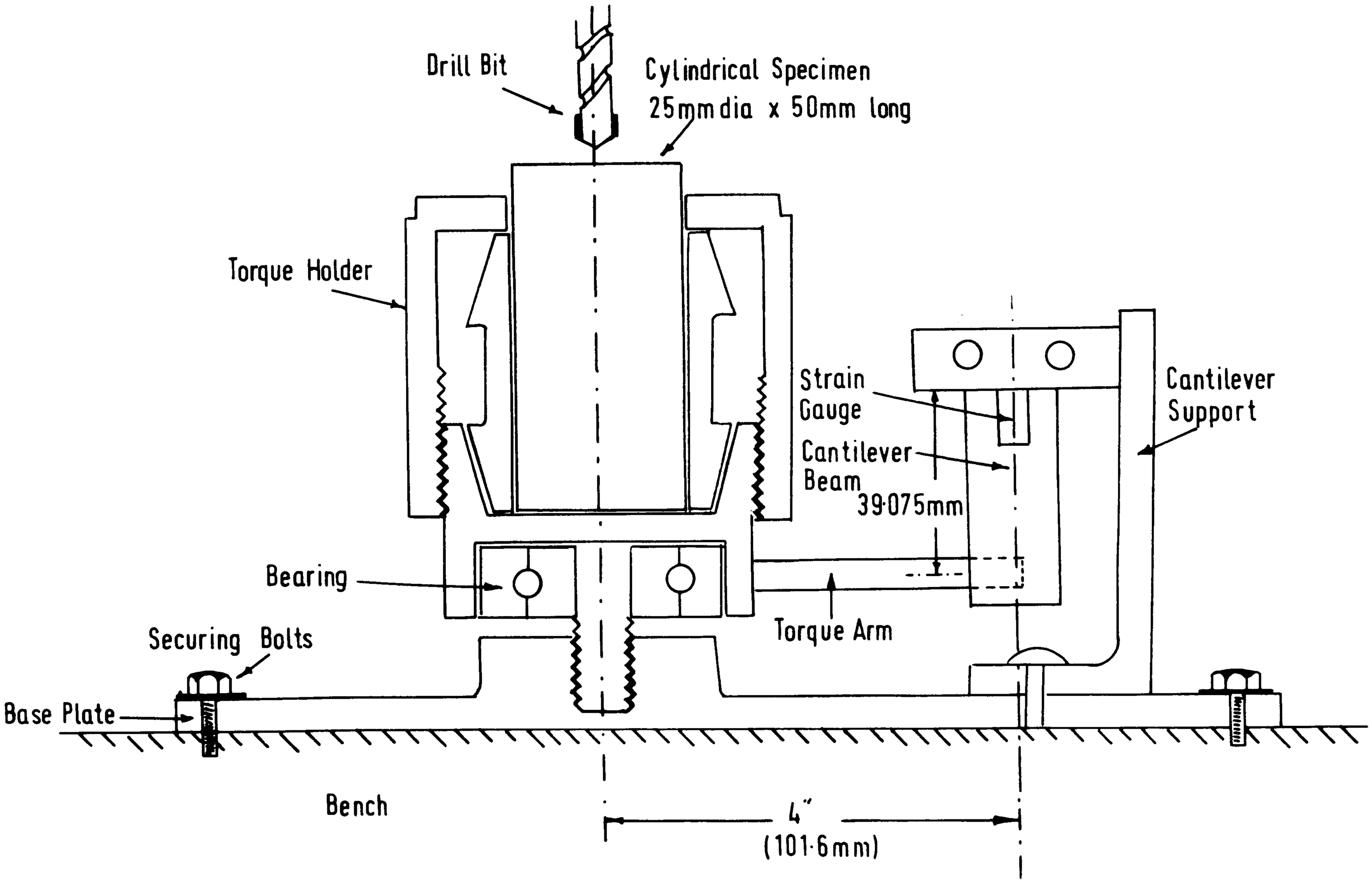

FIGURE 4.10: SCHEMATIC DRAWING OF THE TORQUE MEASURING DEVICE.

4.3 Calibration of the laboratory drills, speed of rotation, percussion and torque.

a) Speed of Rotation Calibration

A stroboscope was used to measure various speeds of rotation given by the variac for drill 1. The corresponding voltages obtained from the tachogenerator were recorded on the Rikadenki. Hence a graph of voltage against speed was plotted for calibration purposes, so that the speed when drilling can be obtained by taking the voltage reading. Figure 4.11 shows the graph of voltage v. speed, which is a linear relationship. The linear regression equation gave a correlation coefficient of 0.999384 and could be used for obtaining the speed from the voltage as well as the graph. Table 26 gives the voltage-speed values in columns 1 and 2.

Regression equation for voltage against speed is

y(speed) = 41.6238x(voltage)+19.9479

correlation coefficient, c.c. = 0.999384

The reason for taking the speed as the y variable and the voltage as the x variable was simply because the Wang computer has the facility for predicting y from a known x by using the established regression equation. This was also done for the percussion and torque calibrations.

b) Percussion Calibration

The percussion rate was calibrated by using the stroboscope to measure the speed of rotation of the armature shaft

in drill 2, for various settings on the variac for drill 2. This was permissible, as using this variac, drill 2 is subjected to a constant load, which is to compress the spring back x inches by use of a rotating double cam. The spring is then released by the cam so allowing it to push the hammer to strike the anvil on the top of the bit shaft. Any other thrusts or vertical forces that might cause a load are taken by the thrust bearing. The armature shaft was extended so that measuring the speed was made easier. A graph of variac settings (0-100) against the speeds measured was plotted and is shown in figure 4.12. Again this is a linear relationship and the regression equation is:-

y(speed) = 267.729x(variac reading)-3365.44

correlation coefficient, c.c. = 0.999508

The values for speed of the armature shaft and the variac settings are given in table 26, columns 2 and 3.

Now the speed of the armature shaft was measured this had to be converted to the percussive rate of blows/minute. The armature shaft rotates the cam shaft via two helical gears and the gear ratio is 8.5 to 1 (i.e. 68 teeth to 8 teeth). Hence the speed of the cam shaft is the speed divided by the gear ratio and since there are two cams i.e. a double cam there will be two blows for every revolution.

$$\text{Percussive rate in blows/minute} = \frac{\text{armature R.P.M} \times 2 \text{blows}}{8.5}$$

To evaluate the energy/blow, it is necessary to find

out the actual strain energy imparted by the spring; this can be expressed by the equation:-

$$\text{Strain energy/blow} = \tfrac{1}{2}\, sd^2$$

Where, s is the maximum load divided by the deflection produced by the maximum load on the spring, and d is the distance through which the energy is imparted i.e. the distance the cams lift the spring. d is 3/16", but the hammer is pushed upwards by the bit shaft by 54 thousands of an inch, hence actual d = the distance raised by the cam minus 0.054". S was found by loading the spring in the Instron testing machine and s = 15kg/5.1mm

$$\text{Therefore, the strain energy} = \tfrac{1}{2} \times \frac{15 \times g}{5.1\text{mm}} \times (0.1875" - 0.054")^2$$

$$= \tfrac{1}{2} \times \frac{15 \times g}{5.1} \times (3.3909\text{mm})^2 \ldots \text{Nmm}$$

$$= \underline{0.16588\text{Nm/blow}}$$

$$\text{Hence the Power input} = {}^{\text{Nm}}/_{\text{blow}} \times {}^{\text{blow}}/_{\text{min}}$$

$$= 0.16588 \frac{\text{Nm}}{\text{blow}} \times \frac{\text{armature R.P.M.}}{8.5} \times 2 \text{ blows}$$

$$= \frac{0.16588\text{Nm}}{4.25} \times \frac{1\text{min}}{60\text{secs}} \times \frac{\text{rev}}{\text{min}}$$

$$\text{Percussive Power Input} = \text{armature speed} \times 0.00065051 .. \frac{\text{Nm}}{\text{sec}} .. \text{Watts}$$

The armature speed is obtained from the regression equation for a variac setting, so the percussive power input can be calculated by multiplying the speed by 0.00065051.

c) Torque Calibration

Torque was calibrated by applying known torques using

a torque wrench. This applied torque was then registered on the Rikadenki chart recorder, the voltage signal coming from the strain gauges due to the cantilever beam being deflected by the torque arm. Table 26 lists the recorded voltage and applied torque in columns 5 and 6. The graph of applied torque versus the voltage is shown in figure 4.13 and the linear regression equation given below:-

y(torque) = 0.14676x(voltage)-0.05921

correlation coefficient, c.c. = 0.999526

So that the drilling torque can be easily obtained from the recorded voltage when drilling.

TABLE 26

Calibration values for speed of rotation, percussion and torque

Speed of Rotation		Percussion		Torque	
Voltage volts	Speed of rotation	Variac setting	Speed of armature	Voltage m volts	Torque lb ft
0	0	35	5,800	22.0	3.0
11.0	500	40	7,250	27.5	4.0
19.5	850	45	8,800	34.0	5.0
25.0	1,100	50	10,050	41.0	6.0
31.0	1,250	55	11,450	52.0	7.5
33.5	1,410	60	12,700	58.0	8.5
38.0	1,600	65	13,900		
39.5	1,650	70	15,800		
48.0	2,000	75	16,800		
48.0	2,050	80	18,100		
59.5	2,500	85	19,200		
60.0	2,520	92	21,100		
		98.5	23,000		

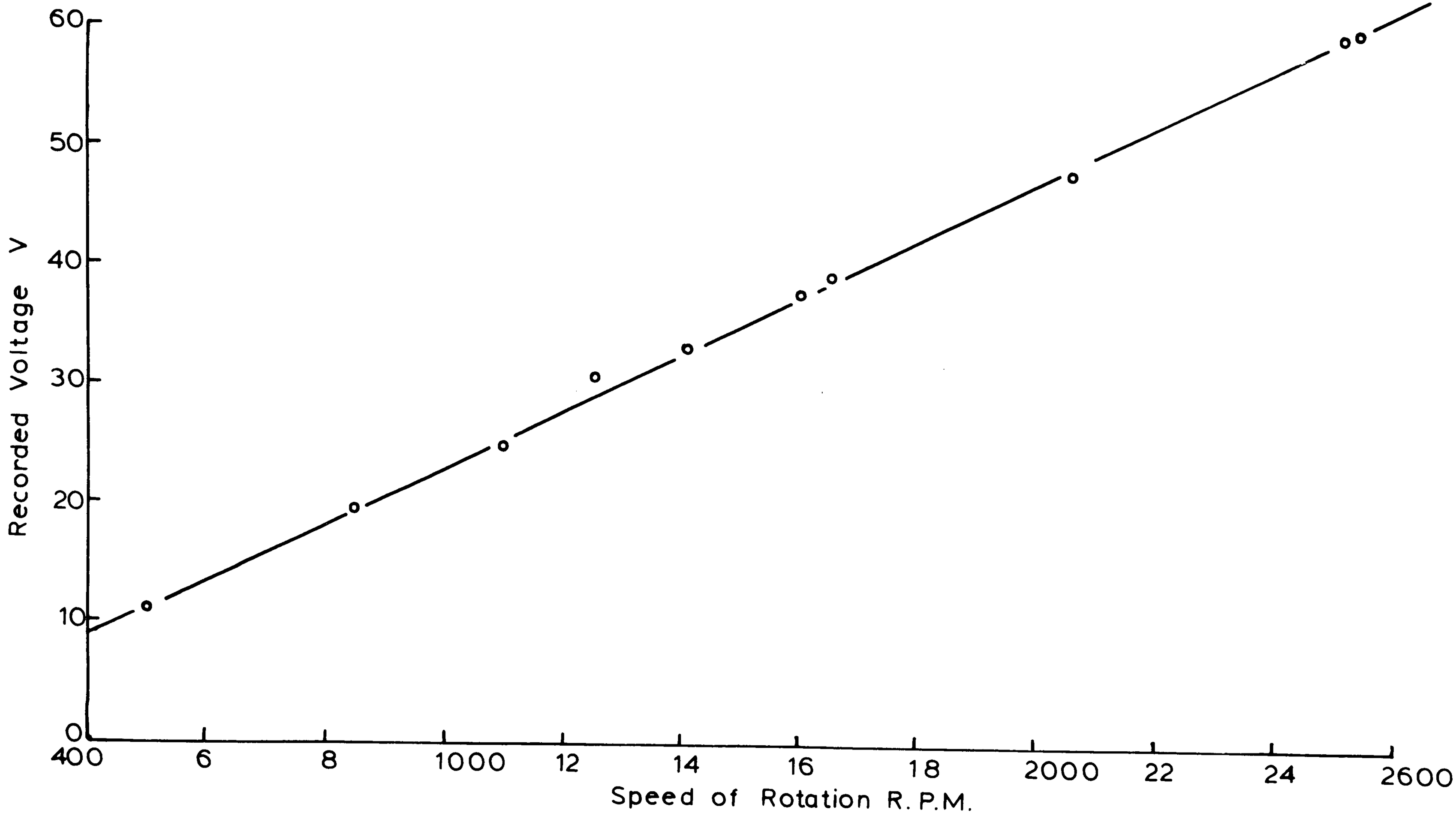

FIGURE 4.11: SPEED OF ROTATION CALIBRATION.

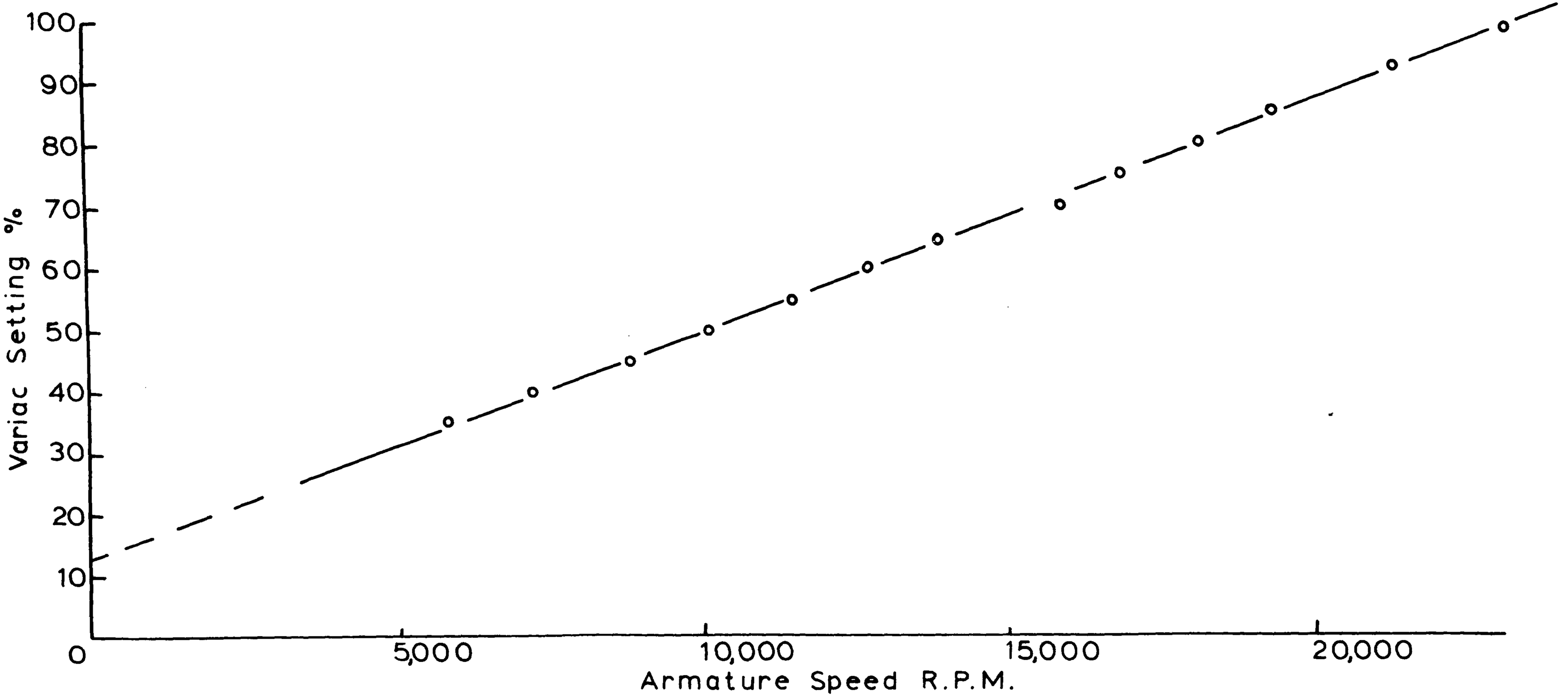

FIGURE 4.12 : PERCUSSION CALIBRATION.

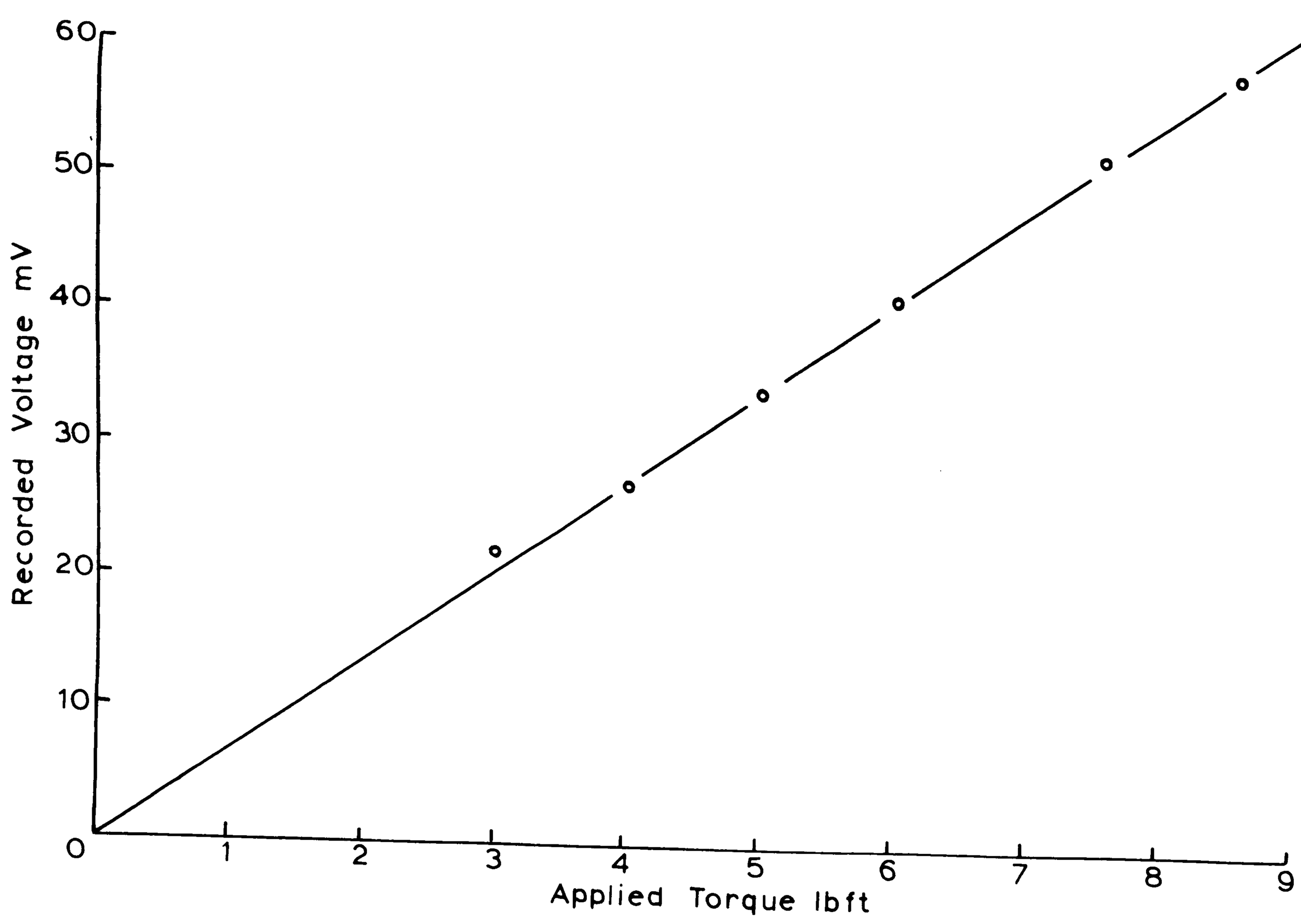

FIGURE 4.13 : TORQUE CALIBRATION.

4.4. The Drilling Operation

The drilling rig is free to slide vertically on the centre post when drilling. At the start of drilling the whole rig is supported by the drill bit resting on the centre of the cylindrical specimen. The drilling distance (approximately 14mm) is set between the contact switch and the contact plate. The contact plate can also slide up and down the centre post, so that the drilling distance can be set. After setting the distance, the plate is secured to the post and will support the rig after drilling, when the rig comes to rest on the plate.

Switching on the system, simultaneously starts the drills to commence drilling and the digital timer to measure the time of drilling. The drill carriage travels the set drilling distance down the post and comes to rest on the contact plate where, the contact switch simultaneously switches off the drills and stops the timer.

The torque, speed of rotation voltages are recorded and the cuttings collected. The cylindrical specimen is unscrewed from the torque holder and the depth of penetration is measured for that thrust, speed and percussion. Hence, all six drilling parameters (thrust, speed of rotation, torque, percussion, drill cuttings and penetration rate) can be measured for different combinations.

4.5. Preliminary Drilling Tests on the Laboratory Drill Rig

The preliminary tests on the laboratory drill rig were

conducted in order to establish that the rig does exhibit rotary-percussive characteristics. Darley Dale sandstone and Cornish granite were chosen for the preliminary tests as they have widely different physical properties.

a) Thrust tests

i) Penetration rate - thrust tests for maximum rotary-percussive and maximum rotary drilling.

These tests were carried out in the same manner as those on the Black and Decker GD4 drill which were described earlier in this chapter (4.1). With this new drilling rig it was possible to apply greater thrusts at maximum speed of rotation and percussion before the anomaly in the penetration rate/ thrust graphs occured.

Tests were also conducted on the two rocks at maximum speed without any percussion in order to examine the penetration rate - thrust graphs of pure rotary drilling compared to rotary - percussive drilling. The difference between the two gives the percussion effect.

The total weight of the drilling rig is 24lbs and increased thrusts were obtained by securing weights on top of the percussive drill (drill no. 2). Penetration rate was averaged from the drilling of five holes per thrust level.

The results of penetration rate, thrust values are given in table 27 for both rotary-percussion and rotary drilling in Darley Dale sandstone and Cornish granite. The graphs of penetration rate against thrust for the two types of drilling in the two rocks are plotted in figure 4.14.

The results show that each rock exhibits the standard penetration rate/thrust characteristics for both rotary-percussion and pure rotation. Large increases in penetration rate are obtained through the addition of the percussive action. The fact is particularly evident with Cornish granite, where rotation alone produces very little penetration with the 'hard' granite. Indeed, this is the major reason for the addition of percussion to rotary drilling so as to overcome the difficulty of penetration in 'hard', 'strong' rocks.

TABLE 27

Penetration rate P.R. - thrust values for rotary-percussion and pure rotation, drilling in Darley Dale sandstone and Cornish granite.

(at maximum speeds of rotation and percussion)

Darley Dale Sandstone			Cornish Granite		
Thrust lbs	Rotary Perc. P.R.mm/sec	Pure Rota. P.R.mm/sec	Thrust lbs	Rotary Perc. P.R.mm/sec	Pure Rota. P.R.mm/sec
24	10.621	6.201	24	1.789	-
29	11.786	9.057	29	2.358	-
34	12.535	9.595	34	2.611	-
44	14.448	10.510	44	2.919	-
54	16.542	10.825	54	3.449	0.191
64	18.778	11.887	64	4.308	0.290
74	16.751	10.807	74	4.612	0.165

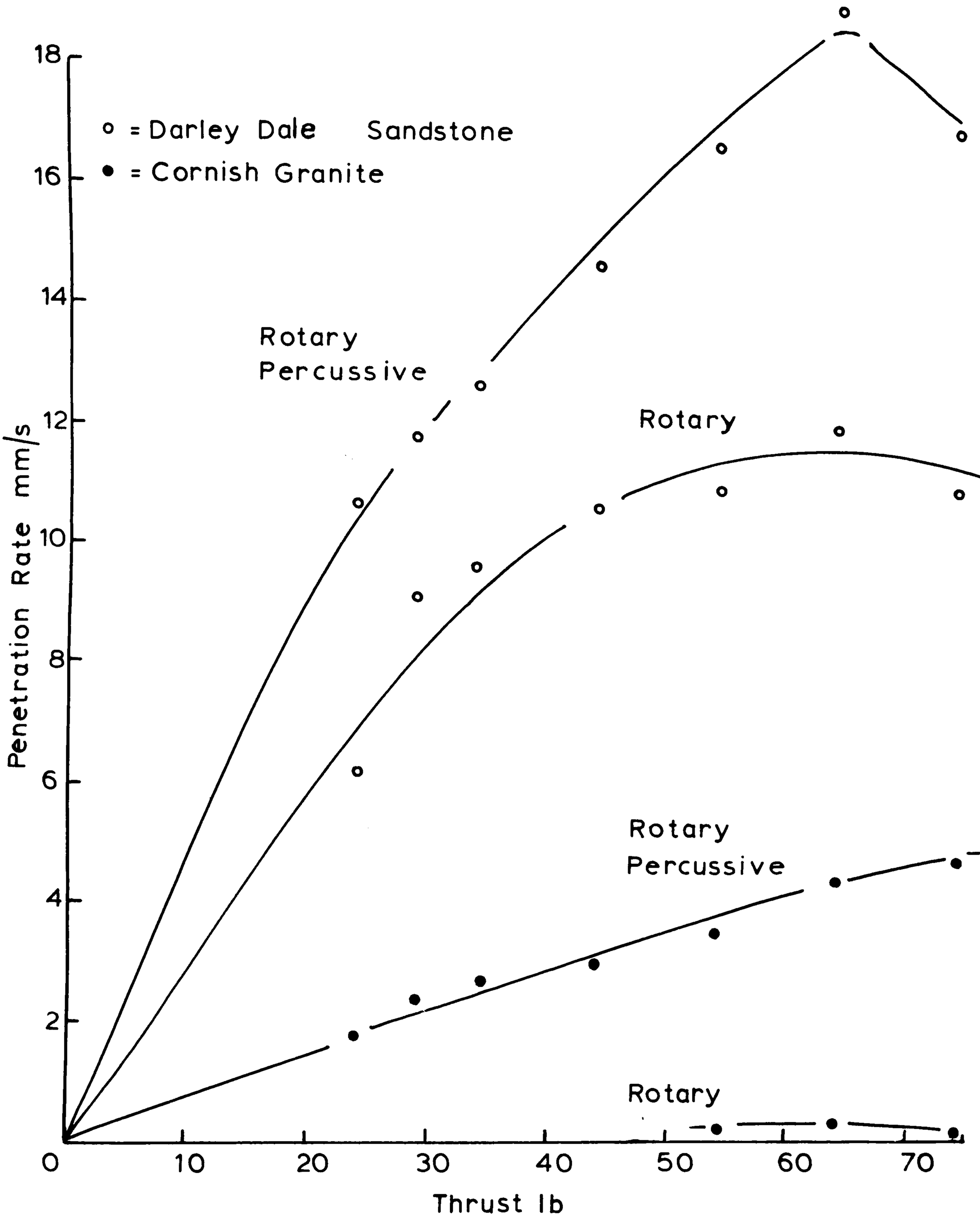

FIGURE 4.14: PENETRATION RATE-THRUST TESTS FOR MAXIMUM ROTARY AND ROTARY-PERCUSSIVE DRILLING.

Cuttings were collected at a thrust value of 64lbs for Darley Dale sandstone to compare the surface areas created/gram for both rotary-percussion and pure rotation. Rotary-percussion drilling gave a value of 0.03505778m^2/gram and rotary drilling for the same thrust 0.0415084m^2/gram. This result agrees with the findings of other workers, where the cuttings show that rotary-percussion is more efficient than rotary in that less energy is wasted in producing fines. The same test for Cornish granite gives an even greater difference between the cuttings, rotary-percussion 0.04261091m^2/gram and pure rotary having an area 0.05109608m^2/gram.

ii) Low speed of rotation and maximum percussion thrust tests.

Tests were now conducted to examine the penetration rate and power for varying thrusts at a low speed of rotation with maximum percussion (15 watts). The speed of rotation and torque are recorded on the Rikadenki and the penetration rate measured for five holes drilled per rock. The drill cuttings for each thrust level were collected and sieved, the fractions weighed and the surface area created/gram computed.

The results for Darley Dale sandstone and Cornish granite are given in table 28, the thrust against penetration rate

is plotted in figure 4.15 and the thrust against power input plotted in figure 4.16. The power input is the total power input equalling the sum of the maximum percussive power and the rotary power (2π x speed x torque).

The penetration rate/thrust graphs at this low speed setting clearly show that anomaly shown in the previous penetration rate/thrust characteristics. However, the anomaly is much larger at this lower speed. Three more rocks were drilled at the same speed setting, measuring the same parameters for varying thrusts. The three other rocks drilled were Bath limestone, Denbigh limestone and Mount Sorrel granite and the results for these are also shown in table 28. The penetration rate and power against thrust are plotted in figures 4.15 and 4.16 respectively with Darley Dale and Cornish granite.

For Darley Dale and Bath limestone intermediate thrusts were applied and the penetration rate measured in order to confirm the shape of the curves, also higher thrusts were applied to extend the curves.

Figure 4.15 verifies for the five rocks, that thrust is a very important drill variable and it is essential that the correct thrust is chosen and maintained to give the best performance, avoiding the anomalies which occur.

The power in figure 4.16 is also considerably affected by the thrust in that the rotary power part increases as the thrust increases. This is due to the thrust affecting the drilling torque. The percussive power is constant as the drill was designed to make the percussive action

TABLE 28

Results of Penetration Rate P.R., Total Power Input P_T, and drill cuttings Ad from drilling five rocks at varying thrust levels at a low speed of rotation and maximum percussion.

	Darley Dale Sandstone			Bath Limestone		
Thrust lbs	P_T watts	P.R. mm/sec	Ad m^2/gm	P_T watts	P.R. mm/sec	Ad m^2/gm
24	20.004	7.828	0.038963	15.799	3.720	-
34	31.295	8.542	0.038006	22.294	4.422	0.027562
44	61.924	7.272	0.037074	24.795	5.401	0.026345
54	77.014	5.576	0.036727	34.995	6.630	0.027787
64	79.692	4.943	0.035128	63.175	5.532	0.0304809
74	68.741	7.047	0.035743	60.560	6.952	0.027583

Extra points	P.R. mm/sec	P.R. mm/sec
69	5.350	6.052
79	7.713	4.617
89	7.211	5.361
94	6.298	5.601
99	5.097	-

	Cornish Granite			Denbigh Limestone		
Thrust lbs	P_T watts	P.R. mm/sec	Ad m^2/gm	P_T watts	P.R. mm/sec	Ad m^2/gm
24	16.661	1.01	-	-	-	-
34	26.678	1.717	0.040714	25.598	2.333	0.032044
44	28.643	1.403	0.042431	30.931	2.385	0.035701
54	29.304	1.041	0.043815	47.378	2.389	0.035242
64	39.403	1.419	0.040591	52.901	2.190	0.035326
74	35.319	1.194	0.043067	40.809	2.976	0.035105

	Mount Sorrel Granite		
24	15.618	0.910	-
34	22.422	0.918	0.040915
44	25.598	1.158	0.042431
54	30.989	1.242	0.043815
64	35.639	1.740	0.040591
74	33.704	1.599	0.043067

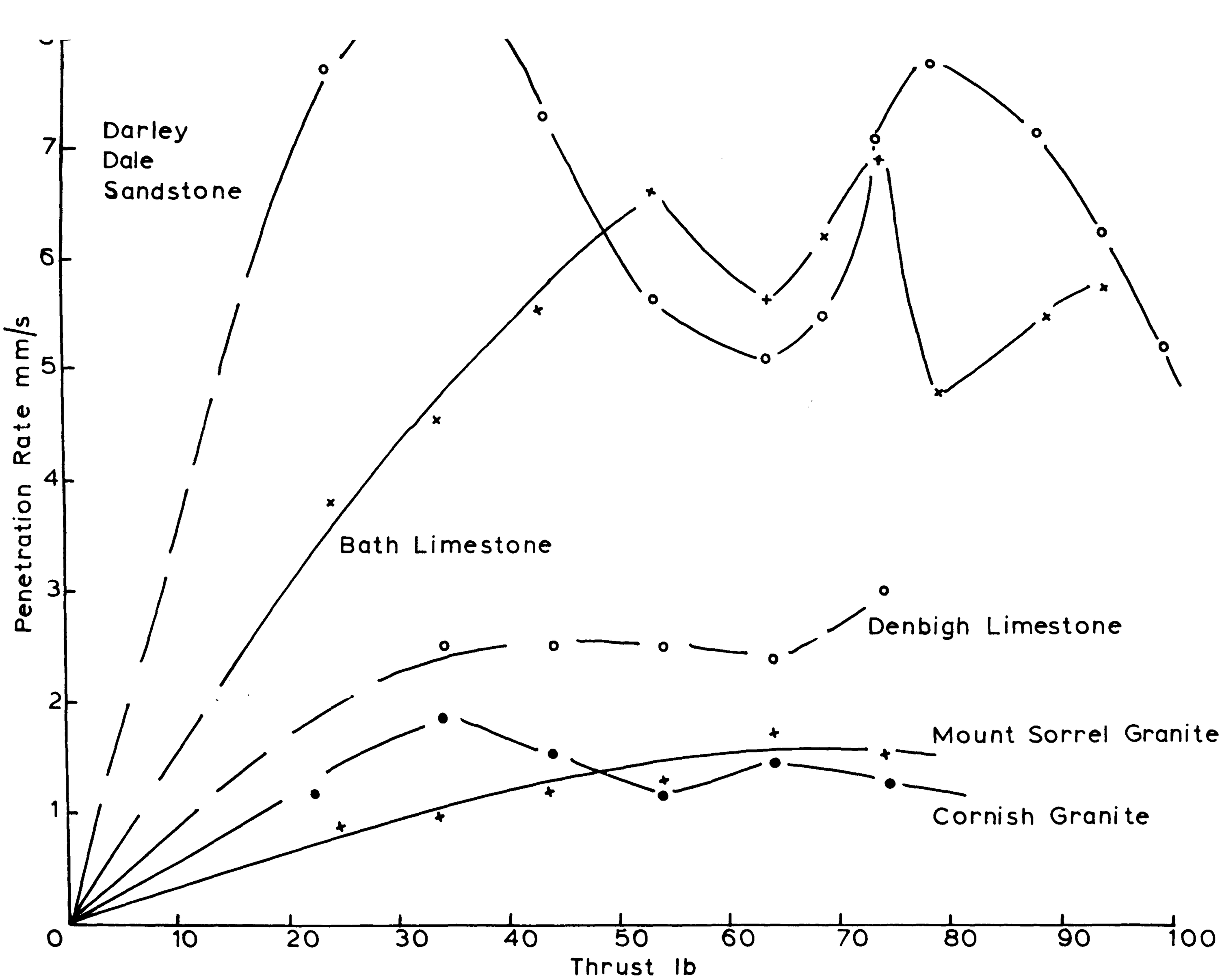

FIGURE 4.15: LOW SPEED OF ROTATION AND MAXIMUM PERCUSSION, PENETRATION RATE - THRUST TESTS.

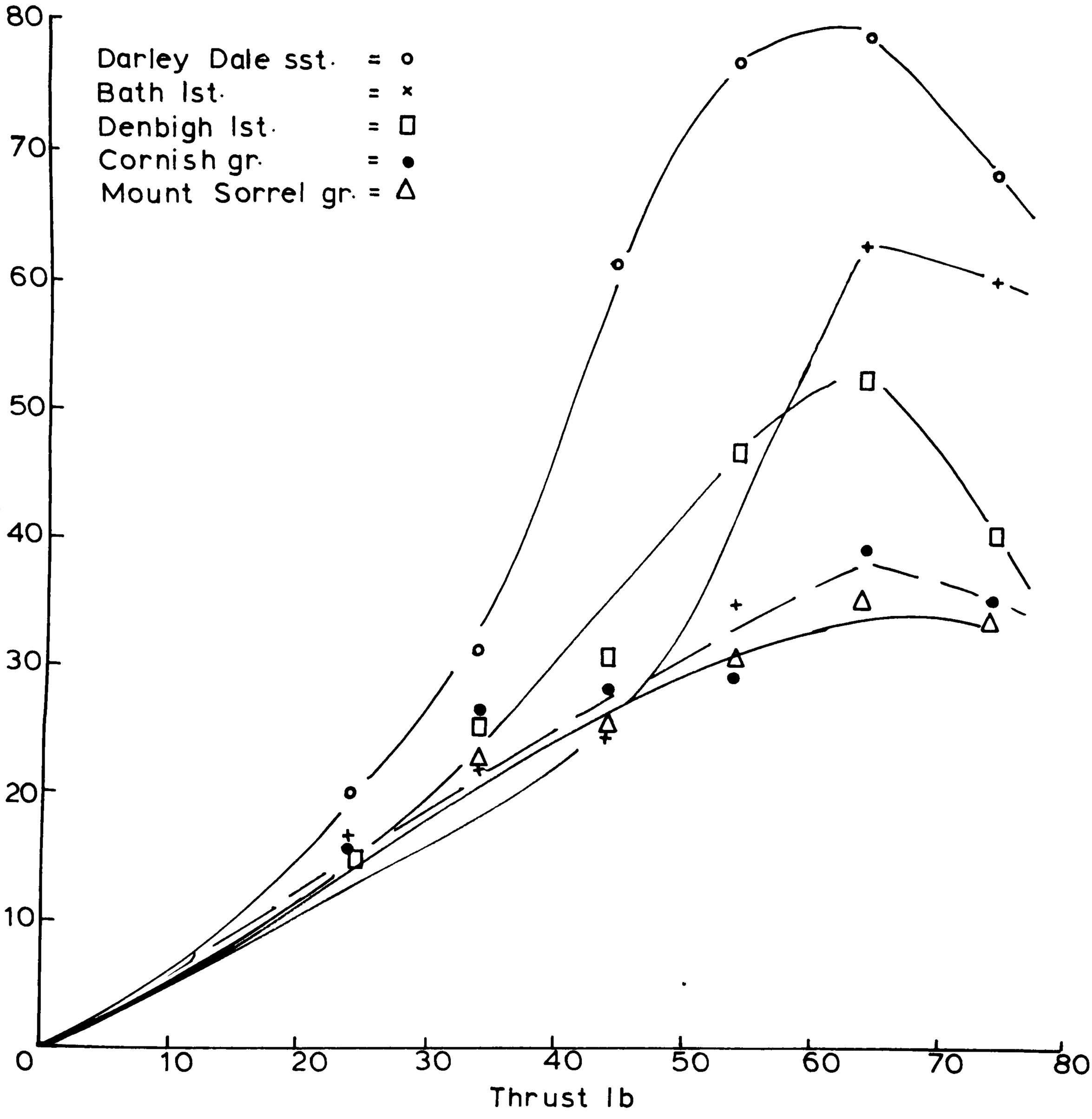

FIGURE 4.16: TOTAL POWER INPUT VERSUS THE VARIED THRUST AT LOW SPEED OF ROTATION AND MAXIMUM PERCUSSION.

independent. In the range of the thrusts applied the power increases to a maximum for the rocks drilled and then begins to decrease.

The computed surface areas from the cuttings collected show that there is a large variation from rock to rock. The cuttings do vary for the different applied thrusts for each rock, but there is no clear relationship except that for Darley Dale where the cuttings become less fine for increased thrust. This reduction in surface area for Darley Dale sandstone indicates that increasing the thrust is more efficient with regard to use of power as the power input increases.

b) Variation of speed of rotation tests

The speed of rotation was varied and recorded on the Rikadenki chart recorder along with the drilling torque, so that the power input can be calculated. The penetration rate was measured with a constant thrust of 64lbs and maximum percussion.

Again, Total Power Input = (Rotary Power+Percussion Power)Wat

= (2π NT+maximum speed of armaturex0.00065051)watts

Where N and T are the drilling speeds and torque respectively

Percussion power = maximum of 15 watts.

The average penetration rate for five holes was determined for that speed setting and a new bit used for each hole. The drill cuttings were collected, sieved and the surface area created per gram computed.

The results of penetration rate, speed of rotation, torque, total power input and surface area/gram of the drill cuttings are given in table 29. The graphs of speed against penetration rate for the two rocks are shown in figure 4.17 and those for total power input against penetration rate in figure 4.18. The graphs of total power input against the surface areas created per gram are shown in figure 4.19.

Figure 4.17 giving speed against penetration rate shows that the penetration rate increases linearly for the increases in speed. The change in penetration rate for Cornish granite is 73.7% and 74.5% for Darley Dale sandstone, showing that increases in speed over the same range are equally advantageous for increasing the percentage penetration rate of the rocks. However, figure 4.18 shows that Darley Dale sandstone has much higher power inputs, which is one reason for the higher penetration rates. The difference in power inputs is due to the values of the drilling torques developed for the same speeds being much larger for Darley Dale than for Cornish. Clearly, the drilling properties are very much dependent on the physical properties of the rock.

The difference between the rocks and the effect on the drill parameters also manifests itself in the drill cuttings where Darley Dale sandstone has a surface area per gram of around 0.035m^2/gram and Cornish granite around 0.040m^2/gram.

TABLE 29

Values of penetration rate P.R., torque, total power input and the cuttings produced when rotary-percussive drilling Darley Dale sandstone and Cornish granite at varying speeds.

(constant thrust of 64 lbs and 15 watts percussion power input)

Darley Dale Sandstone					Cornish Granite				
R.P.M.	P.R. mm/sec	Torque ft. lbs.	Total Power watts	Drill cuttings (Ad) m^2/gram	R.P.M.	P.R. mm/sec	Torque ft. lbs.	Total Power watts	Drill cuttings (Ad) m^2/gram
320	4.068	0.37372	31.910	0.034941	280	1.055	0.19027	22.533	0.039371
695	6.035	0.46911	61.101	0.034498	720	1.874	0.20495	36.327	0.039673
980	6.649	0.35860	64.692	0.035128	1020	2.419	0.16921	39.404	0.040598
1230	8.756	0.37372	79.998	0.035538	1220	2.685	0.16920	42.760	0.042090
1480	9.784	0.35904	90.138	0.035683	1550	3.438	0.15358	48.660	0.041973
1900	15.910	0.36610	113.301	-	1900	3.801	0.13891	52.319	0.042782

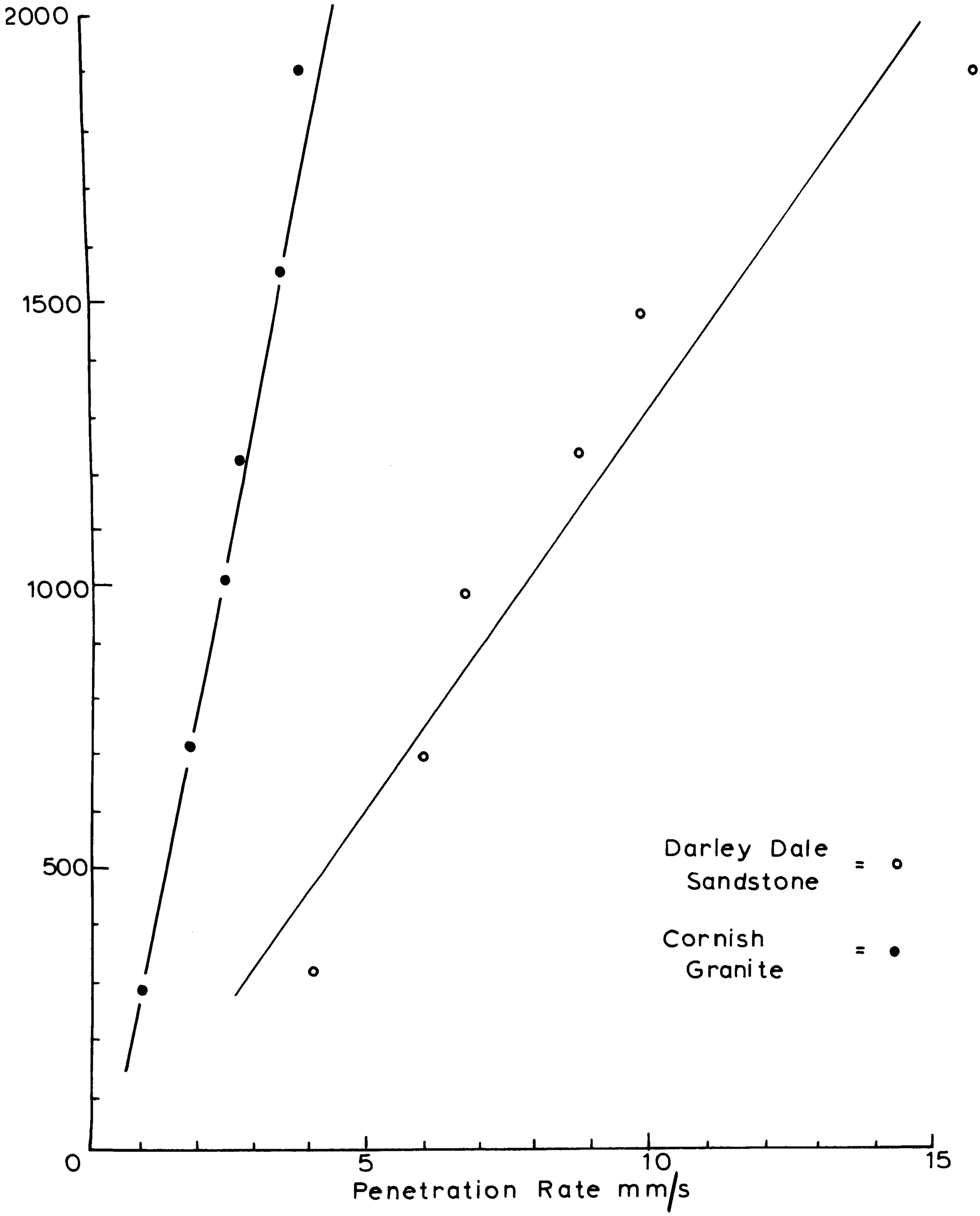

FIGURE 4.17: VARIATION OF SPEED OF ROTATION VERSUS PENETRATION RATE.

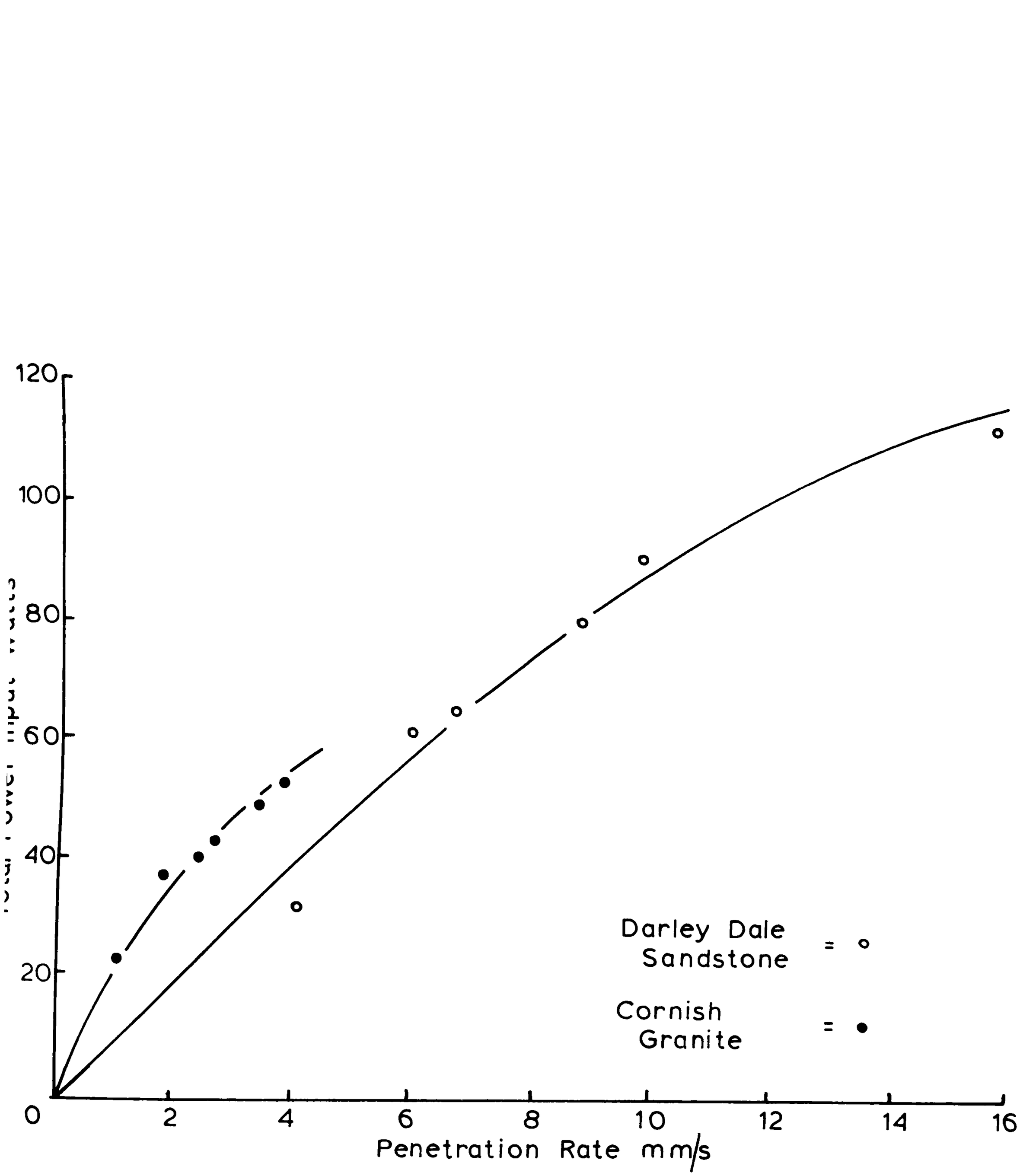

FIGURE 4.18: TOTAL POWER INPUT FOR VARIATION OF SPEED OF ROTATION VERSUS PENETRATION RATE .

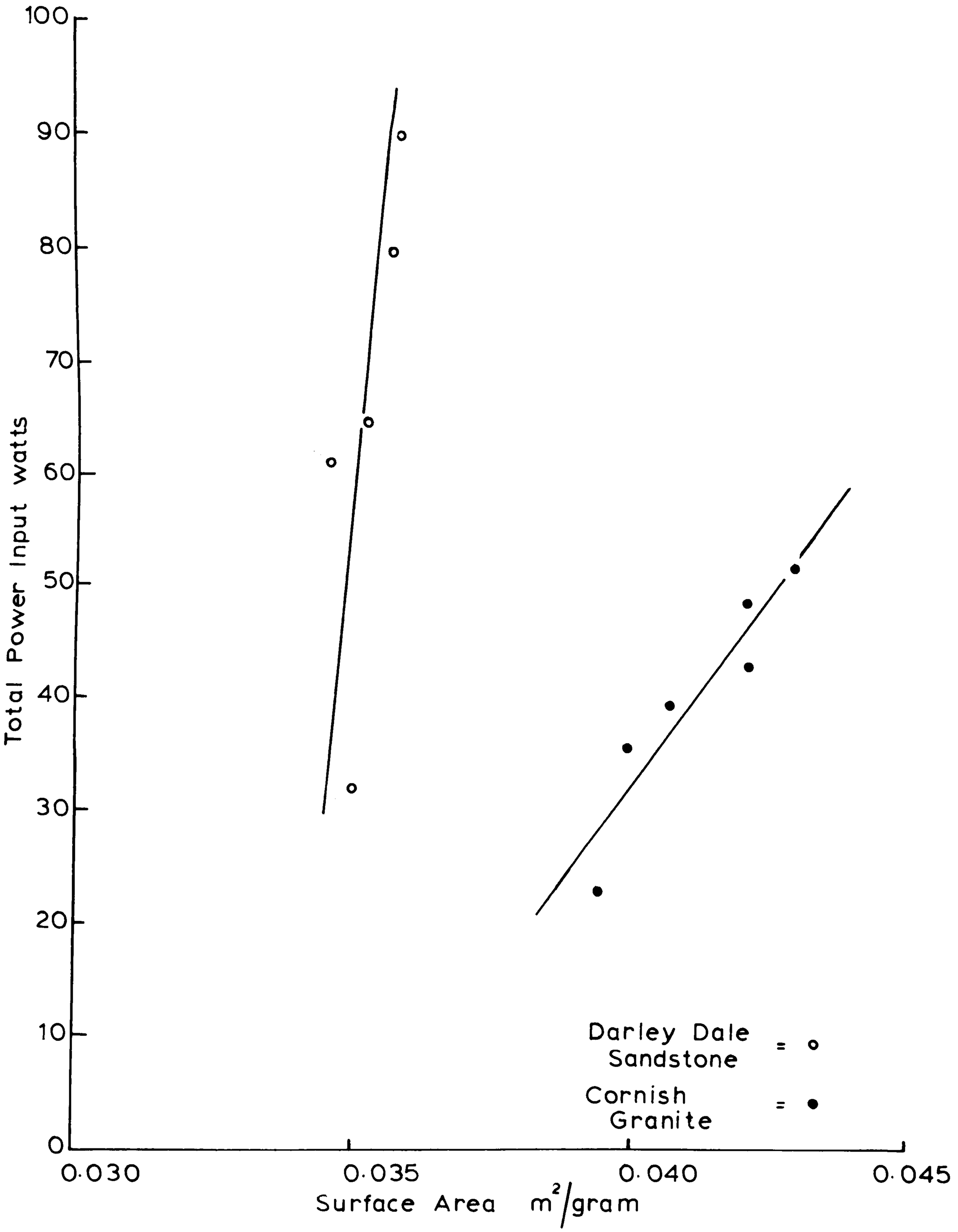

FIGURE 4.19: TOTAL POWER INPUT VERSUS SURFACE AREA OF DRILL CUTTINGS FOR SPEED OF ROTATION VARIATION.

The graphs in figure 4.19 show that the power input is proportional to the surface area per gram created. Increasing the speed of rotation does produce increased penetration rate, but some of the increased energy is wasted in producing more fines. The effect in change in surface area produced for speed increases with laboratory drilling is not as obvious with Darley Dale sandstone as it is with Cornish granite. The reason being that the increased rotation power produces more grinding with the granite giving the greater change in surface area per gram.

To summarise, increasing the energy input by increasing rotation increases the penetration rate for both rocks and increases the surface area per gram. With the granite less power is produced for input due to the smaller torques being developed and the granite has a larger surface area per gram compared to the sandstone. Increasing the energy of rotation produces further regrinding giving the larger surface areas. With Darley Dale increasing the energy input by increasing the speed does not produce as large an increase in the surface area per gram as the granite does. This means that less of the energy is wasted in further grinding, showing that increasing the speed of rotation is doing more useful work in the sandstone. The developed torque is dependent on the physical properties of the rock and determines the power input to the rock which goes to determine the drill performance together with the physical properties again and this reflects in the drill

cuttings. Hence, the performance, power and the drill cuttings are all very much interrelated with the physical properties of the rock and each other.

c) Variation of Percussion Tests

The variac setting for drill 2 was changed to give increasing values of percussive power for a low speed of rotation and constant thrust of 46lbs. The low speed of rotation was chosen in order to emphasize the percussion. The speed and torque values at different percussion levels were recorded on the Rikadenki. The penetration rate measured and the cuttings collected from drilling five holes with new bits at each percussion level.

The results are tabulated in table 30 and the percussion power increase against penetration rate graphs for the two rocks are given in figure 4.20. The total power input of percussion plus rotary is calculated and also tabulated in table 30, the graphs for total power against penetration rate are shown in figure 4.21.

These figures show that increasing percussion power gives a proportional linear increase in penetration rate and similarly for the total power input. The change in penetration rate due to the same increase in percussion power is 61% for the granite and 32% for the sandstone. This clearly shows the advantage of using increased percussion power particularly in 'harder' rocks such as granite.

The surface areas/gram of the cuttings collected show that for Darley Dale sandstone there is an increase in

surface area for the increased percussion power. The Cornish granite has a reducing area for the increased percussion power indicating that increasing the percussion part, drilling becomes more efficient for the drilling of 'harder' rocks. The increased energy to the granite does go to produce the higher change in penetration rates and less grinding of the cuttings takes place, whereas with the sandstone the same increase of energy produces half the penetration rate percentage increase of the granite and the amount of grinding increases. For the rocks tested this is in fact opposite to what happened in the speed tests as regards the cuttings, showing the effect that the different combinations have produced.

TABLE 30

Values of penetration rate (P.R.), torque, speed of rotation, drill cuttings (Ad) rotary power, percussive power and total power input when rotary-percussive drilling Cornish granite and Darley Dale sandstone at different percussion levels.

(constant thrust 46lbs)

Variae setting %	P.R. mm/sec	Torque ft.lbs	Speed R.P.M.	Drill Cuttings Ad:m^2/gm	Rotary Power watts	Percussive Power watts	Total Power watts
Darley Dale Sandstone							
35	4.741	0.11689	789	0.038759	13.057	3.773	16.830
45	5.368	0.11754	769	0.039022	13.010	5.810	18.734
55	5.810	0.11689	789	0.039311	13.057	7.448	20.505
77	6.502	0.10956	769	0.039701	11.915	10.733	22.648
90	6.731	0.08754	904	0.039823	11.195	13.563	24.758
Cornish Granite							
35	0.602	0.08020	800	0.042977	9.077	3.773	12.850
45	0.876	0.08311	816	0.042310	10.011	5.810	15.821
55	1.101	0.09488	821	0.041819	11.017	7.448	18.465
77	1.361	0.10956	810	0.040045	12.560	10.733	23.293
90	1.494	0.08754	831	0.039684	10.294	13.563	23.857

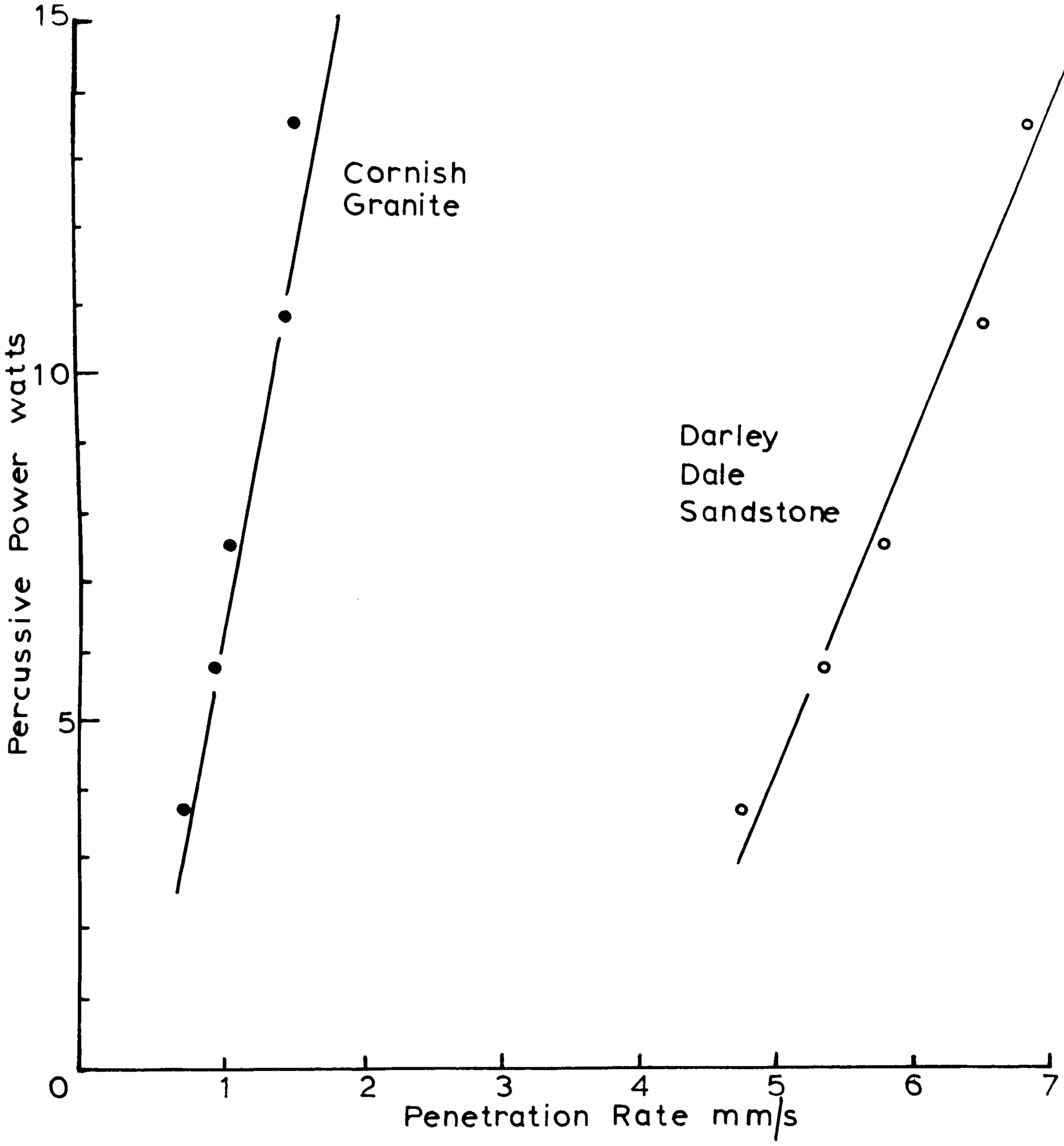

FIGURE 4.20: VARIATION IN PERCUSSION VERSUS PENETRATION RATE.

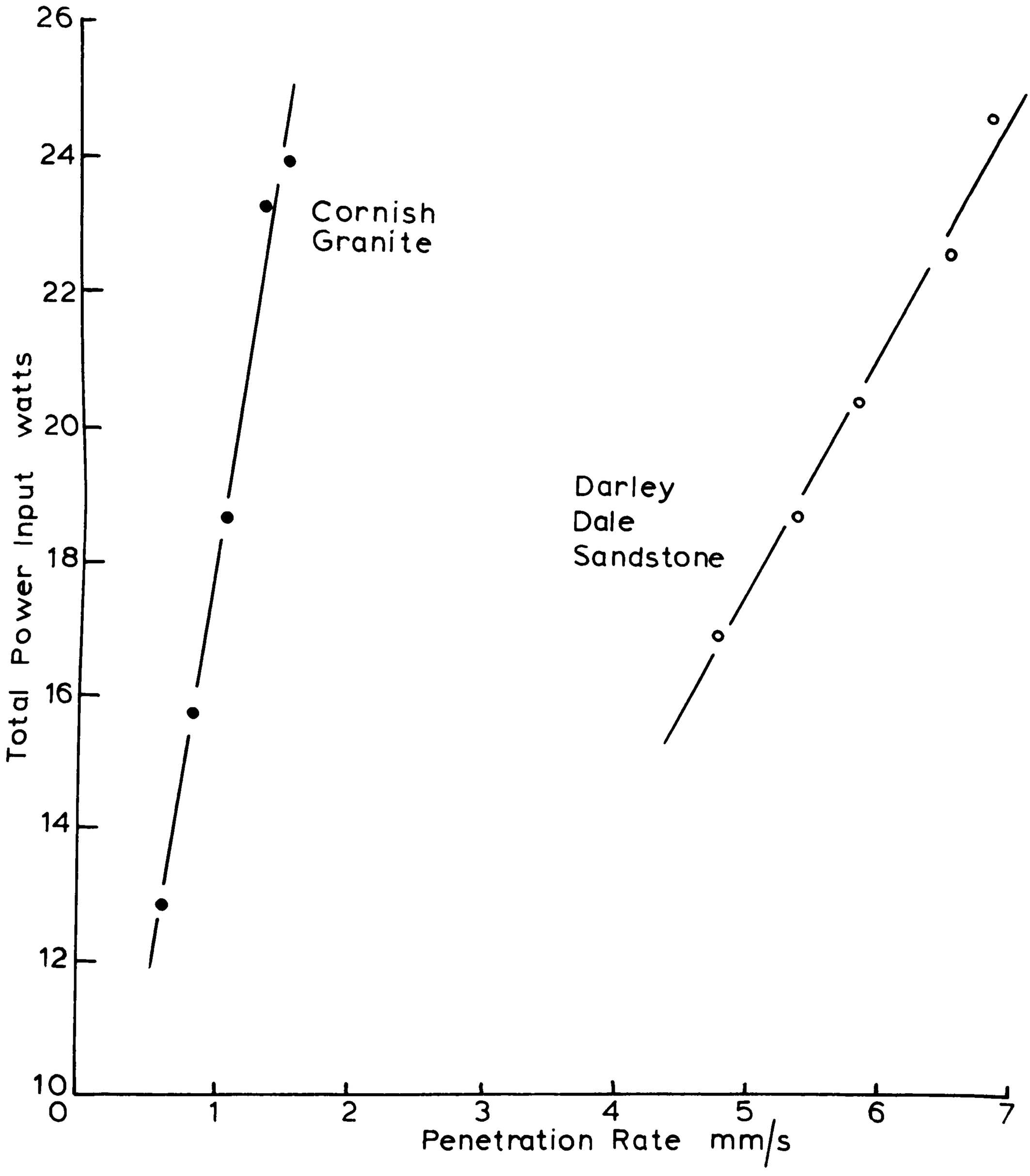

FIGURE 4.21: TOTAL POWER INPUT FOR VARIATION IN PERCUSSION VERSUS PENETRATION RATE.

CONCLUSIONS FROM THE PRELIMINARY TESTS

The analysis of the drill cuttings, power inputs and penetration rates has shown that the addition of percussion is more advantageous for the drilling of 'harder', 'stronger' rocks and that mainly rotary drilling is more advantageous for the 'softer', 'weaker' rocks with the larger energy inputs through developing greater torques. Also, by adding a relatively small amount of percussive energy to the rotation, the penetration increases significantly for both rocks and is particularly favourable with the granite.

This preliminary work verifies that the combination of rotary and percussive drilling gives higher performance figures and is definitely suited for drilling, where, different rock types are encountered and the ratio of percussive/rotary energy requirements can be altered to give the best performance.

These tests have shown that even on this scale large variations of thrust, power and penetration rate can be obtained. On the other hand, the change in drill cuttings from tests on one rock are not large because of the bit size used (3/16"). However it is still possible by surface area measurements to accurately quantify the cuttings to compare the different drilling effects as done with the sandstone and granite. Later work in laboratory drilling has proved the drill cuttings, expressed as surface area/gram to be an important variable from rock to rock and do vary from 0.023942m^2/gram to 0.04898m^2/gram for the range of

rocks drilled.

As the laboratory drilling rig does exhibit the characteristics of rotary-percussive drilling, research on such a model does provide useful and valid information for the study of rotary-percussive drilling. The detailed measurement of drill parameters is also justified as the information for the complete analysis of drilling is obtained.

4.6. Laboratory Drilling of a Range of Rocks, Test A

The object of drilling a range of rocks was to find the interrelationship between the drilling parameters firstly by Teale's (51) specific energy concept compared to a rock property. This concept is the same as Hustrulid's (55) except that the unit volume removed is times the rock property, (C_o), as opposed to dividing into the power to give specific energy. (Compressive strength, C_o).

i.e. Teale: $\frac{\text{Thrust}}{A_H} + \frac{\text{Rotary Power}}{\text{P.R.} \times A_H} + \frac{\text{Percussive Power}}{\text{P.R.} \times A_H}$ v. Rock Property

Hustrulid: Total Power v. (C_o, Rock Property) x P.R. x A_H = Power output.

P.R. x A_H = penetration rate x area of hole = unit volume removed.

Thirteen rocks were drilled at the maximum percussion and rotation settings with a constant thrust of 64lbs. This drilling is known as test A. The speed of rotation, torque and penetration rate were measured and the drill cuttings collected. Average values from drilling five holes per rock were taken. The preliminary tests showed that averaging five holes was sufficient, as there was always good agreement between each hole and five holes yielded enough drill cuttings for sieving in order to determine surface area.

The results for the rocks drilled are tabulated in table 31 and the calculated specific energies after Teale, ignoring the thrust as it is constant, are given in table 32. Table 32 also tabulates the power output after Hustrulid.

Two sets of results are calculated for the unit volumes, one using the area of the hole after Teale and Hustrulid, and the others using the surface area of the drill cuttings (Ad) instead of the area of the hole. The figures quoted will not be interchangeable and the exercise is purely to see if the introduction of the drill cuttings causes any improvement in the relationships quoted by Teale and Hustrulid.

When using the compressive strength, C_o, for determining the rock output power the units of $C_o MN/m^2$ are not in energy form, but when multiplied by penetration rate and area of the hole, the product is then in units of power. However, the Drop Hammer Index and Rock Impact Hardness Number are already in units of energy and can be directly related to specific energies and power.

Therefore, following Hustrulid's analysis of power input against power output, the power output was determined from the Drop Hammer Index (E/A units Nm/m^2) so that power output fully expressed is:-

$$\left(\frac{E}{A}\ \frac{Nm}{m^2} \times \text{P.R.}\ \frac{m}{s} \times A_H m^2 \times Ad\frac{m^2}{gram} \times \text{density}\ \frac{gm}{m^2}\right) \quad \text{watts}$$

where, P.R. = penetration rate, A_H = area of hole, Ad = surface area of drill cuttings per gram.

These values for the rocks drilled are also tabulated in table 32.

The graphs plotted were:-

Figure 4.22

E, specific Energy V. Compressive Strength, C_o (a)

$$\left(\frac{\text{Total Power input}}{\text{P.R. x } A_H}\right)$$

V. Drop Hammer Index, E/A (b)

V. Rock Impact Hardness Number, R.I.H.N. (c)

Figure 4.23

E', $\frac{\text{Total Power Input}}{\text{P.R. X Ad}}$ V. Compressive Strength, C_o (d)

V. Drop Hammer Index, E/A (e)

V. Rock Impact Hardness Number, R.I.H.N. (f)

Figure 4.24

P_T, Total Power Input V. C_o x P.R. x A_H (g)

V. C_o x P.R. x A_d

V. E/A x P.R. x A_H x A_d x density (i)

TABLE 31

RESULTS OF LABORATORY DRILLING A RANGE OF ROCKS AT MAXIMUM ROTATION AND PERCUSSION IN TEST A

Rock	Penetration Rate P.R. mm/sec	Speed R.P.M.	Torque ft.lbs	Rotary Power watts	Total Power P_T watts	Drill Cuttings Ad .. m^2/gram	P.R. x A_H $\frac{m^3}{Sec} \times 10^{-6}$	P.R. x Ad $\frac{m^3}{Sec.gram} \times 10^{-3}$
Yellow Oolitic Lst.	42.63	1680	0.4617	111.62	126.62	0.025796	0.75936	1.09968
Darley Dale Sst.	18.513	1900	0.3661	98.33	113.33	0.031027	0.32954	0.57440
Horsforth Sst.	18.511	1820	0.3372	86.73	101.73	0.031349	0.32974	0.58030
St. Bee's Sst.	10.879	1775	0.3661	91.86	106.86	0.036362	0.19379	0.39558
Elland Edge Sst.	7.915	1880	0.3810	101.28	116.28	0.039017	0.14099	0.30882
Bath Lst.	12.348	1900	0.3371	90.54	105.54	0.023942	0.21995	0.29563
Craigenlow Pink Gr.	3.200	1920	0.1389	37.71	52.71	0.043613	0.05700	0.13956
Giggleswick Lst.	4.686	1960	0.1242	34.42	49.42	0.035199	0.08347	0.16494
Cornish Gr.	3.802	1980	0.1433	40.12	55.12	0.0413904	0.06772	0.15737
Denbigh Lst.	5.911	1980	0.0912	25.53	40.53	0.033816	0.10529	0.19989
Whinstone	6.230	1980	0.1903	53.27	68.27	0.032868	0.11097	0.20477
Mount Sorrel Gr.	3.097	1980	0.1242	34.77	49.77	0.042650	0.05517	0.13208
Groby Gr.	6.084	1940	0.1389	38.10	53.10	0.032673	0.10837	0.19878

TABLE 32

ANALYSIS OF RESULTS FROM TABLE 31 WITH THE LISTS OF THREE ROCK PROPERTIES FOR THE RANGE OF ROCKS DRILLED IN TEST A.

	After Teale		After Hustrulid		Rock Output	C_o=Compressive Strength Index E/A=Drop Hammer Index R.I.H.N.=Rock Impact Hardness Number		
	Specific Energy E, Total Power / P.R. x A_H MJ/m^3	E' Total Power/ P.R. x Ad KJ gram	C_oxP.R.xA_H watts	C_oxP.R.xAd kilowatts/gram	(E/A)xP.R.xAdX$A_H$xdensity watts			
						C_o MN/m^2	E/A Nm/m^2	R.I.H.N MJ/m^3
Yellow Oolitic Lst.	166.750	115.142	7.806	11.305	16.016	10.28	309.47	8.02
Darley Dale Sst.	343.903	197.301	13.666	23.820	9.467	41.47	357.47	9.75
Horsforth Sst.	308.516	175.305	14.617	25.725	11.129	44.33	376.22	9.16
St. Bee's Sst.	551.428	270.133	11.089	22.635	7.678	57.22	424.11	10.87
Elland Edge Sst.	824.741	376.531	13.465	29.492	8.070	95.50	554.84	25.60
Bath Lst.	479.826	356.993	10.318	13.868	11.022	46.91	787.18	20.97
Craigenlow Pink Gr.	924.737	377.683	12.831	31.415	6.639	225.1	1009.28	-
Giggleswick Lst.	592.057	299.620	11.005	21.746	8.232	131.84	1042.79	68.93
Cornish Gr.	813.879	350.265	11.397	26.483	8.130	168.29	1094.04	76.09
Denbigh Lst.	384.927	202.765	18.501	35.691	12.839	178.57	1348.56	96.62
Whinstone	615.183	333.402	19.451	35.890	15.634	175.27	1460.82	113.22
Mount Sorrel Gr.	902.172	376.797	13.876	33.222	9.343	251.51	1541.41	91.05
Groby Gr.	489.969	267.126	15.531	28.486	20.939	143.30	2205.60	133.53

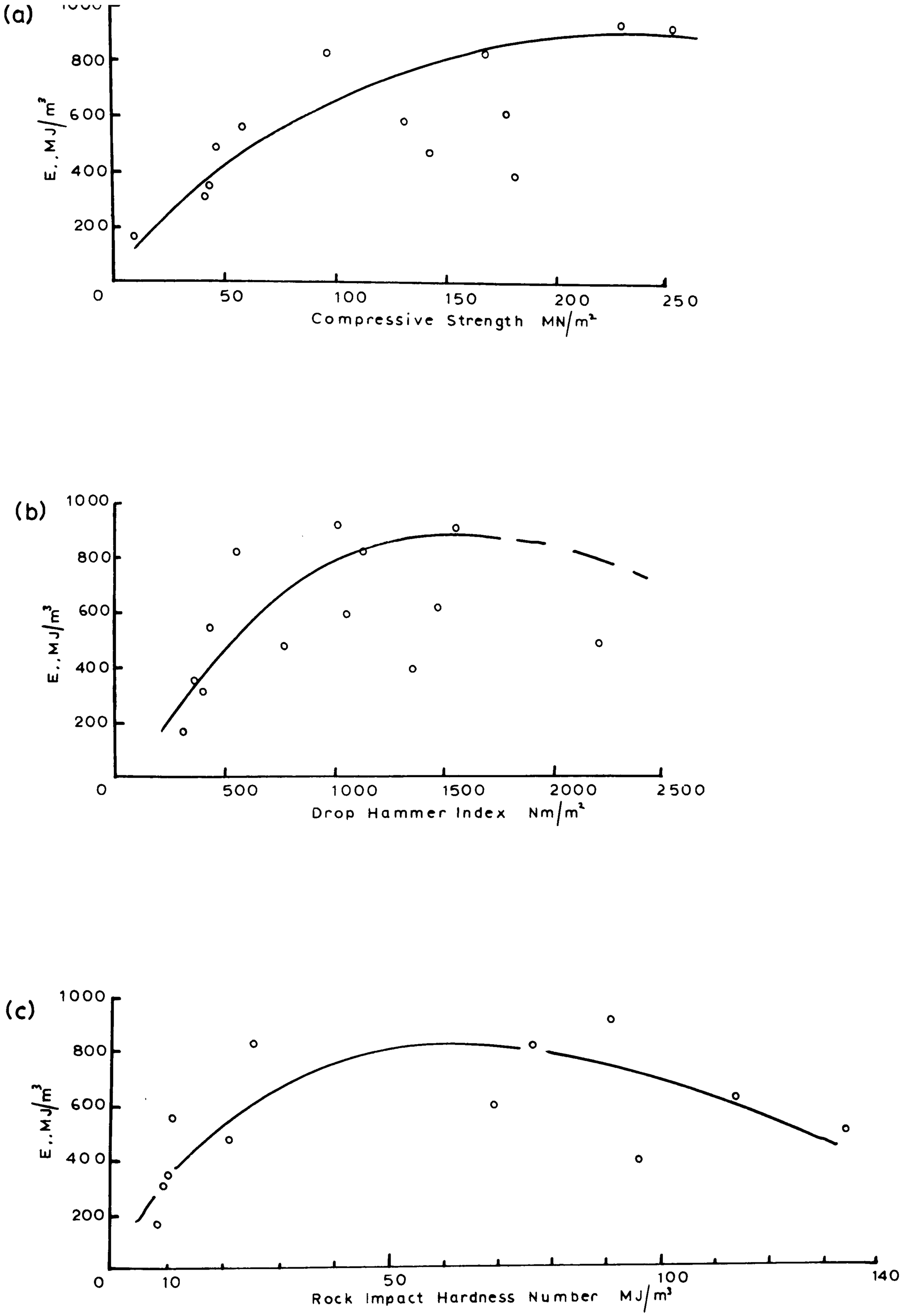

FIGURE 4.22: SPECIFIC ENERGY(E) VERSUS COMPRESSIVE STRENGTH, DROP HAMMER INDEX AND ROCK IMPACT HARDNESS NUMBER.

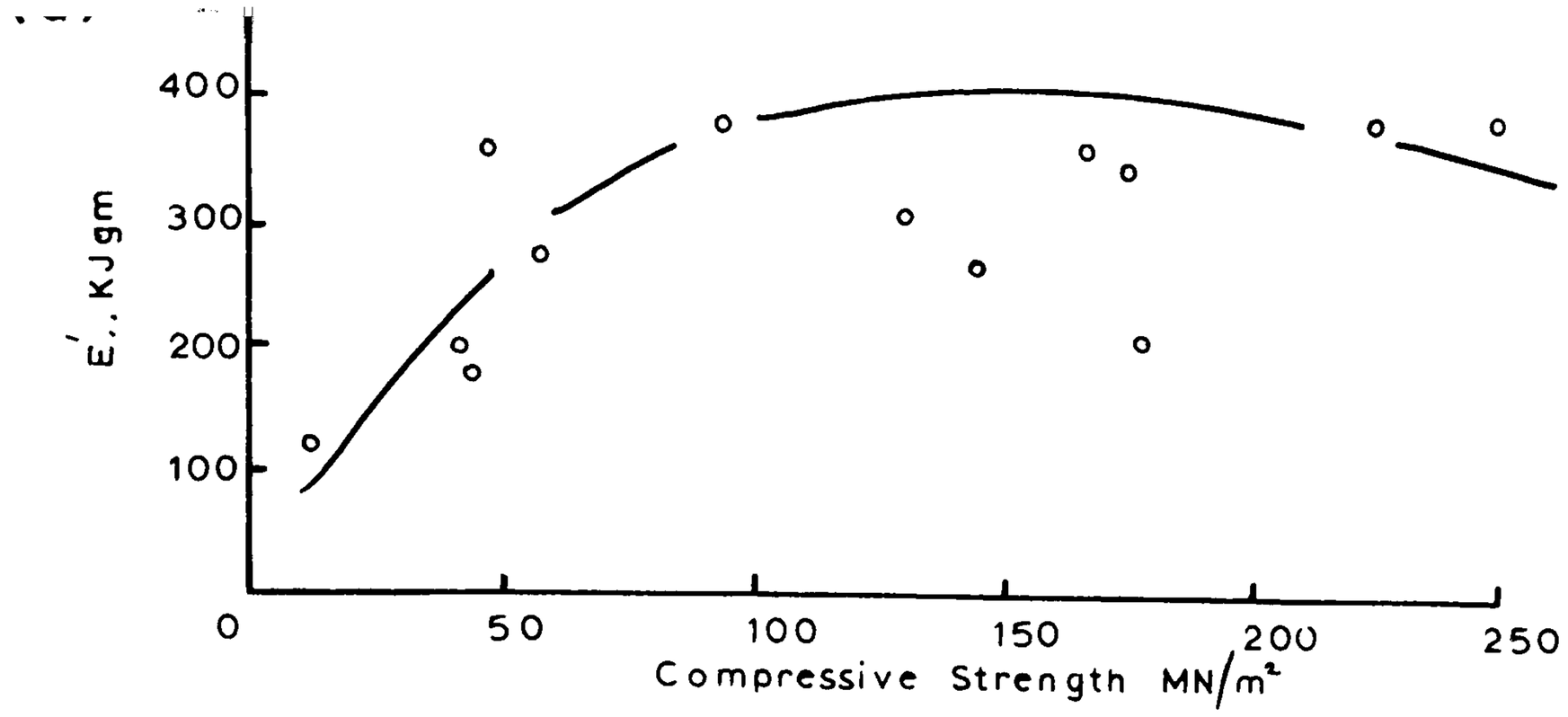

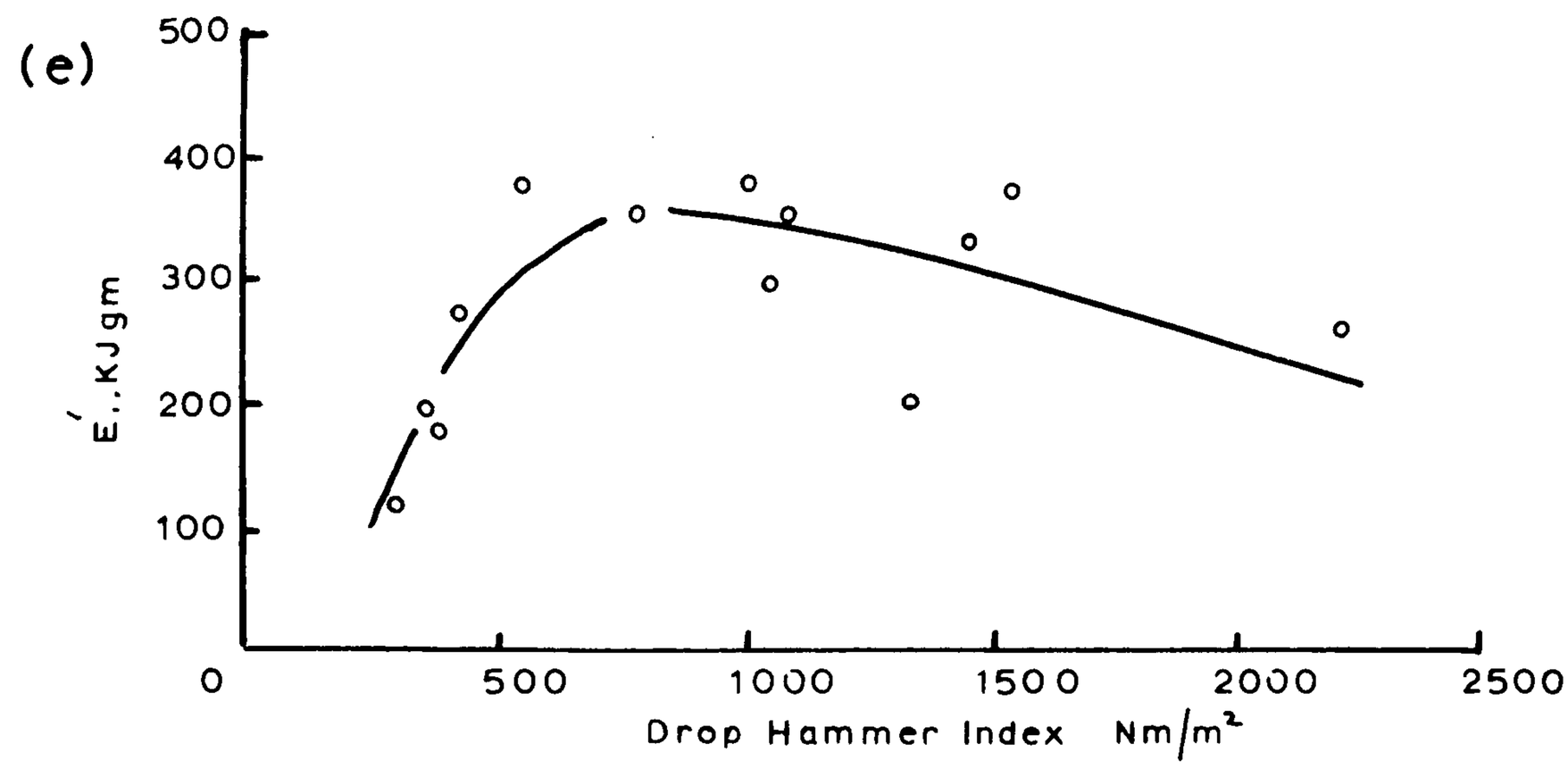

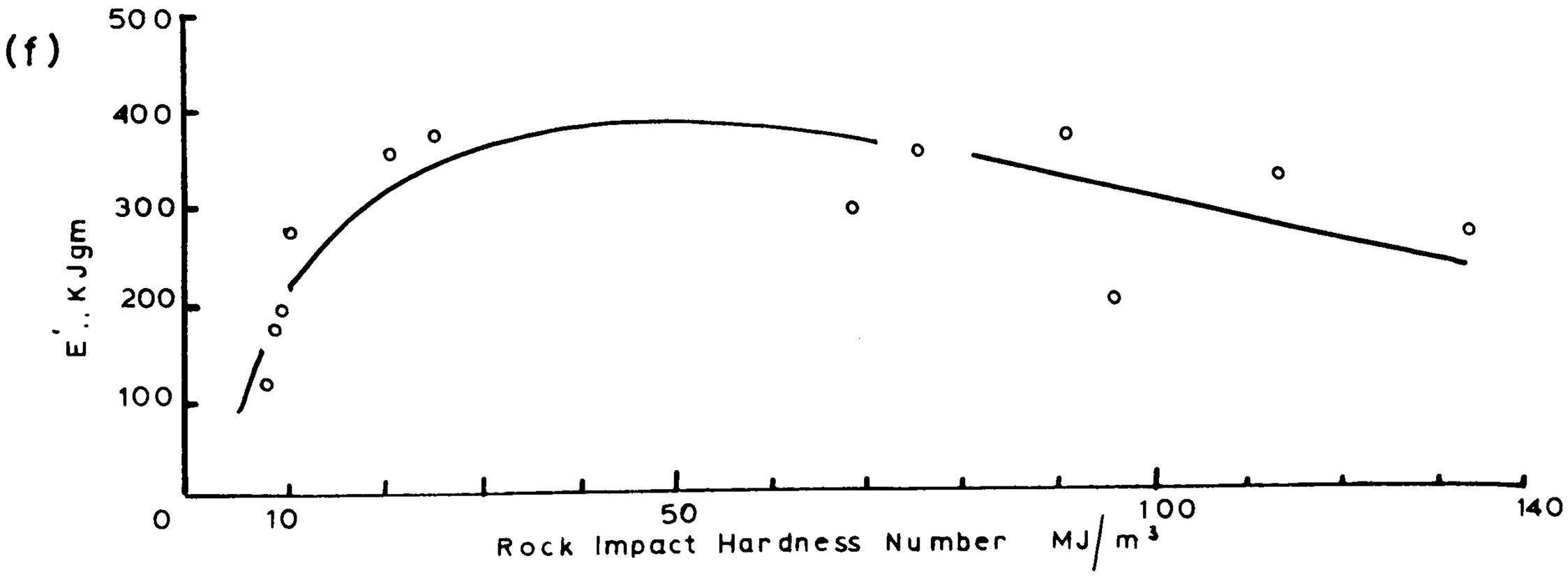

FIGURE 4.23: E' from POWER INPUT / P.R.xA_d VERSUS COMPRESSIVE STRENGTH, DROP HAMMER INDEX AND ROCK IMPACT HARDNESS NUMBER.

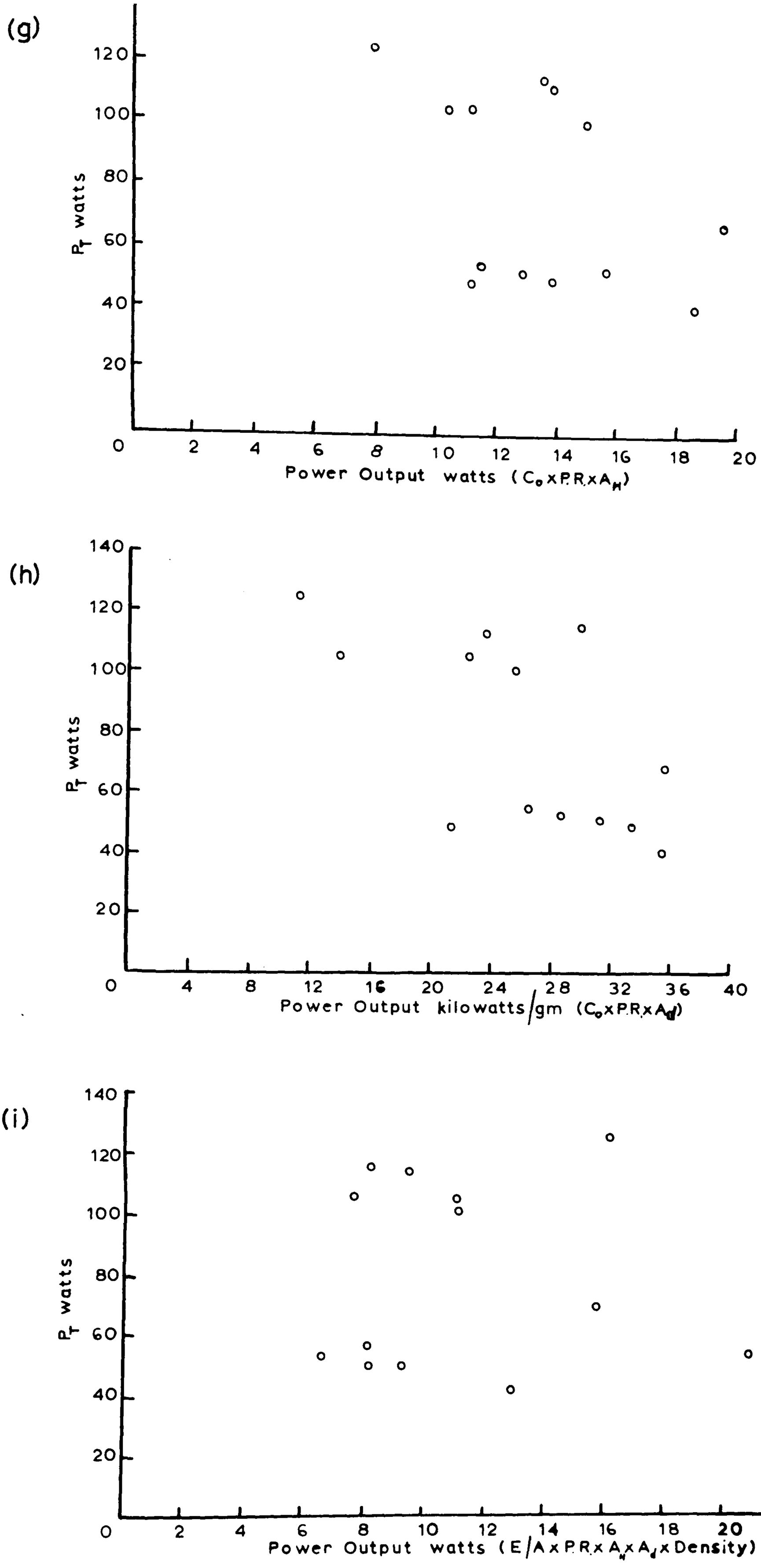

FIGURE 4.24: TOTAL POWER INPUT P_T VERSUS POWER OUTPUT.

4.7. Discussion and further analysis of the results obtained from drilling the range of rocks at maximum rotation and percussion with constant thrust in test A.

The specific energy graphs in figure 4.22, where specific energy is plotted against the three rock properties compressive strength, drop hammer index and rock impact hardness number, all show a large amount of scatter. The specific energy against rock impact hardness number gives the least amount of scatter. With Denbigh limestone and Giggleswick limestone the torques developed are low in relation to their strengths giving low power values, hence the greatest scatter. By measuring the drill cuttings and introducing their surface areas/gram into the specific energy function all three graphs are improved. So that this exercise of introducing the drill cuttings giving the improvement, shows that the drill cuttings are an important factor in the drill analysis.

The power inputs plotted against the power outputs in figure 4.24 show no trend and correlation for all three power output functions considered.

In analysing the drilling parameters obtained from the above testing at maximum rotation, percussion and constant thrust, a relationship was found whereby all the drilling parameters were combined and gave a near perfect correlation against compressive strength. This relationship of the drilling parameters was first developed from multiplying the power input by the penetration rate and later expanded to:-

$$\frac{\text{Power x Penetration Rate x Area of Hole}}{\text{Thrust x Area of drillings /gram.}}$$

This relationship was termed the Performance Factor (P.F.) and has units of energy (Nm, Joules).

Units: $\frac{Nm}{S} \times \frac{1}{N} \times \frac{m}{s} \times \frac{gram}{m^2} \times m^2$ .....Nm

The graph of Performance Factor against compressive strength for the thirteen rocks drilled in test A is shown in figure 4.25 and the Performance Factor values for the rocks drilled are listed in table 33. A rigorous analysis of the curve was made by regression techniques and the equation that gave the best fit and highest correlation is also shown in table 33. This equation was a linear regression of the Performance Factor versus the reciprocal of the square of the natural logarithm of the compressive strength values.

TABLE 33

Values of Performance Factor for drilling at maximum rotation, percussion settings and constant thrust in Test A.

Rock	Performance Factor 10^{-9} Nm	C_o MN/m²	$\frac{1}{(\ell n\ C_o)^2}$
Yellow Oolitic Lst.	13.0901	10.28	0.1842
Darley Dale Sst.	4.2226	41.47	0.0721
Horsforth Sst.	3.7746	44.33	0.0696
St. Bee's Sst.	1.9999	57.22	0.0611
Elland Edge Sst.	1.4755	95.50	0.0481
Bath Lst.	3.4039	46.91	0.0675
Craigenlow Pink Gr.	0.6404	225.10	0.0341
Giggleswick Lst.	1.0832	131.84	0.0420
Cornish Gr.	0.3167	168.29	0.0381
Denbigh Lst.	0.4432	178.57	0.0372
Whinstone	0.8091	175.27	0.0375
Mount Sorrel Gr.	0.2247	251.51	0.0327
Groby Gr.	0.6188	143.30	0.0406

Regression: y = Performance Factor, $x = \frac{1}{(\ell n\ C_o)^2}$,

C_o = compressive strength.

$$y = 85.8645x - 2.5805$$

Correlation coefficient, c.c. = 0.995187

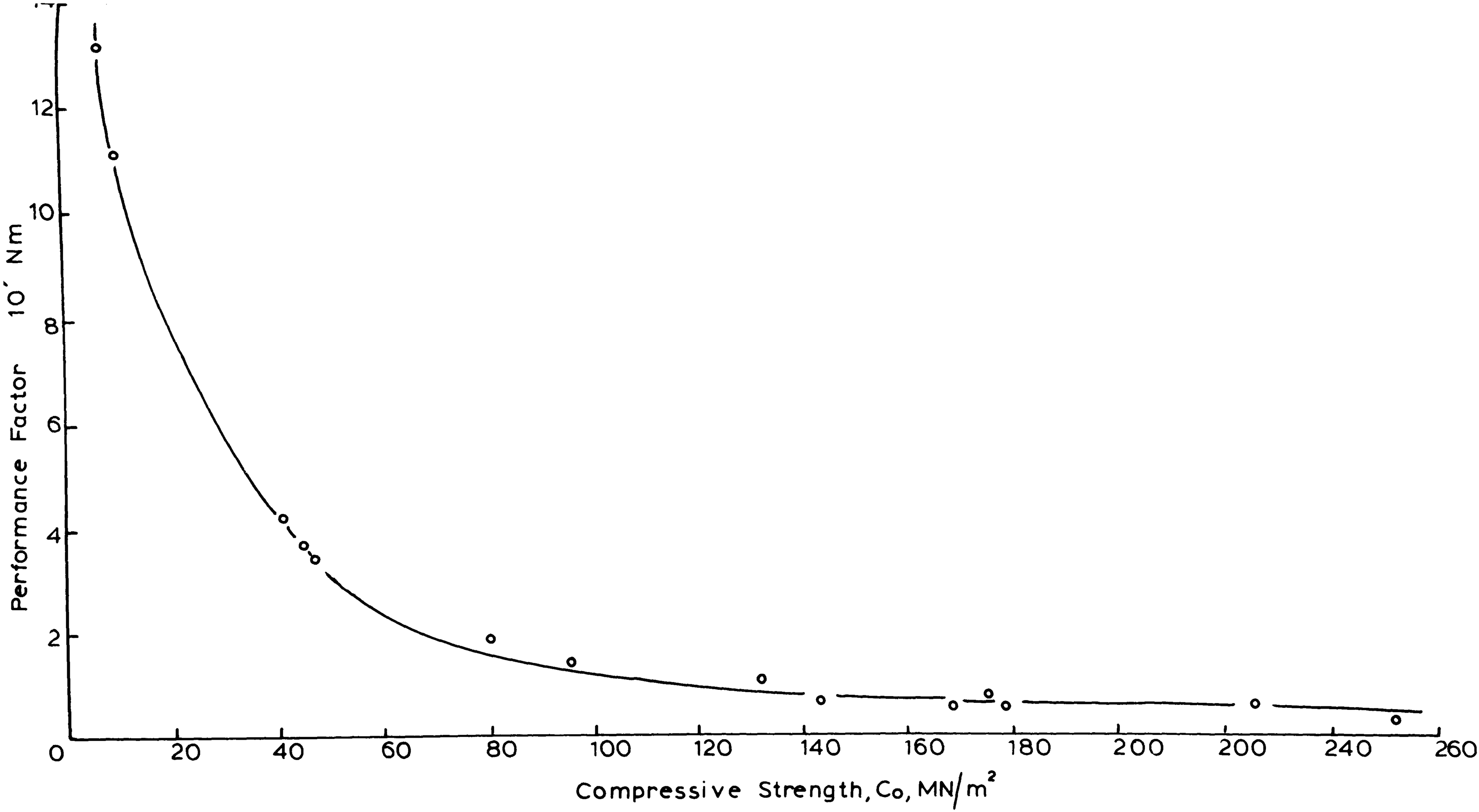

FIGURE 4.25: PERFORMANCE FACTOR VERSUS COMPRESSIVE STRENGTH.
TEST A

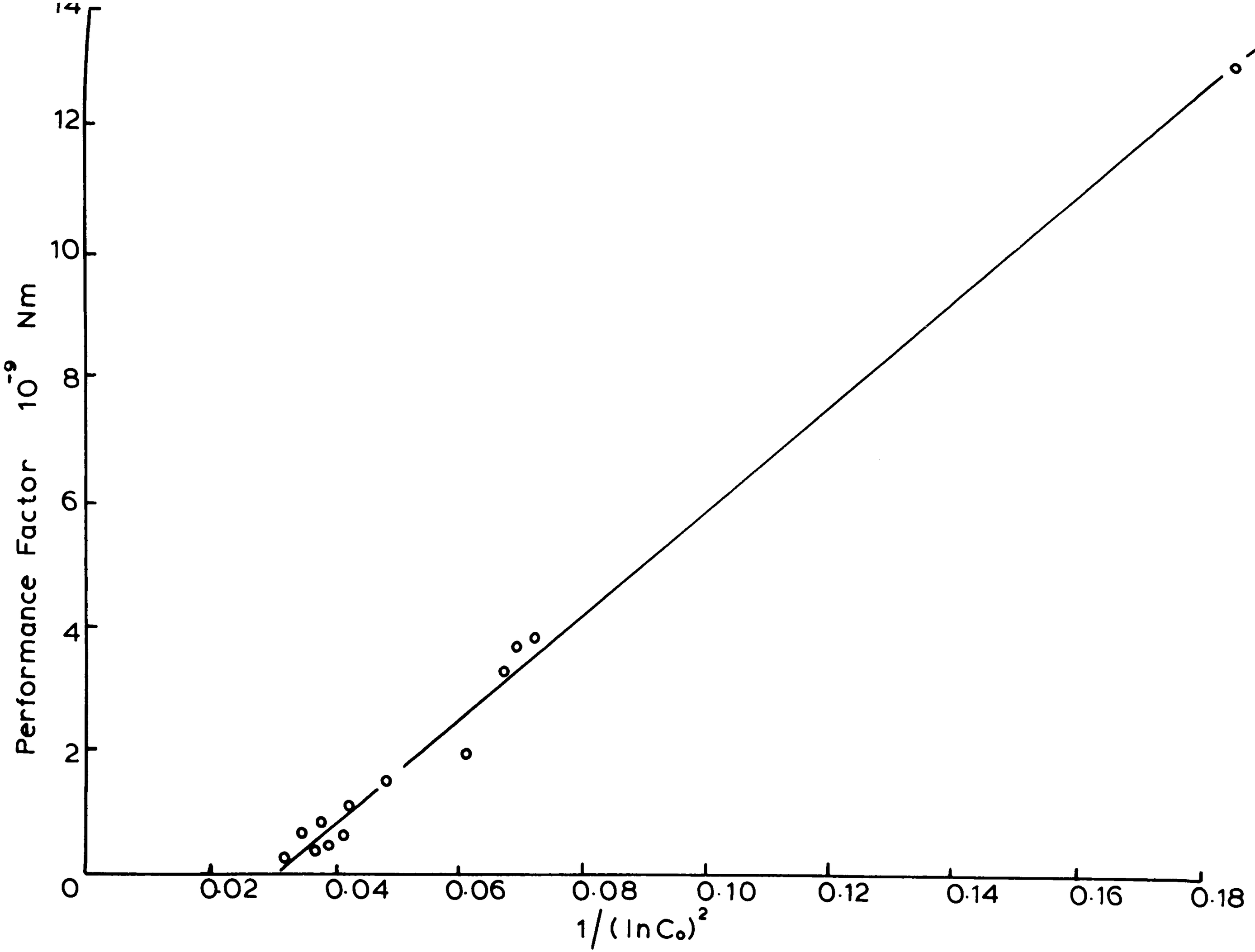

FIGURE 4.26: PERFORMANCE FACTOR VERSUS f(COMPRESSIVE STRENGTH).
TEST A

The plot of performance factor against $\frac{1}{(\ell n\ C_o)^2}$ is shown in figure 4.26 in which it can be seen that Yellow Oolitic limestone (Y.O.) appears to be the major point in determining the regression equation. In view of this, a graph was plotted leaving out Yellow Oolitic limestone and the new correlation coefficient determined from a linear regression. This graph is shown in figure 4.27 and there is still a very good relationship between the performance factor and $\frac{1}{(\ell n\ C_o)^2}$ giving a high correlation coefficient of 0.989105.

Figure 4.27 does however, indicate that the rocks with greater values of compressive strength do have less correlation. Therefore, it was decided to drill a number of different rocks with $\frac{1}{(\ell n\ C_o)^2}$ between 0.029 and 0.050 in order to test the relationship. This test is test B and the different rocks were drilled at the maximum rotation and percussion with a constant thrust of 64lbs, exactly like test A. The results of test B are tabulated in Table 34 and figure 4.28 shows the graph of performance factor plotted against the function $\frac{1}{(\ell n\ C_o)^2}$. This graph also has a very good relationship, especially as the range of the rock strength function has been reduced. The correlation coefficient for the graph in figure 4.28 is 0.986581.

The results of drilling the different rocks in test B should have tied in with the first range of rocks drilled in test A as the same drilling parameters were used. However, they don't, because test B was carried out during the power crises of 1973 when there was a voltage reduction. This

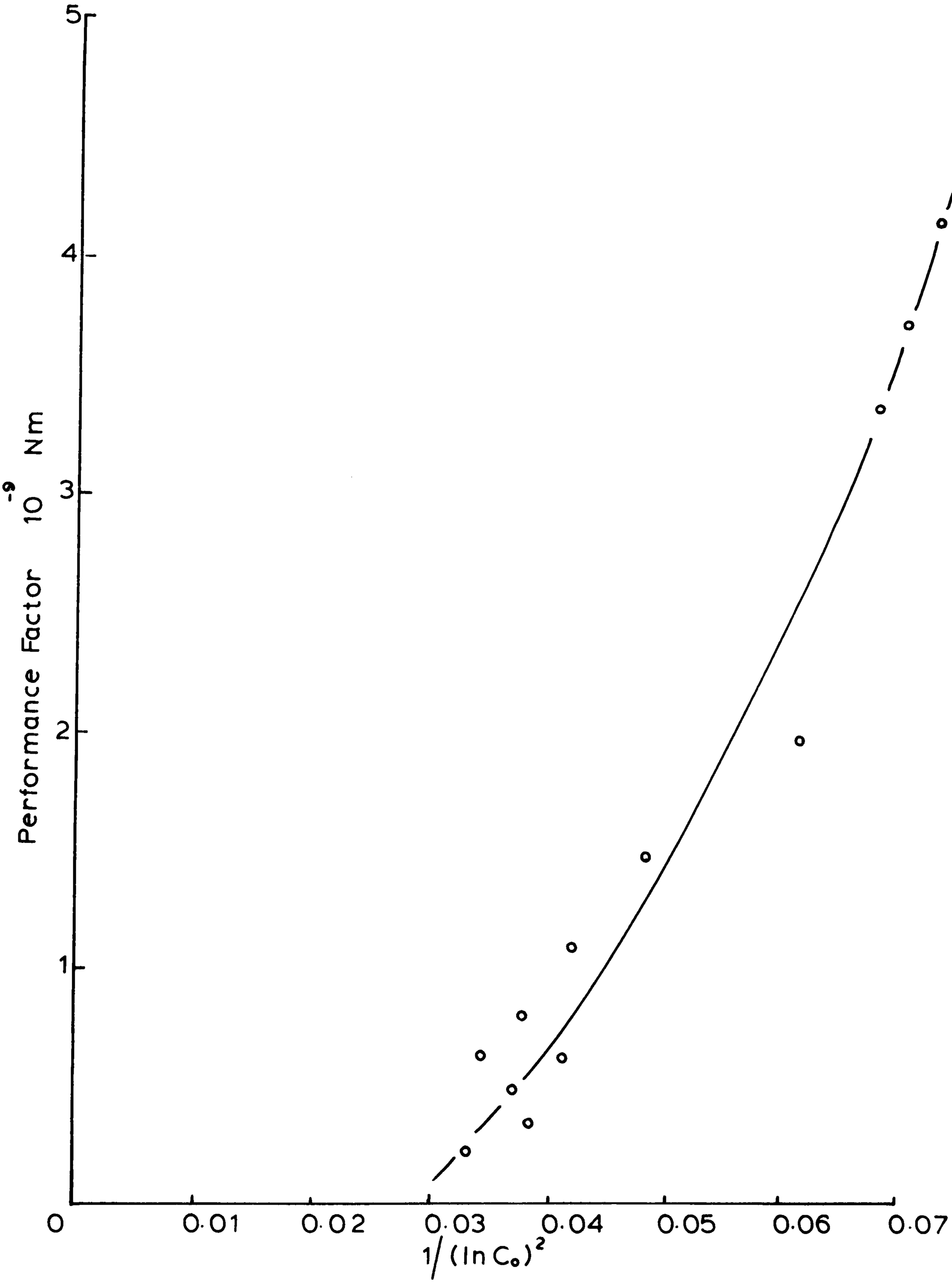

FIGURE 4.27: PERFORMANCE FACTOR VERSUS f(COMPRESSIVE STRENGTH) OMITTING YELLOW OOLITIC LIMESTONE.

TEST A

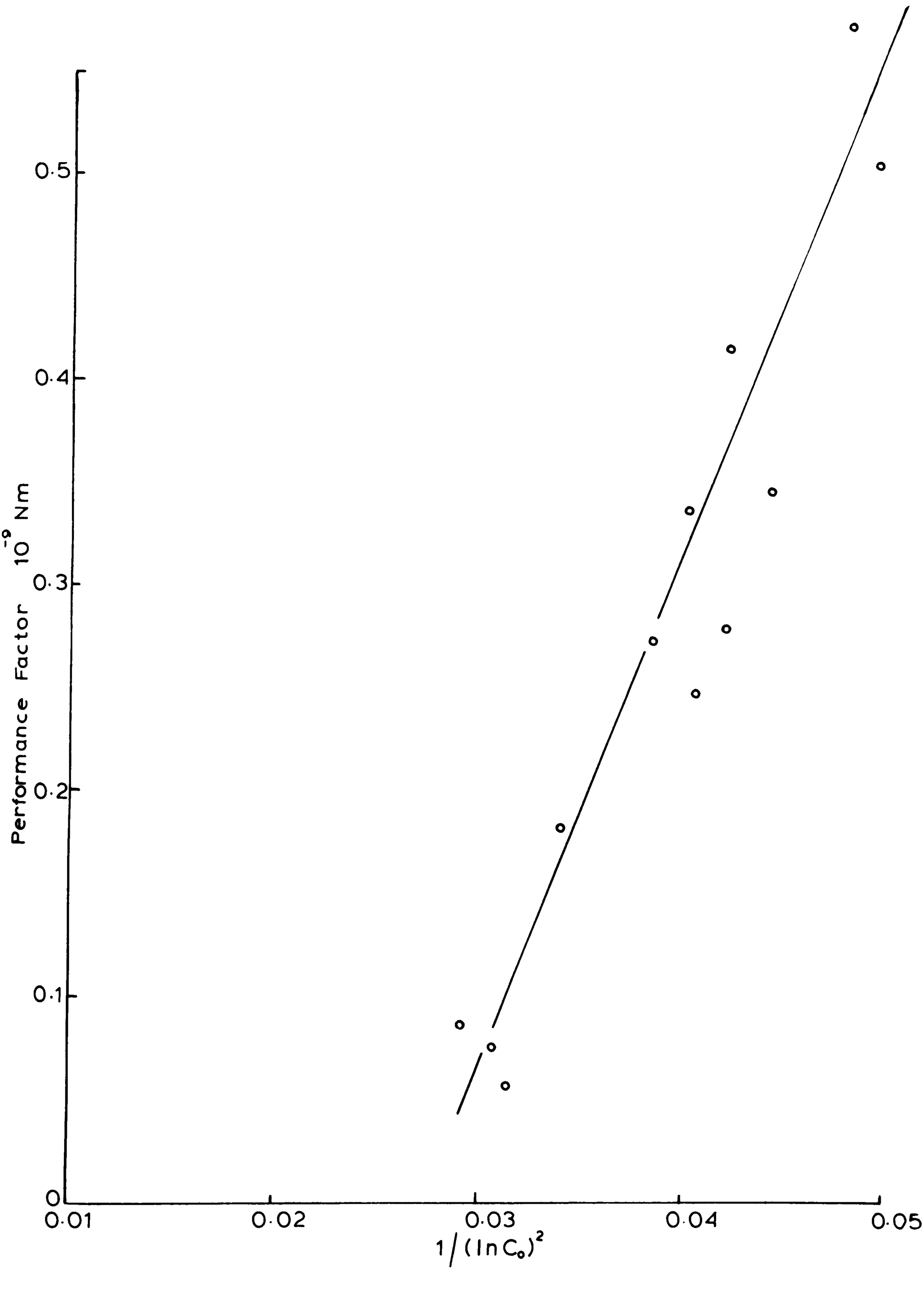

FIGURE 4.28 : PERFORMANCE FACTOR VERSUS f(COMPRESSIVE STRENGTH).
TEST B

gave lower values of drilling torque and a lower maximum speed than normal, so that the total power input was reduced. Fortunately, this was the only test affected and the aim of the test was to determine the linearity of the graph for the smaller range which was achieved in any case.

Two more sets of tests (C and D) were conducted in order to verify the performance factor along with its relationship with the compressive strength under different laboratory drilling conditions. Test C was the drilling of a range of rocks at a low speed setting around 350 R.P.M. with maximum percussion and a constant thrust of 64lbs. The test D was carried out on a range of rocks at a reduced speed of around 800 R.P.M., a reduced constant thrust of 44lbs and a percussion setting of 45% (at 45% variac setting the power input is 5.7244 watts). The speed and torque were recorded on the Rikadenki, the penetration rate measured and the cuttings collected. The results are tabulated in table 35 for test C and table 36 for test D.

The calculated performance factor and $\frac{1}{(\ell n\ C_o)^2}$ are plotted in figure 4.29 and figure 4.30 for the two tests C and D respectively. Again extremely good relationships were obtained and the correlation coefficients are very high. For test C the linear regression gave a correlation coefficient of 0.998718 and for test D 0.98215.

For the three tests B, C and D the specific energies after Teale were also calculated and these values are listed in table 34, 35 and 36. Specific energies were plotted against compressive strength for the three sets of tests and the graphs

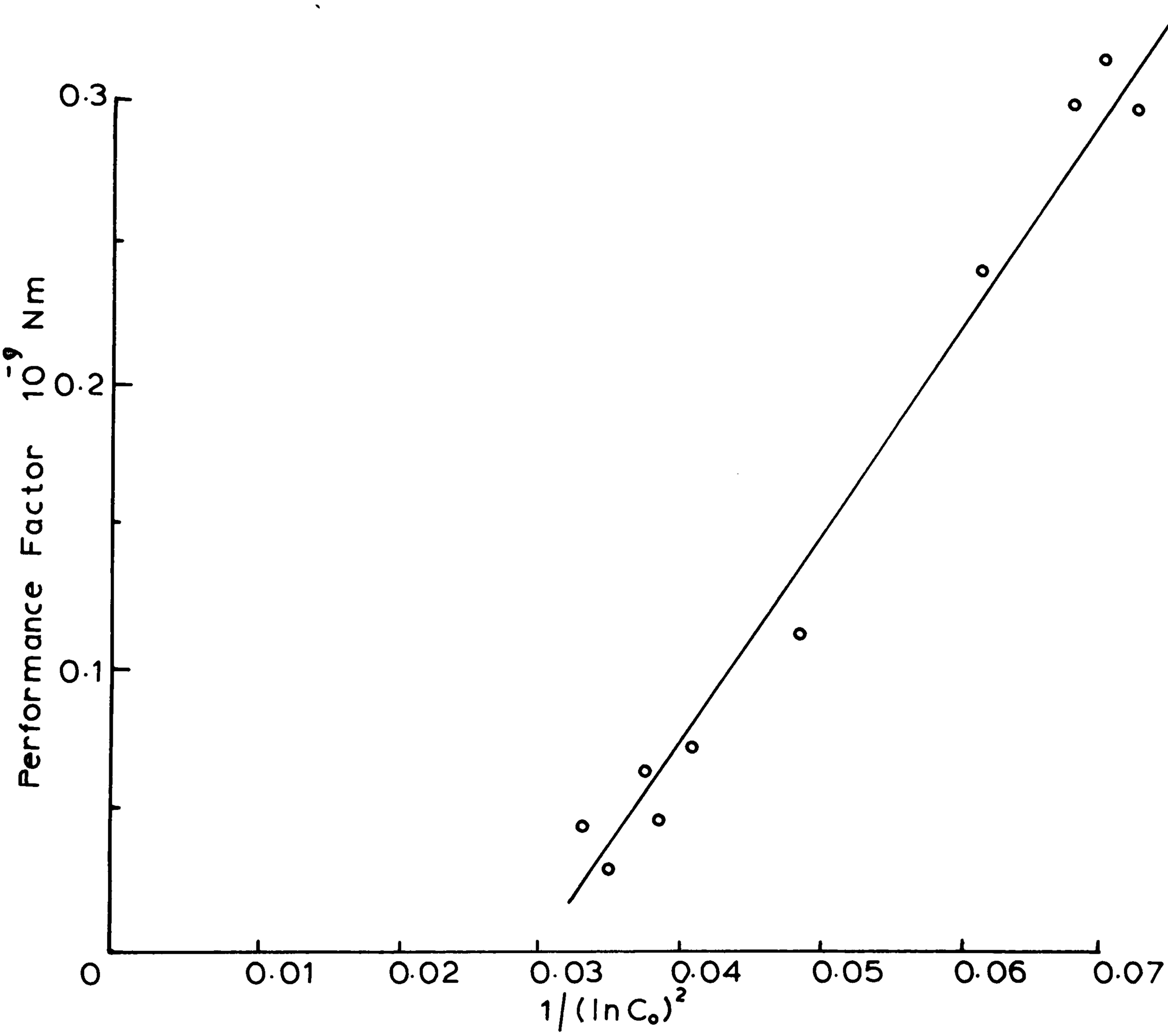

FIGURE 4.29: PERFORMANCE FACTOR VERSUS f(COMPRESSIVE STRENGTH).
TEST C

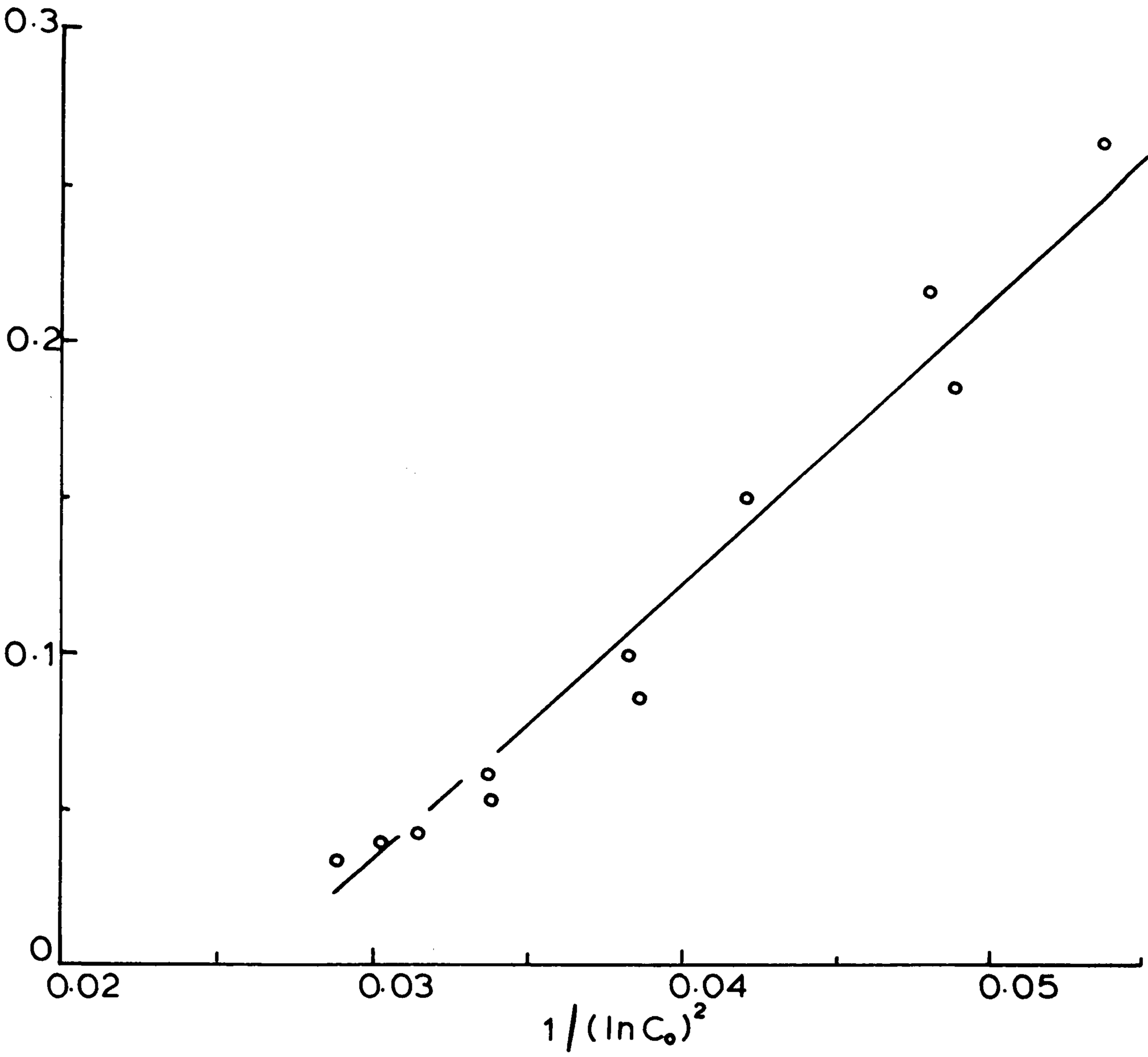

FIGURE 4.30: PERFORMANCE FACTOR VERSUS f(COMPRESSIVE STRENGTH).
TEST D

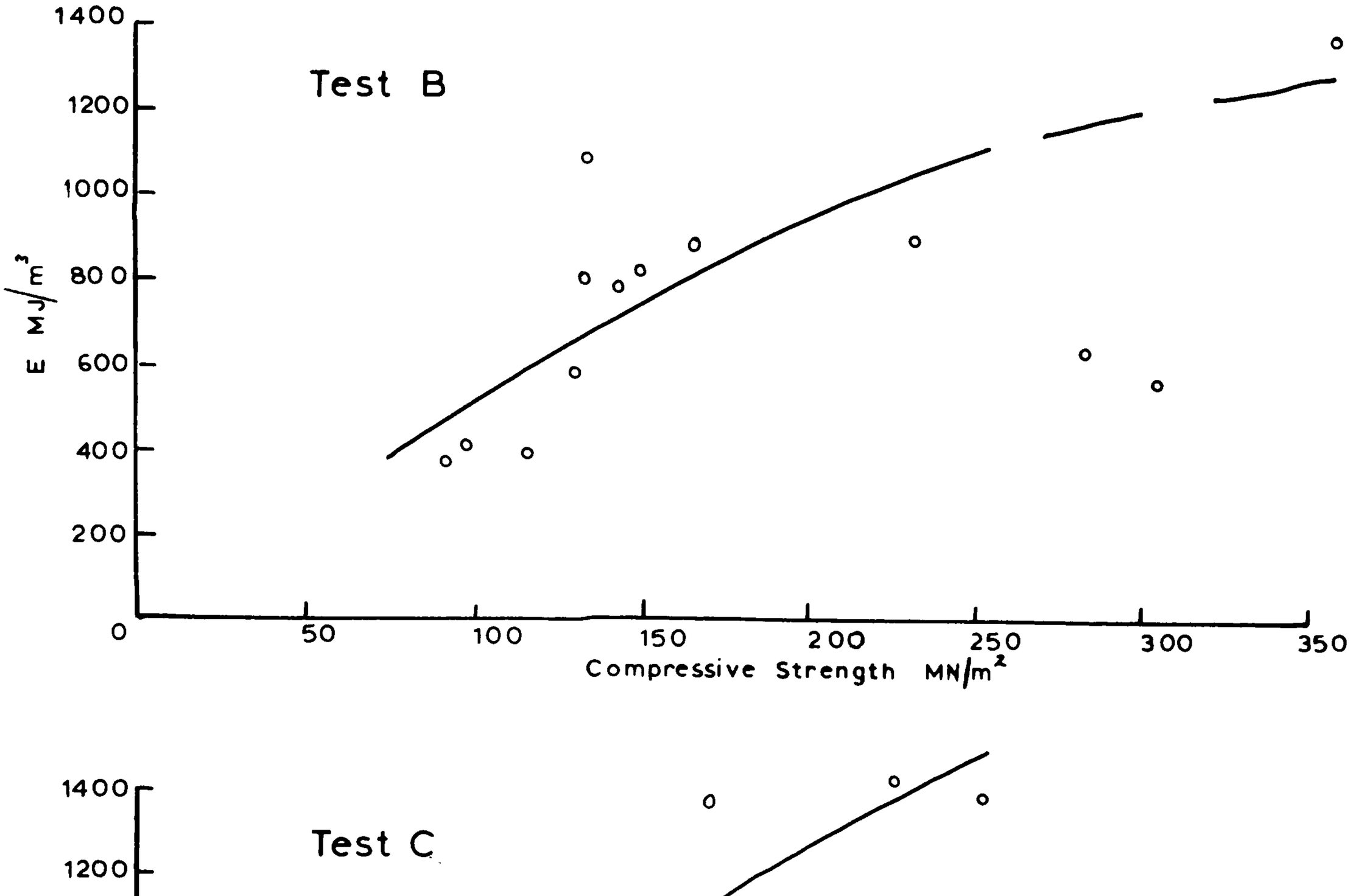

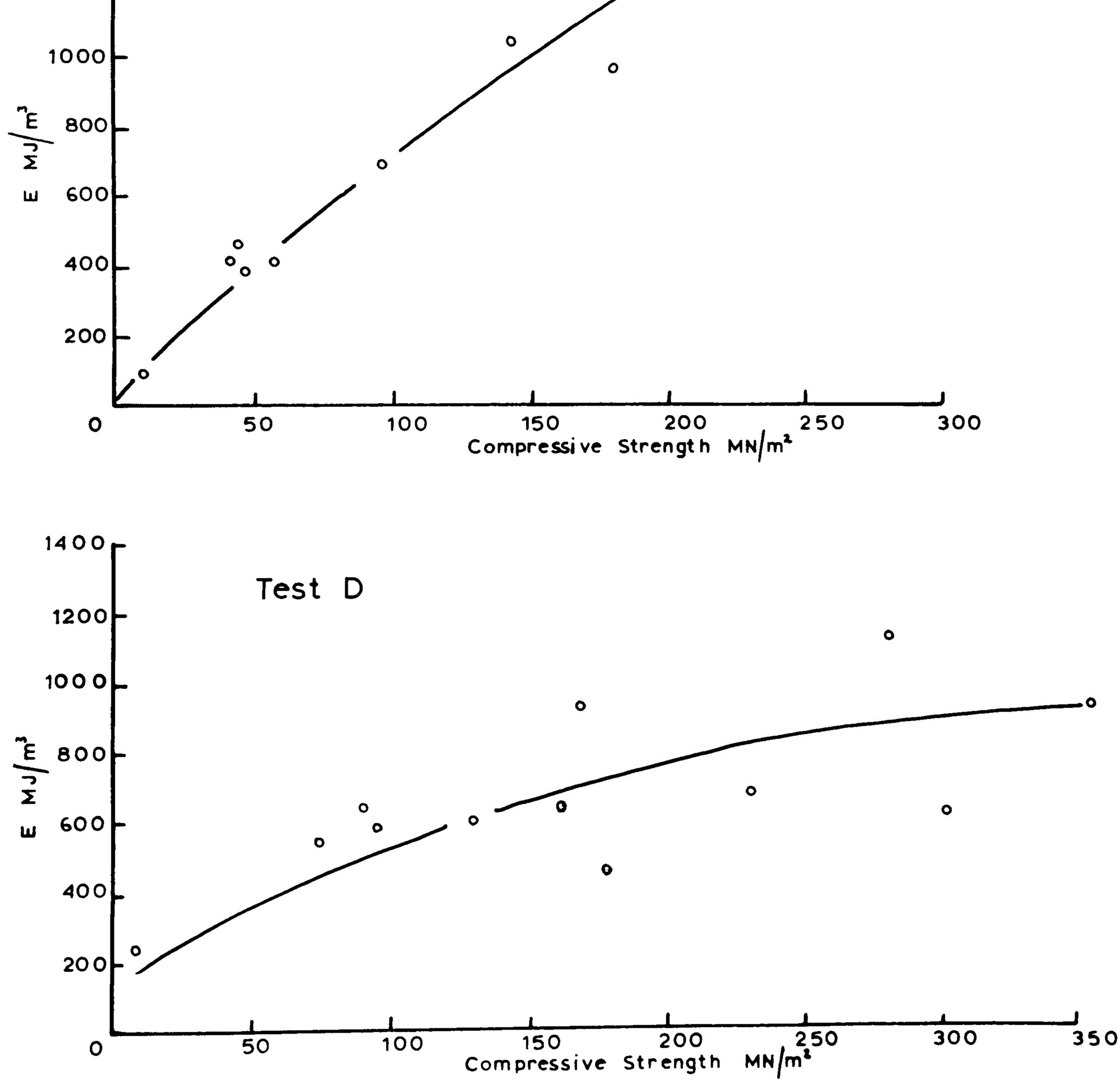

FIGURE 4.31: SPECIFIC ENERGY VERSUS COMPRESSIVE STRENGTH FOR TESTS B, C AND D.

for B, C and D are plotted in figure 4.31. The graphs for specific energy values against compressive strength test B gave a poor correlation, test C, where a low speed was used, a good correlation was obtained and test D gave a general trend.

It can be concluded that the performance factor does provide the best functional relationship of the drilling parameters plotted against the compressive strength and this fact is obtained when the performance factor is plotted against the compressive strength in all four tests. It can also be said that the compressive strength best describes this laboratory drill for the rocks drilled in its relation with the performance factor.

The performance factor has been found to have a linear relationship with the drilling speed and the slope of this line correlates very well with compressive strength.

This analysis was developed by considering the results of the preliminary testing of speed of rotation variation in 4.5 (b) drilling Darley Dale sandstone and Cornish granite. The increase in speed was plotted against the performance factor for Darley Dale sandstone and Cornish granite and was found to be a linear relationship. This was verified by drilling three more rocks, Bath limestone, Denbigh limestone and Mount Sorrel granite, at different speeds, measuring all the parameters as usual and collecting the drill cuttings. The results for Darley Dale and Cornish granite can be seen in the earlier table 29 and those for Bath limestone, Denbigh

limestone and Mount Sorrel granite in table 37. The graphs of performance factor against increase in speed can be seen in figure 4.32. As a linear relationship is obtained and the slope values taken, slope values for other rocks were extrapolated from tests A and C where the same drilling conditions are set and the difference in drilling in maximum speed in A and low speed in C.

Hence the slope values of speed/performance factor shown in table 38 are plotted against compressive strength in figure 4.33. In this case the correlation coefficient 0.960587, is not as high as those in tests A, B, C and D, nevertheless it is a high value considering the number of points involved and the slope values are extrapolated except for those five rocks, (Darley Dale, Denbigh, Cornish, Bath and Mount Sorrel).

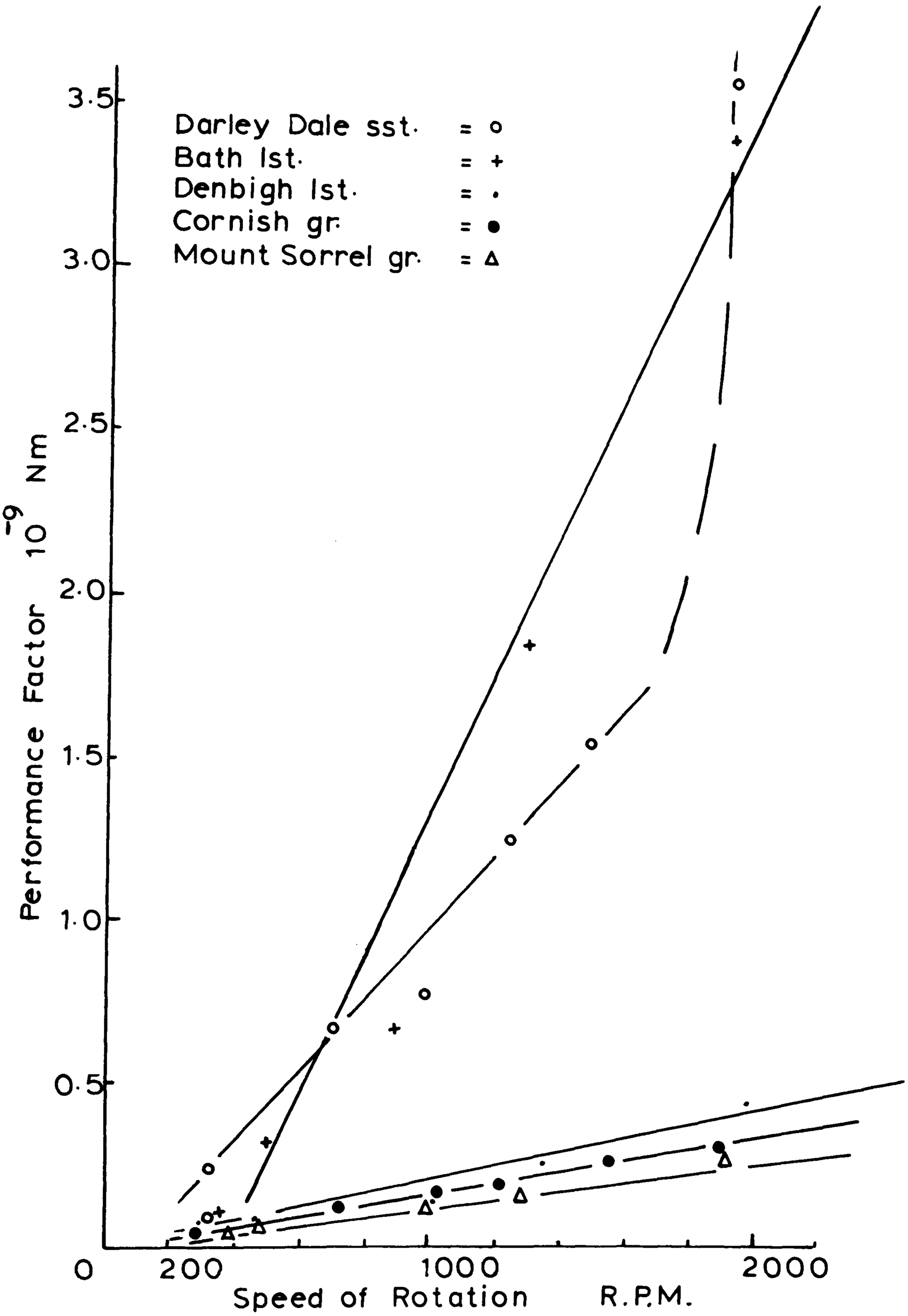

FIGURE 4.32: PERFORMANCE FACTOR VERSUS SPEED OF ROTATION VARIATION.

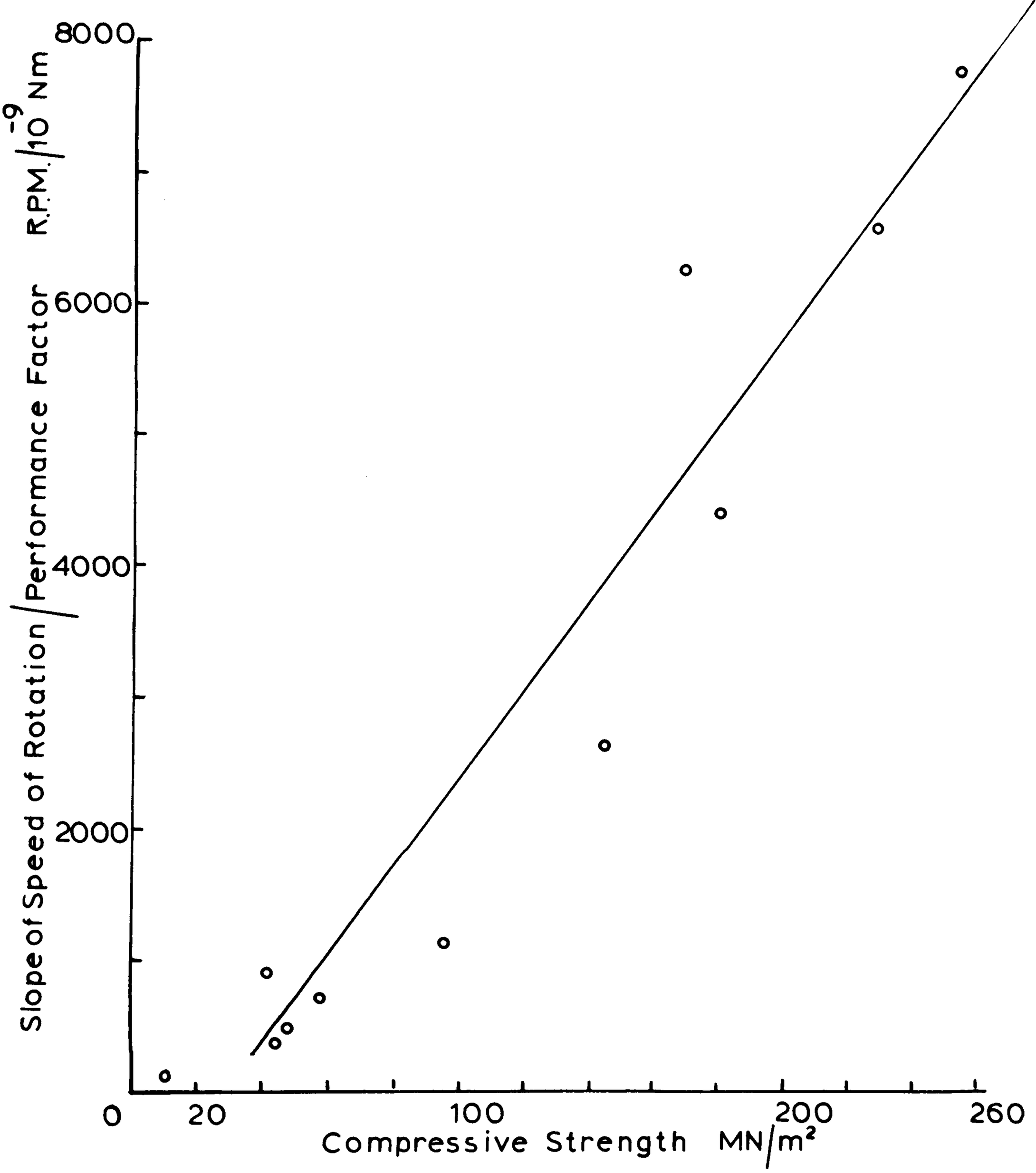

FIGURE 4.33: SLOPES OF SPEED OF ROTATION/ PERFORMANCE FACTOR VERSUS COMPRESSIVE STRENGTH.

TABLE 34

RESULTS OF DRILLING A RANGE OF ROCKS AT MAXIMUM SPEED OF ROTATION AND PERCUSSION WITH A CONSTANT THRUST (64lbs) IN TEST B

Rock	Rotary Power watts	Total Input Power P_T, watts	Penetration Rate P.R., mm/sec	Drill Cuttings Ad, m^2/gm	C_o MN/m^2	$\frac{1}{(\ell n\ C_o)^2}$	Performance Factor $\frac{P.R. x P_T x A_H x 10^{-9} Nm}{Ad x Th}$	Specific Energy $\frac{P_T}{P.R. x A_H}$ .. KJ/m^3
Backwell Lst.	31.619	46.619	2.910	0.030975	163.94	0.0385	0.27401	899.400
Foster Yeoman Lst.	37.182	52.182	2.710	0.031225	131.10	0.0421	0.28232	1084.975
Ramsbottom Wild Sst.	36.130	51.130	7.101	0.039492	96.92	0.0478	0.57510	404.278
Kelmac Lst.	22.917	37.917	5.354	0.039422	114.66	0.0445	0.34817	397.575
Thresfield Lst.	37.951	52.951	3.650	0.035785	146.88	0.0402	0.33784	815.306
Buckton Sst.	32.120	47.120	7.158	0.041650	91.69	0.0490	0.50662	369.553
Holme Park Lst.	28.814	43.814	3.158	0.039610	141.92	0.0407	0.24741	779.934
Tarmac Arcow Greywacke	20.526	35.526	1.432	0.037479	355.83	0.0290	0.08490	1392.728
Horton Mudstone	41.162	56.162	3.914	0.032944	132.33	0.0419	0.41747	805.607
Fairy Cave Lst.	3.541	18.541	1.575	0.034301	282.16	0.0314	0.05331	660.869
Croft Gr.	27.874	42.874	2.262	0.038455	232.62	0.0337	0.18131	916.563
Boon's Nuneaton Quartzite	9.151	24.151	2.317	0.046778	303.32	0.0306	0.07484	585.156

TABLE 35

RESULTS OF TEST C ROTARY-PERCUSSIVE DRILLING AT CONSTANT THRUST (64lbs), MAXIMUM PERCUSSION AND A LOW SPEED OF ROTATION (350 R.P.M.).

Rock	Rotary Power watts	Total Power Input P_T, watts	Penetration Rate P.R., mm/sec	Drill Cuttings Ad, m^2/gm	C_o MN/m^2	$\frac{1}{(\ell n\ C_o)^2}$	Performance Factor $\frac{P.R. x P_T x A_H}{Ad x Th} \times 10^{-9}$ Nm	Specific Energy $\frac{P_T}{P.R. x A_H}$ .. KJ/m^3
Yellow Oolitic Lst.	15.296	30.296	18.471	0.028085	10.28	0.1842	1.24640	92.083
Darley Dale Sst.	20.695	35.695	4.932	0.036711	41.47	0.0721	0.29999	406.465
Horsforth Sst.	22.663	37.663	4.643	0.035072	44.33	0.0696	0.31171	455.389
St. Bee's Sst.	18.926	33.926	3.181	0.040766	57.22	0.0611	0.24262	408.75
Bath Lst.	13.536	28.536	4.210	0.025052	46.91	0.0675	0.30001	380.517
Elland Edge Sst.	16.347	31.347	2.523	0.043508	95.50	0.0481	0.11358	698.326
Denbigh Lst.	9.181	24.181	1.399	0.033561	178.57	0.0372	0.06311	969.597
Cornish Gr.	11.451	26.451	1.072	0.042631	168.29	0.0381	0.04153	1387.782
Groby Gr.	12.122	27.122	1.448	0.033868	143.30	0.0406	0.07265	1053.086
Craigenlow Pink Gr.	8.196	23.196	0.907	0.044084	225.10	0.0341	0.02986	1435.711
Mount Sorrel Gr.	12.745	27.745	1.121	0.042273	251.51	0.0327	0.04502	1390.688

TABLE 36

RESULTS OF TEST D ROTARY-PERCUSSIVE DRILLING AT CONSTANT THRUST (44LBS), 45% PERCUSSION AND AT 800 R.P.M.

Rock	Rotary Power watts	Total Power Input P_T, watts	Penetration Rate P.R., mm/sec	Drill Cuttings Ad, m^2/gm	C_o MN/m^2	$\frac{1}{(\ell n\ C_o)^2}$	Performance Factor $\frac{P.R. x P_T x A_H}{Ad x Th}$ x10^{-9}Nm	Specific Energy $\frac{P_T}{P.R. x A_H}$ .. KJ/m^3
Yellow Oolitic Lst.	27.080	32.804	8.010	0.029458	10.28	0.1842	0.81020	230.169
Cornish Gr.	17.382	23.106	1.402	0.039760	168.29	0.0389	0.07410	926.530
Tarmac Arcow Greywacke	10.036	15.760	0.961	0.039095	355.83	0.0289	0.03523	920.844
Boon's Nuneaton Quartz.	8.354	14.078	1.301	0.043939	303.32	0.0306	0.03788	607.940
York Sst.	27.812	33.536	3.542	0.040052	75.01	0.0536	0.26977	531.527
Ramsbottom Wild Sst.	25.181	30.905	3.013	0.038693	96.92	0.0478	0.21920	575.751
Buckton Sst.	25.709	31.433	2.777	0.041707	91.69	0.0489	0.18771	630.727
Backwell Lst.	12.714	18.438	1.635	0.031921	163.94	0.0385	0.08589	633.081
Croft Gr.	10.817	16.541	1.378	0.036943	232.62	0.0337	0.05597	673.918
Horton Mudstone	19.083	24.807	2.325	0.034400	132.33	0.0419	0.15251	598.983
Fairy Cave Lst.	12.077	17.801	0.881	0.034593	282.16	0.0314	0.04123	1113.567
Denbigh Lst.	11.915	17.639	2.181	0.034366	178.57	0.0372	0.10181	454.089

TABLE 37

RESULTS OF VARYING THE SPEED OF ROTATION MEASURING THE DRILL PARAMETERS AND A LIST OF THE CALCULATED PERFORMANCE FACTOR (P.F.)

Bath Limestone

R.P.M.	P.R. mm/sec	Torque ft.lbs	Total Power P_T, watts	Drill Cuttings m^2/gm	Perf. Factor P.F. x 10^{-9}Nm
321	1.923	0.10589	19.817	0.028008	0.0839
498	4.210	0.191740	28.536	0.025052	0.3000
894	5.131	0.38105	63.172	0.030481	0.6651
1289	10.132	0.38106	84.479	0.028839	1.8564
1900	12.348	0.33711	105.538	0.023942	3.4054

Denbigh Limestone

R.P.M.	P.R.	Torque	Total Power	Drill Cuttings	Perf. Factor P.F.
290	1.413	0.13156	18.404	0.033952	0.0531
467	1.420	0.13890	24.181	0.033868	0.0630
1006	2.100	0.16092	37.900	0.035326	0.1409
1352	3.368	0.09855	33.838	0.033119	0.2411
1980	5.911	0.09121	40.531	0.033816	0.4432

Mount Sorrel Granite

R.P.M.	P.R.	Torque	Total Power	Drill Cuttings	Perf. Factor P.F.
290	0.745	0.13450	20.525	0.040016	0.0236
473	1.120	0.19027	27.122	0.042233	0.0450
998	1.740	0.14625	35.639	0.042296	0.0917
1289	2.221	0.12423	37.651	0.042543	0.1229
1940	3.097	0.13891	53.102	0.042649	0.2412

Darley Dale Sandstone	Speed	320	695	980	1230	1480	1900
	P.F.	0.2324	0.6692	0.7659	1.2331	1.5445	3.5826
Cornish Granite	Speed	280	720	1020	1220	1550	1900
	P.F	0.0378	0.1075	0.1469	0.1704	0.24935	0.2906

TABLE 38

SLOPES OF SPEED/PERFORMANCE FACTOR

Rock	Slopes R.P.M/Nmx10^{-9}	C_o MN/m²
Darley Dale Sst.	903.118	41.47
Bath Lst.	468.342	47.0
Denbigh Lst.	4459.646	178.6
Cornish Gr.	6313.992	168.29
Mount Sorrel Gr.	7864.322	251.5
Extrapolated Slope Values from Tests A and C		
Yellow Oolitic Lst.	88.074	10.28
St. Bee's Sst.	722.495	57.22
Elland Edge Sst.	1142.884	95.50
Horsforth Sst.	386.822	44.33
Craigenlow Pink Gr.	6663.894	225.1
Groby Gr.	2659.80	143.30

Linear regression equation:

Slopes = y, C_o = x

$$y = 33.9056x - 1012.324$$

correlation coefficient = 0.960587

TABLE 39

RELATIVE EFFICIENCIES OF THE RANGE OF ROCKS DRILLED IN TEST A

Rock	% Relative Efficiency $\frac{C_O x P.R. x A_H}{P_T}$	% Relative Efficiency $\frac{E/A x P.R. x Ad x A_H x density}{P_T}$
Yellow Oolitic Lst.	6.16	12.65
Darley Dale Sst.	12.05	8.35
Horsforth Sst.	14.37	10.94
St. Bee's Sst.	10.38	7.19
Elland Edge Sst.	11.58	6.94
Bath Lst.	9.48	10.44
Craigenlow Pink Gr.	24.34	12.59
Giggleswick	22.23	16.66
Cornish Gr.	20.68	14.75
Denbigh Lst.	45.65	31.68
Whinstone	28.49	22.90
Mount Sorrel Gr.	27.88	18.77
Groby Gr.	29.25	39.43

Where, P_T = Total power input, watts

C_O = Compressive strength, MN/m^2

E/A = Drop hammer index, Nm/m^2

P.R. = Penetration rate, m/sec

A_H = Area of hole, m^2

Ad = Area of drill cuttings, m^2/gram

SUMMARY OF LABORATORY DRILLING

(a) The penetration rate-thrust characteristics show that penetration rate increases almost linearly up to a particular thrust for each rock. The slope characteristic for each rock drilled has been used for correlation with rock properties.

The graphs with the least scatter have been presented and are quite good, but the correlation is not significantly better than correlation of penetration rate against the rock properties. The functions considered give very little difference in correlation coefficients of penetration rate/thrust slopes and penetration rates against the rock properties. The advantage of the penetration rate/thrust slopes as opposed to penetration rate for prediction purposes is that the thrust need not be at an optimum or constant value providing the drill is not over thrust and the thrust is known.

The tests on penetration rate-thrust characteristics are a very important part of drilling and have shown that the penetration rate/thrust/strength index relationships display more than just a general trend.

(b) Preliminary thrust tests on the new laboratory drilling rig showed the improvement in penetration rate by adding the percussive action to rotary drilling, particularly in the 'harder' 'stronger' rock . The drill cuttings for rotary drilling were finer than those collected for rotary-percussive drilling, showing that less energy is wasted in producing and regrinding fines in rotary-percussive drilling.

At the low speed of rotation thrust tests the importance of having the correct thrust to avoid low penetration is shown. The power input is also considerably affected by the thrust and the drill cuttings vary from rock to rock. However, the cuttings variation for an individual rock shows no apparent relationship except those for Darley Dale sandstone, where they become less fine indicating less wastage of power.

Increasing the rotary power gives an increase in penetration rate for a constant thrust. The higher penetration rates occured in the sandstone because of the larger developed torques hence greater power input plus the fact that its physical properties allow it to be drilled easier. In this respect increased torque is advantageous, however increasing the thrust at the low speed produced larger torques so increasing the power input and initially the penetration rate, but increasing the thrust too much does produce some lower penetration rates. This must be because the drill is sticking and then freeing giving the anomolies in the thrust tests and with the 'weaker' rocks the anomolies start at lower thrusts. Therefore, producing higher torques by thrust increases is not always a good thing as the too much thrust can cause adverse effects.

Increasing the percussive power increased penetration of both rocks tested, but the granite had the greater percentage improvement in penetration rate. The drill cuttings for both speed and percussion tests were affected by the change of power and measuring the surface area of the cuttings by

sieve analysis has shown this effect.

(c) Drilling a range of rocks with the constant rotation, percussion and thrust when analysed in terms of specific energy gave quite an amount of scatter when plotted against rock properties. This scatter was reduced by introducing the surface areas per gram of the drill cuttings showing that the cuttings are an important part of drill analysis. However, this does not help as regards prediction even if a good correlation could be obtained.

Analysis of power input/output after Hustrulid using both the compressive strength and drop hammer index produced no correlation. Nevertheless dividing the output by the input it is possible to have an idea of the relative efficiency of the drilling. The efficiency is relative depending on which strength index is used. The percentage relative efficiencies for the rocks drilled in test A are listed in table 39, when both compressive strength and the drop hammer indices have been used to determine the relative efficiencies. These efficiencies vary for each rock and on an energy basis we are examining only a small part of the actual energy, most of the energy is being lost. The relative efficiencies would be even smaller if a more efficient breakage energy index was used for comparison, say slow compression instead of drop hammer index.

The efficiency figures are determined from the rock output in terms of power and the power input from the drill,

but the input is also effected by the rock in that the torque developed is dependent on the rock. With some rocks, mainly the 'stronger' ones having low torques giving smaller power inputs, the efficiencies are high. So that in terms of efficiency the rocks with low power inputs have higher efficiencies showing with what power they do have they make the best of it. However, efficiency figures can be misleading in that the best efficiency is not necessarily the best drilling. For example the penetration rate could be very low but if the developed torque is low the efficiency could be quite high and conversely with high penetration rate and high torque. On the other hand as stated, it is possible from the relative efficiencies to see the difficulties involved in drill analysis, where the efficiency changes from rock to rock and quite an amount of energy is lost in the drilling process.

(d) The developed empirical formula called the performance factor which combines the drilling parameters when plotted against the compressive strength gives an excellent correlation for all four tests A, B, C and D. For test C, which was maximum percussion and a low speed a very good relationship was obtained for the specific energy against the compressive strength.

The performance factor when plotted against the speed of rotation increases gave linear relationships and the slopes of the lines for the different rocks also correlates

with compressive strength. The correlation coefficient is not as high as in other tests, but this is understandable because of the large amount of drilling involved and some of the slopes were extrapolated.

The introduction of the performance factor has shown that the drill parameters do correlate with a strength index for different drilling conditions and even for the combination of different drilling speeds where speed/ performance factor slopes have been correlated with compressive strength. The performance factor, apart from showing that there is a near perfect relationship and it would be possible to accurately predict it from the compressive strength, doesn't enable anything else to be determined because it is too complicated in that it has too many unknowns. However, it must be stressed that its introduction was purely to show that a consistent relationship is possible in drilling where previously none has been found.

CHAPTER V

FIELD ROTARY-PERCUSSIVE DRILLING

CHAPTER V

FIELD ROTARY-PERCUSSIVE DRILLING

Introduction

The field drilling was carried out by Halifax Tool Company, who supplied the data from rotary-percussive drilling in a large number of different quarries. Photograph 5 shows one of their rotary-percussive drilling rigs mounted on caterpillar tracks.

The type of bits used are cross bits and button bits with tungsten carbide inserts. In the design of cross bits, four tungsten carbide cutting edges form two mutually perpendicular lines across the diameter of the bit. The button bit has a few small circular tungsten carbide inserts which are placed in any desired pattern on the cutting face of the bit. The advantage of the button bit is that the cutting points or the buttons are more securely retained in the bit than the straight inserts of the cross bit. Generally, the life of the button bit is longer than the cross bit as more inserts can be placed near the periphery of the bit where greatest wear occurs.

The data i.e. penetration rates, optimum thrusts, hammer masses, air pressures, hole sizes, piston strokes, lengths and diameters, feed cylinder and piston rod diameters, and hammer types have been listed in Misra's (34) thesis. The calculated energy output of the hammer per unit time, the thrust on the drill and the volume of rock removed per unit time are also given.

PHOTOGRAPH 5 : Crawler Mounted Rotary-Percussive

Drilling Rig

Therefore, as the data is fully detailed in Misra's thesis only the calculated data that is to be used in this thesis is given (i.e. energy output of the hammer per unit time and the volume of rock removed per unit time). The supplied data along with various determined rock properties were used by Misra in order to investigate the possibilities of mathematical modelling by dimensional analysis to predict the penetration rate. He found the final prediction equation to be extremely complex and the best correlation coefficients were 0.920 for the button bits and 0.857 for cross bits. As these coefficients are quite low, large errors in prediction will occur. Consequently, it seemed a good idea to reanalyse the data from a different angle as there is such a large amount of useful data. By the different analysis it is hoped that a clear picture of the drilling problems will emerge.

5.1 Correlation of Laboratory drilling with Field drilling

The intention of this work was to establish a correlation between the laboratory drilling and the field drilling. So that on being presented with a rock and asked to predict the field drilling performance this could be done by drilling the rock in the laboratory and using the established correlation to predict the field drilling.

The laboratory drilling penetration rates at constant speed of rotation, percussion and thrust, drilling approximately 14mm with new bits for each hole, were determined. The torque and speed were measured so that the power input can be calculated and the specific energy (J/m^3) determined from:-

Total Power Input P_T/Penetration Rate (P.R.) x area of hole(A_H).

The penetration rate for field drilling has to be assumed to be the optimum that can be attained for the drilling conditions. This seems a fair assumption as the operators are in the main experienced and skilful and the drilling performance data supplied is averaged from drilling a large number of holes at each quarry. As the hole sizes drilled in the field do vary the penetration rate is multiplied by the area of the hole drilled so giving the volume of rock removed per unit time, which is a more useful value for correlation in this case. The laboratory drill has a constant area of hole drilled.

The rotation of the drill for all field drilling is kept constant at approximately 30 R.P.M. and the job of rotation is mainly to provide fresh cutting faces for the bit. As the overall contribution of the rotary power is extremely small in variability compared to the percussive power it is omitted from the field calculation.

The specific energy was calculated for the field drill from the power input to the drill divided by the volume of rock removed per unit time. Misra (34) calculated the power input from the air pressure causing a force to move the drill piston to give a theoretical energy output of the hammer per unit time, x, KJ/sec.

$$x = 4.80p^{\frac{3}{2}} \times d^3 \times \ell^{\frac{1}{2}} \times m^{\frac{1}{2}} \times 10^{-7} \text{ ..... KJ/sec}$$

where, p = air pressure kg/cm², d = piston head diameter mm, ℓ = maximum possible stroke length mm, m = mass of piston kg.

The equation is calculated from the force on the piston which is the air pressure times the area of the piston and the work done or energy is obtained by multiplying the force times the stroke length. The power output, x, is then the energy per unit time. The time is obtained by assuming the piston is at rest when the air under pressure is admitted to the cylinder and causes the piston to accelerate the stroke distance.

So that the theoretical energy output/unit time of the hammer, x = force on piston x area of piston x stroke length ÷ unit time = $p \times \pi d^2 \times \ell \div t$.

Unit time is obtained from

$$s = ut + \tfrac{1}{2}ft^2, \quad u = 0$$

$$t = \left(\frac{2 \times \text{stroke length}}{f}\right)^{\frac{1}{2}}$$

and $$f = \frac{\text{force}}{\text{mass}} \qquad \text{(Newton's Law)}$$

$$= \frac{p(\pi d^2/4)}{m}$$

$$t = \left(\frac{8m\ell}{\pi \rho d^2}\right)^{\frac{1}{2}}$$

Doubts have been expressed about the validity of the theoretical energy output of the hammer per unit time equation in that is the piston at rest when the air enters the cylinder and does it accelerate over the stroke distance? Nigel Cox at Halifax Tool Company ran tests on the field drill and by stress wave energetics measured the actual power delivered to the bit. The results are as follows:-

Power input		Power output at bit	
Compressed air working on piston.		determined from stress wave energetics.	
air pressure p.s.i.	kilowatts	kilowatts	% efficiency
100	20.839	4.8	23.0
125	29.123	5.7	19.6
150	38.283	7.3	19.2
150	38.283	8.2	21.5
170	46.189	9.6	20.9

The graph is plotted in figure 5.1 and this shows that for the operating range considered, a linear relationship exists between the power input and the power output at the bit. Therefore, the theoretical energy output of the hammer per unit time equation can be used for the drill input power, but bearing in mind that approximately 3/4 of the energy per unit time can be lost on its way to the bit.

With the laboratory drill the percussive power was constant for a particular variac setting, but some of this power will be lost on its way to the bit as happens with the field drill. This loss is also assumed constant.

The laboratory penetration rates and specific energies are listed in table 40 along with the field volumes of rock removed per unit time, the field power inputs determined from the theoretical equation x, and the field specific energies for twenty-two rocks.

The graphs of (a) laboratory penetration rate against field volume of rock removed per unit time and (b) laboratory specific energy against field specific energy are plotted in

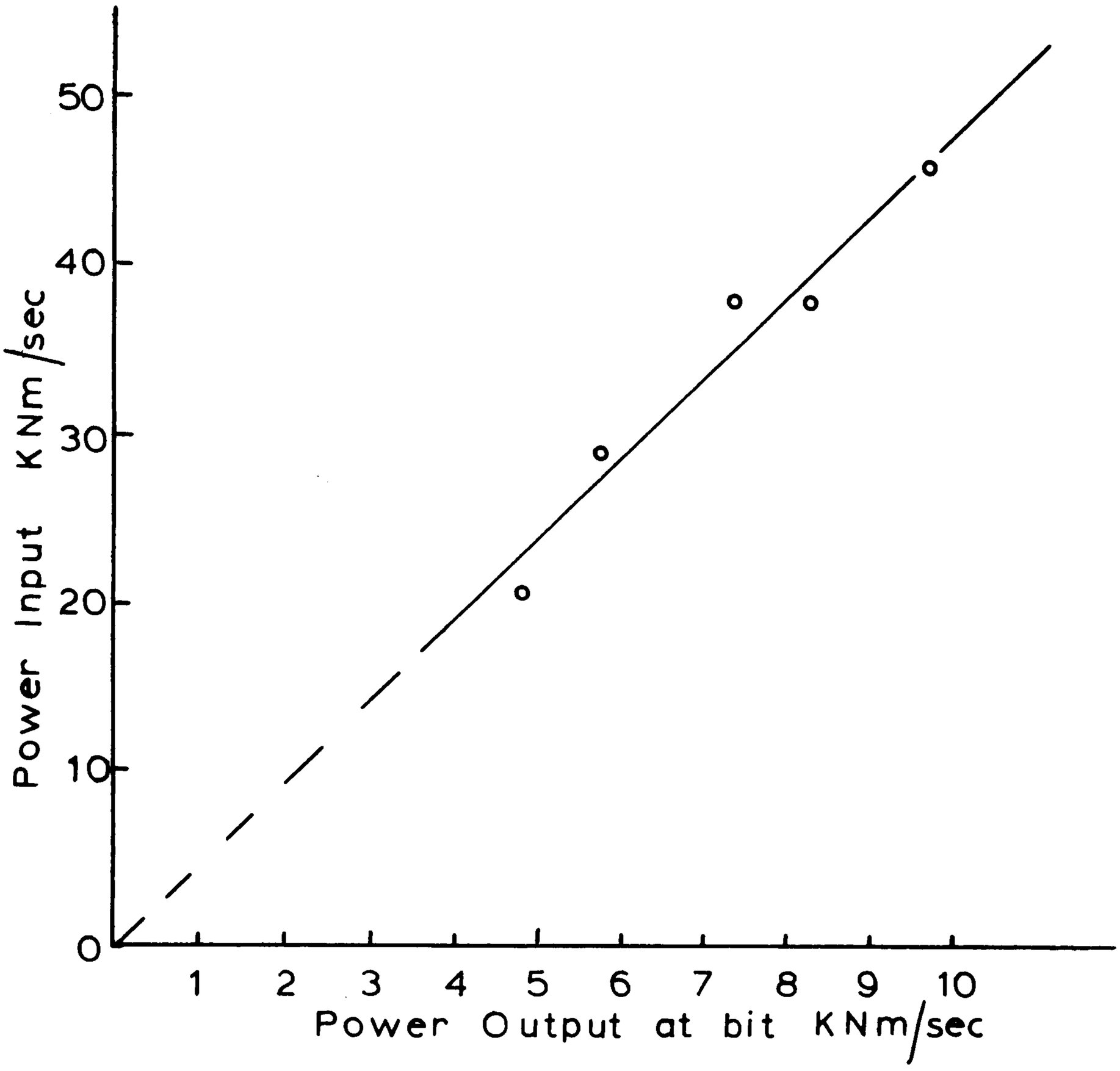

FIGURE 5.1: POWER INPUT V. POWER OUTPUT FOR DA150 DRILL.

Power input by compressed air working on the piston.
Power output at bit determined from stress wave energetics.

TABLE 40

RESULTS OF ROTARY-PERCUSSIVE DRILLING THE SAME ROCKS IN THE LABORATORY AND THE FIELD FOR CORRELATION

Rock	Laboratory Penetration rate P.R., mm/sec	Field Volume of rock removed/sec. P.R. x A_H, V, $cm^3/sec.$	Laboratory Specific Energy MJ/m^3	Field Specific Energy MJ/m^3	Input Power kilowatts.
Button Bit					
Backwell Lst.	3.29	21.3	899.44	875.117	18.64
Foster Yeoman Lst.	2.64	32.23	1084.975	693.481	22.33
Giggleswick Lst.	4.79	26.9	592.951	1007.049	27.08
Kelmac Lst.	5.98	22.1	397.575	711.890	16.16
Rams. Wild Sst.	7.76	31.7	404.278	712.910	22.60
Swinden Cracoe Lst.	5.07	32.2	-	891.583	28.71
Thresfield Lst.	5.31	17.9	815.306	902.771	16.16
Bardon Hill Gr.	2.26	19.9	-	1135.678	22.6
Holme Park Lst.	4.49	48.3	779.934	462.232	22.3
Buckton Sst.	9.26	40.3	369.553	286.615	11.55
Cross Bit					
Croft Gr.	2.48	13.05	916.563	1629.115	21.66
Bardon Hill Gr.	2.26	11.63	-	1495.270	17.39
Cornish Gr.	3.49	58.8	814.012	1127.014	66.27
Bardon Hill Gr.	2.48	12.32	-	1311.688	16.16
Denbigh Lst.	4.10	20.98	384.642	1208.313	25.35
Boon's Nun. Quartz	2.02	8.13	585.156	1218.917	9.91
Springfield Whinstn.	4.38	2.66	614.823	1277.139	3.4
Fairy Cave Lst.	2.58	7.21	660.869	1079.051	7.78
Bardon Hill Gr.	2.26	17.16	-	1317.016	22.60
Buckton Sst.	9.26	21.71	369.553	532.012	11.55
T. Arcow Greywacke	2.58	15.80	1392.728	1022.181	16.16
Horton Mudstone	4.27	37.62	805.607	514.885	19.37

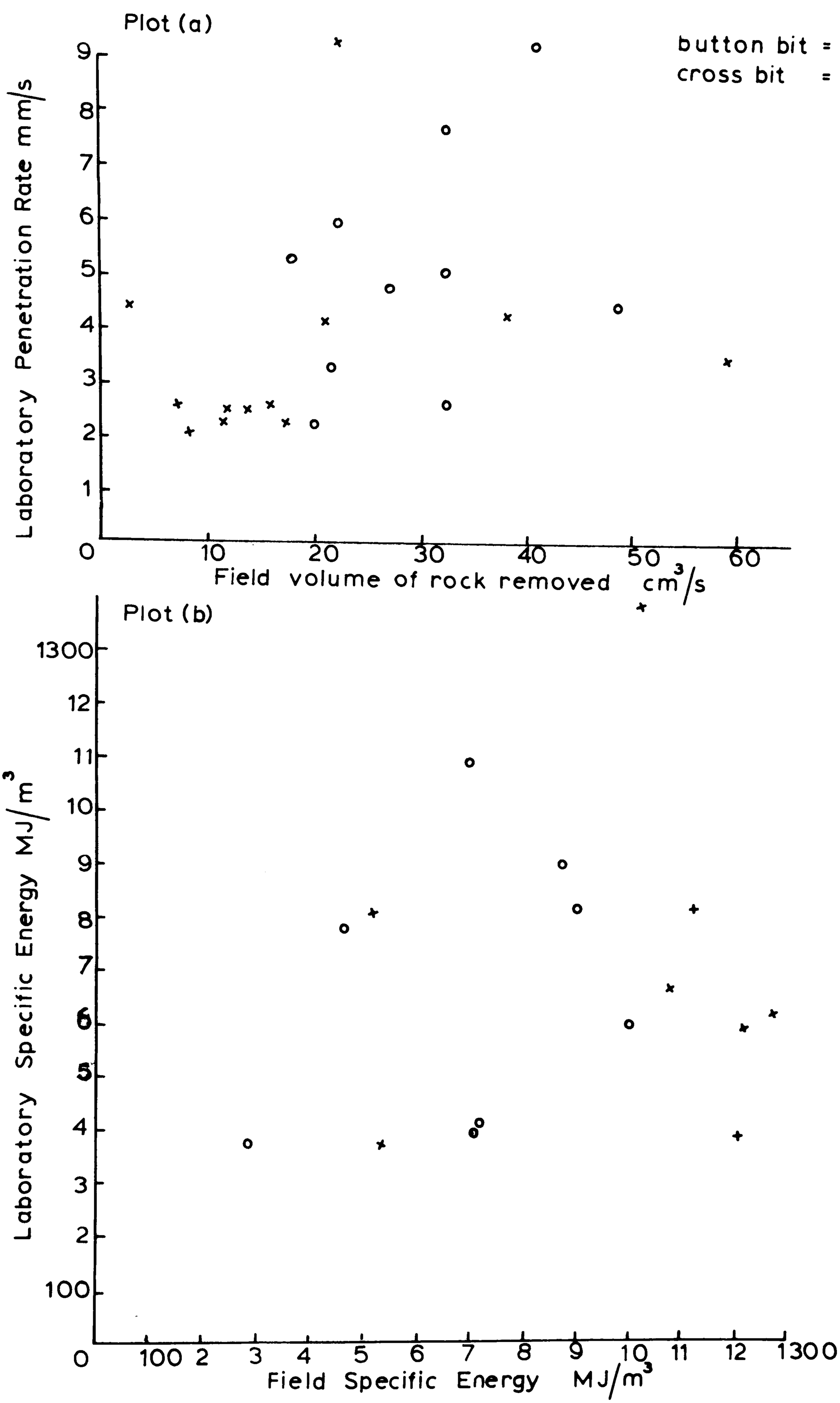

FIGURE 5.2:

(a) Laboratory penetration rate v. Field penetration rate x area of hole drilled.

(b) Laboratory specific energy v. Field specific energy.

figure 5.2. From these graphs it can be seen that in no correlation for either plot (a) or (b).

5.2 Analysis after Teale (51) and Hustrulid (55)

The field data was analysed by using the specific energy values from table 40 separately plotted against two rock properties the compressive strength and rock impact hardness number. (Teale proposed the relation of specific energy to a rock property). The data was also analysed by using the power inputs plotted against the power outputs, the power output being the volume of rock removed per unit time multiplied by the rock property. Again the two rock properties compressive strength and rock impact hardness number were used. (Hustrulid proposed the relation of power input to power output with the power output determined from the compressive strength multiplied by the rock volume removed per unit time).

The two rock indices were chosen because compressive strength is a standard rock property and it would be interesting to test whether or not when used for a large number of rocks it is actually related to the specific energies and powers as proposed by Teale and Hustrulid. Rock impact hardness number was chosen because Misra (34) found it to have the best correlation with the field drill when combined with the compressive strength and modulus of rupture. The index also has units of energy and can be therefore related to specific energies and relative efficiencies more confidently. This is because it has been determined from

measuring the energy required to break the rock as opposed to measuring a force in the compressive strength. However, if either property gave a good relationship it would be extremely advantageous in the design and prediction of drill performance.

The power inputs and outputs for the twenty-two rocks drilled in the field are listed in table 41 with the two rock properties. The field specific energies have been plotted against the compressive strength and rock impact hardness number shown in figures 5.3 and 5.4 respectively. The power inputs plotted against the power outputs one using the compressive strength and the other rock impact hardness number have been drawn in figures 5.5 and 5.6 respectively.

All four graphs have a general trend, but there is a substantial amount of scatter. The specific energy against compressive strength graph is figure 5.3 shows a good relationship up to 200 MN/m^2 compressive strength, but after this point there is a great deal of scatter. Rock impact hardness number against the specific energy in figure 5.4 gives a 'band' of points with a scattering of points within the band. These graphs are very similar to those obtained for the laboratory drill and the specific energy values for both laboratory and field drilling are of the same order.

The power inputs against the power outputs in figure 5.5 and 5.6 show that the rock impact hardness number used to determine the output gives a better graph than using compressive strength. This analysis after Hustrulid, however, gave no correlation for the laboratory drill.

TABLE 41

ANALYSIS OF FIELD RESULTS IN TERMS OF POWER INPUT AND OUTPUT

Rock	Input Power Kilow.	Volume of rock removed/sec P.R.xA_H V,cm^3/sec	Rock Indices C_o MN/m^2	R.I.H.N. MJ/m^3	Output Power VxC_o Kilow.	VxR.I.H.N. Kilow.	Relative Eff. %
Button Bit							
Backwell Lst.	18.64	21.3	163.9	100.68	3.491	2.144	11.50
Foster Yeoman Lst.	22.33	32.2	131.1	85.0	4.244	2.736	12.25
Giggleswick Lst.	27.08	26.9	131.84	68.93	3.546	1.854	6.85
Kelmac Lst.	16.16	22.7	114.6	56.45	2.602	1.281	7.93
Rams. Wild Sst.	22.6	31.7	96.92	34.58	3.072	1.096	4.85
Swinden Crac. Lst.	28.71	32.2	106.21	74.62	3.420	2.403	8.37
Thresfield Lst.	16.16	17.9	146.88	68.65	2.665	1.229	7.64
Bardon Hill Gr.	22.6	19.9	330.4	210.52	6.576	4.189	18.54
Holme Park Lst.	22.3	48.3	141.92	72.52	6.855	3.503	15.71
Buckton Sst.	11.55	40.3	91.92	27.35	3.695	1.102	9.54
Cross Bit							
Croft Gr.	21.66	13.05	232.6	139.08	3.035	1.825	8.43
Bardon Hill Gr.	17.39	11.63	330.4	210.52	3.843	2.448	14.08
Cornish Gr.	66.27	58.80	168.29	76.1	9.896	4.474	6.75
Bardon Hill Gr.	16.16	12.32	330.4	210.52	4.070	2.594	16.05
Denbigh Lst.	25.35	20.98	178.57	96.62	3.746	2.028	8.00
Boon's Nun. Quartz	9.91	8.13	303.32	88.27	2.466	0.718	7.25
Spring. Whinstone	3.4	2.66	175.2	113.2	0.466	0.301	8.85
Fairy Cave Lst.	7.78	7.21	282.2	140.11	2.035	1.010	12.98
Bardon Hill Gr.	22.60	17.16	330.4	210.52	5.670	3.613	15.99
Buckton Sst.	11.55	21.71	20.97	52.2	1.991	0.594	5.14
T. Arcow Greywacke	16.16	15.81	355.8	200.72	5.626	3.173	19.63
Horton Mudstone	19.37	37.62	132.33	66.03	4.978	2.484	12.81

P.R. = Penetration Rate, A_H = Area of hole,

C_o = Compressive strength, R.I.H.N. = Rock Impact Hardness Number.

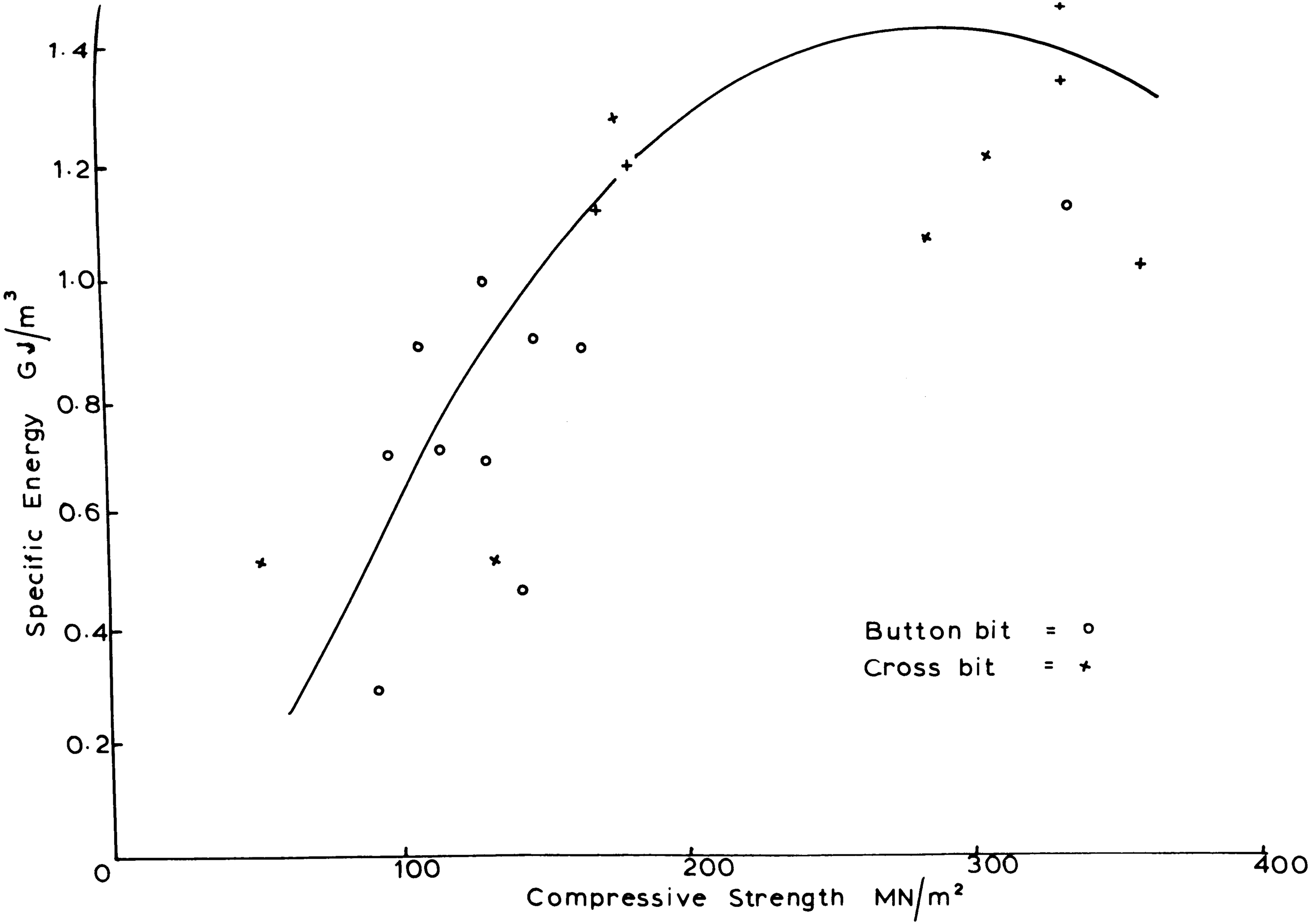

FIGURE 5.3: SPECIFIC ENERGY V COMPRESSIVE STRENGTH.

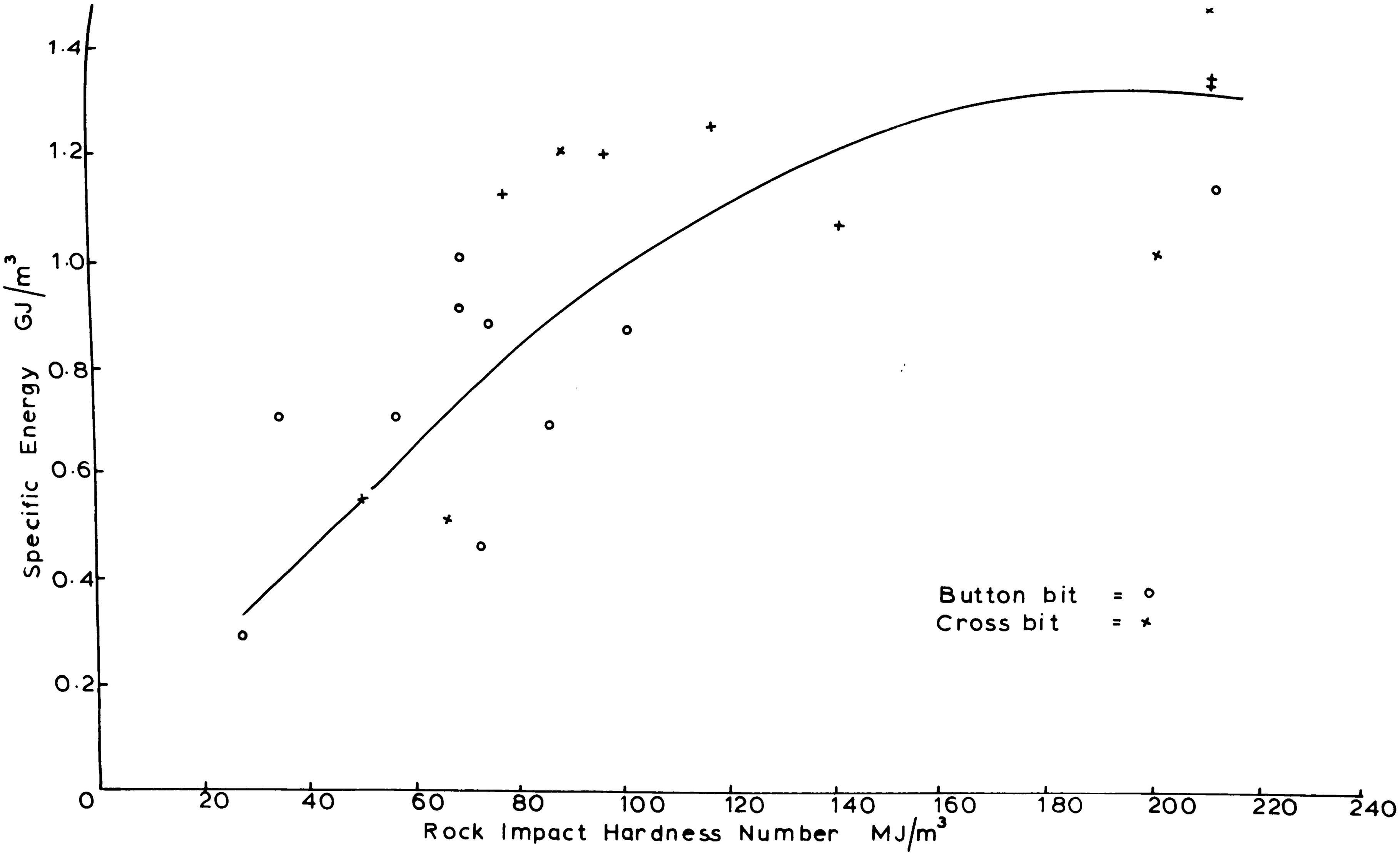

FIGURE 5.4: SPECIFIC ENERGY V ROCK IMPACT HARDNESS NUMBER.

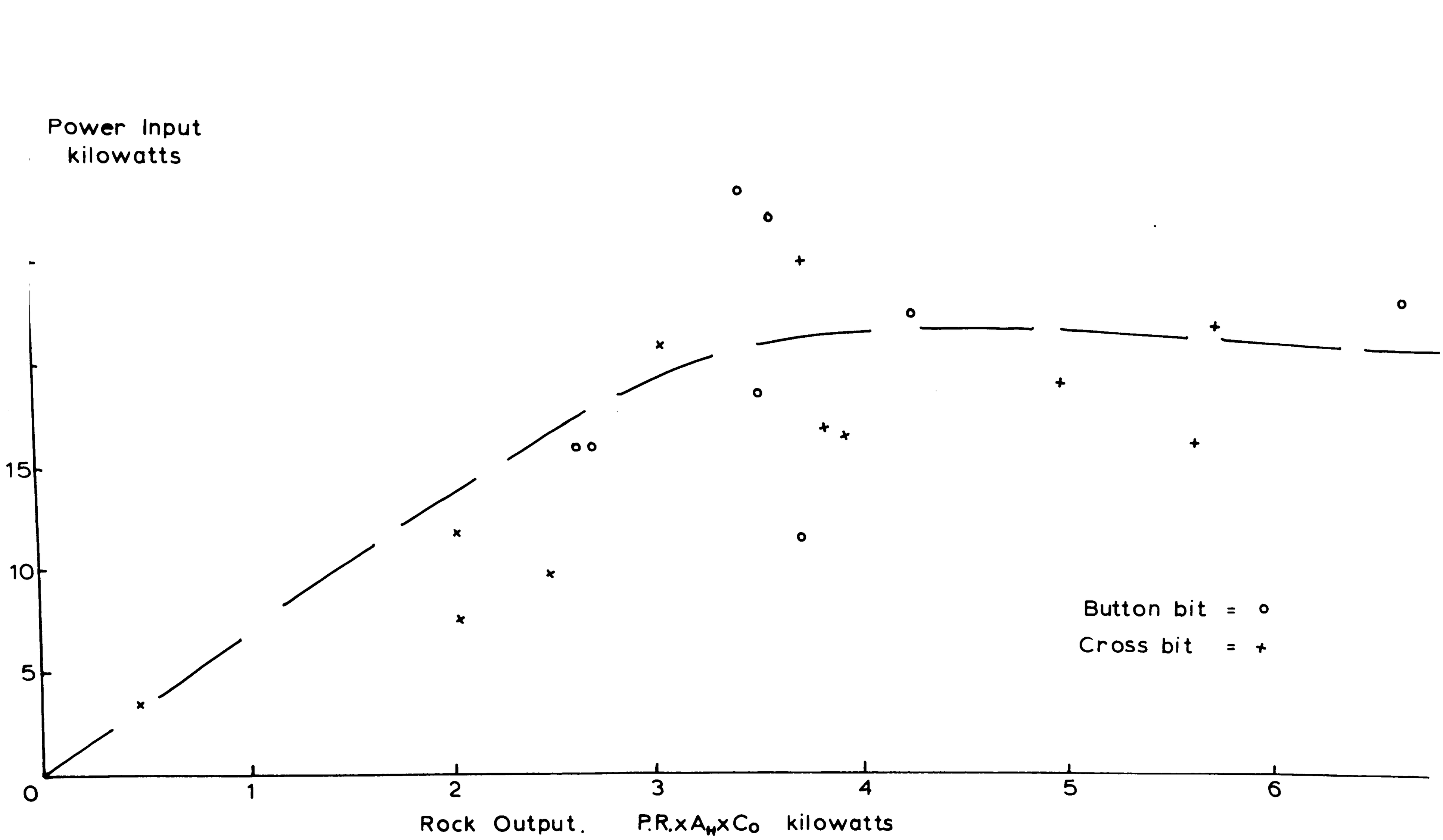

FIGURE 5.5: POWER INPUT V ROCK OUTPUT.

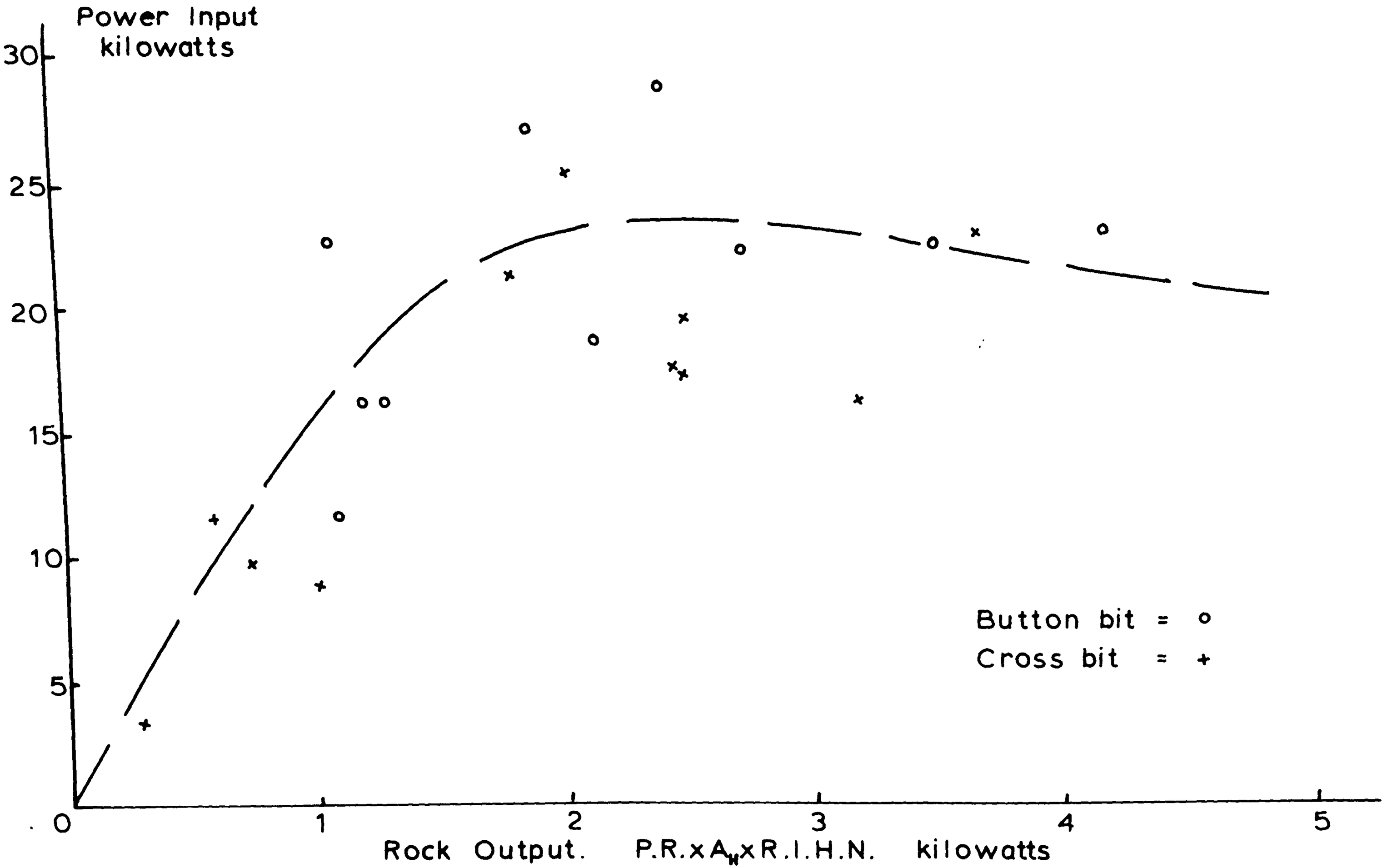

FIGURE 5.6: POWER INPUT V ROCK OUTPUT

5.3. Relative Efficiencies

The efficiencies are calculated from the power output divided by the power input and these are again relative efficiencies depending on which strength index is used. The rock impact hardness number is used for the same reasons as described in 5.2. Therefore, the relative efficiencies are calculated from:-

$$\frac{P.R. \times A_H \times R.I.H.N.}{P_T} \times 100\% = \% \text{ relative efficiency.}$$

where, P.R. = penetration rate, m/s., A_H = area of hole, m^2

R.I.H.N. = rock impact hardness number, MJ/m^3

P_T = power input, kilowatts.

The percentage relative efficiencies are given in table 41 for the field rocks drilled. As the specific energies for the field are of the same order as the laboratory drill, then using the same rock index the relative efficiencies will be of the same order.

These efficiencies do vary for each rock and are quite low, the cross bit having the lowest of 5.14% and the highest of 19.63%. If the efficiency of the power input at the bit determined from stress wave energetics to the rock output is considered then the efficiencies are approximately four times higher.

Also if a different strength index was used the efficiency values would be different, however the percentage relative efficiencies are of the same order whether using rock impact hardness number, compressive strength or drop hammer index. This is to say using one index as opposed to another does not have efficiencies of 0.5% for that index and an order of

50% using another.

It is therefore, hardly surprising that difficulties have arisen where poor relationships have been obtained for energy studies because of the large amounts of energies lost and the variability of the efficiencies both in the laboratory and field analysis. There is also a further probable complication in that the amount of percussive energy reaching the bit when actually drilling will vary from the input power. This is because of the different damping effects caused by different rocks on the generated stress waves and the power at the bit not having a value approximately four times less than air power supply.

Therefore, to accurately measure the percussive input power a continuous recording of the energy input must be made as done with rotation in the laboratory.

5.4. Sampling and Analysis of field drill cuttings.

(a) Drilling at Groby Quarry

Sampling was first carried out at Groby Quarry, Leicestershire whilst drilling in the Groby granite. The drill cuttings are exhausted up the hole and pass into a cyclone for the removal of the very fine cuttings. Samples of drill cuttings were taken at 20 feet depth for two holes A and B drilled 10 feet away from each other. The cuttings were collected at the cyclone outlet as well as without the cyclone which entailed temporarily disconnecting the cyclone.

For both holes the power input (air supply pressure) and the thrust were kept at the same values and the penetration rate was the time taken to drill one 12 feet tube length using a new button bit for each hole.

The samples were each coned and quartered and one of the quarters was further reduced to two halves using a sample splitter, each half weighing approximately 70 grams. The two halves were then separately sieved and weighed to determine the surface area created per gram from

$$\sum \frac{6}{s} \ell n 2 . \frac{\text{wt. of fraction}}{a_1 - a_2}$$ on the Wang desk top computer.

The computed surface areas/gram showed that the cyclone samples contained more fines than without the cyclone. Clearly an amount of regrinding takes place in the cyclone, therefore the cyclone results were rejected and all future sampling was done before the cuttings reached the cyclone.

The results from splitting show quite good agreement as listed over, where the two surface areas/gram of the two

halves are shown with their mean value and penetration rate.

Results of drilling at Groby

	Hole A from cyclone	Hole A without cyclone	Hole B without cyclone
	0.015982	0.014802	0.011749
	0.015720	0.014960	0.011589
Mean value m^2/gm	0.015851	0.014881	0.011669
Penetration rate mm/sec	3.81	3.81	4.924

For the same drill settings the better penetration rate occured with the production of cuttings which were less fine. This indicates that less energy is lost in regrinding the chips and the energy is used in doing work i.e. producing higher penetration rate, assuming that the physical properties of the rock where the two holes were drilled were the same.

(b) Drilling at Foster Yoeman and Swinden Cracoe Limestone Quarries.

Drilling at these two quarries was done with constant power input and varying thrusts. The penetration rate and thrust were measured at the time of collecting the drill cuttings.

At Foster Yoeman two button bit sizes were used whilst drilling at two different test sites I and II. At test site I a 150mm bit size was used and test site II had a 165mm bit size.

The total thrust is the applied thrust at the time of drilling plus the dead weight on the bit which is the weight of the block, shock absorbers and hammer plus the weight of the tubes. At Foster Yoeman the weight of the tubes at test site I was 224lbs and at site II 110lbs, this helped to give some large thrusts in test I. At both sites the power input was held constant with an air pressure of 150 p.s.i. and the weight of the block etc. was 300lbs also constant.

At Swinden Quarry the drill parameters were slightly different with a 127mm button bit size, tube weights 150lbs, weight of block, shock absorbers and hammer 355lbs and the constant power input at 130 p.s.i. air pressure.

As drilling was carried out at two different sites ½ mile apart, at Foster Yoeman, rock samples were collected at each site and the rock impact hardness number determined. At test site I the rock impact hardness number was 85.10 MJ/m^3 and at site II 85.35 MJ/m^3, Misra's (34) result from almost 4 years ago was 84.98 MJ/m^3 for the same quarry. As the two test sites are so close in strength values it is assumed that any difference found between them will be due to the difference in thrust and change of bit size.

At Foster Yoeman tests were carried out drilling different holes up to a depth of 50 feet at the two test sites, whereas at Swinden Cracoe only one hole was drilled, but this was done to a depth of 112 feet. In view of this depth it was decided to test the drill cuttings from Swinden to see whether or not the strength does change as the depth of hole increases.

Samples number 1 and 7 were chosen for testing as 1 is the top of the hole with the largest penetration rate and smallest thrust and 7 is the bottom of the hole with the smallest penetration rate and largest thrust. Samples 1 and 7 were screened to give an approximate size of 3/16" and enough to spread evenly in the small mortar for slow compression testing in the Instron as described in chapter III, section C. The desities of each were determined, no. 1 having a density of 2.712 and no. 7, 2.713.

The results of the slow compression test are given below in table 42 and the graph of energy/gram against area/gram plotted in figure 5.7. The graph shows a linear relationship, so the samples must have the same strength.

TABLE 42

Slow Compression of Swinden Cracoe Drill Cuttings

Crush number	Energy input Nm	Energy/gm Nm/gm	Total Energy/gm Nm/gm	Surface Area/gm m^2/gm
Drill cuttings sample 1.				
I	17.684	1.281	1 281	0.004007
II	8.335	0.610	1.891	0.007256
III	9.318	0.686	2.577	0.010210
Drill cuttings sample 7				
I	16.471	1.467	1.467	0.005594
II	11.559	1.035	2.502	0.010082

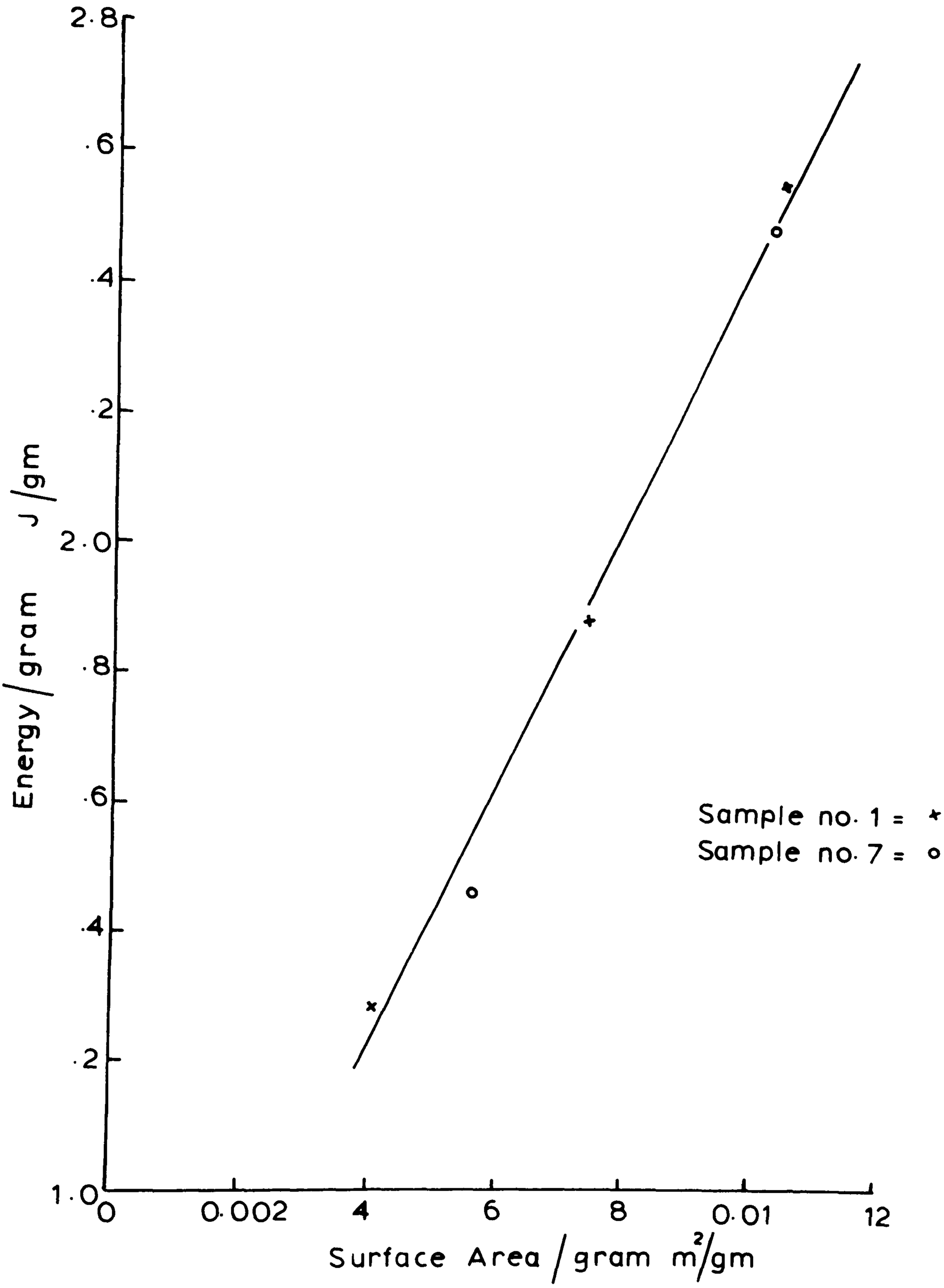

FIGURE 5.7: SLOW COMPRESSION TEST ON SWINDEN CRACOE LST. DRILL CUTTINGS.

The results of drilling at Foster Yoeman and Swinden Cracoe quarries are given in table 43 in which is listed the total thrusts on the bits, the dead weights and the applied thrust pressures, the penetration rates and the surface areas per gram of the drill cuttings. The special features of each drilling (e.g. bit size, tube weights, etc.) are also given in that table.

The plotting of penetration rate against the thrust and the plotting of penetration rate per unit thrust against the surface area of the drill cuttings are given in figures 5.8 and 5.9 respectively.

TABLE 43

RESULTS OF ROTARY-PERCUSSIVE DRILLING AT FOSTER YOEMAN AND SWINDEN CRACOE LIMESTONE QUARRIES

Field Drilling at Foster Yoeman Quarry

Dead weight on bit 300 lbs + wt. of tubes, Total Thrust = Dead wt. + Applied thrust.

I. 150mm bit size, 150 p.s.i. constant power, 224lbs tube weight.

P.R. mm/sec.	No. of tubes	Applied Thrust KN	Total Thrust KN	Drill Cuttings Ad, m^2/gm	P.R./Th. mm/sec.KN
1. 5.952	4	0.785	6.218	0.011977	0.9576
2. 6.410	1	0.196	2.641	0.008271	2.4271
3. 6.944	3	0.491	4.918	0.007489	1.4120
4. 6.173	1	0.785	3.230	0.007432	1.9114
5. 5.952	3	0.491	4.928	0.007654	1.2078
6. 5.952	4	0.491	5.924	0.008552	1.0047

II. 165mm bit size, 150 p.s.i. constant power, 110lbs tube weight.

P.R. mm/sec.	No. of tubes	Applied Thrust KN	Total Thrust KN	Drill Cuttings Ad, m^2/gm	P.R./Th. mm/sec.KN
1. 5.815	3	0	2.964	0.004435	1.9620
2. 5.297	3	0	2.964	0.004814	1.7872
3. 4.686	4	0	3.453	0.005831	1.3571
4. 6.345	4	0.491	3.944	0.005449	1.6089
5. 7.614	1	0.491	2.475	0.004001	3.0762

(Table 43 cont).

Field Drilling at Swinden Cracoe Quarry

Dead weight on bit = 355lbs + wt. of tubes, Total Thrust = Dead wt. + Applied Thrust.

127mm bit size, 130 p.s.i. constant power, 150lbs tube wt.

P.R. mm/sec	No. of tubes	Applied Thrust KN	Total Thrust KN	Drill Cuttings Ad, m^2/gm	P.R./Th. mm/sec.KN
1. 5.805	1	1.963	4.411	0.015209	1.3160
2. 5.896	4	1.374	5.824	0.013110	1.0123
3. 5.113	5	0.981	6.099	0.010044	0.8383
4. 4.861	6	0.981	6.767	0.010568	0.7183
5. 4.572	7	0.981	7.435	0.016178	0.6150
6. 4.810	8	0.834	7.954	0.015140	0.6050
7. 4.059	9	0.736	8.524	0.009926	0.4762

Performance Factor Values, Nm x 10^{-3}.

Foster Yoeman Quarry

I.		II.	
1.	54.100	1.	362.174
2.	198.517	2.	303.934
3.	127.549	3.	190.511
4.	173.519	4.	241.692
5.	106.751	5.	629.356
6.	79.476		

Swinden Cracoe Quarry

1. 33.851
2. 30.212
3. 32.655
4. 26.593
5. 14.871
6. 15.627
7. 1.873

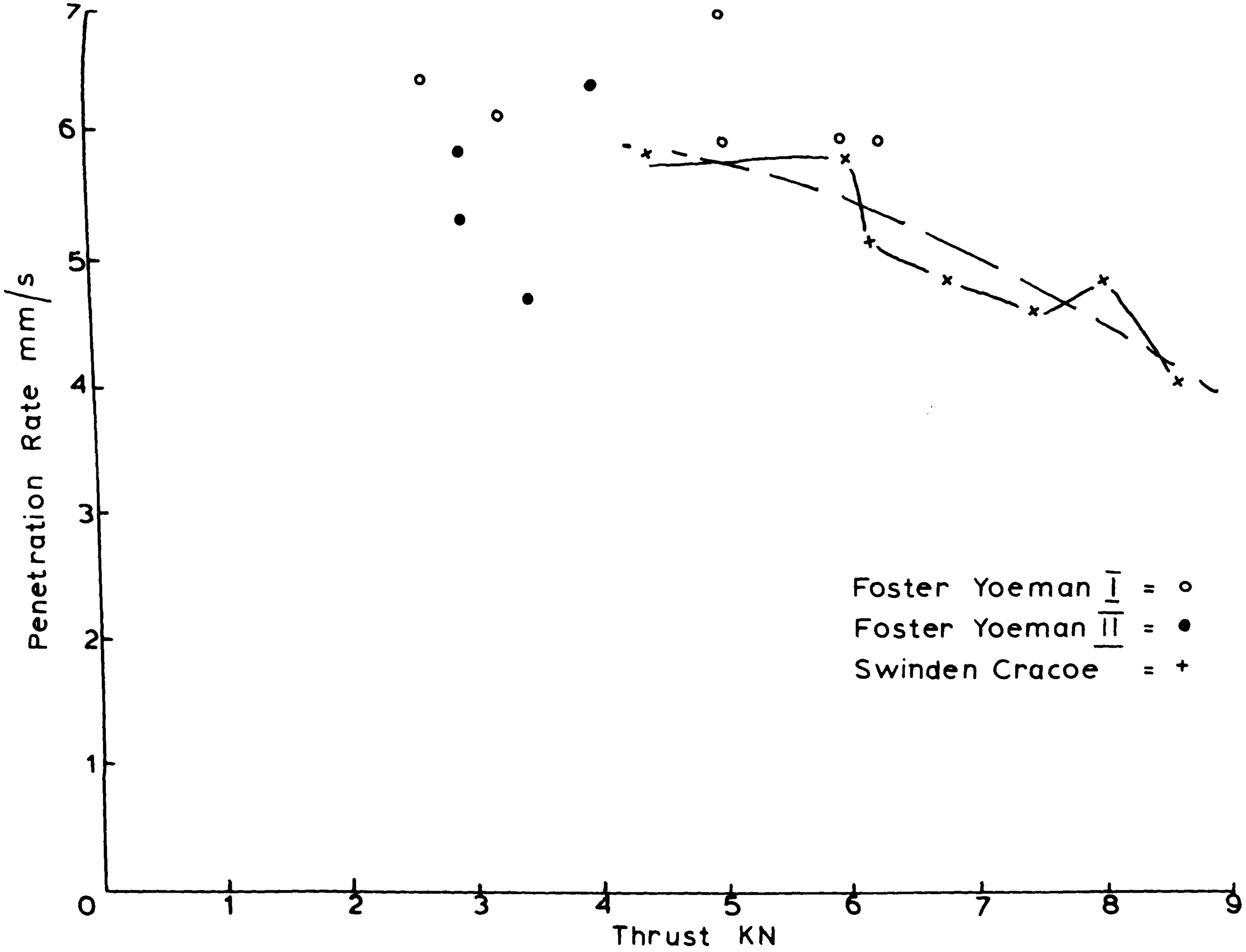

FIGURE 5.8: PENETRATION RATE V THRUST.

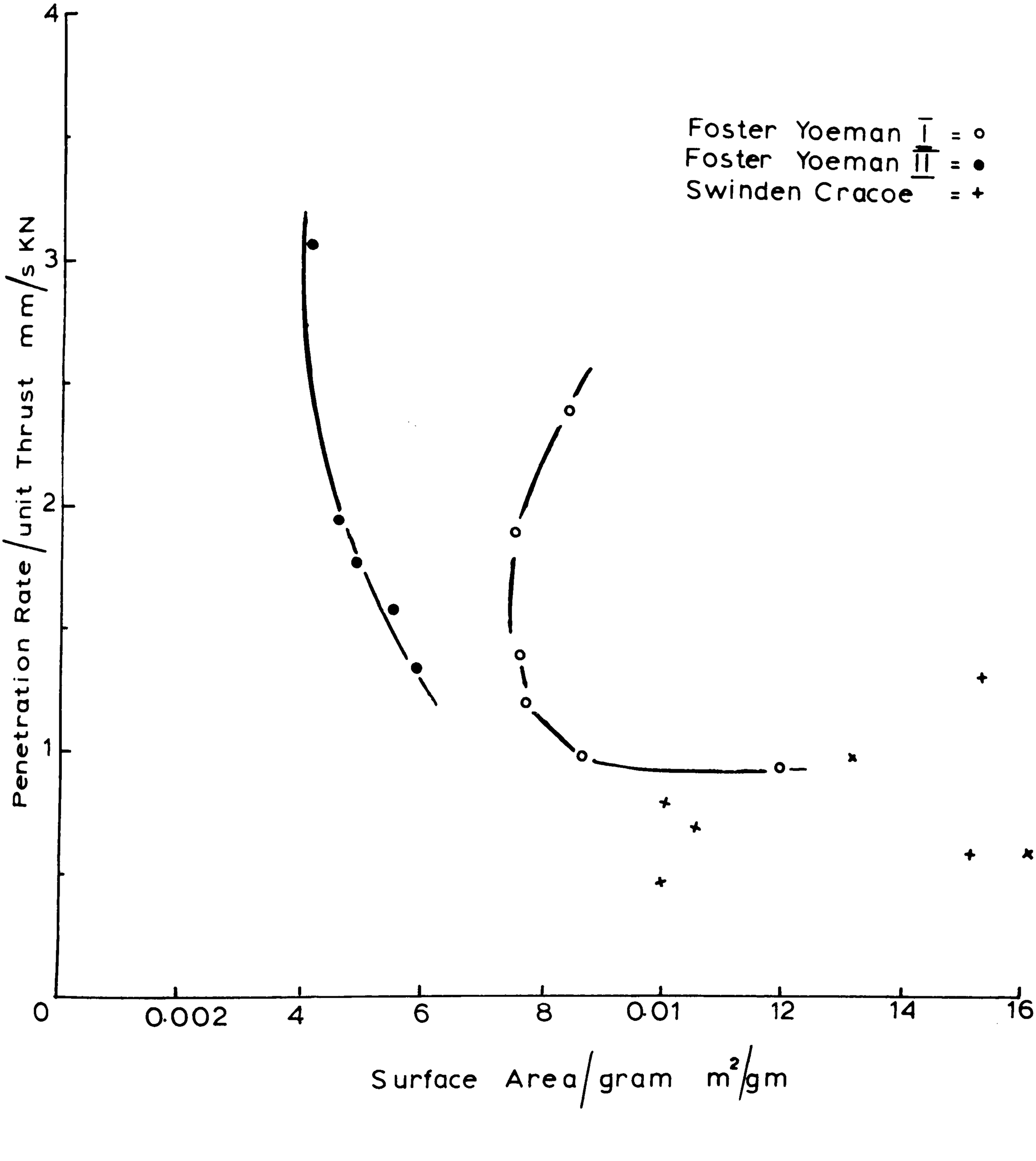

FIGURE 5.9: PENETRATION RATE PER UNIT THRUST VERSUS THE SURFACE AREA OF THE DRILL CUTTINGS.

DISCUSSION

There is no apparent relationship between the penetration rate against the thrust for the Foster Yoeman tests shown in figure 5.8, but Swinden Cracoe has a general decrease of penetration rate as the thrust increases. In figure 5.9 penetration rate per unit thrust against the surface area of the drill cuttings shows some sort of relationship for the Foster Yoeman tests, but none for the Swinden Cracoe.

With Foster Yoeman tests the change in bit size has made a substantial contribution to the change in surface area values. The large bit size in test II must be enabling the cuttings to be cleared away to give the smaller surface areas per gram instead of being reground, producing more fines. The curving characteristic for test I indicates that with the high thrust there is more regrinding because of clogging, hence the greater surface areas/gram. With the highest penetration rate per unit thrust the drill exhaust is unable to clear away the cuttings fast enough because of the high production rate of cuttings therefore causing some regrinding again in test I.

Performance factor values (P.R. x P_T x A_H ÷ Th. x A_d) were calculated for the drilling results at the two quarries and these values are also listed in table 43. Figure 5.10 shows the performance factor plotted against the penetration rate (graph A) and against the penetration rate per unit thrust (graph B). As found with the laboratory drill, the performance factor does provide a relationship of the drill parameters, again this only shows that a consistent relationship is possible.

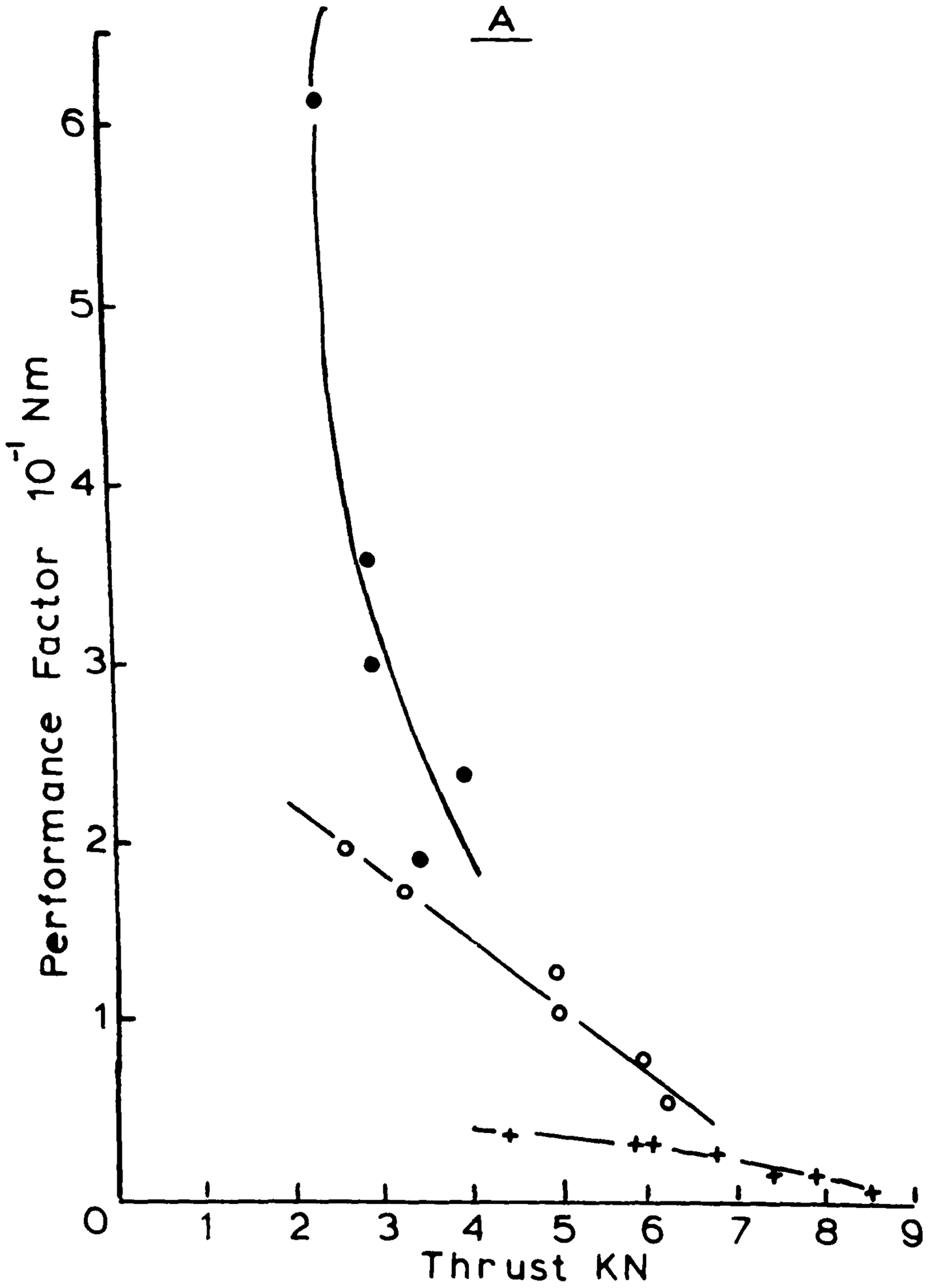

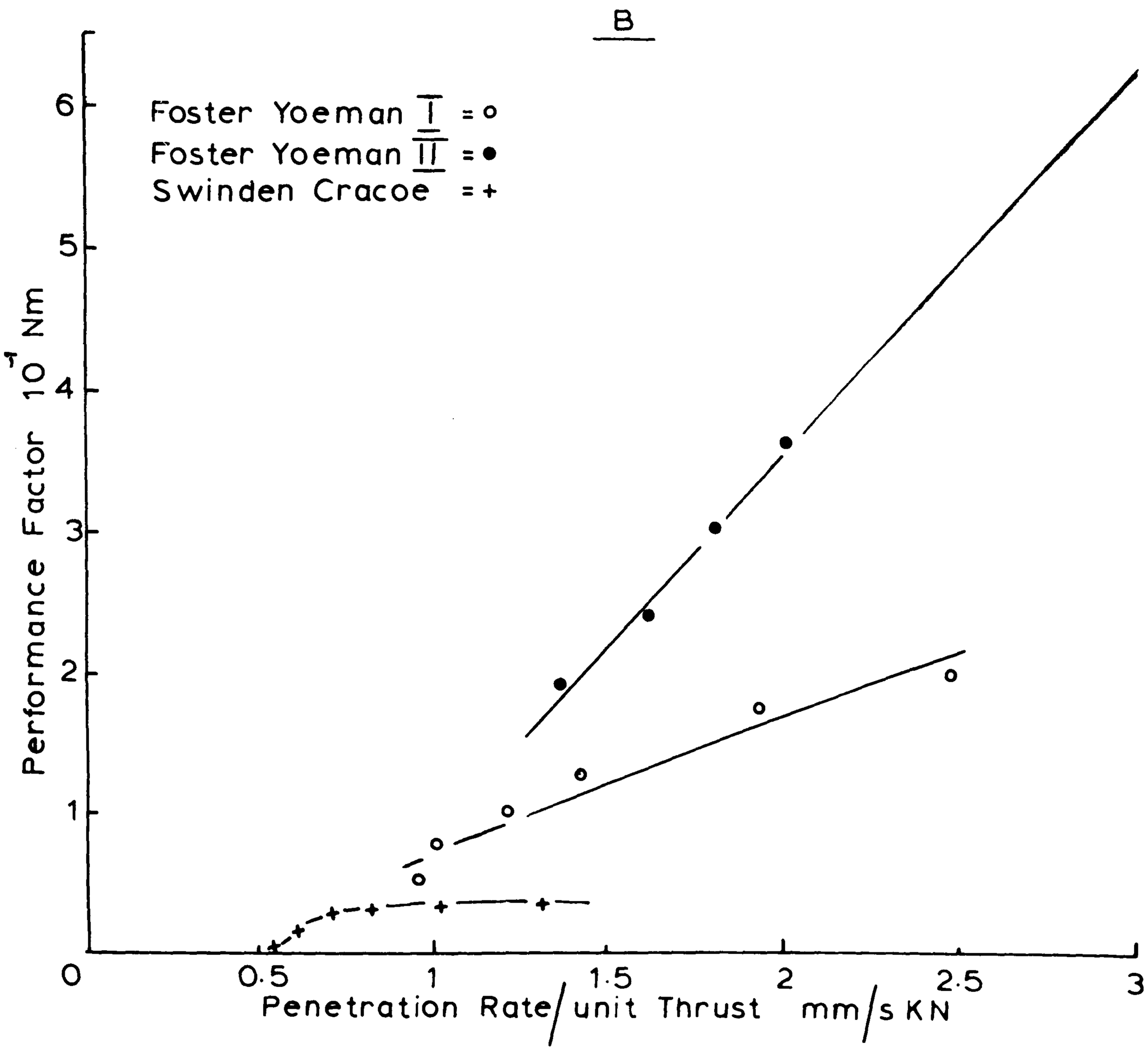

FIGURE 5.10:
PERFORMANCE FACTOR V THRUST(A) AND PENETRATION RATE PER UNIT THRUST(B).

SUMMARY OF FIELD DRILLING

(a) Unfortunately the laboratory drill values plotted against the field drill values gave no correlation.

(b) Analysis by Teale (51) and Hustrulid (55) gave graphs that exhibited a general trend, but with a substantial amount of scatter and could not be used for accurate prediction.

(c) The relative efficiencies showed that the drilling efficiency varies for each rock and the values for relative efficiency are quite small all less than 20% determined from air pressure input and rock impact hardness number. However, stress wave energetics have shown that a lot of the energy is lost before it reaches the bit. So that the efficiency of transfer from the bit to the rock is approximately four times higher than the relative efficiency values, but even allowing for this the efficiencies still vary from 20.56% to 78.52%. There is also further probable variations if the energy losses through to the bit are not a constant proportion of the air pressure energy input. Certainly, this problem needs to be unravelled, but whether such work will help in view of so many variations giving such a complex process remains to be seen.

(d) A large variation in the collected field drill cuttings has been found by surface area measurements. Change of bit sizes has had a large effect on the drill cuttings at Foster Yoeman quarry and the thrust variation at both quarries has also produced a varying effect on the cuttings.

Tests on the drill cuttings collected at Swinden Cracoe at two extreme drill depths produced the same strength characteristic when tested in the laboratory by slow compression. The result of this test in the laboratory by slow compression is very interesting in that it is feasible to actually use the drill cuttings for strength determinations and has the possibilities of 'on line' strength determinations.

There is no clear relationship between the measured drill variables at Foster Yoeman and Swinden Cracoe, but the performance factor did provide a linear relationship when plotted against the penetration rate per unit thrust for all three tests. This again shows that a consistent inter-relationship can be achieved.

CHAPTER VI

GENERAL CONCLUSIONS AND SUGGESTIONS FOR FURTHER WORK

CHAPTER VI

GENERAL CONCLUSIONS AND SUGGESTIONS FOR FURTHER WORK

The detailed study of rock breakage in the laboratory by measuring the energy input and the surface area of rock created has enabled an accurate index to be determined with a graphical comparison of laboratory breakage efficiencies. The intention of developing an accurate index by measuring energy and area was for correlation with rotary-percussion drilling. So that an improved correlation on rock impact hardness number and coefficient of rock strength could be obtained. Also as the measurement involved energy inputs and surface area outputs this would be relevant to drilling as it was proposed to examine the rock output of penetration rate and the drill cuttings incorporating this accurate index. However, in drill correlations and relative efficiency determinations this idea did not give the desired results, as shown in the penetration rate - thrust slope correlations in 4.1 and laboratory input/output drill analysis in 4.6. Therefore, for use in these sorts of situations the rock impact hardness number sufficed.

In the laboratory rock breakage work, three methods of breakage were considered, drop hammer and stamp mill methods for correlation in drilling and slow compression method as the standard for efficiency of breakage. The graphical comparisons of the different methods of breakage showed that the drop hammer has a greater utilization of energy in

producing surface area at the larger sizes and this is most evident in this study with the 'softer, 'weaker' rocks. As the size of rock reduces, breakage by slow compression then becomes very efficient compared to the drop hammer. If slow compression could be adopted for commercial breakage of finer material and the same crushing rates could be maintained, then there would be substantial savings in energy expenditure.

The stamp mill having a small drop height compared to the drop hammer also becomes more efficient than the drop hammer at the finer sizes, but not to the same extent as slow compression.

The measurement of surface area has been applied for the accurate quantification of drill cuttings both in the laboratory and the field. Work has shown that the drill cuttings play an important role in the study of drilling.

In laboratory drilling an extensive survey of drilling has been made. The characteristics of rotary-percussive drilling have been shown along with a detailed presentation of the interrelationships of the drill parameters explaining how rotary-percussion drilling can be used to suit the rock type.

The analysis by specific energy and power and the graphical comparisons using the rock strength properties gave general trends, but with quite an amount of scatter. The difficulties involved in correlating different rocks covering a wide range of physical properties is understandable when one sees that the relative efficiencies of drilling vary considerably. Similar analysis of the field drilling has

also shown the difficulties involved, though in the field the powers involved are much greater the specific energies and relative efficiencies are of the same order as laboratory drilling.

It must be emphasised however, that the drilling relationships considered were for ranges of rocks at set drilling conditions in the laboratory or at optimum drilling conditions in the case of field drilling. So that as difficulties in correlations have arisen under these separate conditions, then the combining of different conditions for correlation by specific energy, power input and output would be even more difficult.

The performance factor for laboratory drilling provides very good relationships when previously there has been none. Unfortunately, the performance factor as yet, does not provide a useable answer for drilling.

The correlation of laboratory drilling with field drilling did not give the desired result, however as the drill variables are interrelated with physical rock properties, further work introducing a rock property or properties may produce a correlation.

Field work at Foster Yoeman and Swinden Cracoe limestone quarries has shown that the bit size and thrust affect the size of the drill cuttings. The drill cuttings have been used to determine the strength of the rock encountered at different depths by slow compression and a linear relationship was obtained between the energy per gram and area per gram.

The performance factor again gave a relationship of the drill variables.

SUGGESTIONS FOR FURTHER WORK

1. To develop a rock strength index first by laboratory work using drill cuttings to find out whether a consistent index will occur. This seems quite probable if closely graded cuttings are used as done with the Swinden Cracoe drill samples and the stamp mill charges where small size rock particles, carefully graded, having approximately the same volumes were used. Also slow compression tests for galena, fluorspar and Elland Edge had graded charges of approximately the same volumes for crushing in the small mortar. With the drop hammer apparatus replacing the larger sizes for Bath limestone and leaving out the fines still gave the same linear relationship for the energy/area graph. When a comparison was made between the stamp mill and the drop hammer using Bath limestone with the stamp mill charge in the drop hammer apparatus, the initial energy/area relationship was obtained. However, as the charge being replaced in the drop hammer mortar became smaller the breakage became inefficient and the curve began to steeply rise away from the area per gram axis. In view of this it would be better to work with slightly larger sizes in the charge. So that the simple drop hammer apparatus would be used in the field and the strength index determined 'on line'.

If this development could be achieved it would be extremely advantageous saving some of the heavy costs incurred for diamond drilling sample cores both in the field and laboratory and allowing in-situ strength determinations.

2. The energy/area measurements gave consistent relationships and there is the possibility that further work on other types of rock breakage indices could also do this. Therefore, having all the rock breakage indices reduced to a common denominator of energy and area. The measurement of larger areas outside the sieve range used would have to be studied and standardised. As it is possible to have a consistent measure with the smaller sizes, it should be possible to have one for the larger pieces.

3. The laboratory drilling has been extensively covered, but stress energetics could be employed to actually measure the variations in energy losses for drilling different rocks. Further field work could be carried out drilling a range of rocks using the measuring techniques described in this work and if possible by stress wave energetics measure the percussive power input at the bit when drilling as well as all the other drill parameters. Collecting the drill cuttings for analysis of performance and possible strength determinations.

If finally after this work a logical analysis doesn't

give the answer, then the performance factor should be calculated to see if this formula still gives the best relationships of the drill variables and correlates with a rock property.

- o - O - o -

APPENDIX

True Rock Densities gm/cc.

Rock	True density
Yellow Oolitic limestone	2.642
Darley Dale sandstone	2.588
Horsforth sandstone	2.860
St. Bee's sandstone	2.569
Elland Edge sandstone	2.644
Bath limestone	2.659
Denbigh limestone	2.674
Whinstone	2.932
Giggleswick limestone	2.687
Cornish granite	2.651
Mount Sorrel granite	2.576
Craigenlow Pink granite	2.646
Groby granite	2.681
Bardon Hill granite	2.849
Backwell limestone	2.718
Foster Yoeman limestone	2.705
Kelmac limestone	2.539
Ramsbottom Wild sandstone	2.671
Swinden Cracoe limestone	2.712
Thresfield limestone	2.736
Holme Park limestone	2.746
Buckton sandstone	2.566
Croft granite	2.714

Appendix cont)

Rock	True density
Boon's Nuneaton quartzite	2.652
Fairy Cave limestone	2.678
Tarmac Arcow greywacke	2.671
Horton mudstone	2.791
Crystalline limestone	2.784
Larvikite	2.773

REFERENCES

1. Lacabanne, W.D. and Pfleider, E.P. "Rotary-Percussion Blast hole Machine May Revolutionise Drilling" Mining Engineering, Sept. 1955, vol. 7, no. 9, pp. 850-855.

2. Fish, B.G. "Percussive Rotary Drilling". The Mining Magazine, March 1956, pp. 133-142.

3. Guppy, G.A. "An Examination of the Salzgitter V100 Percussive Rotary Drilling Machine and Comparison with Hausher DKES Model". N.C.B., M.R.E. Report no. 2116, 1958,

4. Fish, B.G. "A Description of Techniques for the Measurement of Abrassive Bit Wear in Rock Drilling Studies" N.C.B., M.R.E. Technical Memorandum no. 24, 1957.

5. Teale, R. "Studies in Rock Working. 11. Some Fundamental Considerations: The Concept of Specific Energy". N.C.B. M.R.E. Report no. 2154, 1960.

6. Hartman, H.L. "Basic Studies of Percussion Drilling". Trans. American Inst. Min (metall.) Engineers vol. 214 1959. pp. 68-75.

7. Guppy, G.A. "The Percussive Energy Factor in Percussive-Rotary Drilling". N.C.B. M.R.E. Report no. 2199, Nov. 1961.

8. Simon, R. "Theory of Rock Drilling". 6th Annual Drilling Symposium, University of Minnesota, Oct 11-13, 1956. pp. 1-14.

9. Inett, E.W. "Rotary-Percussive Drilling Explains New Drilling Technique". Engineering and Mining Journal vol. 157, no. 8 pp. 75-79. August 1956.

10. Pflieder, E.P. and Lacabanne, W.D.. "Higher Air Pressures for Down-the-hole Percussive Drills" Mine and Quarry Engineering, Nov. 1961, 27, pp. 463-501.

11. De Saint-Venant, B. "Memoir sur le Choc Longitudinal de deux barres elastiques de grosseurs et de Matieres Semblables ou Differentes". Journal Mathematiques, 2e ser. vol. 12 pp. 237-376, (1867).

12. De Saint-Venant, B. "Choc Longitudinal de Deux Barres Elastiques, dont l'une est Extremement Courte ou Extrement Roide par Rapport a L'autre". C.r. hebd. Seanc. Acad. Sci. Paris vol. 66, pp 650-653, (1868).

13. Donnel, L.H. "Longitudinal Wave Transmission and Impact" Trans. Am. Soc. Mech. Engrs. vol. 52, pp. 153-167, (1930).

14. Dahl, H.O. "Hammare och borr". Jernkontorets Annaler, vol. 5, pp. 205-219, (1932).

15. De Juhasz, K.J. "Graphical Analysis of Elastic Bars" Journal Appl. Mech., vol. 9, A122-A128, (1942).

16. De Juhasz, K.J. "Graphical Analysis of Impact of Bars Stressed Above the Elastic Range". J. Franklin Inst. vol. 247, pp 15-48, 113-142, (1949).

17. Fischer, H.C. "On Longitudinal Impact I - III". Appl. Scient.Res. A8 pp. 105-139, 278-308, A9 pp. 9-42, (1959).

18. Fairhust, C. "Wave Mechanics of Percussive Drilling" Mine and Quarry Engineering, vol. 27, 1961.

19. Fischer, H.C "Stress Pulses in Percussive Drilling" Mining Research vol. 2, pp. 833, 1961.

20. Bailey, J.J. "On the Performance of Percussive Drills". Proceeding on the 9th Symposium on Rock Mechanics, Colorado School of Mines, (1967).

21. Simon, R. "Transfer of Stress Wave Energy in the Drill Steel of a Percussive Drill to the Rock". Int. J. of Rock Mechanics. vol. 1, 1964, pp. 397-411.

22. Hustrulid, W.A. and Fairhurst, C. "A Theoretical and Experimental Study of the Percussive Drilling of Rock". Int. J. of Rock Mechanics. vol. 8, pp. 311-333, vol. 8,pp. 335-356 (1971), vol. 9, pp. 417-429, vol. 9, pp. 431-449 (1972).

23. Dutta, P.K. "The Determination of Stress Wave Forms Produced by Percussive Drill Pistons of Various Geometrical Designs". Int. J. Of Rock Mechanics, vol. 5, pp. 501-518 (1968).

24. Lundberg, B. "Energy Transfer in Percussive Rock Destruction". Parts I, II and III. Int. J. of Rock Mechanics vol. 10, no. 5, pp. 381-435, (1973).

25. Harley, G.T. "Proposed Ground Classification for Mining Purposes". Engng. Min. J., vol. 122, pp. 368-372, 413-416 (1926).

26. Gyss, E.E. and Davis, H.G. "The Hardness and Toughness of Rocks". Min. Metall. vol. 28, pp. 261-266. (1927).

27. Alpan, H.S. "Factors Affecting the Speed of Penetration of Bits in Electric Rotary Drilling". Part 2, Trans. Instn. Min. Engrs. vol. 111, pp. 375-389 (1951-52).

8. Kinoshita, S. "Studies in the Drillability of Rocks by Rotary Drills". J. Inst. Min. Met. (Japan), vol.72 pp. 43-48, 1956.

9. Protodyakonov, M.M. "Mechanical Properties and Drillability of Rocks" 5th Symposium on Rock Mechanics, University of Minnesota, pp. 103-118, 1963.

0. Gstalder, S. and Raynal, J. "Measurement of Some Mechanical Properties of Rocks and their Relationship to Rock Drillability". J. Petrol. Technol., vol. 18, pp. 991-996, 1966.

1. Singh, D.P. "Drillability and Physical Properties of Rocks". Proc. Rock Mechanics Symposium, Sidney, Inst. of Engrs., Australia, 1969.

2. Furby, J. "Tests for Rock Drillability". Min. Quarry Engrg., vol. 30, 1964, pp. 292-298.

3. Cook, M.A. "Behaviour of Rock During Blasting". Trans. Am. Inst. Min. Engrs., 235, 1966, pp. 383-92.

4. Misra, B. "Correlation of Rock Properties with Machine Performance". Ph.D. thesis, University of Leeds, 1972.

5. Howard Engineering (Derby) Co. "The N.C.B. Cone Indentor". (British Patent application no. 34743/65) Ashbourne Road, Kirk Langley, Derby.

6. Van del Vlis, A.C. "Rock Classification by a Simple Hardness Test". 2nd Congress of the Int. Soc. for Rock Mechanics. vol. 2, theme 3, p. 23, Belgrade 1970.

7. Paone, J. and Bruce, W.E. "Drillability Studies - Diamond Drilling" Washington, U.S. Bureau of Mines, R.I. 6324, 1963.

38. Paone, J. and Madson, D. "Drillability Studies - Impregnated Diamond Bits". Washington, U.S. Bureau of Mines, R.I. 6776, 1966.

39. Tsoutrelis, C.E. "Determination of the Compressive Strength of Rock In-situ or in Test Blocks using a Diamond Drill". Int. J. of Rock Mechanics Min. Sc. vol. 6, pp. 311-321, 1969.

40. Paone, J., Madson, D., and Bruce, W.E. "Drillability Studies - Laboratory Percussive Drilling" Washington U.S. Bureau of Mines, R.I. 7300, 1969.

41. Protodyakonov, M.M. "Russian Translating Programme," R.T.S. 3637, Ugol. 1950 (9), pp. 20-24.

42. Schmidt, R.L. "Drillability Studies - Percussive Drilling in the Field" Washington, U.S. Bureau of Mine, R.I. 7684, 1972.

43. Summers, D.A. "Disintegration of Rock by High Pressure Jets". Ph.D. thesis, University of Leeds, pp. 42-48, 1968.

44. Misra, B. "Protodyakonov Number and its Relationship with other Measures of Rock Physical Properties". Hons. Dissertation, University of Leeds, 1969.

45. Brook, N. "A Modified Method of Determining the Protodyakonov Number and its Correlation with Compressive Strength" 2nd Congress of Int. Soc. for Rock Mechanics, Belgrade 1970.

46. Brook, N. and Misra, B. "A Critical Examination of the Stamp Mill Method of Determining Protodyakonov Rock Strength and the Development of a method of

Determining a Rock Impact Hardness Number". Chapter 8, pp. 151-165. 12th Symposium on Rock Mechanics, University of Missouri, 1970.

47. Selmar-Olsen, R. and Blindheim, O.T. "On the Drillability of Rock by Percussive Drilling." 2nd Congress of Int. Soc. for Rock Mechanics, 5-8, pp. 65-70, Belgrade 1970.

48. Sievers, H. "Die Bestimmung des Bohrwiderstandes von Gesteinen". Gluckauf 86, 37/38, pp. 776-784, 1950. Gluckauf G.M.B.H., Essen.

49. Broch, E. and Franklin, J.A. "The Point-load Stength Test". Int. J. of Rock Mechanics, vol. 9 no. 6, pp. 669-698, No. 1972.

50. Hartman, H.L. "The effect of Indexing in Percussion and Rotary Drilling". Int. J. of Rock Mechanics vol. 3, 1966, p. 265.

51. Teale, R. "Concept of Specific Energy in Rock Drilling". Int. J. of Rock Mechanics, vol. 2, no. 1, pp. 57-73, 1965.

52. Opoloski, T. "Speed of Advance and Power Consumption in Rotary Drilling". Bergbantechnik, no. 12, pp. 654-658, 1956.

53. Cook, N.G.W. and Hustrulid, W.A. "The Efficiency of a Pneumatic Powered Percussive Rock Drilling System" Res. Lab. of S.A., 82nd Annual Rep. 1971.

54. Hustrulid, W.A. "A Study of Energy Transfer to Rock and Prediction of Drilling Rates in Percussive Drilling" M.S. Thesis, University of Minesota, Duluth, Minn., Jan. 1965, pp. 171.

55. Hustrulid, W.A. "The Percussive Drilling of Quartzite" J. of the S.African Inst. Min. and Metall, July 1971 pp. 245-268.

56. Mellor, M. "Normalisation of Specific Energy Values" Int. J. of Rock Mechanics, vol. 9, no. 5, pp. 661-663, 1972.

57. Hughes, H.M. "Some Aspects of Rock Machining". Int. J. of Rock Mechanics, vol. 9, pp. 205-211, 1972.

58. Unger, H.F. and Fumanti, R.R. "Percussive Drilling with Independent Rotation" Washington, U.S. Bureau of Mines, R.I. 7692, 1972.

59. Selin, A.A., and Bruce, W.E. "Prediction of Penetration Rate for Percussive Drilling" Washington, U.S. Bureau of Mines, R.I. 7396, 1970.

60. Patzold, F. "La Formation Vibree" Revue Ind. Minerale, Dec. 1953, vol. 34, pp. 1058-1065.

61. Barker, J.S. "A Laboratory Investigation Using Large Picks" Int. J. Rock. Mech. Min. Sci. vol. 1, 1964. pp. 519-534.

62. Dubnie, A. and Tervo, R. "Evaluation of Drill Cuttings from a Long-Hole Drilling Project" Mining Research Centre, Internal Report MR 70/97 - 1D, E.M.R. Ottawa, Canada, Oct. 1970.

63. Schmidt, R.L. Engelmann W.H. and Fumanti R.R. "A Comparison of Borer, Ripper and Conventional Mining Products in Illinois no. 6 Coal Seam". Washington U.S. Bureau of Mines, R.I. 7687, 1972.

64. Hartman, H.L. "Crater Geometry Relation in Percussive Drilling. Single Blow Studies". Mine Quarry Engng, vol. 28, 1962, pp. 530-536.

65. Pariseau, W.G. and Fairhurst, C. "Force-Penetration Relationships for Wedge Penetration into Rock". Int. J. of Rock Mechanics Min. Sci. 1967, vol. 4, no. 2.

66. Morris, R.I. "Rock Drillability Related to a Roller Cone Bit" Proceedings of S.P.E., Paper No. SPE 2389 (1969).

67. Lightfoot, R.M. "Drillability and Wear Prediction by Laboratory Techniques and Correlation with Operating Experience". Symposium on Raise and Tunnel Boring, Aust. Geomechanics Soc., Aug. 1970.

68. Kick, F. "The Law of Proportional resistance and its Application to Sand and Explosions". Dinglers J., vol. 247, 1883, pp. 141-145.

69. Rittinger, P.N. "Lehrbuch der Aufbereitungskunde" Berlin, 1867.

70. Bond, F.C. "The Third Theory of Comminution" Trans Am. Inst. Engrs., vol. 193, 1952, pp. 484-494.

71. Hukki, R.T. "Proposal for Solomenic Settlement between the Theories of von Rittinger, Kick and Bond". Trans. Soc. Min. Engrs., AIME, vol. 220, 1961, pp. 403-408.

72. Jowett, A. "An Introduction to the Assessment of Energy Requirements and Product Size in Comminution". Minerals Science and Engineering Oct. 1971, pp. 33-43

73. Walker, W.H. et al. "Principles of Chemical Engineering" 3rd ed. New York, McGraw Hill, 1937.

74. Holmes, J.A. "A Contribution to the Study of Comminution, A Modified Form of Kick's Law" Trans. Inst. Chem. Engrs., vol. 35, 1957, pp. 125-41.

75. Charles, R.J. "Energy-size reduction Relationships in Comminution". Trans. Am. Inst. Min. Engrs., vol. 208, 1957, pp. 80-88.

76. Schuhmann, R. "Principles of Comminution. Part I. Size Distributions and Surface Calculations" Min. Technol., vol. 4, no. 4, July 1940. (T.P. 1189).

77. Carey, W.F. and Stairmand, C.J. "A Method of Assessing the Grinding Efficiency of Industrial Equipment" Symp. Inst, Min. and Metall. Sept. 1952, Session 2, pp. 117-136 in book "Recent Developments in Mineral Dressing" 1953.

78. Carey, W.F. and Stairmand, C.J. "Communications on the Particle Size Analysis of Crushed Products". Inst. Mech. Engnrs., London 1950, vol. 162 (3), pp. 384-391.

79. Muta and Watanabe. "Particle Size Distribution of Fine Powders". p.181, p.193 in book "Particle Size Analysis". Groves and Wyatt Sargent, 1970, University of Bradford, Conference on Particle Size.

80. Hindle, A.C. "A Review of Real Time Size Analysis" J.S. African Inst. Min. and Metall., March 1973, pp. 261-267.

81. Frangiskos, A.Z. "The Effect of Some Surface Active Reagents on the Comminution of Quartz and Limestone" Ph.D. Thesis, University of Leeds, Aug. 1956.

82. Chakravarti, A. "Energy Consumption in Mineral Comminution". Ph.D. Thesis, University of Leeds, Nov. 1963.

83. St. Clair, H.W. and Brown, R.E. "An Experimental Study of Particle Size and Size Distribution of Minerals Crushed by Impact". U.S. Bureau of Mines (Washington). R.I. 7615, 1972.

84. Schoenert, K. "Role of Fracture Physics in Understanding Comminution Phenomena" AIME Transactions, vol. 252, March 1972, pp. 21-26.

85. Griffith, A.A. "Philosophical Transactions, Royal Society A, vol. 221, 1920, p. 163.

86. Bradley, A.A., Hindle, A.L. and Lloyd, P.J. "The Determination of the Efficiency of the Milling Process". J.S. Afr. Inst. Min. and Metall., June 1972, pp. 277-281.

87. Jomoto, K. and Majima, H. "Criterion of Comminution" C/M Trans., vol. LXXV, pp. 326-331, 1972.

88. Rose, H.E., "Drop-weight Tests as the Basis for the Calculation of the Performance of Ball-mills" 10th Int. Mineral Processing Congress, London 1973.

89. Rumpf, H. "Physical Aspects of Comminution and New Formation of a Law of Comminution" Powder Techn. vol. 7, 1973, pp. 145-159.

90. Agar, G.E. and Somasumdaran, P. "Rationalization of Energy-particle Size Relationship in Comminution".

10th Inst. Mineral Processing Congress, London 1973, Paper 16.

91. Bond, F.C. "Standard Grindability Tests Tabulated" Trans. Am. Inst. Min. Engrs., vol. 183, 1949, pp. 313-29.

92. Bond, F.C. "Confirmation of the Third Theory" Trans. Am. Inst. Min. Engnrs, vol. 217, 1960, pp. 139-153.

93. Meyers, J.F., Michaelson, S.D. and Bond, F.C. "Rodmilling-plant and Laboratory Data". Trans. Am. Inst. Min. Engrs., col. 183, 1949, pp. 299-309.

94. Smith, R.W. and Lee, K.H. "A Comparison of Data from Bond Type Simulated Closed-circuit and Batch Type Grindability Tests". Trans Am. Inst. Min. Engrs. vol. 241, 1968, pp. 91-9

95. Thill, R.E. and Peng, S.S. "Statistical Comparison of the Pulse and Resonance Methods for Determining Elastic Moduli". Washington, U.S. Bureau of Mines, R.I. no. 7831, 1974.

BIBLIOGRAPHY

B1. Somerton, W.H. "A Laboratory Study of Rock Breakage by Drilling". A.I.M.E. Trans. no. 216. 1959.

B2. Fish, B.G. "The Basic Variable of Rotary Drilling" Mine Quarry Engng. vol. 27, 1961, pp. 29-34.

B3. Hartman, H.L. "Stress Distribution Beneath a Wedge-Shaped Drill Bit Loaded Statically" Inter. Symposium on Mining Res. vol. 2, 1961, pp. 799-812.

B4. Wheelan, J.A. "Laboratory Studies of Variables in Rotary Drilling". Washington U.S. Bureau of Mines, R.I. no. 6121, 1962.

B5. Fairhurst, C. "Drilling and Rock Destruction". 5th Symposium on Rock Mechanics, May 1962, University of Minnesota, Pergamon Press (Oxford) 1963.

B6. Teale, R. "Mechanical Excavation of Rock-Experiments with Roller Cutters". Int. J. of Rock Mech. vol. 1, 1964.

B7. Maurer, W.C. "The State of Rock Mechanics in Drilling". 8th Symposium on Rock Mechanics, Sept. 1966, University of Minnesota, Pub. A.I.M.E. 1967, Chapter 15, p. 355.

B8. Bailey, J.J. and Dean R.C., "Rock Mechanics and the Evolution of Improved Cutting Methods". 8th Symposium on Rock Mechanics, Sept. 1966. University of Minnesota, Pub. A.I.M.E. 1967, Chapter 16, p.396.

B9. Cheatham, J. and Gnirk, P.F. "Mechanics of Rock Failure Associated with Drilling at Depth" 8th Symposium on Rock Mechanics, Sept. 1966, University

of Minnesota, Pub. A.I.M.E. 1967, Chapter 17, p. 439.

B10. Geller, L.B. "Research in Improved Methods of Rock Breakage". Inst. Min. and Metall. vol. 76, no. 728, July 1967.

B11. Aredissan, Y.M. and Wood, L.E. "Prediction of Compressive Strength of Rock from its Sonic Properties" 10th Symposium on Rock Mechanics, p. 55, 1968.

B12. Bur, Thill and Hjelmstad. "An Ultrasonic Method for Determining the Elastic Symmetry of Material" Washington, U.S. Bureau of Mines, R.I. 7333, Dec. 1969.

B13. Maurer, W.C. "Novel Drilling Techniques" Pergamon Press 1968.

B14. Hartman, H.L. "Exploitation - Unit Operations Drilling" Surface Mining, Editor Pfleider, 1968, Section 6.

B15. White, C.G. "A Rock Drillability index". Quarterly Colorado School of Mines, 1969.

B16. Bruce, W.E. and Paone, J. "Energetics of Percussive Drills". Washington, U.S. Bureau of Mines, R.I. 7253, April 1969.

B17. Lundquist, R.G. and Anderson, C.F. "Energetics of Percussive Drills - Longitudinal Strain Energy" Washington, U.S. Bureau of Mines, R.I. 7329, Dec. 1969.

B18. Franklin, J.A. et al. "Logging the Mechanical Character of Rock". Inst. Min. and Metall, Jan 1971, pp. A1-A9.

B19. Dubnie, A and Gyenge, M. "Studies of Long-hole Drilling". Can. Min. J. Dec. 1972, pp. 44-53.

B20. Hardy, M.P. and Fairhurst C. "Chip Formation by Drag Cutters". 6th Con. on Drilling, Univ.Tex. Jan 1973.

B21. Everall, M.D. et al. "A Preliminary Control Strategy for the Automatic Control of an Instrumented Diamond Drill". 6th Conference on Drilling and Rock Mech., Univ. Texas, Jan 1973.

B22. Singh, D.P. "The Drillability of Rock" Min. Sci. Engng. vol. 5, no. 3, July 1973.

B23. Wilson, J.W. and Millar, H.D.S. "Drilling and blasting in Thin Tabular Stopes at Depth in Hard Rock". Inst. Min. and Metall, July 1973, pp. A101-A110.

B24. Whittaker, B.N. and Szwilski, A.B. "Rock Cutting by Impact Action" Int. J. of Rock Mechanics, vol. 10, no. 6, 1973.

B25. Just, G.D. "Application of Size Distribution Equations to Rock Breakage by Explosives" Rock Mechanics, vol. 5, no. 3, Sept. 1973.

B26. Szlavin, J. "Relationships Between Some Physical Properties of Rock Determined by Laboratory Tests" Int. J. of Rock Mechanics, Feb. 1974, vol. II, no. 2.

B27. Gates, A.O. "Kick vs. Rittinger, An Experimental Investigation in Rock Cutting Performed at Purdue University. "Inst. Min. Metall. Eng., 52, pp. 875-909 (1915).

B28. Tartaron, F.X. "Foundation of a General Theory of Comminution". Trans. Soc. Min. Engrs. June 1964, pp. 120-125.

B29. Beke, B. "Principles of Comminution". Akademiai, Kiado, Budapest, 1964.

B30. Crabtree, D.D. et al. "Mechanisms of Size Reduction in Comminution Systems". Trans. Soc. Min. Engrs., June 1964, Part I, pp. 201-206, Part II pp. 207-210, and A.I.M.E. vol. 229, 1965.

B31. Austin, L.G. et al. "Solutions to Batch Grinding Equations Leading to Rosin-Ramler Distributions" Trans. Soc. Min. Engrs. A.I.M.E. vol. 252, March 1972, pp. 87-94.

B32. Edgar, J. and Pfleider, E.P. "Mining and Milling, an Integrated Fragmentation System". Trans. Soc. Min. Engnrs. A.I.M.E. vol. 252, March 1972, pp. 46-49.

B33. Draft International Standard ISO/DIS 2591, 'Test Sieving'. April 1972.

B34. Bergstrom, B.H. et al. "Energy and Single Particle Crushing". Trans. Am. Inst. Min. Engrs., vol. 220, 1961, pp. 367-72, and pp. 373-9, vol. 226 1963, pp. 433-41.

ACKNOWLEDGEMENTS

The author wishes to express his gratitude to Dr. N. Brook, Senior Lecturer, and Professor P.A. Young, Head of Department, both of the Department of Mining and Mineral Sciences of the University of Leeds, for their continuous encouragement and valuable suggestions.

His thanks are also due to Dr. A. Jowett, Senior Lecturer of the Department of Mining and Mineral Sciences, University of Leeds, for his helpful advice and discussion on the comminution aspects.

The author would like to acknowledge Mr. A. Shaw, Mr. N. Cox and Mr. R. Holroyde for their interest and co-operation in the collection of the field data.

Finally, author's thanks are due to N.E.R.C. whose grant made this investigation possible.

LOCATION OF ROCKS

Yellow Oolitic Limestone	Guiting stone, Bath Stone Co., Bath, Somerset.
Darley Dale Sandstone	Darley Dale, nr. Sheffield, Yorkshire.
Horsforth Sandstone	Briggs Quarry, Horsforth, nr. Leeds, Yorkshire.
St. Bee's Sandstone	Bunter Sandstone, source near Carlisle.
Elland Edge Sandstone	Elland Edge Quarry, Rastrick, near Brighouse, Yorkshire.
Yorks. Sandstone	a local flagstone, exact source unknown.
Bath Limestone	White lst., Bath Stone Co., Bath, Somerset.
Denbigh Limestone	Craig Quarry, Denbigh, Denbighshire.
Whinstone	Springfield, Fifeshire, Scotland.
Giggleswick Limestone	Giggleswick Quarry, Giggleswick, Settle, Yorkshire
Cornish Granite	Carmarthen Redruth, Redruth, Cornwall.
Mount Sorrel Granite	Mountsorrel Quarry, Mountsorrel, Leicestershire.
Craigenhow Pink Granite	Dunecht Quarry, nr. Aberdeen, Scotland.
Groby Granite	Groby Quarry, Newtown Lane, Groby, Leicestershire.
Bardon Hill Granite	Bardon Hill Quarries, Bardon Hill, nr. Leicester. Leicestershire.
Backwell Limestone	Backwell Quarry, Backwell, Somerset.
Foster Yoeman Limestone	Foster Yoeman Quarry, Shepton Mallet Road, Frome, Somerset.
Kelmac Limestone	Dunald Mill Quarry, Nether Kellet, Carnforth, Lancashire.
Ramsbottom Wild Sandstone	Wild's Quarry, Ramsbottom, Lancashire.
Swinden Cracoe Limestone	Cracoe Quarry, Grassington, nr. Skipton, Yorkshire
Thresfield Limestone	Threshfield Quarry, Grassington, nr. Skipton, Yorkshire.
Holme Park Limestone	Holme Park Quarry, Burton (Westmorland) via Carnforth, Lancashire.
Buckton Sandstone	Buckton Quarry, North Yorks., Yorkshire.
Croft Granite	E.C.C. Quarry, Croft, Nr. Leicester, Leicestershir
Boon's Nuneaton Quartzite	Midland Granite Quarries, Tuttle Hill, Nuneaton, Warwickshire.
Fairy Cave Limestone	Fairy Cave Quarry, Nr. Shepton Mallet, Somerset.
Tarmac Arcow Greywacke	Arcow Quarry, Helwith Bridge, Horton-in-Ribblesdal Nr. Settle, Yorkshire.
Horton Mudstone	Horton Quarry, Horton-in-Ribblesdale, nr. Settle, Yorkshire.
Crystalline Limestone	Dry Rigg Quarry, Horton-in-Ribblesdale, nr. Settle Yorkshire.
Larvikite	Obtained through Andrews and Sons (Marbles & Tiles Ltd., Meanwood Road, Leeds 7.